

TELOMERE LENGTH
IN
CARDIOVASCULAR DISEASE AND TYPE 2 DIABETES

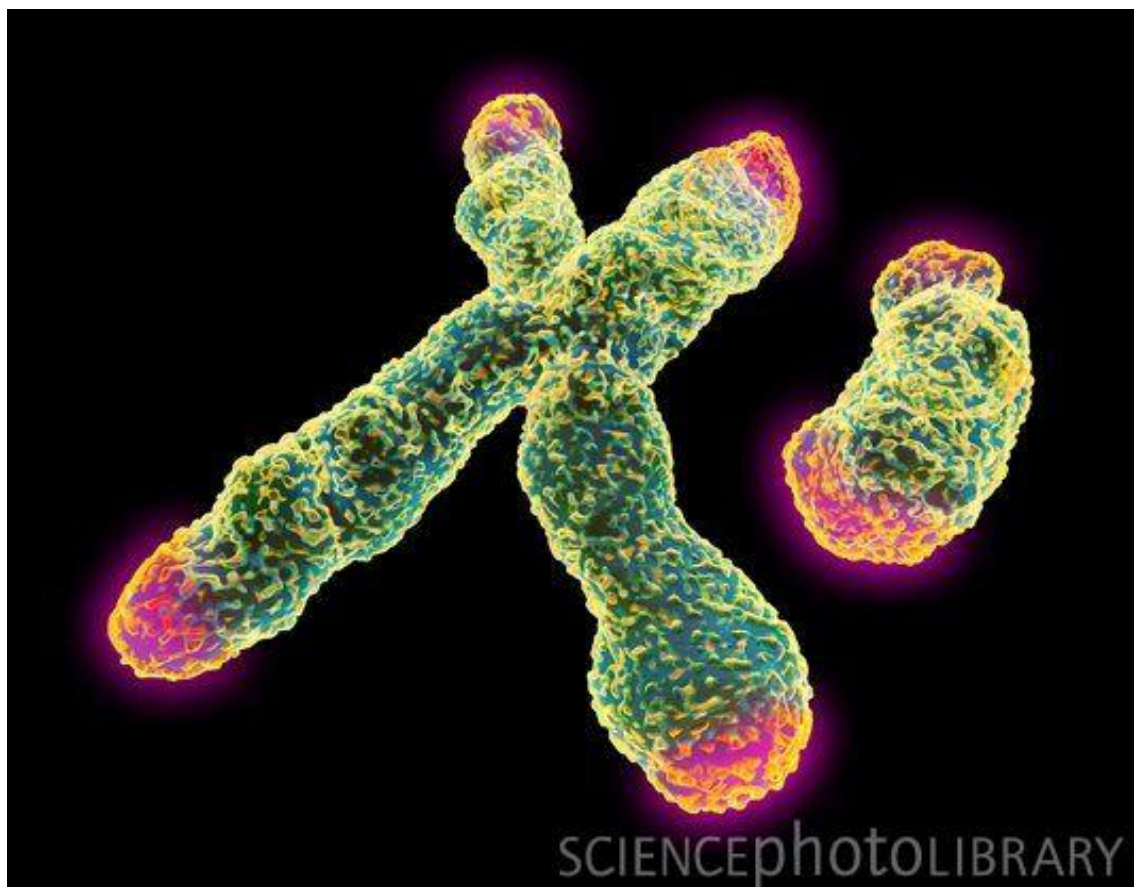
Kalliopi Klelia Salpea

UCL

Thesis submitted for the degree of
Doctor of Philosophy

“Imagination is more important than knowledge”

Albert Einstein (1879 – 1955)



Credit: Pasioka/Science photo library

Caption: Telomeres at X and Y chromosomes. Computer artwork of an X (left) and a Y (right) chromosome.

To my parents

DECLARATION

I, Kalliopi-Klelia Salpea confirm that the work presented in this thesis is my own.
Where information has been derived from other sources, I confirm that this has been indicated in the thesis.

ACKNOWLEDGEMENTS

First and foremost, I would like to thank my supervisors, Professor Steve E. Humphries and Professor Philippa J. Talmud for giving me the opportunity to undertake a PhD and for making it such an educational and pleasant experience. During my PhD studies, they motivated me, taught me how to approach a research question and how to seek a solution to a problem, provide me with all kind of opportunities in order to evolve as a scientist, and taught me how to collaborate with others. Working with them, I did not only enriched my knowledge in science, but most importantly, I learned how to be a researcher. Above all, I am very grateful to them because they were a source of inspiration.

I would like to thank BHF for their generous financial support which allowed the realization of my project. Many thanks to the principal investigators of the studies used in this thesis: EARSII, UDACS, HIFMECH, FH-SB, FH-RF and CABG. Among them I would like particularly to thank Dr Jeffrey Stephens who also performed the oxidative stress measurements in UDACS and Ms Viviane Nicaud who performed the analysis of the EARSII data. I want to also thank Dr Nikos Gkranias who collected the samples and data for the follow up of UDACS. I am very grateful to Dr Scott Brouillette and Professor Nilesh Samani who provided me with samples in order to validate the telomere length assay when I first set it up in our lab. I would like to thank Dr Derek Gilroy for showing me how to use the flow cytometer.

Moreover, I want to deeply thank all past and present members of CVG who have been extremely kind and helpful to me. Especially, I would like to thank Dr Cecilia Maubaret for the wonderful teamwork, fruits of which are the *in vitro* study of telomere shortening and the study of telomere length in monogenic and polygenic CVD. Dr Maubaret performed the PCR assays for the telomere length measurement in HIFMECH and CABG studies and the second measurement of apoptosis and ROS in the *in vitro* experiment presented in the last result chapter. Together with Dr Maubaret we carried out the growing of fibroblast cultures for the *in vitro* study of telomere shortening. Also, I would like to thank Dr Fotios Drenos who was always kind enough, not only to answer my questions on statistics, but also spend time explaining to me the theory behind in more detail. A great help with statistical analysis came from Ms Jackie Cooper, to who I owe a big thank you. Ms Jackie Copper performed the statistical analysis for the HIFMECH, CABG and FH studies, as well as for the follow up data in

UDACS, and helped me to perform the analysis myself in other occasions. Dr Gie Kendror advised me on the statistical analysis of the *in vitro* experimental data. Very important was the help I received from our lab manager Dr Jay Acharya, as well as Ms Jutta Palmen, Ms Ros Whittall, Ms KaWah Li and Ms Wendy Putt, who showed me many techniques and facilitated enormously my research by taking care of the lab orders, preserving the DNA samples and providing help and advice with troubleshooting. Particularly, Ms KaWah Li who performed the genotyping of *MNSOD* and *GPXI* polymorphisms. I am very thankful to you all. Also Dr Sukhbir Dhamrait, who had previously genotyped the *ACE* polymorphism in UDACS. Furthermore, I would like to thank the master and bachelor students that I supervised for their contribution to my experiments. Mr Kavin Abelak for his contribution to the UDACS telomere length measurement, Ms Annegret Kathagen for her contribution to the estimation of mtDNA copies/per nucleus and the measurement of *TFAM* expression levels in fibroblasts, and Dr Anjly Jain for her contribution to the measurement of telomere length in the FH studies. I also owe a big thank you to my fellow PhD students, Dr Simon Thompson, Dr Melissa Smart-Halajko, Mr Donald Pang and Mr Angus Dike, who, over the years, supported me and put up with my occasional stress and frustration, but also shared the moments of excitement and happiness that PhD life offers. I want also to thank them for always having the time to discuss each others' projects.

Finally, I would like to thank my family, for their unconditional support. First of all, I am grateful to my parents who seeded early in my life the love and enthusiasm for science, the admiration to research, and who keep encouraging me to continue studying and seek higher goals. They have always been my example in life. My sister Evi, with who we walked side by side in our lives, studying together, helping each other, believing to each other, encouraging each other and sharing the same love and enthusiasm for life sciences and research. Evi, most of the times you helped me think clearer and find a solution or come up with an idea when I confronted problems with my PhD. Maybe I have never told you how much I enjoy our conversations on science. Maria and Eleni, my beloved aunts, who are always there to console me, congratulate me and encourage me to keep up the effort. Last but not least, I would like to thank Adonis for being always there for me, listening to me, caring about me, supporting me and giving me the strength to carry on, thank you for coming in to my life.

ABSTRACT

Telomere attrition during mitosis is thought to be a mechanism for cell senescence, which is induced when the mean length reduces below a critical value. Oxidative DNA damage has been suggested to cause greater telomere loss per cell division. Thus telomere length indicates the cells' replicative capacity and "biological age". Premature tissue ageing and senescence are major features of cardiovascular disease (CVD) and type 2 diabetes (T2D), and as such telomere length might play an important role in their pathogenesis. The aim of this thesis was to explore the association of telomere length with CVD and type 2 diabetes (T2D) as well as the CVD/T2D risk factors determining telomere length.

The present study showed that telomere length is shorter in CVD and T2D patients compared to healthy subjects. As to what determines telomere length, I found that at least in the case of CVD, it can in part be partly attributed to inherited short telomeres, expressing the family history of the disease. At the same time, in diabetes patients I have observed that high oxidative stress, probably induced by the disease risk factors in the patients, is associated with greater telomere shortening. The later was consistent with the association found between variation in genes regulating reactive oxygen species levels, and shorter telomeres. I further examined the possible determinants of telomere shortening with in vitro experiments on ageing fibroblasts. In this case, the effect of glucose-induced oxidative stress and/or pro-inflammatory conditioning on telomere shortening was tested. The results showed that pro-inflammatory conditioning, partly by inducing an increased cell turnover, aggravates the shortening of telomeres in long-term culture.

Telomere length may prove to be very useful in the management and possibly the prediction of CVD and diabetes, representing the contribution to their pathology of age, oxidative stress and chronic inflammation.

Total thesis word count: 80,880

PUBLICATIONS RESULTING FROM THE WORK IN THIS THESIS

1) **Salpea KD**, Humphries SE. Telomere length in atherosclerosis and diabetes. *Atherosclerosis*. 2010;209:35–38.

2) **Salpea KD**, Talmud PJ, Cooper JA, Maubaret CG, Abelak K, Stephens JW, Humphries SE. Association of telomere length with type 2 diabetes, oxidative stress and *UCP2* gene variation. *Atherosclerosis*. 2010;209:42–50.

➤ Young Investigator Award, *British Atherosclerosis Society Autumn Meeting*. September 18, 2009, Cambridge, UK.

3) **Salpea KD**, Nicaud V, Tiret L, Talmud PJ, Humphries SE; EARS II group. The association of telomere length with paternal history of premature myocardial infarction in the European Atherosclerosis Research Study II. *J Mol Med*. 2008;86(7):815-24.

4) Maubaret CG, **Salpea KD**, Jain A, Couper JA, Hamsten A, Sanders J, Montgomery H, Neil A, Nair D, Humphries SE, HIFMECH consortium, Simon Broome Research Group. Telomeres are shorter in myocardial infarction patients compared to healthy subjects; correlation with environmental risk factors. *J Mol Med*. 2010;88(8):785-94.

OTHER PUBLICATIONS PRODUCED DURING THESIS

1) **Salpea KD**, Gable DR, Cooper JA, Stephens JW, Hurel SJ, Ireland HA, Feher MD, Godsland IF, Humphries SE. The effect of WNT5B IVS3C>G on the susceptibility to type 2 diabetes in UK Caucasian subjects. *Nutr Metab Cardiovasc Dis*. 2009;19(2):140-5.

2) Masi S, **Salpea KD**, Li K, Parkar M, Nibali L, Donos N, Patel K, Taddei S, Deanfield JE, D'Aiuto F, Humphries SE. Oxidative stress, chronic inflammation, and telomere length in patients with periodontitis. *Free Radic Biol Med*. 2010 Dec 29.

3) Eisenberg DT, **Salpea KD**, Kuzawa CW, Hayes MG, Humphries SE; on Behalf of the European Atherosclerosis Research Study II Group. Substantial variation in qPCR measured mean blood telomere lengths in young men from eleven European countries. *Am J Hum Biol*. 2011.

TABLE OF CONTENTS

I. INTRODUCTION	36
1. IMPACT	36
1.1 IMPACT OF CARDIOVASCULAR DISEASE.....	36
1.2 IMPACT OF DIABETES.....	38
2 CARDIOVASCULAR DISEASES	41
2.1 THE CARDIOVASCULAR SYSTEM.....	41
2.1.1 The heart	41
2.1.2 The systemic circulation	41
2.1.3 The vascular wall.....	42
2.2 WHAT IS CARDIOVASCULAR DISEASE.....	43
2.3 ATHEROSCLEROSIS.....	44
2.3.1 Stages of atherosclerosis	44
2.3.2 The process of plaque development	47
2.3.3 Plaque vulnerability and rupture	48
2.3.4 Thrombosis.....	50
2.4 AETIOLOGY	51
2.4.1 Classical risk factors.....	51
2.4.2 Emerging risk factors.....	55
2.4.3 Enviroment - Lifestyle.....	57
2.4.4 Genetic predisposition	59
3 TYPE 2 DIABETES	64
3.1 THE PANCREATIC ISLETS	64
3.2 INSULIN	64

3.3 TYPES OF DIABETES	66
3.4 PREDIABETES CONDITIONS.....	67
3.5 PATHOGENESIS OF TYPE 2 DIABETES	69
3.5.1 Insulin resistance	69
3.5.2 B cell failure.....	71
3.5.3 Risk factors	72
3.5.4 The role of genetics	73
3.6 DIABETES COMPLICATIONS	77
4 THE ‘COMMON SOIL’ HYPOTHESIS.....	78
4.1 OXIDATIVE STRESS.....	79
5. THE BIOLOGY OF AGEING.....	83
5.1 THE EVOLUTION OF AGEING	83
5.2 MOLECULAR PATHWAYS OF AGEING.....	85
5.3 CELLULAR SENESCENCE.....	87
5.4 EUKARYOTIC CELL DIVISION	88
5.5 THE END-REPLICATION PROBLEM.....	90
6. TELOMERE BIOLOGY.....	92
6.1 TELOMERE STRUCTURE.....	92
6.2 GENETICS OF TELOMERE LENGTH	94
6.3 TELOMERASE	95
6.4 TELOMERE FUNCTION.....	97
6.5 TELOMERE HYPOTHESIS IN AGEING.....	99
7. TELOMERE LENGTH IN CARDIOVASCULAR DISEASE AND DIABETES	101

7.1 TELOMERE LENGTH IN CARDIOVASCULAR DISEASE.....	101
7.2 TELOMERE LENGTH IN TYPE 2 DIABETES.....	104
7.3 MECHANISMS	105
8. GENERAL HYPOTHESIS	106
8.1 WORKING HYPOTHESES:	107
<i>II. GENERAL METHODS</i>	<i>108</i>
1. GENERAL STOCK SOLUTIONS.....	108
2. DNA EXTRACTION	109
2.1 DNA EXTRACTION FROM WHOLE BLOOD WITH THE SALTING-OUT METHOD.....	109
2.1.1 Protocol.....	109
2.1.2 Standardisation of DNA stock arrays	111
2.2 DNA EXTRACTION FROM CULTURED HUMAN CELLS.....	113
3. RNA EXTRACTION FROM CULTURED HUMAN CELLS	115
3.1 CDNA SYNTHESIS	116
4. POLYMERASE CHAIN REACTION (PCR)	117
4.1 REAL-TIME PCR.....	120
4.2 PCR FLUOROGENIC CHEMISTRIES	122
4.3 TAQMAN TECHNOLOGY APPLICATIONS	126
4.3.1 Determination of expression levels by TaqMan assays.....	126
4.3.2 TaqMan Genotyping	127
5. TAGGING SNPS – HAPLOTYPE ANALYSIS	131

5.1 GENOME VARIATION AND LINKAGE DISEQUILIBRIUM DATABASES	132
5.2 HAPLOTYPE DATA ANALYSIS.....	135
6. HUMAN CELL CULTURE	136
6.1 GROWING OF HUMAN CELLS	136
6.2 FREEZING OF HUMAN CELLS	137
6.3 MEASUREMENT OF CELL CULTURE APOPTOSIS AND NECROSIS	138
6.4 MEASUREMENT OF INTRACELLULAR REACTIVE OXYGEN SPECIES	
.....	142
<i>III. FIRST RESULT CHAPTER: “TELOMERE LENGTH MEASUREMENT” ...</i>	<i>149</i>
.....	
1. SELECTION OF A METHOD FOR QUANTITATIVE ANALYSIS OF MEAN	
TELOMERE LENGTH.....	149
2. ADPTATION OF CAWTHON’S PCR METHOD IN OUR LABORATORY	153
2.1 APPLICATION ON THE ROTORGENE MACHINE	153
2.2 OPTIMISATION OF TELOMERE AND SINGLE COPY GENE PCRS	154
2.3 METHOD OF ANALYSIS OF QUANTITATIVE PCR DATA	164
3. VALIDATION OF THE ADAPTED PCR METHOD IN OUR LABORATORY	
.....	169
3.1 QUALITY CONTROL – STANDARD CURVES.....	169
3.2 REPRODUCIBILITY OF THE METHOD	171
3.3 COMPARISON WITH THE TRADITIONAL METHOD FOR TELOMERE	
LENGTH MEASUREMENT	173

4. ADAPTION OF ABSOLUTE QUANTIFICATION OF TELOMERE LENGTH USING THE PCR METHOD.....	175
4.1 PRINCIPALS OF ABSOLUTE QUANTIFICATION USING THE PCR METHOD.....	176
4.2 OPITMISATION OF THE USE OF SYNTHESISED OLIGONUCLEOTIDENUCLEOTIDES AS CALIBRATORS	177
4.3 CALCULATIONS FOR THE ABSOLUTE TELOMERE LENGTH QUANTIFICATION.....	181
4.4 PROBLEMS IN THE APPLICATION OF THE ABSOLUTE QUANTIFICATION.....	184
5. ADAPTION OF MULTIPLEX MONOCHROME QUANTITATIVE PCR (MMQPCR) FOR TELOMERE LENGTH MEASUREMENT	187
5.1 PRINCIPLES OF THE MMQPCR METHOD	188
5.2 MMQPCR OPTIMISATION	192
5.3 VALIDATION OF MMQPCR ADAPTION	204
5.3.1 Quality Control – Standard Curves	204
5.3.2 Reproducibility of the MMQPCR method.....	206
5.3.3 Comparison with the traditional TRF method for telomere length measurement	206
<i>IV. SECOND RESULT CHAPTER: “TELOMERE LENGTH IN CARDIOVASCULAR DISEASE AND T2D DIABETES PATIENTS”.....</i>	<i>211</i>
1. TELOMERE LENGTH IN CORONARY HEART DISEASE PATIENTS.....	211
1.1 INTRODUCTION.....	211
1.2 METHODS.....	212

1.2.1	Subjects.....	212
1.2.2	Phenotypic variables.....	215
1.2.3	Measurement of leukocyte telomere length.....	215
1.2.4	Statistical analysis	216
1.3	RESULTS.....	217
1.3.1	General characteristics of study subjects.....	217
1.3.2	Age and gender differences in telomere length.....	219
1.3.3	Lifestyle-related differences in telomere length	220
1.3.4	Geographical differences in telomere length	220
1.3.5	The effect of CHD risk factors on telomere length.....	221
1.3.6	Polygenic CHD case–control differences in telomere length.....	223
1.3.7	Monogenic CHD case–control differences in telomere length.....	223
1.3.8	Overall association of CHD with telomere length / meta-analysis	226
1.4	Discussion.....	227
2.	LEUKOCYTE TELOMERE LENGTH IN TYPE 2 DIABETES PATIENTS	233
2.1	INTRODUCTION.....	233
2.2	METHODS.....	234
2.2.1	Subjects.....	234
2.2.3	Measurement of leukocyte telomere length.....	236
2.2.4	Statistical analysis	236
2.3	RESULTS.....	237
2.3.1	Study cohorts – Ethnic/geographical diversity	237
2.3.2	The effect of T2D risk factors on telomere length	241
2.3.3	Case-Control differences	244
2.4	DISCUSSION.....	247

3. LEUKOCYTE TELOMERE LENGTH IN TYPE 1 DIABTES PATIENTS...	251
4 LEUKOCYTE TELOMERE LENGTH IN CO-EXISTENCE OF CARDIOVASCULAR DISEASE AND TYPE 2 DIABETES	254
V. <i>THIRD RESULT CHAPTER: “DETERMINANTS OF SHORT TELOMERES IN CARDIOVASCULAR DISEASE AND DIABETES”</i>.....	256
1 ASSOCIATION OF FAMILY HISTORY WITH TELOMERE LENGTH	256
1.1 INTRODUCTION.....	256
1.2 METHODS.....	257
1.2.1 Subjects.....	257
1.2.2 Biochemical measurements	258
1.2.3 Measurement of leukocyte telomere length.....	259
1.2.4 Statistical analysis	259
1.3 RESULTS.....	260
1.3.1 Study cohort	260
1.3.2 Geographical differences	260
1.3.3 Case-control differences	264
1.3.4 Association of mean telomere length with classical risk factors and paternal age at birth.	266
1.4 DISCUSSION.....	268
2 ASSOCIATION OF SYSTEMIC OXIDATIVE STRESS WITH TELOMERE LENGTH.....	272
2.1 INTRODUCTION.....	272
2.2 METHODS.....	273
2.2.1 Subjects.....	273

2.2.2 Determination of plasma total antioxidant status (TAOS)	273
2.2.3 Leukocyte telomere length measurement	275
2.2.4 Statistical analysis	275
2.3 RESULTS	276
2.4 DISCUSSION	278
3. ASSOCIATION OF VARIATION IN GENES REGULATING REACTIVE OXYGEN SPECIES WITH TELOMERE LENGTH.....	282
3.1 INTRODUCTION.....	282
3.2 METHODS	286
3.2.1 Study sample	286
3.2.2 Genotyping.....	286
3.2.3 Statistical analysis	286
3.3 RESULTS	287
3.4 DISCUSSION	293
4. ASSOCIATION OF SYSTEMIC INFLAMMATION WITH TELOMERE LENGTH.....	298
4.1 INTRODUCTION.....	298
4.2 METHODS	299
4.2.1 Subjects.....	299
4.2.2 Measurement of inflammatory markers.....	299
4.2.3 Measurement of leukocyte telomere length.....	300
4.2.4 Statistical analysis	300
4.3 RESULTS.....	301
4.4 DISCUSSION.....	302

5. FACTORS DETERMING THE TELOMERE LENGTH CHANGE OVER FOLLOW UP	304
5.1 INTRODUCTION.....	304
5.2 METHODS.....	305
5.2.1 Study sample	305
5.2.2 Leukocyte telomere length measurement	305
5.2.3 Statistical analysis	306
5.3 RESULTS.....	307
5.3.1 Characteristics of T2D patients with follow up	307
5.3.2 Seven-year change in LTL.....	308
5.3.3 Determinants of longitudinal change in LTL.....	308
5.4 DISCUSSION.....	312
VI. FOURTH RESULT CHAPTER: “IN VITRO INVESTIGATION OF THE DETERMINANTS OF TELOMERE LENGTH DURING AGING”	317
1. THE EFFECT OF PRO-INFLAMMATORY CONDITIONING AND/OR HIGH GLUCOSE ON TELOMERE SHORTENING OF AGING FIBROBLASTS	317
1.1 INTRODUCTION.....	317
1.2 METHODS.....	319
1.2.1 Cell culture	319
1.2.2 Telomere length measurement	320
1.2.3 Mitochondrial DNA (mtDNA) copy number measurement	320
1.2.4 Quantification of apoptosis	326
1.2.5 Measurement of intracellular ROS content.....	326

1.2.6 Gene expression assays.....	326
1.2.7 Statistical analysis	327
1.3 RESULTS.....	329
1.3.1 General characteristics of cultures	329
1.3.2 Growth rate	331
1.3.3 Telomere length.....	334
1.3.4 MtDNA copy number per nucleus	339
1.3.5 Apoptosis and necrosis	344
1.3.6 Intracellular ROS production	344
1.3.7 Gene expression	347
1.4 DISCUSSION.....	349
1.4.1 Discussion of <i>in vitro</i> findings	349
1.4.2 <i>In vitro</i> vs. epidemiological findings.....	354
VII. GENERAL DISCUSSION	355
1. CONCLUSIONS.....	355
1.1 THE ROLE OF TELOMERE LENGTH IN CVD	355
1.2 THE ROLE OF TELOMERE LENGTH IN T2D	356
1.3 THE DETERMINANTS OF TELOMERE LENGTH.....	358
2. THE COMMON SOIL HYPOTHESIS	362
3. FUTURE WORK.....	363
4. FUTURE PERSPECTIVES IN TELOMERE RESEARCH.....	367
VIII. APPENDICES.....	368
APPENDIX I: THE EARSII GROUP	368

**APPENDIX II: THE PRIMARY DATA PRODUCED BY THE *IN VITRO*
EXPERIMENT PRESENTED IN THE FOURTH RESULT CHAPTER. 370**

***IX. REFERENCES* 375**

LIST OF TABLES

Table I-1. Genes reported to be associated with atherosclerotic vascular diseases (CHD, MI, peripheral artery disease, carotid atherosclerosis and ischemic stroke) (Roy <i>et al.</i> 2009).	62
Table I-2. Diagnosis criteria of diabetes mellitus and intermediate hyperglycemia (Report of a WHO/IDF Consultation for the definition and diagnosis of diabetes, http://www.idf.org/webdata/docs).	68
Table I-3. Genes and <i>loci</i> associated with T2D that have been most replicated (Bonnetfond <i>et al.</i> 2010).	75
Table III-1. The combinations of different primer concentrations that were used for the telomere PCR optimisation:	155
Table IV-1. Characteristics of study subjects.....	218
Table IV-2. Partial Pearson correlation coefficients of telomere length with classical risk factors.....	222
Table IV-3. Characteristics of the Caucasian type 2 diabetes (T2D) cases and controls.	240
Table IV-4. Partial Pearson correlation coefficients of age-adjusted telomere length with classical risk factors in Caucasian type 2 diabetes patients.	242
Table IV-5. Age-adjusted telomere length by sex, smoking, hypertension status, age of diabetes onset, duration of diabetes and medication use in Caucasian type 2 diabetes patients.	243
Table IV-6. Characteristics of the Caucasian type 1 diabetes (T1D) cases.....	252
Table V-1. Characteristics at recruitment in EARSII cases and controls.	261
Table V-2. Geometric mean (95% CI) of telomere length (T/S ratio) in cases and control across the Europe.....	263

Table V-3. Partial Pearson correlation coefficients of telomere length with classical risk factors.....	267
Table V-4. Mean leukocyte telomere length (LTL) in tertiles of plasma total antioxidant status (TAOS) in Caucasian type 2 diabetes patients.	277
Table V-5. Age-adjusted leukocyte telomere length and plasma total antioxidant status (TAOS) measures by the different SNP genotypes in 569 Caucasian type 2 diabetes patients.	288
Table V-6. Inflammatory markers in the study samples.	301
Table V-7. Partial Pearson correlation coefficients of age-adjusted telomere length with inflammatory markers.	302
Table V-8. Characteristics of the total of T2D cases and of the subset participating in follow up.	307
Table V-9. Partial correlation coefficients of baseline LTL and % Δ LTL with selected risk factors.	309
Table V-10. Differences in baseline LTL and % Δ LTL by medication and T2D complications.....	311
Table VI-1. Percentage changes in mean telomere length and mtDNA copies per nucleus over the time of culture (days) or cell divisions occurred during the experiment (CPD). The primary experimental data on these parameters are presented in Appendix II (page 370).....	343

LIST OF FIGURES

Figure I-1. Percentage of deaths by cause in Europe for 2007 (British Heart Foundation (BHF) statistics 2007, www.bhf.org.uk).....	37
Figure I-2. Percentage of all-cause mortality attributable to diabetes by age and sex in Europe for 2010 (IDF Diabetes Atlas, Fourth Edition 2009, www.diabetesatlas.org)...	39
Figure I-3. The stages of atherosclerosis (Lusis <i>et al.</i> 2004).	46
Figure I-4. The development of an atherosclerotic plaque progressively from left to right (Sanz & Fayad 2008).	49
Figure I-5. Models representing the mechanism by which common polymorphisms influence the susceptibility to a complex disorder such as atherosclerosis (Hingorani 2001).	60
Figure I-6. The insulin-glucagon balanced regulation of glucose (Diabetes Atlas 4 th edition, IDF 2009, www.diabetesatlas.org).....	65
Figure I-7. Fatty acid- and age-induced insulin resistance in: A) skeletal muscle cells and B) liver cells.	70
Figure I-8. Negative regulation of ROS by activation of UCP2 (Krauss <i>et al.</i> 2005)....	81
Figure I-9. Theories for the evolution of biological ageing. A) The theory of programmed senescence-associated ageing, B) The theory of natural selection shadow in later life, C) The theory of antagonistic pleiotropy, D) The disposable soma theory (Kirkwood & Austad 2000).....	84
Figure I-10. The cell cycle (University of Leicester, Genetics Education Networking for Innovation and Excellence, Virtual Genetics Education Centre, http://www.le.ac.uk/ge/genie/vgec/he/cellcycle.html).....	89

Figure I-11. The replication of DNA in eukaryotic linear chromosomes (Reactome, Telomere maintenance in Homo Sapiens http://www.reactome.org/cgi-bin/eventbrowser?DB=gk_current&ID=157579).....	91
Figure I-12. Schematic presentation of telomeres (Salpea & Humphries 2010).....	93
Figure I-13. Telomerase-mediated replication (University Medical Center Hamburg-Eppendorf, Department of Internal Medicine, www.uke.de/kliniken/medizinische-klinik-1/images_content/klinik-med-I/Telomerase_Abb2.jpg)......	96
Figure I-14. The telomere hypothesis of cellular senescence and immortalization (Royle <i>et al.</i> 2009).....	98
Figure I-15. Schematic presentation of LTL decrease with age in CHD cases (solid line) and controls (dashed line). The double line illustrates the biological age gap between cases and controls.	103
Figure II-1. Schematic presentation of polymerase chain reaction (Source: Florida museum of natural history website, http://www.flmnh.ufl.edu/cowries/amplify.html).	118
Figure II-2. Schematic presentation of the fluorescence signal during real-time PCR.	121
Figure II-3. TaqMan principle (source: (Koch 2004))......	124
Figure II-4. Allelic discrimination plot.	130
Figure II-5. An example of Haploview linkage disequilibrium plot with a selected set of tagging SNPs.	133
Figure II-6. A) Cells from the same flask with (on the left) and without (on the right) Annexin V-Fluorescein labeling. The cells shifted into the gate R1 are Annexin V-Fluorescein positive i.e. apoptotic cells. B) Cells from the same flask with (on the left) and without (on the right) PI labeling. The cells shifted into the gate R2 are PI positive i.e. necrotic cells.	140

Figure II-7. Plots of FL1 against FL2 showing the distribution of the cells according to their fluorescent signals. The left plot shows cells which have not been stained, and the right plot shows cells with the double staining of Annexin V-Fluorescein and PI.	142
Figure II-8. Measurement of cellular ROS with H ₂ DCFDA.....	144
Figure II-9. FL2-to-FL1 plot of cells: a) without staining, b) with double staining of Annexin V-Fluorescein staining and PI. In panel b, the cells at the bottom left quadrante are not stained with either probe, thus these are the viable cells, while the cells shifting to the lower right or the two upper quadrantes are apoptotic or necrotic. The viable cells in the lower left quadrante of panel b were gated (R3) and only these were then used for the ROS measurement.	146
Figure II-10. a) Plot showing the cells shift on the FL1 axis due to the green fluorescence emission from the H ₂ DCFDA dye oxidation by intracellular ROS . b) Histogram of the fluorescence emitted by cells with oxidised H ₂ DCFDA dye.	148
Figure III-1 A) Hybridisation of telomere primers to genomic telomere sequences. B) Possible hybridisation of telomere primers to each other.	151
Figure III-2. A) The amplification plot generated from the telomere PCR when testing the primer combinations of table 1. B) Amplification plot showing only the duplicate and the NTC of the 135nM / 900nM primer combination.	156
Figure III-3. A representative amplification plot of the optimised telomere PCR.	157
Figure III-4. Melting curve of telomere PCR product.	159
Figure III-5. A) The amplification plot of <i>36B4</i> PCR. B) The amplification plot of <i>GAPDH</i> PCR.	161
Figure III-6. A) Melting curve of <i>36B4</i> PCR product. B) Melting curve of <i>GAPDH</i> PCR product.....	162

Figure III-7. Linear regression graph between the telomere length estimates of the same 10 samples measured on two consecutive days.....	163
Figure III-8. Plot of the second derivative of the amplification.	167
Figure III-9. Standard curves of A) Telomere PCR and B) SCG (<i>36B4</i>) PCR.....	170
Figure III-10. Linear regression graph between the telomere length estimates of the same 10 samples measured on two consecutive days ($R^2=0.79$, $p=0.001$).....	172
Figure III-11. Correlation of the PCR-based method with the conventional TRF analysis.....	174
Figure III-12. Telomere PCR standard curve with a dilution series (2.4 - 0.01875 pg/ μ l, two-fold dilution, eight points) of the synthesised 84 bp oligonucleotide.....	178
Figure III-13. SCG PCR standard curve with a dilution series (0.0032 - 0.000025 pg/ μ l, two-fold dilution, eight points) of the synthesised 75 bp oligonucleotide.....	179
Figure III-14. Melting curves including the synthesised calibrators and DNA samples of: A) the telomere PCR products and B) the SCG PCR products.....	180
Figure III-15. Melting curves of FH DNA samples and the synthesised calibrators of: A) Telomere PCR products and B) SCG PCR products.....	185
Figure III-16. A) Hybridisation of new telomere primers to genomic telomere sequences. B) Extension of a fixed-length PCR product initiated by the new telomere primers. C) Hybridisation of new telomere primers to each other.	191
Figure III-17. DNA samples run with and without extra SYBR Green added in their PCR reaction mix. A) Second derivative of the amplification from the channel collecting the telomere PCR fluorescence. B) Second derivative of the amplification from the channel collecting the SCG PCR fluorescence. C) Melting curve of the multiplex PCR products. The melting profile of the MMQPCR consists of two curves of which, the one at lower temperatures corresponds to the melting of the shorter, telomere	

PCR product, and the other at the higher temperatures corresponds to the longer SCGs products.....	193
Figure III-18. DNA samples run with ALB or HBG as SCG. A) Second derivative of the amplification from the channel collecting the SCG PCR fluorescence. Samples with ALB and HBB as SCGs are included. B) Second derivative of the amplification from the channel collecting the SCG PCR fluorescence. Samples with HBB only as SCGs are included. C) Melting curve of the multiplex PCR products including samples with ALB and HBB as SCGs. D) Melting curve of the multiplex PCR products including only samples with HBB as SCGs.	195
Figure III-19. Amplification and melting profiles of the MMQPCR products with: A) Cycling conditions as suggested by Cawthon. B) Cycling conditions with higher annealing temperatures.....	197
Figure III-20 Linear regression graphs between the telomere length estimates (T/S ratios) of the same 19 DNA samples measured on two consecutive days. A) Cycling conditions as suggested by Cawthon. B) Cycling conditions with higher annealing temperatures.	199
Figure III-21. A) Amplification signal of the telomere MMQPCR in channel (A), B) Amplification signal of the HBB (SCG) MMQPCR in channel (B), and C) Melting profile of both the MMQPCR products.	203
Figure III-22. Standard curves of A) Telomere PCR and B) SCG (<i>HBB</i>) PCR.....	205
Figure III-23. Correlation of the MMQPCR with the conventional TRF analysis.....	208
Figure III-24. Correlation of the MMQPCR with the original qPCR method.	209
Figure IV-1. Decrease of telomere length with age in each study sample.....	219
Figure IV-2. Comparison of mean leukocyte telomere length (kb) between North and South of Europe in HIFMECH study.....	221

Figure IV-3. Comparison of telomere length between CHD cases and controls.	225
Figure IV-4. Odds ratio (OR) for CHD when having LTL in the lowest tertile / meta-analysis.....	226
Figure IV-5. Color-illustrated age-standardised mortality from CVD among men of the age group 45–74 years in Europe (Muller-Nordhorn <i>et al.</i> 2008) and age-adjusted mean LTL (kb) in each of the four recruitment centers (Stockholm, Sweden; London, UK; Marseille, France; San Giovanni Rotondo, Italy) in HIFMECH.....	229
Figure IV-6. Correlation between telomere length and duration of statin use in FH patients.	232
Figure IV-7. Ethnic differences in mean age-adjusted leukocyte telomere length (LTL) of the type 2 diabetes patients.	239
Figure IV-8. The correlation of telomere length (T/S ratio) with age in Caucasian type 2 diabetes patients.....	241
Figure IV-9. Type 2 diabetes case-control differences in mean age-adjusted leukocyte telomere length (LTL).....	245
Figure IV-10. A) The odds ratio of type 2 diabetes for one standard deviation decrease in age-adjusted telomere length when comparing the cases with i) the HIFMECH controls, ii) the EARSII controls and iii) the combined controls. B) The odds ratio of type 2 diabetes for each tertile of age-adjusted telomere length when comparing the cases with the combined controls.	246
Figure IV-11. Type 1 and type 2 diabetes case-control differences in mean age-adjusted leukocyte telomere length (LTL).....	253
Figure IV-12. The odds ratio of coronary heart disease for each tertile of age-adjusted telomere length among patients with type 2 diabetes.	255

Figure V-1. Distribution of leukocyte telomere length in each European region for the combined cohort.	262
Figure V-2. Distribution of telomere length in each European region for the cases and the controls.	265
Figure V-3. The correlation of age-adjusted telomere length (T/S ratio) with plasma total antioxidant status (TAOS) in Caucasian type 2 diabetes patients.	276
Figure V-4. The mean age-adjusted telomere length in tertiles of plasma total antioxidant status (TAOS) measures in Caucasian type 2 diabetes patients. (The error bars represent 95% confidence intervals).	277
Figure V-5. Proposed mechanism in cardiovascular disease and type 2 diabetes.....	281
Figure V-6. The mean age-adjusted telomere length in Caucasian type 2 diabetes patients carrying or not the <i>UCP2</i> -866 G>A variant (The error bars represent 95% confidence intervals).....	292
Figure V-7. Proposed mechanism.....	297
Figure V-8. Correlation graph of baseline LTL with % Δ LTL (LN change).	310
Figure V-9. Correlation graph of CRP with % Δ LTL (LN change).....	310
Figure VI-1. A) Mitochondrial single copy gene (<i>MTND1</i>) PCR standard curve. B) Genomic single copy gene (<i>36B4</i>) PCR standard curve.	323
Figure VI-2. Linear regression between measurements of mtDNA copy number measurement with the quantitative PCR in 16 samples acquired on two consecutive days ($R^2=0.52$, $p=0.002$).	325
Figure VI-3. Microscope pictures of cultures, after 62 days of treatment in each of the experimental conditions.	330

Figure VI-4. The cumulative population doublings (CPD) over the time of culture in each treatment (growth rate). A) In pooled data from all four donors, B) In each of the four donors separately.	332
Figure VI-5. The shortening of mean telomere length over time of culture in each treatment. A) In pooled data from all four donors, B) In each of the four donors separately.	336
Figure VI-6. The shortening of mean telomere length over the number of cell divisions occurring during the experiment, as reflected by the cumulative population doublings (CPD), in each treatment.	338
Figure VI-7. The change in the number of mitochondria per cell, as reflected by the copy number of mtDNA per nucleus, over time in each of the treatments. A) In pooled data from all four donors, B) In each of the four donors separately.	340
Figure VI-8. The change in the number of mitochondria per cell, as reflected by the copy number of mtDNA per nucleus, over the number of cell divisions occurred during the experiment [cumulative population doublings (CPD)] in each treatment.	342
Figure VI-9. The percentage of cells at any stage of apoptosis or necrosis in each treatment after 7 days of treatment.	345
Figure VI-10. The intracellular ROS content of viable cells in each treatment after 7 days of treatment.	346
Figure VI-11. The change in <i>TFAM</i> expression levels after 45 days of treatment in each of the five conditions.	348
Figure VII-1. Mean leukocyte telomere length plotted against mean age in each of the study samples employed in the present thesis.	359

LIST OF ACRONYMS

36B4 or RLP0: acidic ribosomal phosphoprotein PO

ACE: Angiotensin I-converting enzyme

ACTB: beta actin

ALB: albumin

ApoE: Apolipoprotein E

BHF: British heart foundation

BMI: Body mass index

BP: Blood pressure

BSO: L-buthionine-[S,R]-sulphoximine

CABG: Coronary artery bypass grafting

CASIS: Coronary artery surgery inflammation study ()

CEPH: Centre d'Etude du Polymorphisme Humain DNA samples in HapMap

CHB: Chinese DNA samples in HapMap

CHD: Coronary heart disease

CI: Confidence intervals

CPD: cumulative PD

CQ: comparative quantification

CRP: C-reactive protein

CVD: Cardiovascular disease

CYBA: Cytochrome b-245 alpha subunit

DBP: Diastolic blood pressure

DMSO: dimethylsulfoxide

DTT: Dithiothreitol

EARSII: European atherosclerosis research study II

EDTA: Ethylenediaminetetraacetic acid

FCS: Foetal calf serum

FGM -AA: fibroblast growth medium lacking ascorbic acid

FH: Familial hypercholesterolaemia

FH-RF: FH study recruited from the Royal Free Hospital, London

FH-SB: Simon Broome Familial Hyperlipidaemia Register Group and Scientific Steering Committee study.

GAPDH: glyceraldehydes-3-phosphate dehydrogenase

GLUT4: glucose transporter member 4

GPX: glutathione peroxidase

GPX1: Glutathione peroxidase 1

GVS: Genome variation server

HBA1c: hemoglobin A1c or glycosylated hemoglobin

HBB: hemoglobin beta

HDL: High density lipoprotein

HIFMECH: Hypercoagulability and impaired fibrinolytic function mechanisms predisposing to myocardial infarction study.

HRM: High resolution melt

IDF: International diabetes federation

IFN γ : Interferon γ

IGF-1: Insulin growth factor 1

IL1: Interleukin 1

IL1B: Interleukin 1 beta

IL6: Interleukin 6

IQR: Inter-quartile range

JPT: Japanese DNA samples in HapMap

KCNJ11: potassium channel, inwardly rectifying, subfamily J, member 11

LDL: Low density lipoprotein

LOD: logarithm of odds score for linkage disequilibrium

Lp(α): Lipoprotein α

LTL: Leukocyte telomere length

M-CSF: macrophage colony-stimulating factor

MI: Myocardial infarction

MMP: Matrix metalloproteinases

MMQPCR: Multiplex monochrome quantitative PCR

MNSOD: Manganese superoxide dismutase

mtDNA: Mitochondrial DNA

MTND1: Mitochondrial subunit 1

NHDF: Normal human dermal fibroblasts

NO: Nitric oxide

NTC: no-template controls

P: p value

PAI-1: Plasminogen activator inhibitor 1

PBS: Phosphate buffered saline

PCR: Polymerase chain reaction

PD: population doublings

PGI₂: Prostacyclin

PI: propidium iodide

PI3K: phosphoinositide 3-kinase

PPARG: peroxisome proliferator-activated receptor-gamma

qPCR: quantitative polymerase chain reaction

ROS: Reactive oxygen species

SBP: Systolic blood pressure

SCG: Single copy gene

SD: standard deviation

SE: standard error

SMC: Smooth muscle cells

SOD: superoxide dismutase

T/S ratio: relative concentration of Telomere repeats / relative concentration of Single copy gene copies

T1D: Type 1 diabetes

T2D: Type 2 diabetes

TAOS: total antioxidant status

TC: total cholesterol

TCF7L2: transcription factor 7-like 2

TE: Tris-EDTA

TERC: Telomerase RNA component

TERT: Telomerase reverse transcriptase

TFAM : mitochondrial transcription factor A

TGF β : transforming growth factor β

TNF α : Tumor necrosis factor α

TNS: trypsin inhibitor

TOR: target of rapamycin

TRF: terminal restriction fragment

TRF1: telomeric repeat-binding factor 1

TRF2: telomeric repeat-binding factor 2

TRL: triglyceride-rich lipoprotein

UBC: ubiquitin C

UCP2: uncoupling protein 2

UDACS: University College London diabetes and cardiovascular disease study

VCAM-1: vascular cell adhesion molecule 1

WHO: World health organisation

WOSCOPS: West of Scotland primary prevention study

XRCC1: X-ray repair, complementing defective in Chinese hamster 1

YRI: Yoruban (West African) DNA samples in HapMap

Δ LTL: LTL change

I. INTRODUCTION

1. IMPACT

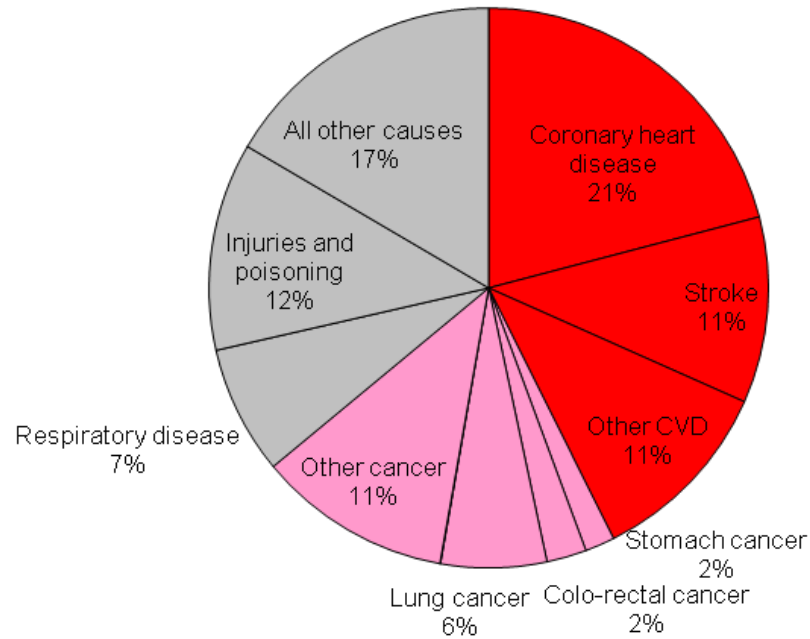
1.1 IMPACT OF CARDIOVASCULAR DISEASE

The years following World War II cardiovascular disease (CVD) replaced infectious diseases as the leading cause of deaths. Today more people worldwide die from the complications of CVD than from any other cause. According to the World Health Organization (WHO), 17.1 million people died from CVD in 2004, representing 29% of all global deaths. An estimated 7.2 million of these deaths were due to coronary heart disease (CHD) and 5.7 million were due to stroke. By 2030 another 23.6 million people are expected to die from CVD (WHO, Fact sheet on cardiovascular disease, www.who.int).

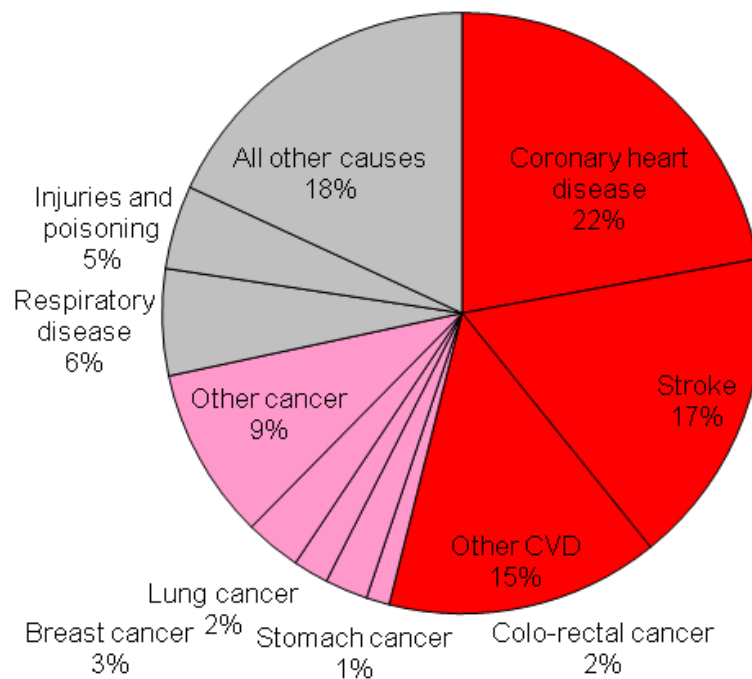
More than 190,000 deaths in the United Kingdom (UK), a third of all deaths, were caused by CVD in 2007. CVD is also a major cause of premature death (death before the age of 75) accounting for almost a third (29%) of premature deaths in men and over a fifth (21%) in women (British Heart Foundation (BHF) statistics 2007, www.bhf.org.uk). The main components of CVD are CHD and stroke. Around half of all CVD deaths are from CHD and about a quarter from stroke. CHD, by itself, is UK's number one killer and the most common cause of premature death, with approximately 2.6 million people in the country currently suffering from CHD (BHF, UK CHD statistics 2009-10, www.bhf.org.uk). This is illustrated for Europe in figures 1A and 1B.

Figure I-1. Percentage of deaths by cause in Europe for 2007 (British Heart Foundation (BHF) statistics 2007, www.bhf.org.uk).

A) In men.



A) In women.



Medical care of CVD patients is costly and usually prolonged. By itself the care of CHD patients costs the health system of UK around £3.2 billion a year (British Heart Foundation, UK CHD statistics factsheet 2009-10, www.bhf.org.uk). Nonetheless, estimating the costs of CVD to the health care system underestimates the total cost to the society's resources. CVD affects people in their peak mid-life years, disrupting the future of the families dependent on them and depriving the society of a highly productive and experienced working force (International Cardiovascular Disease Statistics of the American Heart Association, www.americanheart.org).

1.2 IMPACT OF DIABETES

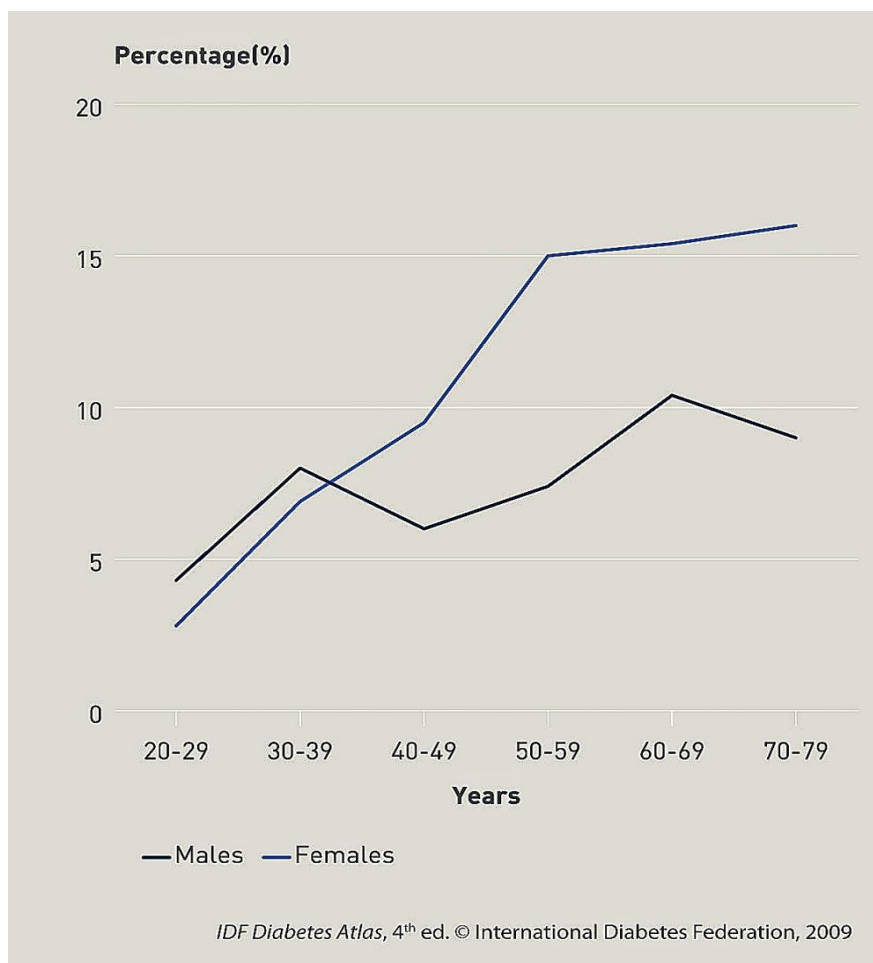
According to the International Diabetes Federation (IDF) estimates, 285 million people worldwide have diabetes and this number is expected to reach 438 million people by 2030, corresponding to the 7.8% of the adult population (IDF Diabetes Atlas, Fourth Edition 2009, www.diabetesatlas.org). The increasing prevalence and severity of diabetes creates one of the most challenging health problems of our century

In the UK around 1.9 million people have been diagnosed with diabetes and another 600,000 people are estimated to have undiagnosed diabetes. The prevalence of diabetes has been continuously increasing also in the UK, as in most countries around the world, with estimates reaching 3 million people by 2010 (British Heart Foundation, UK CHD statistics factsheet 2009-10, www.bhf.org.uk).

Diabetes impact on society is very significant. Approximately four million deaths in the 20-79 age group are attributable to diabetes in 2010, accounting for 6.8% of global all-cause mortality in this age group. These deaths are expected to double between 2005 and 2030. For Europe, the mortality percentages attributable to diabetes

are shown in figure 2. While the cost of diabetes to the healthcare systems around the world is estimated to be very high (around 376 billion US Dollar in 2010), the largest economic and social burden is associated with disability and loss of life as a result of the disease itself and its related complications (IDF Diabetes Atlas, Fourth Edition 2009, www.diabetesatlas.org).

Figure I-2. Percentage of all-cause mortality attributable to diabetes by age and sex in Europe for 2010 (IDF Diabetes Atlas, Fourth Edition 2009, www.diabetesatlas.org).



Despite the significant advances in the prevention and treatment of CVD and diabetes in recent years, these still represent the prime health problems around the globe with immense impact on society's prosperity, rendering the need for deeper understanding of their pathology and improvement in their prevention an urgent issue.

2 CARDIOVASCULAR DISEASES

2.1 THE CARDIOVASCULAR SYSTEM

The cardiovascular system consists of the heart, the vessels and the blood. Its main function is to transport and distribute essential substances, such as oxygen, nutrients, water and electrolytes, to all tissues and to remove byproducts of metabolism. The cardiovascular system also serves homeostatic mechanisms such as the regulation of body temperature and humoral communication among tissues and organs (Robert M. Berne 1993a).

2.1.1 The heart

The human heart is a muscular pump serving two distinct blood circulations, the pulmonary circulation, where the blood is impelled towards the lungs for the exchange of oxygen and carbon dioxide, and the systemic circulation, where the blood is impelled towards all other body tissues. The interior of the heart is divided into four chambers, two atria and two ventricles. The atria are responsible for receiving blood from the veins leading to the heart and in turn they deliver the blood into the ventricles. During contraction the ventricles pump the blood out of heart with enough pressure in order to pass through all body tissues and return back to heart. The heart valves are responsible for the unidirectional blood flow (Robert M. Berne 1993a).

2.1.2 The systemic circulation

The systemic circulation is an extended network of vessels, which consists of a series of distributing and collecting large vessels and an extensive system of thin vessels with capillary endings which allow the exchange of substances between the intracellular

matrix of tissues and the blood. The blood is pushed away from the heart through the aorta and its arterial branches. These are progressively divided into smaller arteries and even thinner vessels the arterioles which eventually end in capillaries. The blood from the capillaries then flows into thin vessels called venules, which drain into larger vessels, the veins. The veins progressively increase in size, until the blood is transferred back to heart into the right atrium.

A special part of the systemic circulation is the coronary circulation, a network of vessels, which supply with blood the myocardium. The right coronary artery supplies blood principally to the right atrium and ventricle, and the left coronary the left atrium and ventricle with a partial overlap. The blood from the heart tissues is mainly collected by the coronary sinus which returns the blood to the right atrium. Another special circulation, again part of the systemic, is the cerebral circulation, which distributes blood to the brain tissues. The vertebral arteries in conjunction with branches of the internal carotid artery form a network called the circle of Willis, which supplies the brain with blood (Robert M. Berne 1993a).

2.1.3 The vascular wall

The vascular wall consists of three distinct layers, which from the inner to the outer are the intima, the media, and the adventitia. These layers are separated by two elastic laminae. The intima is mainly composed of a single layer of endothelial cells facing the lumen and a small amount of sub-endothelial connective tissue. The neighbouring endothelial cells are connected with tight junctional complexes. The endothelium forms a barrier between the blood and the arterial wall and is a dynamic cellular layer regulating a number of functions such as vascular tone, leukocyte adhesion and thrombosis. The media is the thickest layer which provides structural

support and consists of multiple layers of smooth muscle cells (SMC) held together by an extracellular matrix, consisting mainly of elastic fibres, collagen, and proteoglycans. The adventitia is composed of a loose matrix of SMC, fibroblasts, collagen and elastin. In the adventitia are located vessels nourishing the vascular wall tissues (vasa vasorum) and autonomic nerves (nervi vasorum) (M. C. Stuhlinger 2003).

The walls of arteries are thicker than that of veins in order to withstand the higher blood pressure (BP). The arterial thickness and the media composition depend on the location, size and function of the artery. For example in large arteries, the media is abundant in elastic fibres, while in medium-sized arteries the media is abundant in SMCs (M. C. Stuhlinger 2003).

2.2 WHAT IS CARDIOVASCULAR DISEASE

Cardiovascular disease is an umbrella term for all diseases of the heart and blood vessels. The two main diseases in this category are CHD, with the end points of angina and myocardial infarction (MI), and cerebrovascular disease, with the end point of stroke. Moreover, CVD includes peripheral artery disease, rheumatic heart disease and congenital heart disease. CHD, cerebrovascular disease and peripheral artery disease are diseases of the blood vessels, mainly caused by the development of plaques on their inner wall. This process is described as atherosclerosis. The plaques eventually lead to a blockage of the arteries supplying blood to the heart and brain, which is the most common reason for MIs and strokes, respectively. MIs and strokes are usually acute events, which often cause either fatality or permanent disability (WHO, cardiovascular disease, www.who.int).

2.3 ATHEROSCLEROSIS

Atherosclerosis is a chronic vascular disease of medium and large arteries. During atherosclerosis a plaque is formed in the inner vascular wall resulting in the thickening and remodelling of the wall which obstructs the blood flow. These plaques are often vulnerable and therefore may rupture, trigger thrombosis and lead to an occlusion of the artery. Depending on its location, the plaque formation in the vascular wall can lead to ischemia or infarction of the heart, brain, or extremities (Ross 1999).

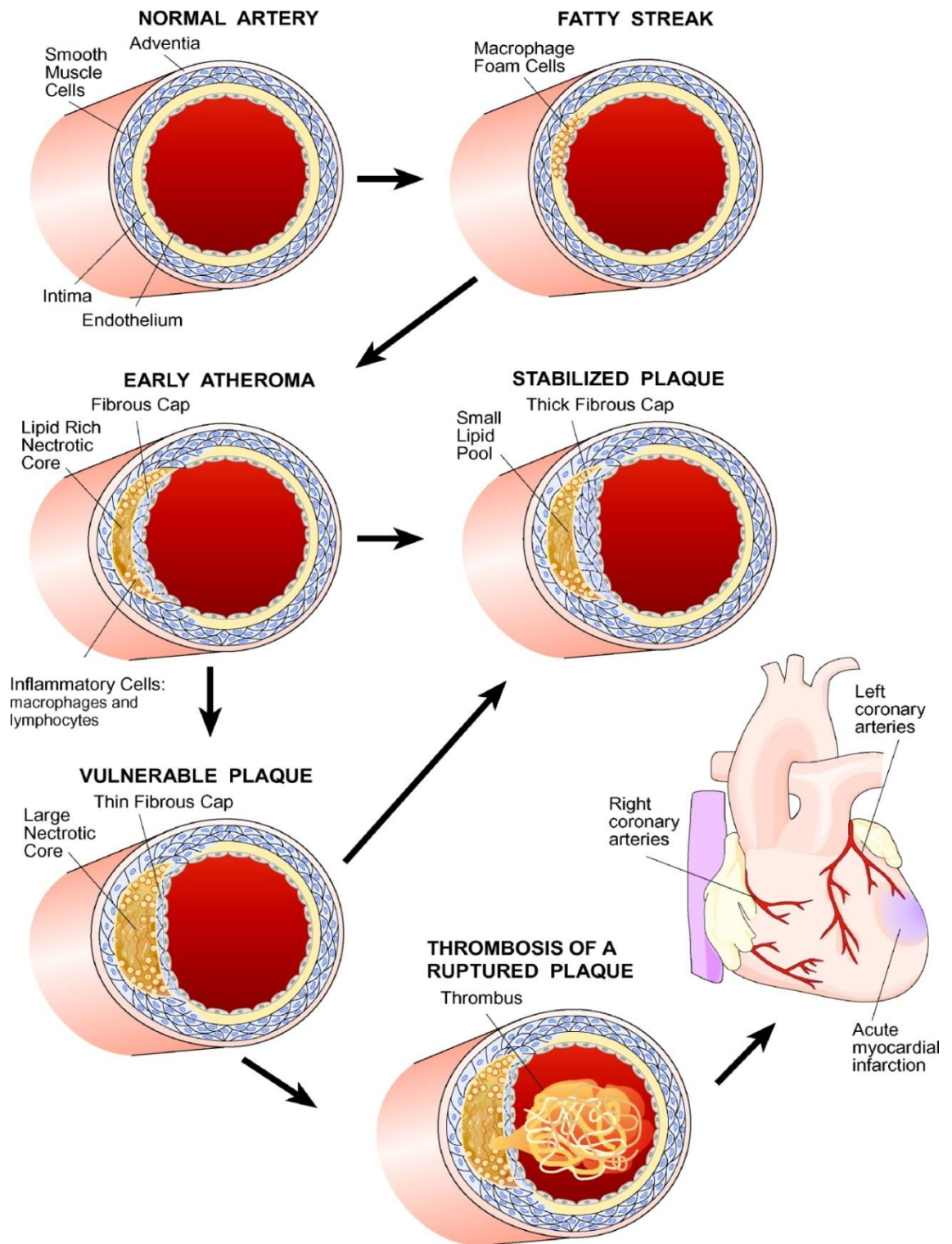
The process of atherosclerosis, from a physiological point of view, aims at protecting the endothelium and SMC of the vascular wall from all kinds of insults [e.g. mechanical, injury, toxins, viruses, oxidised low density lipoprotein (LDL)]. Essentially, it is an inflammatory response accompanied by the formation of fibro-fatty lesions at the site of endothelial damage. When this response is excessive, it becomes a disease which may occlude the artery (Ross 1993).

2.3.1 Stages of atherosclerosis

The development of atherosclerosis begins with the formation of the “fatty streaks”, the earliest recognisable lesions. These lesions consist of accumulated lipid-rich macrophages, called foam cells, under the endothelium, in the intima layer of the vascular wall. In the next stage, a lipid-rich necrotic core is built-up, which is surrounded by SMCs and covered by a fibrous cap. Monocytes and T lymphocytes, some activated, also participate in the composition of the atherosclerotic lesions. The fibrous plaques increase in size and can develop in different ways. In some cases calcification, haemorrhages into the lesion, ulcers at the luminal surface, or projection into the lumen may occur. The increasing volume of the plaque may partially block the blood flow and cause ischemia. However, the most crucial point into the development

of those atherosclerotic plaques is whether they will evolve into stable plaques with a small lipid-rich necrotic core, or in vulnerable plaques with a large lipid-rich necrotic core and thin fibrous cap. These vulnerable plaques may rupture and result in a formation of a thrombus and the subsequent occlusion of the artery (Ross 1993; Lusis *et al.* 2004) (Figure 3).

Figure I-3. The stages of atherosclerosis (Lusis *et al.* 2004).



2.3.2 The process of plaque development

The endothelium has a major role in the maintenance of vascular homeostasis. Although a single-cell layer, it is involved in a number of important functions. 1) It regulates the vascular tone by releasing key molecules such as nitric oxide (NO) and endothelin, 2) regulates the exchange of substances and cells with the circulation, and has the ability to modify (oxidise) lipoproteins during their transportation into the vascular wall 3) participates to the inflammatory response, by producing growth factors and cytokines and controlling the adhesion of leukocytes, 4) controls thrombogenesis and 5) plays an important role in vascular remodelling. Thus, endothelial damage and/or dysfunction triggers a number of processes initiating or intensifying the formation of atherosclerotic lesions (Ross 1993; Luscher & Barton 1997).

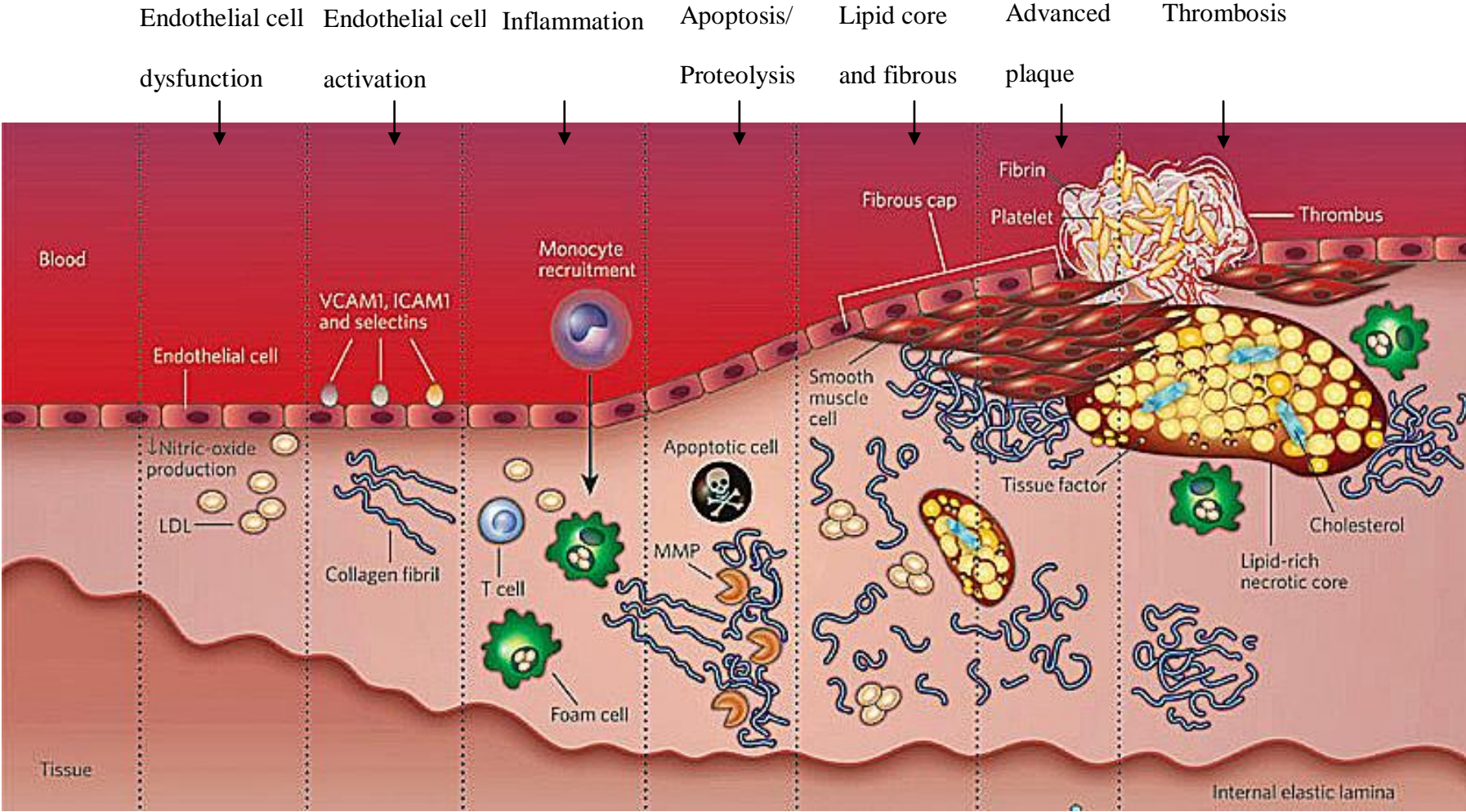
A prime event in the initiation of the atherosclerotic process is the diffusion through the endothelium and accumulation in the intima of lipoprotein particles, mainly LDL, but also lipoprotein remnants as well as lipoprotein a [Lp(a)]. When transferred, these lipoproteins can be oxidised, if not being oxidised already, and become pro-inflammatory. A molecule having a substantial contribution to the oxidation of LDL is the endothelial derived nitric oxide (NO). Subsequently, as part of an inflammatory response, the endothelial cells project specific adhesive glycoproteins on their surface, such as the vascular cell adhesion molecule-1 (VCAM-1)], which attach to circulating monocytes and T lymphocytes and facilitate their transfer into the intima. The endothelial cells also secrete growth factors with the macrophage colony-stimulating factor (M-CSF) being the most important among them. Thus, the trapped monocytes proliferate and differentiate into macrophages, which then take up the accumulated oxidised LDL and become foam cells. The foam cells, as well as the T cells, produce cytokines and growth factors [e.g. interleukin 1 (IL-1), tumour necrosis factor α

(TNF α), transforming growth factor β (TGF β) and interferon γ (IFN γ)], which activate the migration of SMC to the intima, their proliferation and the secretion of collagen. The secreted collagen builds up to form the fibrous cap. The cholesterol-rich foam cells and the accumulated SMC are eventually led to apoptosis and necrosis, contributing to the enlargement of the lipid-rich necrotic core of the plaque. From then on, continuing cell and lipid influx, accompanied by SMC migration to the intima and collagen secretion, leads to advanced fibrous plaques (Ross 1993; Lüscher *et al.* 2004) (Figure 4).

2.3.3 Plaque vulnerability and rupture

The rupture of a plaque, with the concomitant formation of a thrombus resulting in the occlusion of the artery, depends predominantly on the vulnerability of the plaque rather than its size. The stability of the plaque is determined by the proportion of the fibrous cap to the lipid-rich necrotic core. Vulnerable plaques have thin fibrous caps, large lipid-rich necrotic cores and a high concentration of inflammatory cells and molecules (Davies *et al.* 1993). The development of a stable fibrous cap requires SMC proliferation and production of extracellular matrix including collagen. Thus, a weak fibrous cap is primarily a result of SMC loss due to early apoptosis (Clarke *et al.* 2006). T lymphocytes and macrophages also contribute to the weakening of the fibrous cap. The T lymphocytes produce IFN γ , which inhibits the production of matrix by SMCs, and the macrophages produce matrix metalloproteinases (MMPs), that degrade SMC matrix and eventually lead to the rupture of the fibrous cap. Thus, particularly inflamed plaques tend to have thinner caps and are more likely to rupture. Other factors and characteristics of the plaque like intimal calcification, ulceration, neovascularisation and haemorrhages into the plaque, also contribute to its vulnerability and rupture (Lüscher *et al.* 2004) (Figure 4).

Figure I-4. The development of an atherosclerotic plaque progressively from left to right (Sanz & Fayad 2008).



2.3.4 Thrombosis

The endothelium plays a critical role in both the thrombotic and coagulant activities. It secretes antithrombotic molecules like NO and prostacyclin (PGI₂) and binds factors preventing coagulation. In addition, the endothelial cell production of plasminogen activator and urokinase regulate the balance between coagulation and fibrinolysis (Ross 1993). On the other hand, when the endothelial cells are exposed to oxidised LDL, they secrete tissue factor, a key protein in the initiation of the coagulation cascade and plasminogen activator inhibitor 1 (PAI-1) which prevents fibrinolysis (Drake *et al.* 1989; Latron *et al.* 1991). In this way, when a plaque ruptures, the pro-thrombotic tissue factor and the anti-fibrinolytic PAI-1 are exposed to the blood from the circulation resulting in thrombus formation. In the majority of cases, the thrombus is lysed and the fracture in the artery resealed, although this leads sometimes to an enlargement of the plaque at that site, and only in a small portion of cases the formation of the thrombus results in total occlusion of the artery (Libby 2008). However, thrombosis constitutes the cause of most of the acute manifestations of atherosclerotic disease. The majority of thromboses results from the disruption of the plaque's fibrous cap, which occurs usually in plaques causing 50% or less stenosis of the artery. Because of the critical role of the disruption of fibrous cap in triggering artery thrombosis, factors determining the vulnerability of fibrous cap (as described in the above paragraph), have attracted a great research interest (Libby 2000).

2.4 AETIOLOGY

Atherosclerosis is a complex multi-factorial disease of the arteries resulting from the interactions of various environmental factors with the genetic background of each individual (Roy *et al.* 2009). Dyslipidemia, hypertension, and diabetes mellitus are well-established risk factors for CVD. Nevertheless, there are several other traditional and emerging risk factors contributing to the risk of developing CVD.

2.4.1 Classical risk factors

Age: There is undoubtedly a strong and independent contribution of age to the occurrence of atherosclerotic CVD. Multivariate analysis of the prospective data in the Framingham study shows the independent effect of age on CVD incidence, taking all the major risk factors into account. The effect of age on CVD risk was evident even in subjects at the low risk category by current risk factor guidelines, pointing out the substantial contribution of age to an individual's risk for CVD (Kannel & Vasani 2009a). CVD is a disease of maturity related to tissue deterioration with age. The concept of tissues' biological ageing in CVD is discussed in more detail in chapter 5 of the "Introduction" (page 83).

Gender: For many years now, it has become clear that men are more prone to CVD than women, especially prior to menopause. This results in the delay of CHD onset in women by approximately 10-15 years compared to men, and the greater life expectancy in women, which is on average 81 years compared to the 74 years in men. However, menopause is considered as the marker for the end of natural protection against atherosclerotic CVD (Brochier & Arwidson 1998), suggesting that female hormones play a protective role against the development/onset of atherosclerosis.

Lipid disorders: Hypercholesterolaemia (total cholesterol >5 mmol/l and/or LDL cholesterol >3.0 mmol/l, according to WHO Guidelines for assessment and management of cardiovascular risk 2007, www.who.int) is acknowledged as the major risk factor for atherosclerosis progression and a powerful predictor of premature CVD manifestations. Several large studies have shown the significant benefit of cholesterol reduction, in particular LDL cholesterol, in primary and secondary prevention. The cholesterol-rich, small dense LDL particles are highly atherogenic as a result of their prolonged plasma half-life and low resistance to oxidative stress. These LDL particles, upon entrance in the arterial intima, get oxidised and are consequently taken on by macrophages, which constitutes a trigger for the initiation and exacerbation of the atherosclerotic process (Chapman *et al.* 1998).

Another frequent form of lipid disorder, with a recently established association with CVD risk, is elevated plasma concentrations of triglyceride-rich lipoproteins (triglyceride plasma levels >2 mmol/l, according to WHO Guidelines for assessment and management of cardiovascular risk 2007, www.who.int). The triglyceride-rich lipoproteins (TRLs) appear to be pro-inflammatory, cause endothelial dysfunction, upregulate expression of endothelial adhesion molecules and promote macrophage chemotaxis. TRLs are also prone to enter the arterial wall, where they are uptaken by macrophages like the oxidized LDLs (Kannel & Vasan 2009b).

In recent years another lipid disorder, that of low high density lipoprotein (HDL) plasma levels (HDL cholesterol <1 mmol/l in men and <1.3 mmol/l in women, according to WHO Guidelines for assessment and management of cardiovascular risk 2007, www.who.int), has attracted great attention. High levels of HDL are associated with reduced CVD risk. The mechanism through which HDL confers its beneficial effects has been attributed in part to its ability to mediate reverse cholesterol transport,

as well as its anti-inflammatory, antiapoptotic, antioxidative, and antithrombotic actions (Hausenloy & Yellon 2009). All the above lipid disorders are metabolically linked and often appear in combination.

Diabetes: Diabetes is characterised by hyperglycaemia (fasting plasma glucose concentration >7 mmol/l or a 2 hours postprandially >11 mmol/l, according to WHO Guidelines for assessment and management of cardiovascular risk 2007, www.who.int) and glucose intolerance, due to insulin deficiency or impaired effectiveness of insulin action, or both. The development of diabetes is accompanied by elevated BP, lipoprotein abnormalities, and inflammation. The risk for CVD is doubled among people with diabetes, after adjusting for classic risk factors (Kannel & McGee 1979). Approximately 50% of diabetes patients die from CVD complications, such as MI and stroke (WHO, Diabetes, www.who.int). The mechanism by which diabetes is involved in the pathogenesis of CVD is complex, and involves the direct toxic effects of hyperglycaemia and advanced glycation end products (Reusch & Draznin 2007), along with the impact of abnormal lipid levels (DeFronzo 2010) and inflammation (Maiti & Agrawal 2007), which lead to atherosclerosis. The diabetic state also promotes oxidative stress mediated by reactive oxygen species (ROS), which may aggravate the atherosclerotic progression (Baynes & Thorpe 1999). Diabetes is described in more detail in chapter 3 of the “Introduction” (page 64).

Hypertension: Hypertension is the term to describe the chronic elevation of systemic arterial BP. High arterial BP [systolic blood pressure (SBP) >140 mmHg and diastolic blood pressure (DBP) >90 mmHg, according to WHO Guidelines for assessment and management of cardiovascular risk 2007, www.who.int] is a leading risk factor for CVD. Several major prospective, observational and epidemiological studies have shown that lower DBP within the usual range (i.e. 70-110 mm Hg) is

associated with lower risk of stroke or CHD. This means that, not only in hypertensive, but also among normotensive individuals, lower DBP is related to lower CVD risk. More specifically, a 5 mmHg lower DBP is associated with about a one-fifth lower risk of CHD and a one-third difference in stroke risk (Collins & MacMahon 1994).

The deleterious effect of elevated BP on the cardiovascular system appears to be mainly due to the mechanical stress placed on the heart and blood vessels. Humoral factors and vasoactive hormones such as angiotensin, catecholamines and prostaglandins may also play a role in the fibromuscular thickening of the intima and media with luminal narrowing of the arteries. Hypertension increases the susceptibility of arteries to atherosclerosis and accelerates progression particularly in the coronary and cerebral vessels. Moreover, hypertension increases the likelihood of plaque rupture and thrombotic occlusion of blood vessels, especially in the brain (Hollander 1976).

Obesity: Overweight and obesity are defined as abnormal or excessive fat accumulation that presents a risk to health. Overweight or obese people, in particular with abdominal obesity, have an increased risk of developing CVD (WHO, Obesity, www.who.int). An individual with body mass index (BMI) $>25 \text{ kg/m}^2$ is characterised as overweight and with BMI $>30 \text{ kg/m}^2$ obese. There are other parameters used in order to define central obesity. Waist circumference greater than 102 cm in men and 88 cm in women, or waist-to-hip ratio over 1 in men and 0.8 in women denote abdominal obesity, which has been shown to significantly increase the risk for CVD (The National Research Council, Guidelines on overweight and obesity 1998, www.nhlbi.nih.gov/guidelines/obesity). For example, men in the uppermost quintile of waist-to-hip ratio have a three times higher risk of developing CHD compared to those in the lowest (Rimm *et al.* 1995). Obesity can contribute to CVD directly by aggravating the lipid accumulation *per se*, but also indirectly by increasing insulin

resistance and thus promoting the development of diabetes (Bjorntorp 1991). Obesity, like atherosclerosis, was once considered to be simple lipid-storage disease. Nowadays, obesity and atherosclerosis are considered as chronic inflammatory states, with processes such as inflammatory cell infiltration, cytokine production, and cell death, in addition to the lipid accumulation, contributing to the two diseases interplay, and their complications (Rocha & Libby 2009).

2.4.2 Emerging risk factors

C-reactive protein (CRP): The hepatocyte-derived acute-phase reactant CRP is a non-specific marker of systemic inflammation and has been associated with high risk for CHD events as well as with increased carotid intima-media thickness, a sub-clinical measure of atherosclerosis. The role of CRP in the pathogenesis and risk prediction of CVD has attracted an intense research interest, which provided controversial data the previous years. However, recent studies and a systematic review of published data show that measurement of CRP has limited utility in the screening or prediction of CVD (Shah *et al.* 2009). Once established risk factors have been evaluated to estimate absolute risk, CRP concentration appears to provide very modest incremental risk information (Hingorani *et al.* 2009).

Regarding the implication of CRP in the pathogenesis of CVD, Mendelian randomisation studies have shown a lack of concordance between the effect of CRP genotypes on CHD risk and CRP levels, which argues against the causality of CRP (Casas *et al.* 2006; Kivimaki *et al.* 2008; Elliott *et al.* 2009). It seems more likely that the association of CRP with atherosclerosis is a result of reverse causality, i.e. CRP levels are altered as a result of atherosclerosis rather than being a cause of it, or confounding, i.e. the association of CRP with atherosclerosis arises from the common

association of the two with other causative factors (Kivimaki *et al.* 2008). Although the totality of evidence at present favors the interpretation that elevated CRP does not cause CVD, a human intervention trial with a specific CRP inhibitor is still missing in order to give the final answer (Nordestgaard 2009).

Homocysteine: Homocysteine is an amino acid synthesised during the metabolism of an essential amino acid, the methionine. Circulating levels of homocysteine are normally low due to its rapid metabolism and clearance and high levels of circulating homocysteine have been suggested to have a causal relationship with the development of atherosclerosis (McCully & Wilson 1975). A meta-analysis of retrospective data showed that an increase of 5µmol/l was associated with 20-30% higher CVD risk (Ueland *et al.* 2000). The mechanism underlying this association remains to be elucidated.

Fibrinogen: Fibrinogen is a key molecule in the clotting cascade. In the final step of the process, thrombin cleaves fibrinogen to produce fibrin, which in turn polymerises to produce the structural backbone of a thrombus. Higher levels of fibrinogen are considered as a risk factor contributing independently to a higher risk for CVD (Heinrich *et al.* 1994).

Lp(α): Lp(α) is a circulating lipoprotein which is deposited in the arterial wall along with LDL and triglyceride-rich lipoproteins. The contribution of this particular lipoprotein to atherosclerosis lies with its ability to interfere with fibrinolysis by competing plasminogen (Angles-Cano *et al.* 2001). Large-scale prospective data have demonstrated an independent, continuous and modest association of Lp(a) levels with the risk of CHD in a broad range of individuals, with levels of Lp(a) being highly stable within individuals across many years and only weakly correlated with known risk

factors (Bennet *et al.* 2008; Erqou *et al.* 2009). But most importantly, variants in the gene of Lp(a) have been strongly associated with both an increased level of Lp(a) lipoprotein and an increased risk of CHD, which provides support for a causal role of Lp(a) lipoprotein in CHD (Clarke *et al.* 2009).

2.4.3 Environment - Lifestyle

Smoking: Smoking and lipid disorders are the two most important risk factors for CHD worldwide, accounting for about two-thirds of the population attributable risk for a MI. The INTERHEART study showed that the association of smoking with MI is graded, without either a threshold or a plateau in the dose response, with smoking even five cigarettes per day to increase the risk (Yusuf *et al.* 2004). There is a large body of evidence from prospective cohort studies regarding the beneficial effect of smoking cessation on CVD mortality. There are several potential mechanisms by which smoking may increase the risk of CVD. Smoking causes damage to the endothelium, abnormal lipid levels, increased BP, insulin resistance; increased oxidative stress and decreased activity of endothelial NO, all of which promote atherosclerosis. Also, smoking activates platelets, increasing the risk of thrombus formation with consequent artery occlusion (Erhardt 2009).

Alcohol: Many epidemiological and clinical studies have shown a U-shaped association of alcohol consumption with CVD risk and total mortality in middle-aged and elderly men and women (Rehm *et al.* 2003) (Rimm *et al.* 1999). A light-to-moderate consumption confers a lower risk and death rate than that of abstainers, while those who drink large amounts have a higher risk and death rate compared to both the other two categories (Gaziano *et al.* 2000). The plausible mechanisms for the putative cardioprotective effects include increased levels of HDL (Rimm *et al.* 1999), prevention

of formation and promotion of dissolution of blood clots, reduced platelet aggregation, and lowering of plasma Lp(a) concentration (Agarwal 2002). Nonetheless, people who drink heavily have a high mortality from all causes and CVD, including sudden death and haemorrhagic stroke, which is attributed to increased clotting, rise in LDL cholesterol (Rehm *et al.* 2003) and lower threshold for ventricular fibrillation (Greenspon & Schaal 1983).

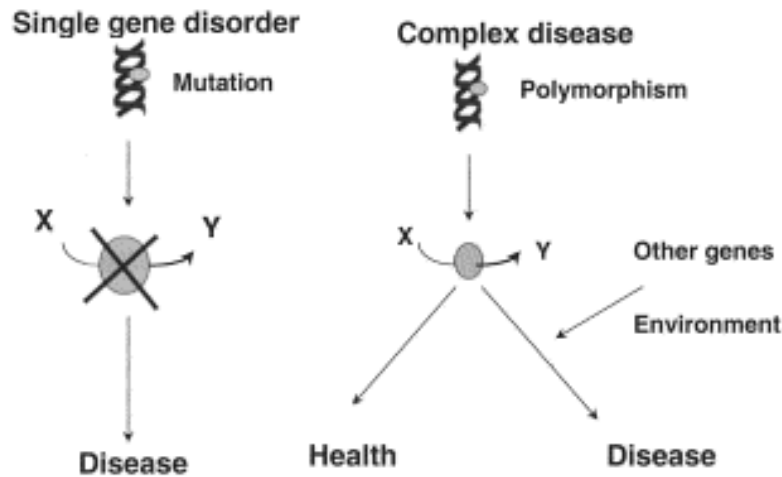
Physical activity: Sedentary lifestyle is associated with increased risk of CVD, while observational studies have shown that leisure-time physical activity is associated with reduced CVD risk and mortality in both men and women and in middle-aged and older individuals. The physical activity beneficiary effect on CVD can be attributed to improvement of endothelial function as well as contribution to weight loss and glycaemic control (Yung *et al.* 2009; Kokkinos *et al.* 2011).

Diet: Atherosclerosis is widely considered to have a nutritional background. In several cross sectional studies high dietary intakes of fat, cholesterol and sodium or low consumption of fruits, vegetables and fish are linked to CVD risk (WHO Guidelines for assessment and management of cardiovascular risk 2007, www.who.int). For example, in the INTERHEART study, the daily consumption of fruits and vegetables conferred a 30% reduction in the odds for MI while the lack of daily consumption accounted for 13.7% of the population attributable risk for MI (Yusuf *et al.* 2004).

2.4.4 Genetic predisposition

Complex diseases such as CVD arise due to ineffective maintenance of homeostasis within a physiological system. This may be attributed to failure at the genetic level, or to exposure to a detrimental environment, but it usually occurs due to an interaction between the two. Failure at the genetic level involves mutations altering the composition or structure of the proteins encoded for by genes, or the inappropriate amount of protein synthesised (Stephens & Humphries 2003). There are some monogenic causes of early CVD, such as familial hypercholesterolemia (FH), with a frequency for the heterozygous state, approximately 1 in 500 members of the general population. In monogenic forms, a single functional mutation in a single important homeostatic gene, like the gene coding for the LDL receptor in the case of FH, are sufficient to cause the disease. However, the common form of the disorder is polygenic and heterogeneous (Humphries *et al.* 2004). Complex disorders such as atherosclerosis are usually the result of several common polymorphisms causing subtle alterations in the expression or activity of the encoded proteins which individually are compatible with health. However, interaction among several of these polymorphisms combined with an adverse environmental influence leads to the development of the disease (Hingorani 2001) (Figure 5).

Figure I-5. Models representing the mechanism by which common polymorphisms influence the susceptibility to a complex disorder such as atherosclerosis (Hingorani 2001).



Many family and twin studies have examined the contribution of genetics in CVD and have found heritability to often exceed 50% (Lusis *et al.* 2004). Atherosclerosis is a multistep process involving the interaction of many different key pathways, including lipoprotein metabolism, coagulation, inflammation oxidative stress, cellular proliferation and tissue remodelling. Variation in genes encoding key proteins in any of these metabolic pathways can upset the delicate balance of homeostasis and result in the development of the disease (Roy *et al.* 2009). Over the last 10 to 15 years variants, functional variants in genes with a key role in processes involved in the pathogenesis of CVD have been investigated for their effect on disease predisposition. More recently after the mapping of linkage disequilibrium blocks in the genome has become available, single nucleotide polymorphisms (SNPs) tagging the variation in and flanking the candidate genes are also being studied followed by investigation for the functional variants. The use of the candidate gene approach through association studies

in prospective analysis or case control studies has led to the identification of many common polymorphisms associated with CVD. Meta-analyses have confirmed the association of several of those polymorphisms with CVD, with the best example being that of apolipoprotein E gene (*APOE*). Two common polymorphisms in this gene result in the coding of three different isoforms of the protein, the strong effects of which on plasma lipids and their modest effects on CHD risk has been confirmed by many independent studies.

The last couple of years, the technological advances have provided the possibility for genome-wide screening of cases and controls in order to discover new loci associated with CVD. This hypothesis-free approach has confirmed several previously identified CVD associated loci, but most importantly has revealed many new ones. The discovery of these new loci has triggered further research aiming at identifying the functional variants related to the newly identified loci and their involvement in processes predisposing to CVD. In this way new directions have been given to the research field and also new questions have been raised.

Table 1 summarises the most important genes that have been associated with atherosclerotic CVD.

Table I-1. Genes reported to be associated with atherosclerotic vascular diseases (CHD, MI, peripheral artery disease, carotid atherosclerosis and ischemic stroke) (Roy *et al.* 2009).

Pathophysiological processes	Susceptibility genes
LDL metabolism	<i>LDLR, LDLRAP1, LRP, LRP6, APOB, APOE, PCSK9, CYP7A1, SREBP-2/SCAP, USF1, PSRC1</i> and <i>CELSR2</i>
HDL metabolism	<i>LCAT, APOA-1, ABCA1, SR-B1, PON, LIPC, CETP</i>
Triglyceride metabolism	<i>LPL, APOA5, APOC-III</i>
Lipoprotein(a)	<i>APO(a)</i>
Endothelial dysfunction	<i>NOS3, MnSOD, KDR</i>
Oxidative stress	<i>CYBA, MPO, EC-SOD, GPX1, GST, UCP2, HO-1</i>
Inflammation	Interleukins: <i>IL-1, IL-1Ra, IL-6, IL-10</i> Cytokines and cytokine receptors: <i>TNF-α, TNF-receptor, LTA</i> Adhesion molecules: <i>selectins, ICAM-1, VCAM-1, PECAM</i> Chemokines and chemokine receptors: <i>CX3CR1, CCR5, CCR2, CXCL12, RANTES, MCP-1</i> Eicosanoids: <i>ALOX5, ALOX5AP, LTA4H, LTC4S, PTGS1, PTGS2, L-PGDS</i> Others: <i>Connexin 37, MEF2A, TLR-4, CRP, TNFS4, MHC2TA</i>
Vascular remodeling	<i>TGF-β1, MMP-1, MMP-3, MMP-7, MMP-9, MMP-12</i>
Arterial thrombosis	Hemostatic system: <i>fibrinogen, prothrombin, factor V, factor VII, Factor XIII, thrombomodulin</i> Fibrinolytic system: <i>PAI-1, TAFI, t-PA</i> Platelet surface receptors: <i>glycoprotein IIb/IIIa, Ia/IIa, Ib</i>
Cell cycle regulators	<i>CDKN2A, CDKN2B</i>
Vascular progenitor cell regulators	<i>CXCL12, GATA2</i>

Miscellaneous	<i>PPARγ, PPARα, thrombospondins, ACE, angiotensin II type 1 receptor, angiotensinogen, MTHFR, PDE4D, ANRIL, VAMP8, HNRPUL1, KIF6</i>
---------------	---

Although the list of candidate loci has grown with the contribution of genome wide association studies (GWAS), the SNPs currently identified only explain a portion of the heritability estimate for CVD. Since there is robust evidence for the heritability of CVD, the fact that this heritability cannot be explained means that the nature and number of genetic factors involved in the disease pathogenesis remains partly elusive. Therefore, more genetic factors need to be explored in order to elucidate their contribution in the disease heritability. These include rare mutations, telomere length, copy number variations and epigenetic modifications such as DNA methylation.

Genetic research in CVD aim is to reveal a set of genetic factors which could improve the risk prediction algorithms by adding information over and above the classical risk factors. Improving the sensitivity and specificity of risk prediction is very important, since with the use of the current algorithms a large percentage of individuals, who go on to develop CVD, is not identified in time to prevent the disease complications. Moreover discovering the genetic factors contributing to the disease development offers new drug targets and helps to more effective treatment strategies for primary or secondary prevention.

3 TYPE 2 DIABETES

3.1 THE PANCREATIC ISLETS

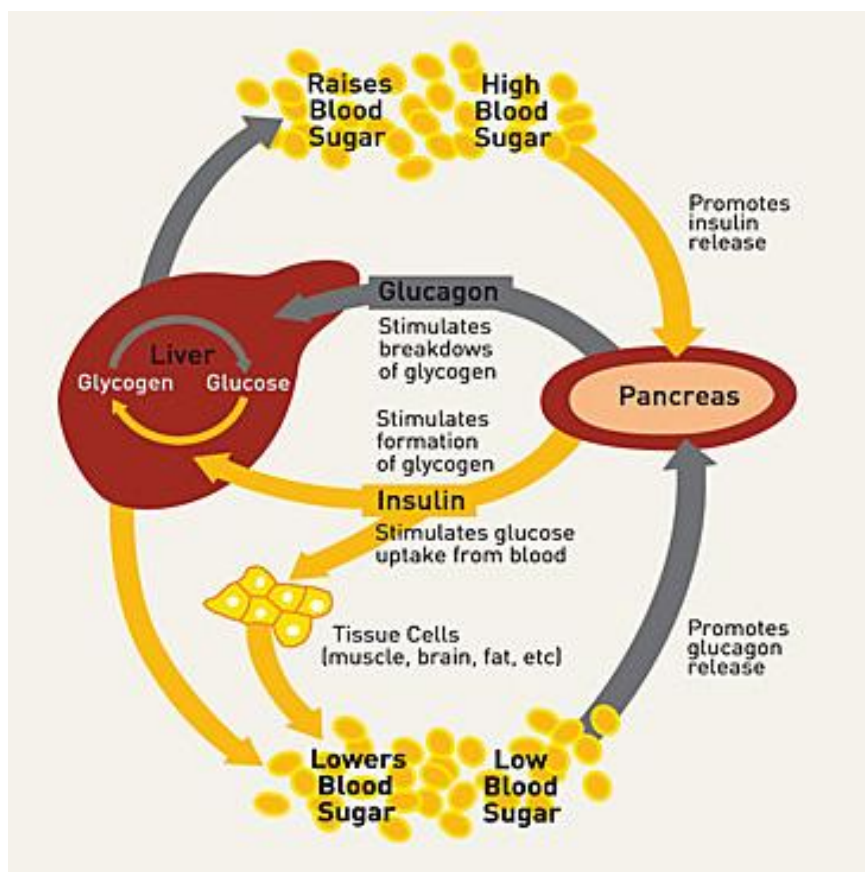
The pancreas serves an endocrine and exocrine function and consists of two distinctly different tissues. The bulk of its mass is exocrine tissue, which produces digestive enzymes which are delivered to the small intestine to facilitate digestion. Scattered throughout the exocrine tissue are clusters of several hundred thousand endocrine cells, the pancreatic islets or islets of Langerhans. These endocrine cells produce two very important hormones, insulin and glucagon. Insulin is secreted by the β cells, which are the majority of cells in the pancreatic islets, and glucagon from the α cells. Insulin and glucagon together regulate the uptake, storage and use of exogenous glucose mainly, but also free fatty acids and amino acids, in order to cover the energy needs of tissues. Insulin is an anabolic hormone promoting the uptake and storage of fuels after food intake, while glucagon acts in the opposite way to insulin promoting the mobilisation of fuels during fasting or exercise (Cooperstein 1981; Robert M. Berne 1993b) (Figure 6).

3.2 INSULIN

Insulin is the major glucoregulatory hormone. It consists of two polypeptide chains held together by disulfide bonds and synthesised from a single chain precursor proinsulin. The secretion of insulin is stimulated by food intake, gastrointestinal peptides, cholinergic and β -adrenergic stimuli. Its release is inhibited by fasting and exercise, conditions where fuel mobilisation is required.

The regulatory role of insulin is accomplished through its action in various sites of the body. Insulin action in the liver leads to inhibition of gluconeogenesis or glycogenolysis and glucose release, as well as stimulation of glycogen synthesis. In muscle cells insulin signals the inhibition of proteolysis, the stimulation of glucose uptake and storage as glycogen. Finally, in adipose tissue insulin inhibits lipolysis and ketogenesis and stimulates the glucose uptake from blood (Figure 6).

Figure I-6. The insulin-glucagon balanced regulation of glucose (Diabetes Atlas 4th edition, IDF 2009, www.diabetesatlas.org).



The signal transduction pathway of insulin in the cells of these tissues begins with its binding to a plasma membrane receptor with tyrosine kinase activity, called the insulin receptor. Insulin binds and activates the tyrosine kinase subunit, which phosphorylates intracellular substrates, such as kinases, phosphatases or G proteins, which in turn may trigger a number of cascades (Robert M. Berne 1993b). It is now established that the phosphatidylinositol 3-kinase in particular plays a pivotal role in the signal-transduction pathways linking insulin with many of its specific cellular responses (e.g. glycogen synthesis, cell proliferation, differentiation and apoptosis) (Shepherd *et al.* 1998). One of the cellular responses triggered by the activation of phosphatidylinositol 3-kinase is the projection to the cell membrane of the facilitated glucose transporter member 4 (GLUT4) in order to enhance glucose uptake by muscle and adipose tissue cells when circulating glucose levels are increased (Thong *et al.* 2005). Thus, insulin signalling in muscle and adipose tissue is important for keeping plasma glucose levels within acceptable limits (approximately 3.4-6.4 mmol/l) (Robert M. Berne 1993b).

3.3 TYPES OF DIABETES

Diabetes, also called diabetes mellitus, is a group of heterogeneous disorders having as common features hyperglycaemia and glucose intolerance, which arises as a result of insufficient production of insulin due to failure of the pancreatic β cells, insulin resistance or both. According to the aetiology and the clinical presentation, diabetes is classified in two main types, 1 and 2.

Type 1 diabetes (T1D): T1D, also called insulin-dependent, immune-mediated or juvenile-onset diabetes, is caused by complete failure of the β cells of the pancreas,

and thus insufficient or null production of insulin. This β cell failure is predominantly caused by an auto-immune reaction; the aetiology of which is not fully understood (Bloomgarden 2006). T1D can affect people of any age, but typically its onset occurs during childhood or adolescence. This form of the disease is severe, with T1D patients being dependent on exogenous insulin administration (Diabetes Atlas 4th edition, IDF 2009, www.diabetesatlas.org and WHO, Diabetes, www.who.int).

Type 2 diabetes (T2D): T2D, the common form of the disease, is caused by insulin resistance and relative insulin deficiency due to relative β cell failure. The onset of T2D, in contrast to T1D, usually occurs later in life, during middle-age and thereafter. However, T2D can remain undetected for years, with its diagnosis being made often from the associated complications or an incidental detection of abnormal circulating glucose levels (Table 2). Most T2D patients are not dependent on exogenous insulin, like T1D, but may require insulin for control of hyperglycaemia if this is not achieved with diet and oral hypoglycaemic agents (Bloomgarden 2006) (Diabetes Atlas 4th edition, IDF 2009, www.diabetesatlas.org and WHO, Diabetes, www.who.int).

3.4 PREDIABETES CONDITIONS

Impaired glucose tolerance and impaired fasting glucose are asymptomatic conditions preceding diabetes development and are also caused by insulin resistance and a low grade of insulin deficiency (Ferrannini *et al.* 2011). Impaired glucose tolerance is characterised by elevated levels of blood glucose two hours after an oral glucose challenge, while impaired fasting glucose is characterised by elevated fasting glucose levels in plasma (Table 2) (Bloomgarden 2006) (Report of a WHO/IDF Consultation for the definition and diagnosis of diabetes, <http://www.idf.org/webdata/docs>). In both

cases the plasma glucose levels are not as high as in developed diabetes; however people with prediabetes are at high risk of developing T2D and CVD (Twigg *et al.* 2007). This increased risk for CVD in prediabetes is multifactorial, with etiologies including insulin resistance, hyperglycemia, dyslipidemia, hypertension, systemic inflammation, and oxidative stress (Hsueh *et al.* 2010).

Table I-2. Diagnosis criteria of diabetes mellitus and intermediate hyperglycemia (Report of a WHO/IDF Consultation for the definition and diagnosis of diabetes, <http://www.idf.org/webdata/docs>).

Diabetes	
Fasting plasma glucose	≥ 7.0 mmol/l
<i>or</i> 2hrs plasma glucose*	≥ 11.1 mmol/l
Impaired Glucose Tolerance (IGT)	
Fasting plasma glucose	< 7.0 mmol/l
<i>and</i> 2hrs plasma glucose*	≥ 7.8 and < 11.1 mmol/l
Impaired Fasting Glucose (IFG)	
Fasting plasma glucose	> 6.1 and < 6.9 mmol/l
<i>and</i> if measured 2hrs plasma glucose**	< 7.8 mmol/l

* Venous plasma glucose 2hrs after ingestion of 75g oral glucose load

** If 2hrs plasma glucose is not measured, status is uncertain as diabetes or IGT cannot be excluded.

3.5 PATHOGENESIS OF TYPE 2 DIABETES

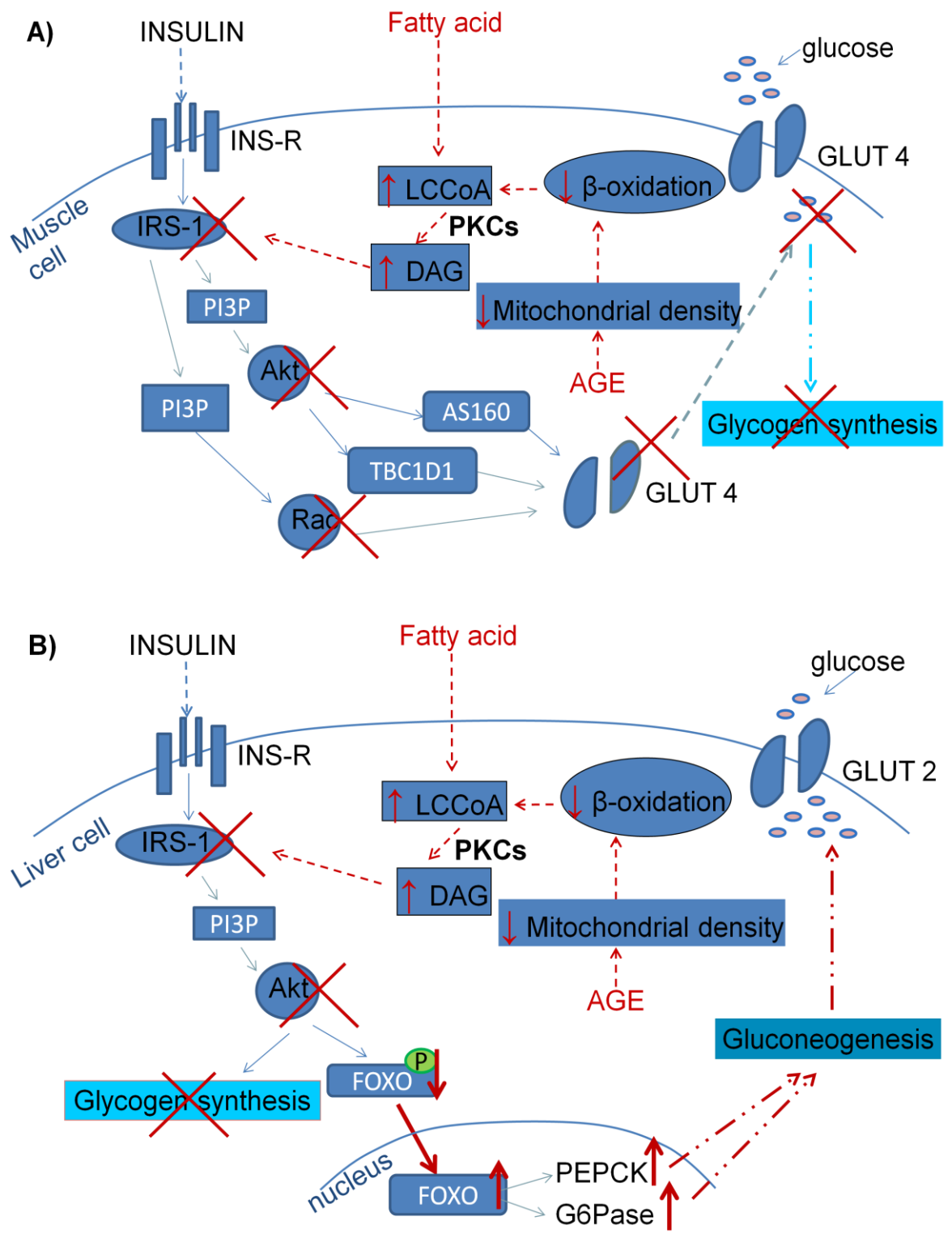
T2D mainly rises from the failure of glucose homeostasis maintenance, which depends on the balance between the target's tissue sensitivity to insulin and the insulin secretion from β cells. Insulin resistance alone is not sufficient to disturb glucose homeostasis as long as the β cells function normally and secrete insulin in adequate amounts, in order to compensate for the defective tissues' insulin response. Thus, T2D onset requires the development of both insulin sensitivity and insulin secretion (DeFronzo & Tripathy 2009).

3.5.1 Insulin resistance

Insulin resistance is considered to be the initiating defect, which might occur decades before, resulting in β cell failure and overt hyperglycemia. Insulin resistance is defined as a reduced, compared to normal, response to insulin of target tissues, such as the skeletal muscle, liver, and adipocytes. In particular the response of skeletal muscle cells to the insulin signal is mainly responsible for the glucose uptake and glycogen synthesis after food intake, determining the postprandial blood glucose levels and the time of clearance (Krook *et al.* 2000). Therefore, the reduced response of skeletal muscle to insulin is considered as the hallmark in T2D pathogenesis (Goldstein 2002).

The molecular mechanism leading to skeletal muscle insulin resistance is triggered by high levels of free fatty acids and cytokines as well as glucose itself (DeFronzo & Tripathy 2009). There is compelling evidence that an increase in free fatty acids causes skeletal and liver insulin resistance (Petersen & Shulman 2002), as shown in figure 7.

Figure I-7. Fatty acid- and age-induced insulin resistance in: A) skeletal muscle cells and B) liver cells.



Legend: A) Increased fatty acid availability and/or age-induced decrease in mitochondrial β -oxidation in skeletal muscle cells result in high levels of intracellular long-chain acylcoenzyme A (LCCoA) and diacylglycerol (DAG). This in turn induces serine/threonine phosphorylation of IRS-1 sites, thereby inhibiting IRS-1 phosphorylation and activation of phosphatidylinositol 3-phosphate (PI3P) signaling. This leads to reduced levels of glucose transporter 4 (GLUT4) synthesis and consequently to low insulin-stimulated muscle glucose uptake and diminished glycogen synthesis. B) Similarly, increased fatty acid availability and/or age-induced decrease in mitochondrial β -oxidation in liver cells result in reduced insulin-stimulated IRS-1 and consequent inhibition of the PI3P signaling. This leads to lower forkhead box protein O (FOXO) phosphorylation, which in turn results in lower insulin-stimulated liver glycogen synthesis and increased hepatic gluconeogenesis (Savage et al. 2007).

The resistance of adipose tissue cells to the insulin signal for inhibition of lipolysis might be the cause of the elevated free fatty acids, which in turn leads to skeletal muscle and liver insulin resistance and consequent β cell failure. Thus, adipose tissue insulin resistance might precede the skeletal muscle resistance and represent the initial trigger in the pathogenesis of T2D (DeFronzo & Tripathy 2009).

3.5.2 B cell failure

B cell failure is the *sine qua non* for the development of T2D and involves a decrease in β cell mass due to apoptosis as well as a decline of key β cell functions. The pathways leading to β cell failure are not yet fully understood. Current evidence suggests that β cell failure is a consequence of 'glucolipotoxicity', i.e. a combination of hyperglycaemia and high levels of free fatty acids, rather than exposure to each nutrient alone (Poitout *et al.* 2010). Various mechanisms, explaining the effect of the metabolic overload (glucose and fatty acids) on β cells, have been proposed. To begin with, metabolic overload of the β cell mitochondria results in basal insulin hypersecretion and

loss of glucose-stimulated insulin secretion, through upregulation of the pyruvate cycling. This metabolic overload might lead to increased production of ROS and altered uncoupling protein 2 (*UCP2*) expression, which might play a role in β cell failure, although the exact mechanism has not yet been defined. In addition, the increased demand for insulin biosynthesis gradually leads to ER stress, with consequent protein misfolding and cell death (Muio & Newgard 2008). Finally, insulin hypersecretion is accompanied by amylin hypersecretion, which accumulates as amyloid plaques at the β cell surface inducing severe dysfunction and apoptotic death (Muio & Newgard 2008). Thus, metabolic overload in combination with an increased demand for function are the main causes for β cell failure.

3.5.3 Risk factors

T2D is often associated with obesity and its occurrence is highly familial. Most of T2D risk factors are shared with those for CVD (see chapters 2.3.1.1 and 2.3.3 of the Introduction).

Age: T2D, as well as CVD, is considered an age-related disease, associated with tissue deterioration and decline from normal functions in a biologically aged organism. The biology of ageing and its possible role in T2D are discussed in more detail in chapter 5 of the “Introduction” (page 82).

Obesity: Excess adiposity is considered the most important risk factor, which itself can cause insulin resistance and lead to elevated blood glucose levels. This risk increase is mainly conferred by intra-abdominal and intra-hepatic fat depots. Accumulation of ectopic lipids in muscle and islets is also involved in the pathogenesis of the disease (Joost 2008). Indicative of the effect of obesity is that in the Health Professionals Follow-up Study, 56% of the T2D cases could be attributed to a weight

gain of 7 kg or greater and 20% to a waist gain of 2.5 cm or greater (Koh-Banerjee *et al.* 2004).

Physical activity and diet: Human cohort studies have provided convincing evidence that nutritional and lifestyle variables are independent risk factors for T2D. Specifically, sedentary lifestyle can increase almost 3-fold the risk for T2D, while physical activity has a protective effect which is independent of the weight reduction. Regarding the role of diet, a beneficial nutritional pattern has been identified consisting of a high consumption of fruits in combination with a low consumption of red meat, beer, soft drinks and white bread. This dietary pattern has been associated with an approximately 80% reduction of T2D risk (Joost 2008).

Sub-optimal intrauterine environment: In recent years, it has become evident that a disturbed nutritional environment of the foetus is a risk factor for T2D. There are now several human epidemiological studies showing that both a nutrient poor and a nutrient abundant intrauterine environment may compromise the adult health of the fetus by increasing susceptibility to insulin resistance, glucose intolerance and diabetes (Reusens *et al.* 2007).

3.5.4 The role of genetics

There is compelling evidence to support a major genetic component to T2D susceptibility (Gloyn & McCarthy 2001). According to the thrifty gene hypothesis, certain genetic variants have developed in some populations as a fitness advantage in poor nutritional environments, but in an environment of increased food supply these same variants now predispose to insulin resistance and diabetes (Carulli *et al.* 2005). The genetic contribution is well recognised in the diverse forms of both juvenile-onset diabetes (monogenic) and adult-onset diabetes (complex). Evidence supporting the

genetic basis to T2D includes its greater prevalence in particular ethnic groups (Gloyn & McCarthy 2001), the higher concordance rate observed in monozygotic than dizygotic twins (Newman *et al.* 1987) and the identification of susceptibility loci by GWAS (Zeggini *et al.* 2007; McCarthy & Zeggini 2009).

The primary methods used to explore the genetic basis of diabetes were linkage analysis (analysis of shared DNA segments inherited from common ancestors coupled with phenotypic information) and candidate gene approaches. These approaches revealed few genes [e.g. peroxisome proliferator-activated receptor-gamma (*PPARG*) and potassium channel, inwardly rectifying, subfamily J, member 11 (*KCNJ11*), Table 3], with most important the breakthrough of the transcription factor 7-like 2 gene (*TCF7L2*) discovery by linkage analysis (Table 3). The *TCF7L2* gene has a strong effect on the risk for T2D which has been replicated in many ethnicities (Frayling 2007).

In the past three years, GWAS for T2D in several European populations revealed 25 new *loci*, several of which encode proteins of the cell cycle, and represent putative new pathways involved in the pathogenesis of the disease which can also serve as new targets for therapeutic interventions (Bonnetfond *et al.* 2010) (Table 3).

Table I-3. Genes and *loci* associated with T2D that have been most replicated (Bonnetfond *et al.* 2010).

Gene	Loci	Protein	Assumed effect of risk allele
Candidate gene studies			
<i>PPARG</i>	3p25	Peroxisome proliferator-activated receptor- γ	Decreased insulin sensitivity, decreased insulin clearance
<i>KCNJ11</i>	11p15.1	K inwardly-rectifying channel, subfamily J, member 11	Decreased β -cell function, decreased glucose-stimulated insulin secretion (GSIS), decreased insulin sensitivity
<i>HNF1B</i>	17cen-q21.3	Hepatocyte nuclear factor 1-beta	Decreased β -cell function
<i>WFS1</i>	4p16	Wolfram syndrome 1 (wolframin)	Decreased β -cell function, decreased insulin secretion
<i>GCK</i>	7p15.3-p15.1	Glucokinase (Hexokinase 4)	Decreased β -cell function, decreased GSIS, increased fasting glucose, increased glycated hemoglobin
Linkage analysis			
<i>TCF7L2</i>	10q25.3	Transcription factor 7-like 2 (T-cell-specific, HMG-box)	Decreased β -cell function, decreased incretin-stimulated insulin secretion, decreased GSIS, decreased proinsulin conversion, decreased insulin sensitivity, decreased disposition index, increased fasting glucose, increased 2h-glucose
GWAS for T2D			
<i>CDKN2A/2B</i>	9p21	Cyclin-dependent kinase inhibitor 2A/2B	Decreased β -cell function, decreased GSIS, decreased disposition index
<i>CDKAL1</i>	6p22.3	CDK5 regulatory subunit associated protein 1-like 1	Decreased β -cell function, decreased GSIS, decreased proinsulin conversion, decreased disposition index
<i>SLC30A8</i>	8q24.11	Solute carrier family 30 (zinc transporter), member 8	Decreased β -cell function, decreased GSIS, decreased proinsulin conversion, decreased disposition index, increased fasting glucose, increased 2h-glucose, increased glycated hemoglobin
<i>IGF2BP2</i>	3q27.2	Insulin-like growth factor 2 mRNA binding protein 2	Decreased β -cell function, decreased GSIS, decreased disposition index

Gene	Loci	Protein	Assumed effect of risk allele
<i>HADA</i>	2p21	Thyroid adenoma associated	Decreased β -cell function, decreased insulin sensitivity, decreased second-phase insulin secretion, decreased disposition index, decreased GLP-1 and arginine-stimulated insulin response
<i>NOTCH2</i>	1p13-p11	Neurogenic locus notch homolog protein 2 (<i>Drosophila</i>)	NA
<i>CDC123</i>	10p13	Cell division cycle 123 homolog (<i>Saccharomyces cerevisiae</i>)	Decreased β -cell function, decreased insulin secretion
<i>CAMK1D</i>		Calcium/calmodulin-dependent protein kinase type 1D	
<i>HHEX</i>	10q23	Hematopoietically expressed homeobox	Decreased β -cell function, decreased GSIS, decreased insulin sensitivity, decreased proinsulin conversion, decreased disposition index
<i>IDE</i>		Insulin-degrading enzyme	
<i>TSPAN8</i>	12q14.1-q21.1	Tetraspanin 8	Decreased β -cell function, decreased insulin secretion, decreased insulin sensitivity
<i>LGR5</i>	12q22-q23	Leucine-rich repeat-containing G protein-coupled receptor 5	
<i>ADAMTS9</i>	3p14.3-p14.2	ADAM metalloproteinase with thrombospondin type 1 motif, 9	Decreased insulin sensitivity
<i>JAZF1</i>	7p15.2-p15.1	Juxtaposed with another zinc finger protein 1	Decreased β -cell function, increased insulin secretion, increased fasting insulin
<i>IRS1</i>	2q36	Insulin receptor substrate 1	Increased insulin resistance, decreased insulin sensitivity, increased fasting insulin, increased 2h-insulin
<i>KCNQ1</i>	11p15.5	K voltage-gated channel, KQT-like subfamily, member 1	Decreased β -cell function, decreased insulin secretion, decreased insulin secretion
<i>FTO</i>	16q12.2	Fat mass and obesity-associated protein	Increased risk of obesity, increased body mass index, increased fat mass, increased triglycerides and cholesterol

Worthy of remark is that most of the variants detected with GWAS influence the β cell function and insulin secretion, which strongly suggests that susceptibility to T2D is mainly caused by genetic defects in β cell function (Billings & Florez 2010; Bonnefond *et al.* 2010; Grarup *et al.* 2010).

Similar to the genetics of CVD, the T2D-associated genetic variants discovered so far, only explain a small portion of T2D heritability. There is again an issue with the “missing heritability” which requires new directions in genetic research. These new directions include the investigation of rare variants with large effects on T2D risk, copy number variations, epigenetic modifications (Billings & Florez 2010; Bonnefond *et al.* 2010) and possibly telomere length.

3.6 DIABETES COMPLICATIONS

Chronic diabetes eventually leads to tissue damage in many organ systems. The kidneys, the eyes, the peripheral nerves and the vascular vessels are manifesting with the most significant diabetes complications of nephropathy, retinopathy, neuropathy and cardiovascular disease. The mechanism by which diabetes leads to these complications is not yet fully understood, but hyperglycaemia, abnormal lipid levels and high BP are all likely to play a role in accelerating the deterioration of tissues and lead to organ damage (Melendez-Ramirez *et al.* 2010; Stolar 2010).

4 THE 'COMMON SOIL' HYPOTHESIS

T2D is undoubtedly a major risk factor for atherosclerotic CVD, however atherosclerosis may precede the development of T2D, suggesting that rather than atherosclerosis being a complication of diabetes, both conditions rise from a "common soil." According to the "common soil" hypothesis a certain genetic background combined with adverse environmental conditions, perhaps even in uterus, result in susceptibility to both diabetes and atherosclerotic CVD. For example, insulin resistance is a key risk factor for T2D and some of its features, like high triglyceride levels, low HDL levels and hypertension are also documented risk factors for CVD (Stern 1995).

At the molecular level, both atherosclerosis and T2D development involves "cross-talk" between different complex processes, including inflammation, glucose and lipoprotein metabolism and oxidative stress. In particular, oxidative stress has been proposed as the pathogenic mechanism linking insulin resistance with dysfunction of both β cells and endothelium, eventually leading to overt diabetes and cardiovascular disease. Further support for this hypothesis is provided by pharmacological intervention studies aiming at reducing CVD, which used agents with intracellular preventive antioxidant activity. Therapy with statins in the WOSCOP study (Freeman *et al.* 2001), with angiotensin-1 converting enzyme inhibitors in the HOPE (Yusuf *et al.* 2001) and CAPP studies (Hansson *et al.* 1998), and with angiotensin II type 1-receptor antagonists in the LIFE study (Dahlof *et al.* 2002) resulted in a substantial reduction in the development of T2D, in parallel to the CVD risk, presumably through an underlying common mechanism (Ceriello & Motz 2004).

4.1 OXIDATIVE STRESS

Oxidative stress and consequent damage are considered the main component of the “common soil” hypothesis for the pathogenesis of CVD and T2D (Ceriello & Motz 2004). High oxidative stress is associated with many of the risk factors implicated in the pathophysiology of atherosclerosis and diabetes, such as hypercholesterolaemia, renal failure, ageing, hypertension, smoking and ageing (Harrison *et al.* 2003). Oxidative stress is caused by high levels of ROS, molecules containing oxygen and having one or more unpaired electrons in their atomic structure, which renders them highly reactive. These include the hydrogen peroxide (H_2O_2), the superoxide anion (O_2^-), the hydroxyl radical (OH^\cdot) and the peroxynitrite radical (OONO^\cdot). One to five percent of inhaled oxygen becomes active oxygen species, which are approximately 25,000,000,000 molecules per cell in a day’s time (Maritim *et al.* 2003).

The mitochondria constitute a major source of cellular ROS, which are produced during the final step of nutrient oxidation for energy production. When excessive NADH, produced in the citric acid cycle, cannot be dissipated by oxidative phosphorylation, the mitochondrial proton gradient increases, and single electrons are transferred to molecular oxygen, resulting in the formation of superoxide (Maechler *et al.* 1999). Another major source of ROS is the enzymatic activity of the membrane-associated NADPH oxidase, whose primary function is to catalyse the transfer of electrons from NADPH to molecular oxygen resulting in the generation of superoxide. In addition, the enzymatic activity of xanthine oxidase may result in the formation of superoxide as byproduct (Droge 2002). Similarly, NO generation, which reacts with O_2^- to form OONO^\cdot , occurs through specific nitric oxide synthase isozymes, including mitochondrial nitric oxide synthase (mtNOS), neuronal NOS (nNOS), endothelial NOS

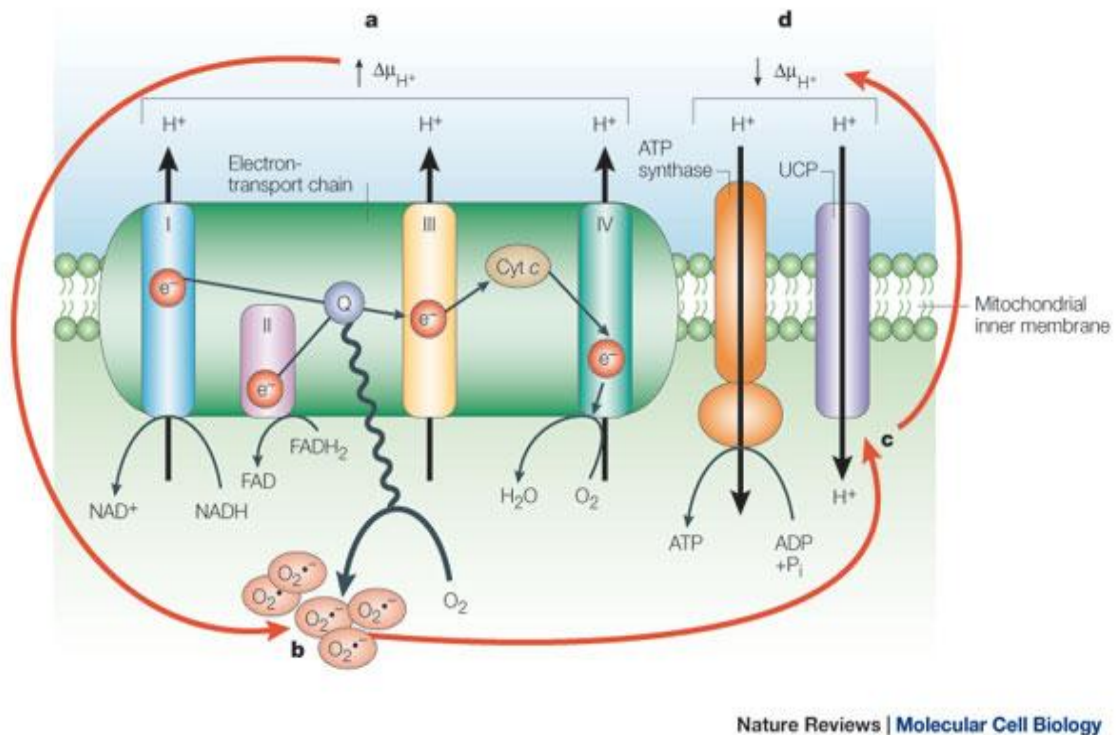
(eNOS), and inducible NOS (iNOS). Other sources of ROS, mainly H₂O₂, include the microsomes and peroxisomes (Trachootham *et al.* 2008).

Oxidative stress is essentially a redox imbalance which results from a disparity between ROS production and antioxidant defences (Maritim *et al.* 2003). Cells are equipped with enzymatic and nonenzymatic antioxidant systems to eliminate ROS and maintain redox homeostasis. The antioxidant defences come from endogenous systems including uncoupling proteins of the respiratory chain, mitochondrial, cytoplasmic and peroxisomal enzymes, which exist to reduce oxidative stress. Of particular importance for the antioxidant defence is the conversion of O₂⁻ to H₂O₂ by superoxide dismutase (SOD) in the mitochondria and then the further detoxification of H₂O₂ to form H₂O by the action of glutathione peroxidase (GPX) in the cytoplasm or the the action of catalase in the peroxisome (Trachootham *et al.* 2008). In specific, the conversion of reduced glutathione (GSH) to oxidized glutathione (GSSG), which is catalyzed by GPX is a major antioxidant system that reduces a broad range of hydroperoxides. GSH, in addition to being a cofactor of various antioxidant enzymes, is the most abundant peptide in cells and possesses a plethora of functions. These include direct scavenging of HO⁻, singlet oxygen, and regeneration of other antioxidants such as vitamin C and E to their active forms (Nakamura *et al.* 1997).

Key role in the antioxidant defence play the uncoupling proteins (UCPs), especially the ubiquitously expressed UCP2. UCP2 dissipates the electrochemical proton gradient generated across the mitochondrial membrane by the electron transport chain. As shown in figure 8, superoxide production in the mitochondrial electron-transport chain activates UCP, which transfers protons to the internal side of the mitochondrial inner membrane. This proton leak causes a decrease in mitochondrial

membrane potential, which limits the production of superoxide in an autoregulatory feedback loop (Krauss *et al.* 2005).

Figure I-8. Negative regulation of ROS by activation of UCP2 (Krauss *et al.* 2005).



Nature Reviews | Molecular Cell Biology

Legend: The proton gradient across the mitochondrial inner membrane (H^+) is created by the export of protons (H^+) from the mitochondrial matrix across the inner mitochondrial membrane (a), which also leads to electron reductions of molecular oxygen at complexes I and III of the mitochondrial electron-transport chain and the formation of superoxide (b). When this export of protons increases the membrane potential and consequently the production of superoxide in the inner side of the membrane also increase. The increased levels of superoxide anions in the inner side of the membrane active UCP2, which transfers protons from the mitochondrial matrix across the mitochondrial inner membrane (c). This proton leakage, in turn, causes a decrease in mitochondrial membrane potential (d), which limits the production of superoxide from the mitochondrial electron-transport chain as a result of this regulatory feedback mechanism.

Uncoupling leads to a higher flow rate through the electron chain and a reduced formation of ROS, which protects the cell from high oxidative stress at the cost of wasting energy as heat. UCP2 activity is induced by byproducts of lipid peroxidation and intra-mitochondrial superoxide (Echtay *et al.* 2002), serving as a negative regulator of ROS generation. The widespread UCP2 tissue distribution is, to some extent, due to expression in immune cells which are generators of large amounts of ROS especially under conditions of stress.

In its most severe form, redox imbalance may result in cell death following widespread macromolecule oxidation, while more subtle changes appear to play a role in modulating a range of signal transduction pathways (Suzuki *et al.* 1997). All molecules are potential targets for ROS (proteins, lipids and DNA), but because of their propensity to contain double bonds, unsaturated lipids are more often targeted (Evans *et al.* 2002). Nonetheless, oxidative DNA damage is of particular importance, since it may trigger DNA damage response pathways which influence the cell cycle (Zhan *et al.* 2010).

5. THE BIOLOGY OF AGEING

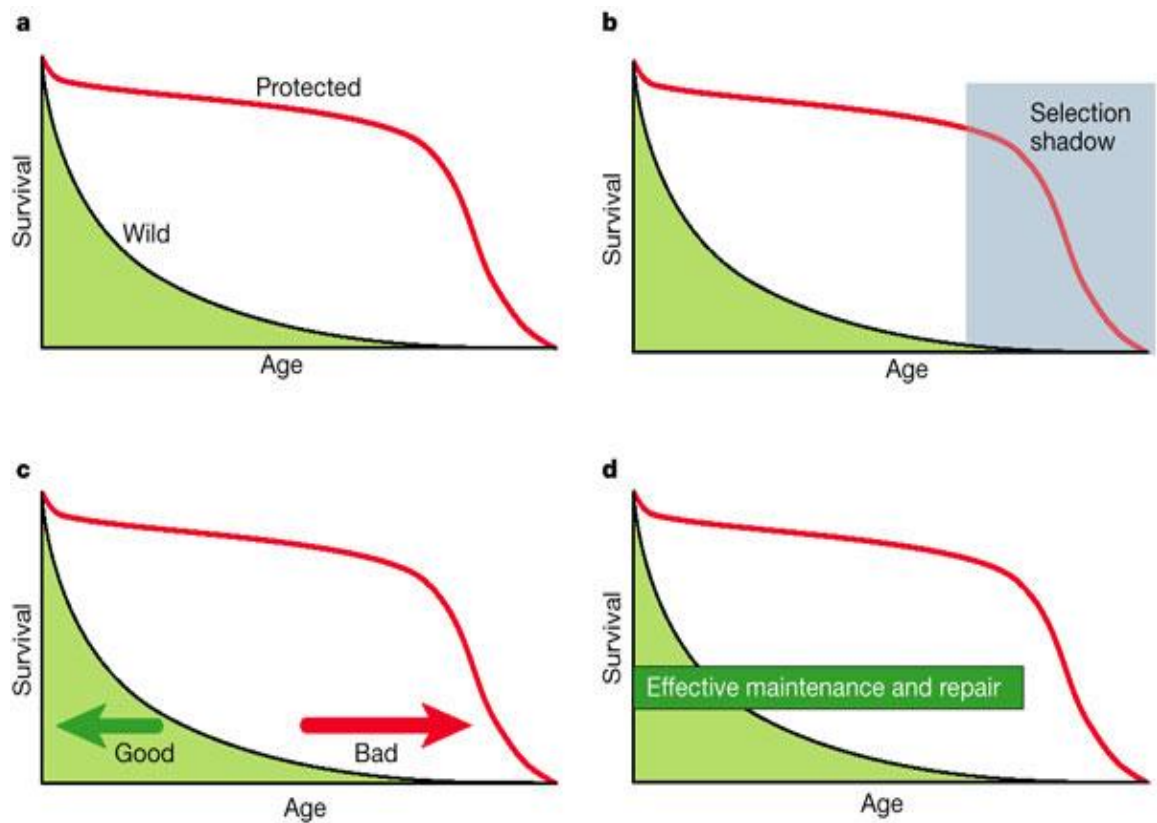
Chronological age is a measure of the period of time that an organism exists and proceeds at the same rate in all individuals of every species. On the other hand, the biological age reflects the physical state of an organism and does not proceed at the same rate in all individuals. Biological ageing is a result of tissue deterioration and progressive loss of function accompanied by a gradual decrease in fertility and increase in the probability of death. This tissue deterioration and loss of function is often responsible for the development of age-related diseases, which lead to higher morbidity and mortality.

5.1 THE EVOLUTION OF AGEING

There are different evolution theories to explain how natural selection is implicated in the development of the mechanisms governing ageing. One explanation is that programmed senescence-associated mortality has evolved in order to limit the population size, or enhance the turnover of generations, helping the population to adapt in changing environments. However, in the wild mortality is mainly determined by extrinsic hazards and occurs in younger ages, long before senescence-associated mortality arise (Figure 9A). Thus the evolution of genetic factors leading to programmed senescence-associated death appears unlikely. Due to high extrinsic mortality, only a small number of subjects in a population reach old ages, and thus, natural selection has limited opportunity to act, creating a natural selection “shadow” at old ages (Figure 9B). For this reason, not only are genetic factors leading to programmed death unlikely to be favoured, but nor will the accumulation of mutations with late-acting deleterious effects be opposed by natural selection. Therefore, given

that unselected deleterious mutations accumulate, the distribution of these mutations in a population is expected to be highly heterogeneous (Kirkwood & Austad 2000).

Figure I-9. Theories for the evolution of biological ageing. A) The theory of programmed senescence-associated ageing, B) The theory of natural selection shadow in later life, C) The theory of antagonistic pleiotropy, D) The disposable soma theory (Kirkwood & Austad 2000).



In 1957, Williams suggested another theory for the evolution of ageing, that of “antagonistic pleiotropy” (Figure 9C). According to this theory genes with beneficial effects early in life would be favoured by natural selection even if these same genes led

to a deleterious effect, such as senescence, later in life. A small beneficial effect of a pleiotropic gene early in life, before reproduction, grants a more important fitness advantage compared to the disadvantage of a deleterious effect later in life, even if that leads to premature ageing and death (Williams 1957). This theory led Kirkwood to suggest the theory of “disposable soma” (Figure 9D). This theory is based on the concept that metabolic resources are allocated between somatic maintenance and reproduction as effectively as possible. In that sense somatic maintenance is required for as long as the organism has a reasonable chance to survive in the natural environment. Extending the theory of Williams, Kirkwood suggested that an organism will benefit by investing any spare resource into preserving a good physiological condition until reproduction, rather than into a better repair capacity later on, even though that would result in less damage accumulation and slower ageing (Kirkwood 1977).

5.2 MOLECULAR PATHWAYS OF AGEING

Ageing is no longer thought to be an entropic process of tissue deterioration that occurs in a random way. We now know that the ageing process, like all biological processes, is subject to regulation by classical signalling pathways and that its role is partly genetically determined. Interestingly, ageing research has shown that mutations that slow ageing also postpone age-related disease (Kenyon 2010), which raises the possibility of combating many age-related diseases all at once by targeting ageing, their greatest risk factor.

Studies in organisms ranging from yeast to primates have revealed specific mechanisms that regulate ageing, which involve nutrient sensors and metabolic regulation and genome maintenance mechanisms and DNA damage signalling (Kenyon

2010). Of great importance is the metabolic flux through the insulin/insulin growth factor-1 (IGF-1) pathway and the downstream phosphoinositide 3-kinase (PI3K) signalling (Honjoh *et al.* 2009). Another pathway regulating ageing is the signalling of the kinase target of rapamycin (TOR). TOR kinase is a major amino-acid and nutrient sensor that stimulates growth and blocks salvage pathways such as autophagy when food is plentiful (Kapahi *et al.* 2004; Kaeberlein *et al.* 2005). Another important pathway is that of AMP kinase, a nutrient and energy sensor that activates catabolic pathways and represses anabolic pathways when the cell's AMP/ATP ratio rises (Greer *et al.* 2007). Also, sirtuins, the NAD⁺-dependent protein deacetylases have been demonstrated to play a key role. Sirtuins are important metabolic regulators that respond to dietary restriction (Rogina & Helfand 2004). Finally, mitochondria integrity seems to be crucial, since decreasing mitochondrial reserves and function has been documented in aged human and mouse tissues (Kenyon 2010; Sahin & Depinho 2010).

On the other hand, the preservation of genome integrity has a great impact in the regulation of ageing. Inefficiency of DNA repair (Rossi *et al.* 2007) or oxidative defence systems (St-Pierre *et al.* 2006), as well as shortened, dysfunctional telomeres (Wong *et al.* 2003) have been shown to accelerate premature ageing and diminish lifespan. In particular, there is increasing evidence pointing to age-associated telomere damage and p53-mediated DNA damage signalling as the driving force leading to senescence and apoptosis of tissue stem cell reserves and age-related tissue degeneration (Sahin & Depinho 2010).

As to what causes ageing, it is widely now accepted that ageing is caused by macromolecular damage and a prime candidate for causing this damage are the ROS produced during respiration. Evidence supporting this role of ROS comes from resistant to oxidative stress mutants who exhibit long lifespan (Sun *et al.* 2002), as well as from

the stress-resistant cells of mammalian species that live long (Kenyon 2005). In addition, a moderate inhibition of respiration has been shown to extend the lifespan in a wide variety of species (Kenyon 2010).

5.3 CELLULAR SENESENCE

The ageing process at the cellular level is expressed through senescence. Cellular senescence is seen as permanent growth arrest and appearance of a cell phenotype associated with impairment of cellular homeostasis, which under certain circumstances may lead to apoptosis. Senescence was first described by Hayflick and Moorhead in 1961. They discovered that primary human cells can only divide up to a finite number of times in culture. After this cell-specific limit of replications, now called the “Hayflick limit”, the cells undergo “replicative” senescence. Hayflick and Moorhead interpreting their results, suggested that the cells, in a way, remembered how “old” they were, i.e. how many times they have divided, linking the phenomenon of limited replicative capacity to ageing (Hayflick & Moorhead 1961; Hayflick 1965). However, at the time it was unclear how cells remember how “old” they are. In other words, the mechanism by which the cells register the number of cell divisions that has occurred and the mechanism that controls the trigger of replicative senescence once this cell-specific limit of replications is reached were unknown.

It is now widely accepted, at least in humans, that this role is served by the progressive shortening of telomeres with cell divisions until they reach a critical length, whereby telomere dysfunction is induced. The latter is considered to be the trigger of replicative senescence, by activating the tumour suppressor p53 (the role of telomeres is described in more detail in chapter 6 of the Introduction, page 92) (Allsopp & Harley

1995; Blackburn *et al.* 2006; Finkel *et al.* 2007). Stressful stimuli might also induce cellular senescence, which can be telomere-dependent or –independent. In the second case, cells may undergo an exogenously induced acute growth arrest, which occurs in particularly stressful conditions. This phenomenon is called stress or aberrant signalling-induced senescence “stasis” and is similar to telomere-dependent replicative senescence. However, the telomere-dependent replicative senescence is induced at the M1 or M2 phase of the cell cycle, while during “stasis”, growth arrest is induced at the G1 phase of the cell cycle (Shay & Roninson 2004).

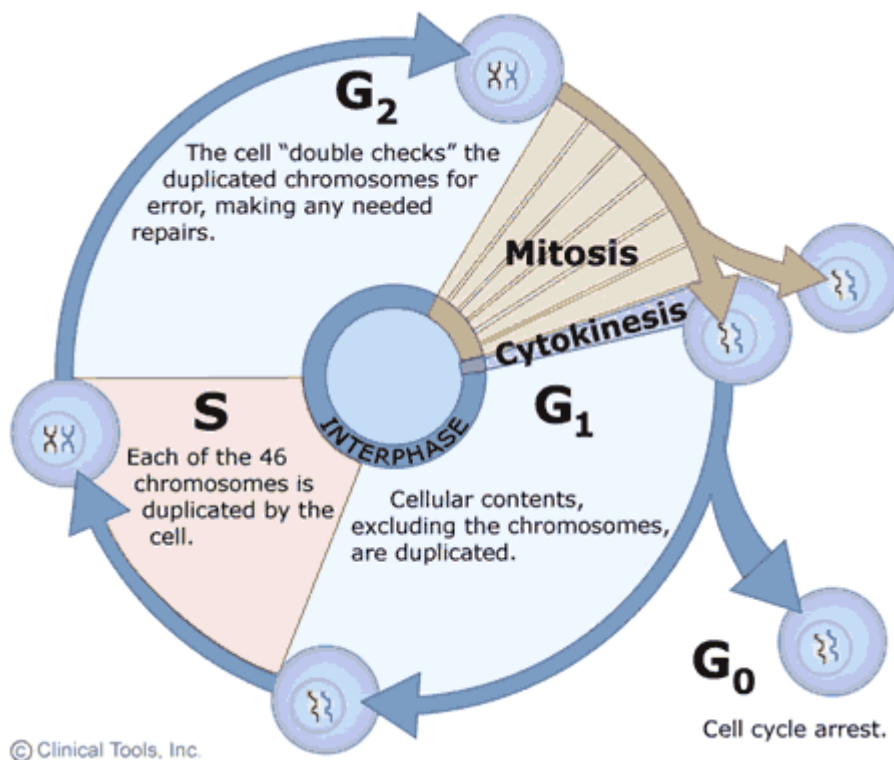
Senescence has probably developed initially as a mechanism of removal of cells which have accumulated genomic damage, protecting in this way against the formation of early onset cancers. Thus the evolution of senescence complies with the antagonistic pleiotropy theory on the evolution of ageing. According to this theory, natural selection would have favoured a mechanism, like senescence, which preserves genomic integrity and health in early life, even if the accumulation of senescent cells in later life would compromise normal tissue function and lead to ageing and age-related diseases (Shay & Roninson 2004).

5.4 EUKARYOTIC CELL DIVISION

The division of the eukaryotic cell is only a small part of the cell cycle and is called the “M” phase. During this phase mitosis (or meiosis in gametes) and cytokinesis take place, resulting in separation of the nucleus and cytoplasm respectively. The rest of the cell cycle consists of the G1 the S and the G2 phases (Figure 10). During G1 and G2 phases the cell grows, and during S phase DNA replication occurs. After a successful cell division, the new cell enters the G1 phase, where it enlarges and makes new

proteins. This phase is critical, as a checkpoint occurs at the end of G₁, just before the S phase, whereby the cell decides whether the conditions are favorable in order to divide. If the conditions are not favorable then the cell enters a non-dividing state called G₀. If the conditions are favorable the cell decides to commit to the cell cycle and divide, and it moves on to the S phase. After the DNA is replicated successfully the cell moves to the G₂, during which the cell prepares itself for division, and finally at the M phase the cell divides (Hunt 2002).

Figure I-10. The cell cycle (University of Leicester, Genetics Education Networking for Innovation and Excellence, Virtual Genetics Education Centre, <http://www.le.ac.uk/ge/genie/vgec/he/cellcycle.html>).

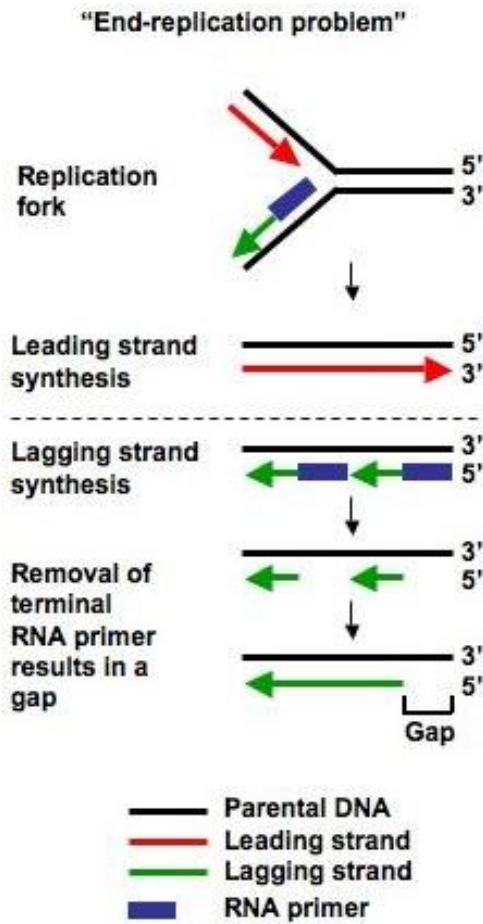


5.5 THE END-REPLICATION PROBLEM

Replication of DNA is governed by the interplay of various proteins, with DNA polymerase, the enzyme which catalyses the synthesis of new DNA strands, having the central role. The first step of the replication is the split of the two antiparallel strands of DNA to form the “replication fork”. The DNA polymerase can only add deoxyribonucleotides to the 3' hydroxyl terminus of a pre-existing strand. Thus, the 5' to 3' leading strand is synthesized continuously to the end of the DNA molecule using DNA polymerase. On the other hand, the 3' to 5' lagging strand cannot be copied continuously due to the incapability of DNA polymerase to add deoxyribonucleotides to the 5' hydroxyl terminus. Thus, the lagging strand is synthesised in discontinuous Okazaki fragments initiated by RNA primers. In the next step, these RNA primers are degraded, the internal gaps are filled and the Okazaki fragments are ligated with the help of DNA ligase. However, this enzyme can only join two strands together, which means that the terminal gaps left from the degradation of the RNA primers cannot be filled. Thus, in each DNA replication the terminal region will be left unreplicated (Figure 11). This phenomenon is called the “end replication problem”.

In 1971 Olovnikov proposed the “marginotomy” theory (Olovnikov 1971), according to which the incomplete replication of the very end sequences of chromosomes, during DNA replication provided an explanation for the Hayflick limit and the trigger of senescence. These distal ends of chromosomes constitute a special structure, called the telomere.

Figure I-11. The replication of DNA in eukaryotic linear chromosomes (Reactome, Telomere maintenance in Homo Sapiens http://www.reactome.org/cgi-bin/eventbrowser?DB=gk_current&ID=157579).



6. TELOMERE BIOLOGY

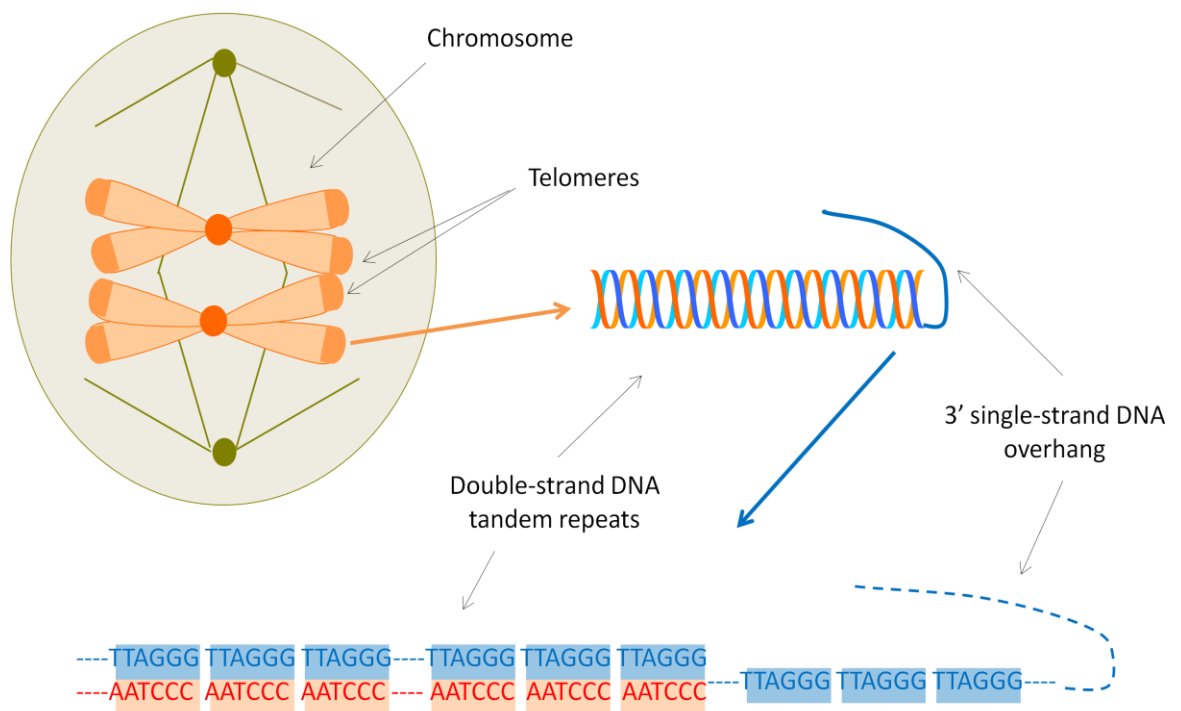
Telomeres (from the Greek words “telos”, meaning “end” and “meros” meaning “component”) are specialised DNA-protein structures at the extreme ends of eukaryotic linear chromosomes. Elizabeth Blackburn, Carol Greider and Jack Szostak won the Nobel Prize in Medicine in 2009 for discovering the molecular structure of telomeres, and how these protect chromosomes from degradation. Their discoveries shed light on a basic biological mechanism which stimulated research in a new exciting field aiming to explore the role of telomeres in normal ageing, cancer and age-related disease pathology.

6.1 TELOMERE STRUCTURE

The essential DNA sequences of telomeres, in most species, are tandem repeats of a short sequence unit. The number of terminal repeats at a telomere displays variability between species and between individuals of the same species. The initial mammalian telomere length is estimated to be at around 17 kb (de Bono 1998). In humans, telomere length is approximately 15 kb in sperm and 10kb in average in somatic tissues. The sequence of the tandem repeats is TTAGGG, thus the double-stranded telomeric DNA, consists of a G rich strand, which is always 5' to 3' and a complimentary C rich strand. Telomeric DNA is double-stranded for most of its length with a 3' G rich single-stranded overhang of a few to several repeats at the very end (150-200 bp). This 3' single-stranded overhang is usually tucked back invading the preceding double-stranded DNA (with a section of the double-stranded DNA also invading the preceding one) resulting in the formation of a loop, the so-called “T-loop”.

However, in dividing cells with active telomerase, telomeres are in a state of flux (Figure 12). Subtelomeric sequences, next to the terminal telomeric repeats, are degenerated telomeric sequences which also contain tandem repeats of shared telomeric sequences (Blackburn 2001; De Boeck *et al.* 2009).

Figure I-12. Schematic presentation of telomeres (Salpea & Humphries 2010).



In all vertebrates, including humans, the distal end of the telomeric DNA is part of a non-nucleosomal DNA-protein complex, with various structural and evolutionarily conserved DNA binding proteins taking part. The interaction between these proteins and the telomeric DNA sequences is essential to the function of telomeres. Two of the most important telomeric sequence-specific binding proteins in mammals are telomeric

repeat-binding factor 1 and 2 (TRF1 and TRF2). TRF2 contributes to the formation of the “T-loop”, which has been shown to protect the telomeric structure *in vivo*. Telomeres which do not form the T-loop are prone to non-homologous end-joining, and fusion (Blackburn 2001; De Boeck *et al.* 2009). In addition, the loss of TRF2 has been shown to activate the p53 pathway and induce senescence (Smogorzewska & de Lange 2002), while overexpression results in prevention of chromosomal aberrations (Karlseder 2003). On the other hand TRF1 binding to double-stranded DNA blocks replication by DNA polymerases (Smucker & Turchi 2001). The proteins which bind along the repetitive telomeric sequences assemble additional proteins to form a higher-order nucleoprotein. For example in humans, the telomeric proteins, TIN2, tankyrase and DNA-repair protein Ku, interact with telomeres via TRF1 binding. It has been proposed that tankyrase-mediated ADP-ribosylation of TRF1 opens the telomeric complex allowing access to the enzyme telomerase (Smith & de Lange 2000), and that TIN2 interacts with TRF1 to suppress telomere elongation in cells with active telomerase (Kim *et al.* 2003). A recent study has suggested that another human telomere protein Pot1 may bind to the 3' end of telomeres and stabilise them whilst in a flux or “open” state during various phases of the cell cycle (Colgin *et al.* 2003).

6.2 GENETICS OF TELOMERE LENGTH

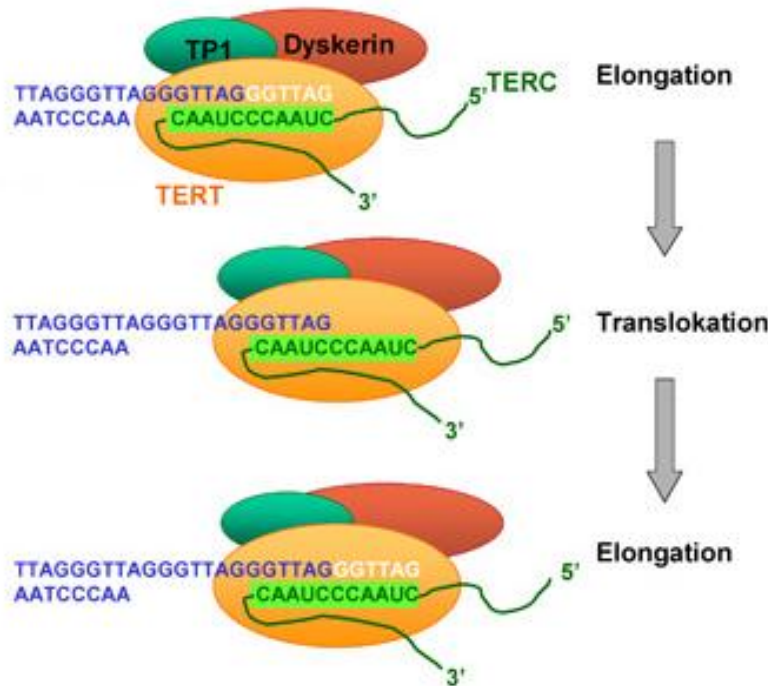
The consistent average length differences between species and chromosome arm differences within species indicate that mean telomere length is genetically determined (de Pauw *et al.* 2005). Telomeres have chromosome-specific lengths which are very similar between homologues of an individual and may differ among individuals. It has been suggested that this chromosome-specific pattern of telomere lengths is defined in

the zygote. Twin and family studies have provided evidence showing that heritability of the inter-individual variation in telomere length ranges from 44% to 80% (Slagboom *et al.* 1994) (Vasa-Nicotera *et al.* 2005; Njajou *et al.* 2007). Quantitative trait linkage (QTL) studies have mapped putative loci for telomere length to human chromosomes 3p26.1, 10q26.13, 12q12.22 and 14q23.2 (Vasa-Nicotera *et al.* 2005; Andrew *et al.* 2006; Mangino *et al.* 2008). Recent GWAS have identified SNPs affecting telomere length on chromosome 18q12.2 (Mangino *et al.* 2009) and chromosome 3q26 at a locus which includes *TERC*, the gene encoding the telomerase RNA component (Codd *et al.* 2010).

6.3 TELOMERASE

In 1984 Carol Greider working with Elizabeth Blackburn discovered the enzyme which forms telomeric sequences (Greider & Blackburn 1985). This enzyme prevents telomere shortening with cell division, which otherwise takes place due to the end replication problem. It is a ribonucleoprotein enzyme containing the rate-limiting catalytic unit of reverse transcriptase (TERT), which is highly conserved, and a RNA primer (TERC), which provides the template for the telomeric repeats to be synthesised and to fill in the gap in telomeres left unrepliated during DNA replication. During telomerase-dependent replication, the enzyme binds to telomeric sequences serving as primers on the 3' end of the G-rich strand of telomeres, so that the reverse transcriptase TERT elongates the G-rich strand using the TERC RNA as template. The complimentary C-rich strand is generated by lagging-strand synthesis, thus a G-rich single stranded overhang is always created (Figure 13) (Greider & Blackburn 1989; Lingner *et al.* 1997).

Figure I-13. Telomerase-mediated replication (University Medical Center Hamburg-Eppendorf, Department of Internal Medicine, www.uke.de/kliniken/medizinische-klinik-1/images_content/klinik-med-I/Telomerase_Abb2.jpg).



Telomerase is not expressed at the same level in all cell types. All foetal tissues have active telomerase at early stages of the development. However, some tissues like liver, lung, testis and spleen have active telomerase until the latest foetal age examined, while brain and kidney tissues only express it up to the 16th week and heart up to the 12th week (Ulaner & Giudice 1997). Most importantly, telomerase is active always in germ cells. The differentiated cells of somatic tissues in most cases do not express telomerase. Nonetheless, there is a low activity of telomerase in hematopoietic progenitor cells, activated lymphocytes (Hiyama *et al.* 1995), the basal layer of skin

(Harle-Bachor & Boukamp 1996) and cells of the premenopausal endometrium (Brien *et al.* 1997). This low activity though, is not sufficient to maintain the telomere length as long as in germ lines (Figure 14).

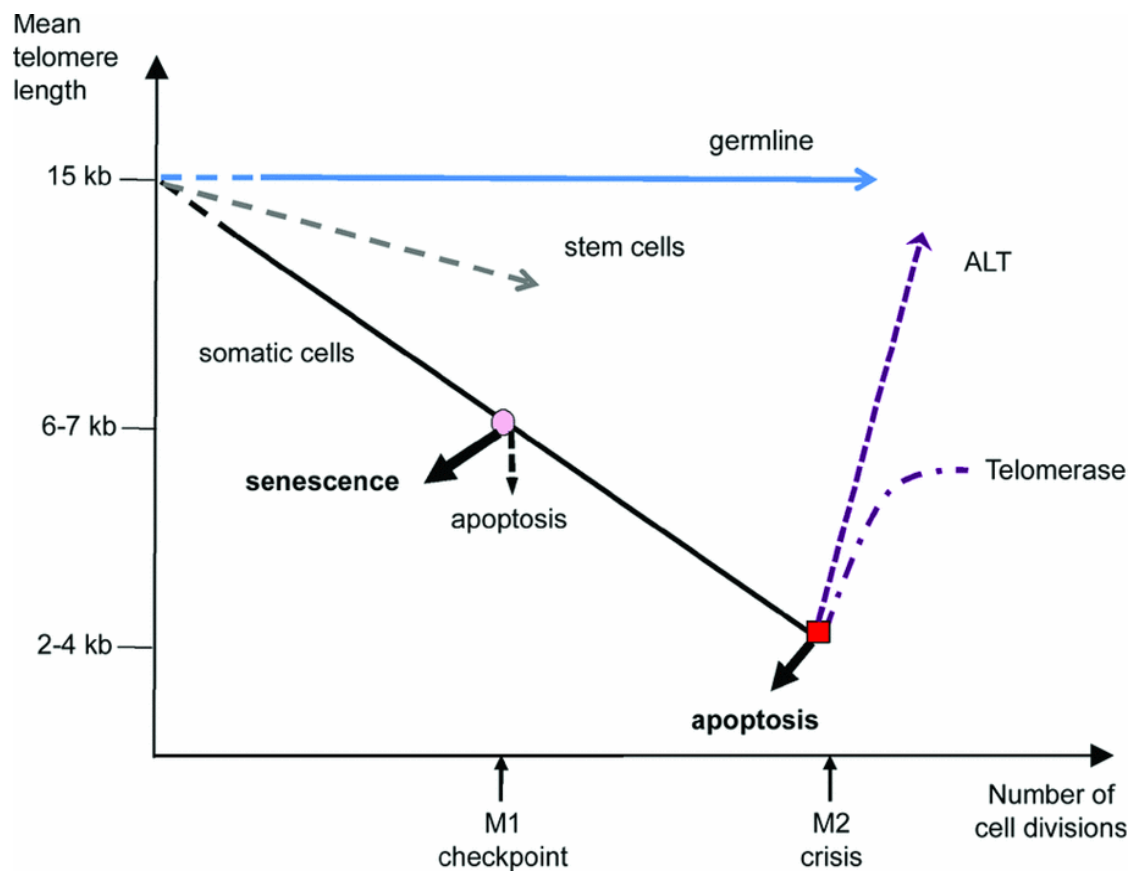
6.4 TELOMERE FUNCTION

Jack Szostak and Elizabeth Blackburn in 1982 revealed that telomeres constitute a fundamental mechanism offering protection to chromosomes from degradation throughout different species (Szostak & Blackburn 1982). More specifically, telomeres protect chromosome ends against cellular exonucleases and non-homologous end-joining, while distinguishing integer chromosome ends from DNA breaks. We now know that telomeres' biological function goes beyond the protection of chromosome ends from degradation or fusion, playing an important role in the cell's ageing process (Blackburn *et al.* 2006).

In somatic cells, where the enzyme telomerase is not expressed, the very end of telomeres is left unreplicated due to the end-replication problem. Thus the length of telomeres becomes shorter with each cell division, and once the length reduces below a critical value, the Hayflick limit, replicative senescence is induced (Sozou & Kirkwood 2001). Telomere length constitutes a mechanism of normal cell senescence (Allsopp & Harley 1995). This normal cell senescence is induced, at the cell cycle checkpoint M1, when the critically short length compromises the telomeric structure inducing DNA damage signaling pathways. Mutations or transformation events may allow cells with DNA damage (such as critically short telomeres) to escape the M1 checkpoint and extend their lifespan (de Lange 2001) (Figure 14). Another checkpoint exists later in the cell cycle, at M2, whereby the cells that escaped M1 usually undergo crisis at M2. In

rare cases of mutations, cells might also escape the M2 checkpoint and become immortal. There is an additional checkpoint later on at the G2 phase of the cell cycle, which is also sensitive to critically short telomeres (Jin *et al.* 1996). The regulator of the senescence response pathway to critically short telomeres is p53 (Itahana *et al.* 2001).

Figure I-14. The telomere hypothesis of cellular senescence and immortalization (Royle *et al.* 2009).



Immortality may be induced when cells, that do not normally have active telomerase, express this enzyme and elongate their telomeres (Figure 14). This telomerase-dependent immortalization occurs in the majority of human cancers. Nevertheless, in 10-15% of human cancers, cell immortalization is achieved through another pathway that does not require the activity of telomerase, the alternative lengthening of telomeres (ALT) pathway (Figure 14). In this case telomeres are elongated through homologous recombination between telomere repetitive DNAs. The ALT phenomenon has been observed only in cancer and genetically modified organisms, but it is possible that it represents the dysregulated version a normal process (Cesare & Reddel 2010).

A potential mechanism for telomere-mediated senescence is the transcriptional silencing of genes adjacent to telomeres. According to this postulated mechanism, called the “telomere positioning effect”, when the length of telomeres becomes very short, it causes the reversible silencing of certain adjacent gene/s. The telomere positioning effect has been shown in *Saccharomyces cerevisiae* but there is little evidence suggesting that this mechanism exists in humans (Wright & Shay 1992; Tham & Zakian 2002).

6.5 TELOMERE HYPOTHESIS IN AGEING

Telomere shortening in somatic tissues “counts” the number of cell divisions and induces senescence at a critical length. In this way the length of telomeres represents the replicative history and capacity of the cells, serving as a “mitotic clock”. The theory that telomere length is a mitotic clock regulating the cellular lifespan was proposed by Harley in 1992 (Harley *et al.* 1992). Since then, this theory has been

supported with increasing evidence. Telomere length has been shown to decrease with ageing of cells both *in vivo* and *in vitro*. More importantly, initial telomere length has been shown to predict the replicative capacity of cell culture generated from a wide range of donor ages. The donor age has also been shown to correlate with the cells telomere length (Allsopp *et al.* 1992; Vaziri *et al.* 1994; Chang & Harley 1995).

The rate of telomere shortening in telomerase negative cells is not only dependant on the number of cell divisions, but also on DNA damage. The processing of telomere ends to reconstitute 3' single-strand overhangs results in telomere loss due to the fact that DNA repair mechanisms, particularly for single-stranded DNA damage, are less efficient in telomeric DNA than elsewhere in the genome. The resulting accumulation of single-strand breaks along the telomere leads to additional DNA damage-dependent shortening during replication (Richter & von Zglinicki 2007). Hence, telomere shortening could serve as an indicator of replicative history and cumulative genomic damage of somatic cells (Petersen *et al.* 1998; Serra *et al.* 2000). Therefore, the length of telomeres indicates the replicative capacity and cumulative genomic damage of somatic cells, reflecting the tissue's "biological age".

In recent years, the role of telomere length in the pathology of CVD and diabetes, where tissue ageing and senescence play major roles, has attracted a continuously growing research interest.

7. TELOMERE LENGTH IN CARDIOVASCULAR DISEASE AND DIABETES

7.1 TELOMERE LENGTH IN CARDIOVASCULAR DISEASE

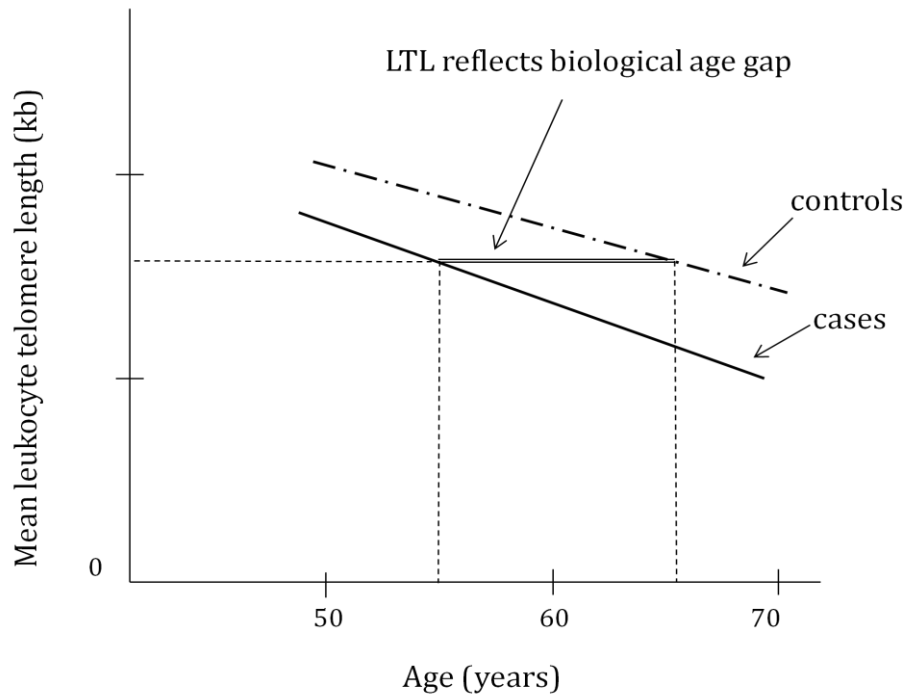
As discussed previously (paragraph 2.4.1 of the “Introduction”, page 51), CVDs, including ischaemic heart disease, heart failure, cerebrovascular disease, aortic aneurysms and renal vascular disease, are all diseases of maturity, closely related to ageing. CVDs mainly arise from the failure to preserve vascular wall homeostasis and normal function. This is usually a result of vascular tissue deterioration and impaired regenerative capacity during the ageing process. The accelerated age-associated changes in vascular structure and function lead to a number of pathologies, causally related to the early development of CVDs; These include endothelial dysfunction (Celermajer *et al.* 1994), atherosclerotic plaque progression (Eggen & Solberg 1968), arterial stiffening and remodeling (Lakatta 2003) as well as impaired angiogenesis (Rivard *et al.* 1999) and defective vascular repair (Weinsaft & Edelberg 2001).

At the cellular level, vascular ageing and the related pathologies possibly arise from the depletion of vascular progenitor cell reserves which impairs the tissue’s regenerative capacity and the accumulation of senescent endothelial and vascular SMCs (VSMCs) (Erusalimsky 2009). Senescent cells undergo distinct changes in gene expression that cause impairment of cellular function. Vascular endothelial and VSMC senescence and consequent dysfunction have been shown to contribute to atherogenesis. Specifically, senescent endothelial cells, which display impaired NO production and overexpress proteins such as interleukin-1 α , intercellular adhesion molecule 1 and PAI-1, characterise the pro-inflammatory and pro-thrombotic phenotype of the endothelium during atherogenesis (Samani *et al.* 2001; Minamino *et al.* 2002).

As expected from the description of telomere length as a marker of tissues biological ageing and a mechanism of cellular senescence (paragraph 6.4 of the “Introduction”, page 97), marked telomere shortening has been detected in endothelial cells of vascular regions susceptible to atherosclerosis (Chang & Harley 1995), while telomere shortening-induced SMC senescence has been shown to contribute to the development of atherosclerotic plaques (Matthews *et al.* 2006). Taking these together, it can be hypothesised that telomere length could serve as an indicator of vascular biological ageing associated with CVD development.

Previous studies have demonstrated an association of telomere length with health and longevity (Terry *et al.* 2008), atherosclerosis (Samani *et al.* 2001), vascular ageing as reflected by arterial stiffness (Benetos *et al.* 2001) and other degenerative diseases, such as dementia and Alzheimer (Honig *et al.* 2006). In this last study, mean telomere length was shorter among patients dying during follow-up than in those surviving. As a result, CHD patients have mean leukocyte telomere length (LTL) equivalent to that of 11 years older healthy subjects (Brouillette *et al.* 2003), which reflects the biological ageing of the vascular wall (Figure 15).

Figure I-15. Schematic presentation of LTL decrease with age in CHD cases (solid line) and controls (dashed line). The double line illustrates the biological age gap between cases and controls.



Short telomeres may be a primary abnormality that renders the organism more susceptible to CVD. However, reduced leukocyte length in CHD patients may also be a consequence of increased cell turnover induced by chronic inflammatory response underlying atherogenesis (Serrano & Andres 2004) or faster shortening due to oxidative stress caused by CHD risk factors (Aviv 2002).

7.2 TELOMERE LENGTH IN TYPE 2 DIABETES

T2D is also considered an age-related disease in terms of its onset and progression. Premature cell senescence has been postulated as an important cause and consequence of T2D and its complications (Sampson & Hughes 2006). The β cell senescence and apoptosis is an indispensable condition for the pathogenesis of T2D. On the other hand the complications of the disease are a consequence of senescent phenotypes in various tissues and organs, including the kidneys, the eyes, the peripheral nerves and the vascular vessels. Thus, it can be speculated that telomere shortening may be the underlying mechanism leading to senescence of beta cells and the onset of the disease, and/or to senescent phenotypes in other tissues contributing to the worsening of the disease.

These shorter telomeres can be either attributed to shorter length at birth in individuals predisposed to diabetes *or* to accelerated telomere loss during cell division caused by T2D risk factors in prediabetic conditions, *or* both. In support of this, shorter telomeres have been observed in circulating epithelial progenitor cells in patients with metabolic syndrome (Sato *et al.* 2008) and in other conditions of high oxidative stress, such as smoking and obesity (Valdes *et al.* 2005).

Accelerated shortening of telomeres during diabetes may also be the underlying mechanism leading to telomere-dependent genomic instability and consequent development of epithelial cancers, senescent retinal and renal phenotypes (expressed as diabetic retinopathy and nephropathy), as well as senescent vascular endothelial and smooth muscle cells (expressed as endothelial dysfunction and accelerated atherogenesis), all contributing to T2D complications (Sampson & Hughes 2006).

7.3 MECHANISMS

As described earlier (paragraph 6.2 of the “Introduction”, page 94), telomere length is documented to have a strong hereditary component (Graakjaer *et al.* 2004). More specifically, Graakjaer *et al.* (Graakjaer *et al.* 2004) demonstrated that any length alteration during the lifespan impacts equally on genetically identical chromosomes. Therefore, mean telomere length at a certain point in lifetime will be a function of the telomere length inherited at birth and the rate of shortening during life.

Increased oxidative stress is associated with many of the risk factors implicated in the pathophysiology of atherosclerosis including diabetes, hypercholesterolaemia, ageing, hypertension and smoking (Harrison *et al.* 2003). Diabetes, in specific, is characterised by increased oxidative stress (Orie *et al.* 2000) and oxidative DNA damage (Sampson *et al.* 2006). Telomeres are particularly prone to oxidative damage at the GGG sequence and consequent single-strand breaks. Telomere ends tend to reconstitute their 3' single-strand overhangs when broken, thus the accumulation of single-strand breaks along telomeres leads to an additional, DNA damage-dependent, shortening during replication (Richter & von Zglinicki 2007). Therefore, the rate of telomere shortening is considered to depend on the balance between intracellular oxidative stress and antioxidant defence. Thus, it can be speculated that increased oxidative DNA damage in CVD and T2D leads to telomeric DNA damage in many cell types, resulting in telomere loss accelerated at cell division, and consequently to senescent phenotypes in multiple cell types (Sampson & Hughes 2006).

Finally, chronic inflammation is an important feature characterizing and preceding both CVD and T2D (Pillarsetti & Saxena 2004; Hulsmans & Holvoet 2010). Pro-inflammatory cytokines released in chronic inflammation may lead to a more rapid

shortening of telomeres most likely through increased cell turnover (Serrano & Andres 2004) but also through the enhancement of free radical production (Hulsmans & Holvoet 2010).

8. GENERAL HYPOTHESIS

Despite the significant advances in identifying risk factors for CVD and T2D, these do not completely explain the inter-individual variability related to predisposition for premature disease. CVD and T2D development is clearly associated with ageing, but chronological age does not reflect the physical state of an organism and does not proceed at the same rate in all individuals. Thus there is a need for a marker of biological age in evaluating the risk for CVD and T2D and telomere length could serve as such.

As described earlier, CVD and T2D are thought to arise from a “common soil” of metabolic abnormalities. This common soil of abnormalities includes oxidative stress but lately chronic inflammation is also considered to be part of it. My hypothesis is that these abnormalities might lead to accelerated telomere shortening during life and extended cell senescence implicated in the pathogenesis of both diseases. Moreover, since there is a strong genetic component in determining telomere length, familial predisposition to CVD or T2D might in part arise from inherited short telomeres at birth leading earlier to senescent phenotypes and disease development.

8.1 WORKING HYPOTHESES:

1) Telomeres will be shorter in patients with CVD and/or T2D where premature tissue ageing and senescence are major features of the disease.

2) The short telomeres in patients are due to:

a) shorter lengths at birth in those predisposed to CVD/T2D

b) faster shortening during life due to oxidative stress caused by CVD/T2D risk factors.

c) faster shortening during life induced by the underlying chronic inflammatory response.

II. GENERAL METHODS

1. GENERAL STOCK SOLUTIONS

- I. *1M MgCl₂*: 20.33gr MgCl₂ dissolved in 100ml in dH₂O.
- II. *1M Tris pH 8.0*: 12.11gr Tris, made up to 100ml in dH₂O, Corrected pH to 8.0 and autoclaved.
- III. *Sucrose lysis mix*: 109.54gr sucrose, 5ml 1M MgCl₂, 10ml 1M Tris pH7.5, 10ml Triton-X-100, made up in 1000ml in dH₂O and stored at 4°C.
- IV. *0.5M Na₂EDTA*: 37.22gr EDTA, made up to 200ml in dH₂O. Adjusted with NaOH to pH 8.0.
- V. *10%SDS*: 10gr Sodium dodecyl sulphate, made up in 100ml in dH₂O.
- VI. *Nuclear lysis mix*: 1ml 1M Tris-HCl pH8.2, 2.34gr NaCl, 0.4ml 0.5M Na₂EDTA pH 8.0, 10ml 10%SDS, made up to 90ml in dH₂O.
- VII. *5M Sodium perchlorate*: 70.24gr sodium perchlorate, made up to 100ml in dH₂O.
- VIII. *TE buffer pH 7.6*: 1.21gr Tris, 0.37gr EDTA, made up to 1000ml in dH₂O.

All reagents were supplied by Sigma (Poole, UK).

2. DNA EXTRACTION

2.1 DNA EXTRACTION FROM WHOLE BLOOD WITH THE SALTING-OUT METHOD

2.1.1 Protocol

DNA was extracted from 5ml of potassium-EDTA or citrated anti-coagulated peripheral blood using the salting out method described by Miller with minor modifications (Miller *et al.* 1988). Before starting the extraction process in batches of 24 samples, the samples identification codes were carefully logged and entered into a database. This DNA extraction process involves several steps, which are described below:

1) Cell and nuclear lysis: Blood samples (10ml) were thawed and transferred into a labeled 30ml polypropylene tube. Twelve ml cold (4°C) sucrose lysis buffer (15ml) were added to each tube and mixed by hand inversion. Tubes were centrifuged at 4°C for 10 min at 1300g (Sorvall RC5 centrifuge using rotor SA-600). The supernatant was carefully discarded without disturbing the pellet; then the pellets were re-suspended in 20ml of sucrose lysis buffer. The samples were subsequently centrifuged for a further 10 minutes. Following centrifugation, the supernatant was discarded, and the pellet was re-suspended in 2ml of nuclear lysis buffer.

2) Deproteinisation: In the re-suspended pellet of the previous stage, 1ml of 5M sodium perchlorate was added and the sample was mixed by inversion. Samples were then left on a shaker for 15 min.

3) DNA extraction: In each tube, 2ml of cold chloroform (-20°C) was added and the sample was mixed by inversion. Samples were then centrifuged at 1300g for 3min at room temperature. Following addition of cold chloroform, the DNA from each sample had been partitioned into the upper aqueous phase within each tube. This upper aqueous phase was then transferred into a fresh 30ml polypropylene tube without disturbing the organic phase.

4) Precipitation and washing: Ten ml of cold (-20°C) 100% ethanol was added slowly in each tube and then mixed by inversion in order to precipitate the DNA. DNA from each tube was then “spooled” using a sterile Pasteur pipette. The “spooled” DNA was washed in 70% ethanol and transferred into a sterile labeled microtube containing 1ml Tris-EDTA (TE) buffer.

5) Dissolving the DNA: The microtubes were then sealed and incubated at 37°C overnight. The samples were then placed in a cold (4°C) cabinet where they were left for a period of at least four weeks to allow complete dissolution of DNA.

Troubleshooting: In cases where no visible DNA was precipitated after the addition of 100% ethanol, the samples were placed in the freezer overnight at -20°C. After that the samples were centrifuged at 1500g for 15 mins. The supernatant was discarded and a small DNA pellet was left. The tubes containing this small pellet of DNA were left to air dry before adding 0.5ml of TE buffer. Then the samples were left overnight at 37°C before re-suspending and transferring the contents into labeled microtubes. The samples were then placed in a cold (4°C) cabinet where they were left for a period of at least four weeks to allow complete dissolution of DNA.

Handling of DNA samples: Stock DNA samples were checked for quality and purity and then were standardised to a concentration of 15 ng/μl, and aliquoted into 96-

well deep Abgene's arrays. These "Stock Arrays" were stored at -20°C. Working arrays were also generated and stored at 4°C.

2.1.2 Standardisation of DNA stock arrays

The process of standardisation to 15 ng/μl is described below:

1) Transfer of DNA: An array sheet from the database of the study sample was prepared. 250μl original DNA was transferred from microtubes into 0.8ml labeled 96-well Abgene's arrays. Two people were required during the process of array making in order to double check that the ID numbers matched those of the prepared array sheet.

2) Preparing 1/10 dilution for the measuring samples' absorption: The 96-well array was spun-down at 3000rpm for 1 min before opening. Ten μl from each DNA sample was pipetted out into the corresponding well of a 96 well Costar UV plate containing 90μl dH₂O and mixed by re-suspending. Four no template controls were kept in wells 12E, 12F, 12G and 12H. The plate was then spun-down, before being placed in the plate reader.

3) Measuring absorption at 260nm and 280nm: This was performed using the Tecan GENios plate reader and the Magellan 3 software package. The 260/280nm filter slide was inserted into the excitation port. The corresponding absorption at 260 and 280nm was then recorded for each well in the plate and exported.

4) Extracted DNA quality control: The quality and purity of the extracted DNA was checked by the absorbance ratios of DNA/protein and DNA/organic contaminants, as measured with the Tecan GENios plate reader. DNA absorbs at A₂₆₀nm, protein at A₂₈₀nm, thus the samples with values of A₂₆₀/A₂₈₀nm ratio lower than 1.8 were excluded from further analysis. Furthermore, organic contaminants absorb

at 230nm (e.g. carbohydrates, peptides, phenol or other aromatic compounds), thus DNA samples with values of A260/230 ratio lower than 1.8 were also excluded from further analysis.

5) Standardisation to 15 ng/ μ l stock arrays using the Beckman Coulter Biomek 2000 Robot (Beckman-Coulter, High Wycombe, UK): After excluding the DNA samples that had not pass the quality control, the concentration data of each array from the plate reader were imported into the Robot. The Robot's software calculated the volume of DNA required for achieving a concentration of 15ng/ μ l when adding 750 μ l of 10mM Tris pH 8.0 dilution into each well. If any of the DNA volumes were above 200 μ l, then the volume was halved and respectively only 375 μ l of 10mM Tris pH 8.0 dilution was added to the respective wells of the array. If any of the DNA concentrations were near 15ng/ μ l, then the DNA was transferred neat. The new Abgene 0.8ml arrays and lids were labeled before placed to the robot. This way stock arrays, standardised to 15 ng/ μ l, were created and stored at -20°C.

6) Creating Working Arrays: Working arrays were made in labelled Matrix ScreenMate plates using Matrix ScreenMate cap mats. The stock array was spun-down before opening and 20 μ l of DNA were transferred to the bottom of the working arrays using filtered tips. Using filtered tips, 40 μ l of 3 mM Tris pH 8.0 was also added to each well in order to create a 1/3 dilution of the stock array i.e. a 5 ng/ μ l concentration in the working array (other dilutions can also be created following the same procedure). The working array was then left overnight to equilibrate before use.

2.2 DNA EXTRACTION FROM CULTURED HUMAN CELLS

Total DNA was extracted from cultured cells (normal human dermal fibroblasts) using the PUREGENE DNA kit (Qiagen, West Sussex, UK) with a minimum starting material of 200,000 cells per sample. To purify the DNA, this kit uses a modified salting-out precipitation method, which leads to a high purification and quality of DNA needed for sensitive downstream applications, such as PCR. This method was chosen for the extraction of DNA from the cultured fibroblasts of the experiment described in the “Fourth Result Chapter” (pages 317-354). The reason was mainly that with this method both high and low molecular DNA (like mitochondrial DNA) could be yielded, since one of the aims of the cell experiment of Result Chapter 4 was to also measure the mitochondrial DNA copies. In contrast, the in-house salting-out method, as used for the whole blood samples, included the “spooling of DNA”, which resulted in the extraction predominantly of high molecular DNA. This kit was also chosen due to other advantages which include the possibility of interruption and storing the partially purified samples during the DNA isolation via convenient stopping points and the possibility of parallel processing of multiple samples; useful advantages in order to meet the high demands of a large scale cell experiment, such as the one carried out in the present thesis (described in the “Fourth Result Chapter”, pages 317-354).

First, the sample of fibroblasts in PBS was centrifuged at 13,200 rpm for 5 seconds and the supernatant was discarded carefully, leaving approximately 20 μ l residual liquid with the pellet. The pellet was resuspended in 150 μ l Cell Lysis Buffer with the use of vortex. After adding 0.75 μ l of RNase A Solution and mixing the solution by inverting 25 times the cells were incubated at 37°C for 8 minutes (up to 1 hour is possible). Subsequently the cells were incubated on ice for 1 min and 50 μ l Protein Precipitation Solution was added and mixed by vortex. The samples were then

centrifuged for 1 min at 13,200 rpm. In the following step only the supernatant was poured into a new tube, where 150 μ l isopropanol were added and mixed in order to remove the proteins by precipitation. The samples were then centrifuged for 1 min at 13,200 rpm and the supernatant was discarded. Following this, the DNA was washed with 150 μ l of 70% ethanol by inverting several times, and centrifuged for 1 min at 13,200 rpm. The supernatant was discarded. After air drying (for 15 min), the DNA was dissolved in 25 μ l of DNA Hydration Solution and incubated at 65°C for 1 hr. The DNA concentration was measured using the Nanodrop ND-8000 (Nanodrop Technologies, USA), a full-spectrum UV/Vis 8-sample spectrophotometer. The same quality control was performed for these samples (described in paragraph 2.1.2 of the “General methods”, page 111) and the samples that did not meet the criteria were excluded from further analysis. Once the DNA concentration had been determined, DNA samples were stored for short-term at 4°C and for long-term at -20°C.

3. RNA EXTRACTION FROM CULTURED HUMAN CELLS

Total RNA was extracted from cultured cells (normal human dermal fibroblasts) soon after the cells were harvested (minimum starting material: 200,000 cells per sample) using the RNeasy Mini Kit 250 (Qiagen, West Sussex, UK). Such kits, due to the simplicity of their method, are useful alternatives to time-consuming and more hazardous methods, like the alcohol precipitation or methods involving toxic reagents such as phenol and/or chloroform. This kit is also designed for parallel processing of multiple samples, providing purified RNA that is ready for use in applications such as cDNA synthesis and real-time RT-PCR.

In the first step, the sample of fibroblasts in PBS was centrifuged at 13,200 rpm for 5 sec and the supernatant was completely removed by aspiration. Buffer RLT was then added to the pellet of fibroblasts at a volume dependent on the number of cells included in the sample (e.g. 350 μ l for 200,000 cells). The samples were then vortexed for 10 sec to enhance the lysis of the cells, and, therefore, to maximise the RNA yield. One volume of 70% (v/v) ethanol was added to the homogenised lysate and mixed well by pipetting. Subsequently, the whole solution was transferred to an RNeasy spin column, placed in a 2 ml collection tube and centrifuged for 15 sec at $\geq 10,000$ rpm. The flow-through was discarded and the collection tube was reused in the next step. For the first washing step, 700 μ l of Buffer RW1 was added to the RNeasy spin column which was centrifuged for 15 sec at $\geq 10,000$ rpm. The flow-through was discarded again and 500 μ l of Buffer RPE was added to the RNeasy spin column which was centrifuged for 15 sec at $\geq 10,000$ rpm for a second wash. The flow-through was discarded, the collection tube was reused and the membrane was washed once more with 500 μ l of Buffer RPE. In contrast to the previous washing step, this time the sample was

centrifuged for 2 min at $\geq 10,000$ rpm. This step ensured the drying of the spin column membrane, so that no ethanol was carried over during the RNA elution. Then the RNeasy spin column was placed in a new 1.5 ml collection tube and 40 μ l of RNase-free water was directly added to the spin column membrane. After a rest period of about 1 min the samples were centrifuged for 1 min at $\geq 10,000$ rpm in order to elude the RNA. RNA quality and concentration were assessed using the Nanodrop ND-8000 spectrophotometer (Labtech, East Sussex, UK). RNA samples with A260/A280 or A260/A230 ratio below 1.8 were excluded from further analysis. The samples of good quality were immediately stored at -80°C .

3.1 CDNA SYNTHESIS

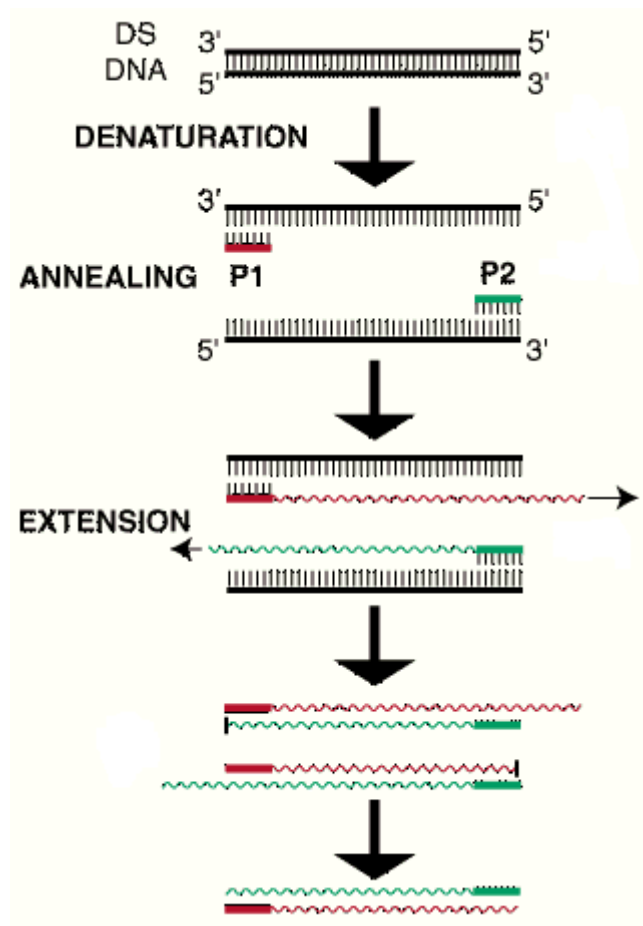
cDNA was synthesised by reverse transcription of total RNA extracted from cultured cells (normal human skin fibroblasts) using the Superscript III Reverse Transcriptase (Invitrogen, Paisley, UK) and random hexamer primers (Rd(N)6, GE Healthcare, Little Chalfont, UK), according to the manufacturer's instructions. In brief, 10 μ l RNA (100ng), 1 μ l random hexamer primers (50-250 ng) and 1 μ l of dNTP mix (10 mM of each) were mixed together in a nuclease-free eppendorf tube. The reaction was incubated at 65°C for 5 min and cooled quickly on ice. In the next step, 4 μ l first-strand buffer (5x) and 1 μ l of 0.1M Dithiothreitol (DTT) and 1 μ l of Superscript III reverse transcriptase (200 units) were added and the mixture was first incubated at 25°C for 5min and then at 42°C for 1 hr. The reaction was stopped by incubation at 70°C for 15 min. In order to remove completely the RNA from the newly synthesised cDNA, 1 μ l *E.coli* RNase H (EPICENTRE Biotechnologies, distributed by Cambio Ltd., Cambridge UK) was added to each sample, which were then incubated at 37°C for 20

min. The synthesised cDNA was subsequently used as a template for amplification in real-time PCR.

4. POLYMERASE CHAIN REACTION (PCR)

The Polymerase Chain Reaction (PCR) is based on the self-replicating nature of DNA, which allows short primers to be used in order to initiate synthesis of a target sequence in the presence of a DNA polymerase. As shown in figure 1, during the first step of the PCR, the double stranded DNA is heated up to a high temperature for a short period of time in order to denature DNA into single strands (denaturation step). Then a period of lower temperature follows, during which the primer oligonucleotides anneal to the complementary bases on the single strands of DNA, flanking the DNA target sequence (annealing step). Then the polymerase initiates the synthesis of a new complimentary strand at the 5' end of each primer using trisphosphate deoxyribonucleotides (dNTPs: dATP, dCTP, dGTP and dTTP) (extension step). This process is repeated many times during a PCR, resulting each time in the synthesis of new pieces of double stranded DNA. During the second cycle of this process, extension can occur on both the genomic DNA strands but also on the newly synthesised DNA pieces which are shorter and are limited in length precisely to the target sequence. In the end, this technique allows the use of a small initial amount of DNA to produce a large amount of copies of a specific sequence of interest. Typically, the DNA polymerase used in PCRs is derived from the bacterium *Thermus aquaticus* (*Taq*), which is not denatured by the fluctuating temperatures of the PCR.

Figure II-1. Schematic presentation of polymerase chain reaction (Source: Florida museum of natural history website, <http://www.flmnh.ufl.edu/cowries/amplify.html>).



P1: Forward primer, P2: reverse primer

Theoretically, each cycle of a PCR results in the doubling of the target sequence. In practice this exponential increase in the PCR product occurs only for a limited number of cycles while the reagents are still in excess. After a number of cycles the rate of amplification reaches a plateau phase, due to a number of reasons including the

saturation of the amplified target sequence, the eventual failure of the DNA polymerase and the consumption of dNTPs. After the plateau phase is reached subsequent cycles lead to eventual formation of primer-dimer and non-specific products.

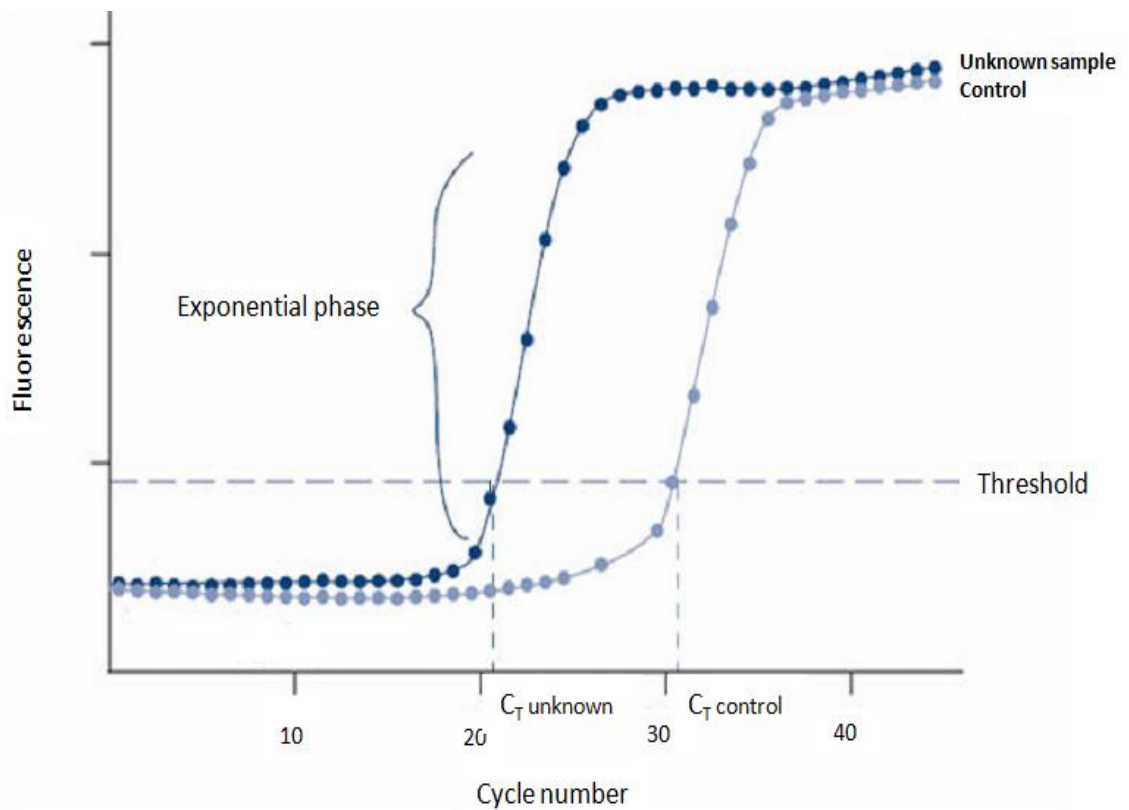
There are two kinds of PCR depending on the purpose it serves. These are the “end-point PCR” and the “real-time PCR”. The purpose of multiplying a specific sequence of interest using PCR is to facilitate its study. If the aim of the study is to detect a specific sequence and thus its multiplication will allow its determination, then the end-point PCR is employed. In this case, once the reaction is completed the PCR product is determined by either sequencing or gel electrophoresis or high resolution melting. Generally, methods that can determine the length or the base consistency of a PCR product are used depending on the purpose of the study. The end-point PCR is used for many applications such as the detection of mutations or polymorphisms, the detection of infectious agents and DNA fingerprinting.

On the other hand, when the target sequence needs to be quantified, then real-time PCR is employed. In a real-time PCR the amplification of the PCR product is measured in each cycle by the fluorescence emitted from a DNA intercalating fluorescent dye or from fluorescent probes. Through the monitoring of the amplification in each PCR cycle, the exponential phase of the PCR can be determined. Then at this phase the rate of amplification of the sequence of interest is compared to that of a control target sequence and the relative concentration is estimated. The real-time PCR also has many applications, such as the quantitation of mRNA expression levels and the measurement of mean telomere length, which will be described in detail in the “First result chapter” of the present thesis (pages 149-210).

4.1 REAL-TIME PCR

During the real-time PCR or quantitative PCR (qPCR), the fluorescence emitted during the reaction is recorded in each cycle. This fluorescence emission is proportional to the PCR product generated, thus by recording the amount of fluorescence produced it is possible to detect when the exponential phase of the reaction occurs. At this phase the rate of the fluorescence increase correlates directly to the amount of the initial target sequence. Usually a threshold of the fluorescence is set, and the earliest cycle that a sample reaches this threshold (Ct value, Figure 2), the higher is the number of initial copies of the target sequence in that sample relatively to the others in the same PCR run. This way the relative starting amount of copies of the target sequence is determined relatively to a control sample (normalised) in a real-time PCR.

Figure II-2. Schematic presentation of the fluorescence signal during real-time PCR.



The real-time PCR can provide quantification of the starting concentration of the target sequence either in relation to a reference sequence or absolute quantification. In the second case a standard curve is constructed by serial dilution of a DNA sample of known concentration which is included in the same PCR run. The methods of analysis of real-time PCR data are described in the “First result chapter”, paragraph 2.3 (pages 164-168).

An important aspect of the quantification of a target sequence with real-time PCR is the amplification efficiency. In theory, during the exponential phase of the PCR reaction the amount of the target sequence is doubled in each cycle. In reality this is not

quite true because the efficiency of the reaction is not 100%. The conditions of the reaction and the purity of samples are factors that play a major role in determining the performance of a PCR. Thus it is very important when optimising a real-time PCR to achieve as close to 100% efficiency as possible. This can be examined by carrying out a standard curve of serial dilutions of a DNA sample; the efficiency (E) can be calculated by the slope (M) of the curve with the formula:

$$E = 10^{-1/M}$$

From the standard curve, it can also be examined whether there is a linear correlation between the serial dilutions and the amount of target sequence copies measured, which indicates the accuracy of the quantification using the real-time PCR data. Thus, examining these estimates of a standard curve is considered a quality control of real-time PCR.

4.2 PCR FLUOROGENIC CHEMISTRIES

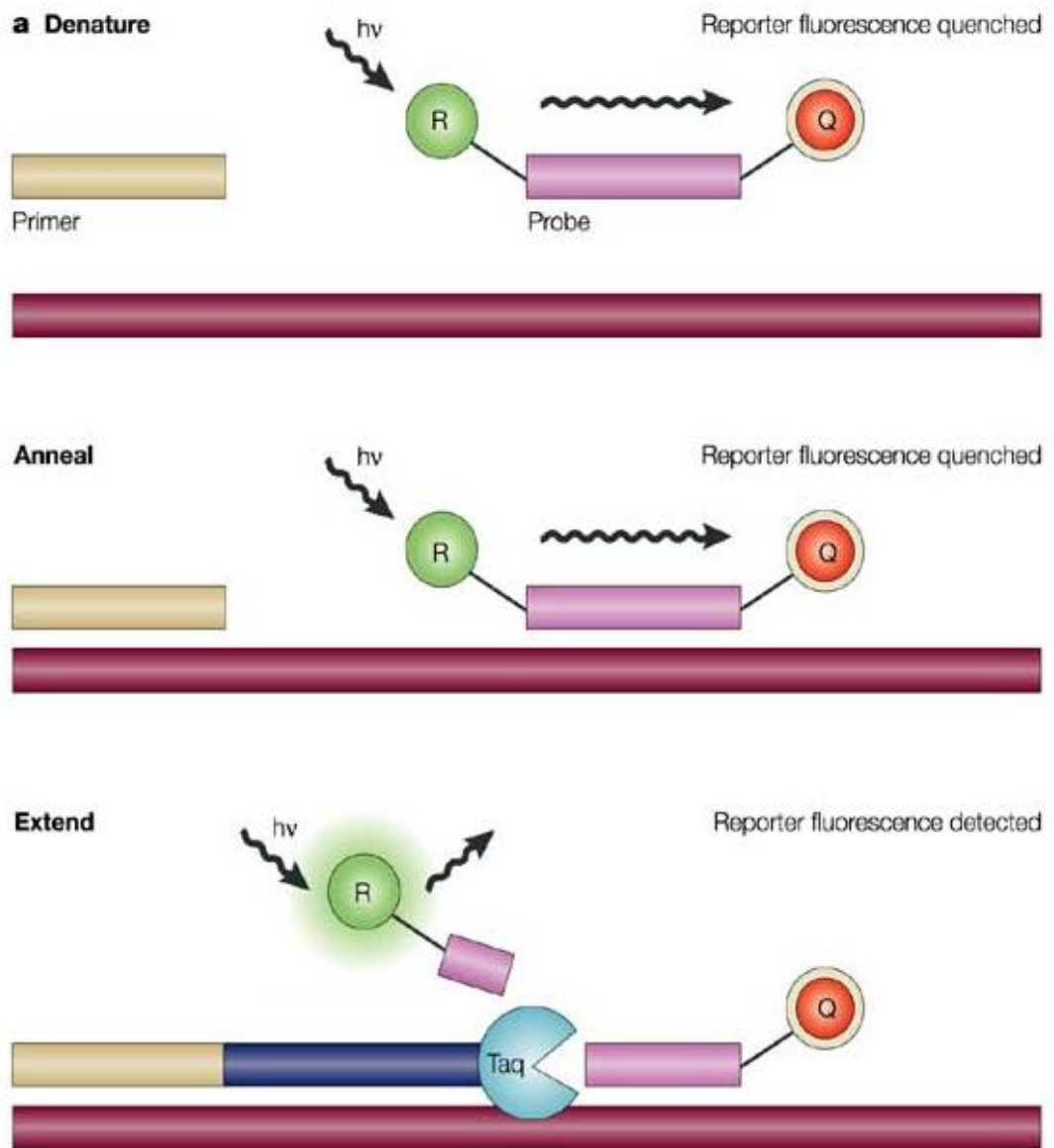
The detection of the PCR products is performed by the generation of a fluorescent signal from different kind of chemistries. These chemistries include intercalating fluorescent dyes such as SYBR Green, TaqMan probes, Molecular Beacons and Scorpions.

Intercalating fluorescent dyes: Such dyes (e.g. SYBR green) are the simplest chemistry for detecting the DNA product in real-time PCRs. These dyes exhibit little fluorescence when in solution, but emit a strong fluorescent signal upon binding to double-stranded DNA. Thus, as the number of copies of DNA increases during the reaction, the fluorescent signal increases. The advantages of such dyes are that they are

inexpensive, simple and sensitive; major disadvantages are the lack of specificity, since such dyes will bind to any double-stranded DNA generated during the PCR reaction and the need for extensive optimization (Gudnason *et al.* 2007).

TaqMan probes: Generally, fluorescent probes are pieces of DNA, labelled with a fluorescent dye, which are complimentary to the specific sequence of interest. The most commonly used type of these probes is the TaqMan. The TaqMan technology is based on the 5' nuclease activity of the DNA polymerase to hydrolyse an oligonucleotide which has been hybridised to the target sequence (Holland *et al.* 1991). The TaqMan probes are labelled with a fluorescent dye -the "reporter"- at the 5' end, and a molecule capable of quenching the reporter's fluorescence -the "quencher"- at the 3' end. This coupling of reporter and quencher prevents the emission of fluorescence. During PCR the TaqMan probe binds to the sequence of interest, and when the DNA polymerase acts to replicate the sequence where the probe is already bound to, the 5' nuclease activity of the polymerase cleaves the probe (Figure 3). This cleavage of the probe by the polymerase physically separates the reporter and the quencher and allows the fluorescence emission. Therefore, the fluorescence increases in each PCR cycle proportionally to the amount of probe cleaved, which is in turn proportional to the amount of target sequence copied. (Heid *et al.* 1996).

Figure II-3. TaqMan principle (source: (Koch 2004)).



(R): Fluorescent reporter, (Q): Quencher molecule, ($h\nu$): Excitation light

The advantages of TaqMan probe technology are that little optimisation is required compared to the intercalating fluorescent dyes, and that it can be used for multiplex assays. However, these probes are expensive, with a separate probe designed for each target sequence.

Molecular beacons: These are another commonly-used type of fluorescent probe, which are also small pieces of DNA, complementary to the sequence of interest and labelled with a fluorescent reporter and a quencher molecule on opposite ends. These probes when free (not hybridised) in solution are fold on to themselves forming a hairpin stem, which brings the reporter and quencher into close proximity and prevents fluorescent emission. When the probe binds to the sequence of interest, it takes up a linear conformation and the reporter and quencher are separated. This results in the desired increase in fluorescence. Molecular beacon probes are not cleaved by the polymerase but are just set free again and rebind to the target sequence in the next PCR cycle (Kostrikis *et al.* 1998).

Scorpions: The Scorpion probes are single oligonucleotides, specific for the sequence of interest, which again have a fluorescent dye attached to the 5' end and a quencher molecule at the 3' end. The Scorpion probes, when they are not hybridised, maintain a hairpin loop configuration which prevents fluorescence emission. The 3' fraction of the Scorpions contains a sequence which is complementary to the extension product of the primer. This sequence is linked to the 5' end of a specific primer (Scorpion primer) through a non-amplifiable monomer. After extension of the Scorpion primer, the specific probe sequence is able to bind to its complementary sequence within the extended PCR amplicon, thus causing the opening of the hairpin loop. This brings apart the fluorescent dye from the quencher and allows the fluorescence emission (Whitcombe *et al.* 1999).

4.3 TAQMAN TECHNOLOGY APPLICATIONS

4.3.1 Determination of expression levels by TaqMan assays.

Relative quantification of the mRNA of the genes of interest was performed with Taqman probes, after amplification and detection with the ABI prism 7900HT sequences detection system (Applied Biosystems, Cheshire, UK). The reverse transcribed cDNA was used as the template for real time PCR.

TaqMan probes and primers: Forward and reverse primers and probes for the genes of interest and selected housekeeping genes were ordered and supplied on demand from Applied Biosystems, Cheshire, UK. The probes used for the housekeeping genes were: ubiquitin C (*UBC*) (Hs00824723_m1), beta actin (*ACTB*) (Hs99999903_m1) and glyceraldehydes-3-phosphate dehydrogenase (*GAPDH*) (Hs99999905_m1). All probes were labeled at the 5' end with 6-carboxyfluorescein (FAM), and at the 3' end with a non-fluorescent quencher.

Real-time PCR protocol: Each PCR reaction had 5 μ l volume and consisted of 2.5 μ l Taqman Gene expression master mix (Applied Biosystems, Cheshire, UK), 0.25 μ l of (20x) assay on demand probes (containing the relevant primers), 1.25 μ l of RNase free water and 1 μ l of cDNA template. The thermal cycling was performed as follows: 50°C for 2 min, 95°C for 10 min, followed by 40 cycles of 95°C for 15 sec and 60°C for 1 min. The raw data of the real-time PCR were analysed with the S.D.S.2.1 Applied Biosystems software. The cycle threshold (Ct) was automatically set at the beginning of the exponential phase of each of the PCR amplifications, in each well on the 384-plate. The fractional PCR cycle number, at which the fluorescence emitted from a particular well rose above the threshold, was defined as the well's Ct value. Each sample was run

in triplicate and the mean Ct value used for analysis. The lower the Ct value, the higher the amount of cDNA –and therefore mRNA- in the sample tested.

Relative expression analysis: The relative quantification of the genes' of interest cDNA was performed using *UBC*, *ACTB* and *GAPDH* cDNA as endogenous control (housekeeping genes), to normalise for differences in total amounts of DNA that may be present in the samples. The BestKeeper software (Pfaffl *et al.* 2004) was used to check the stability of the three housekeeping genes. The software estimated the correlation between the expression of a particular housekeeping gene and a BestKeeper index (geometric mean of all the housekeeping genes) in a repeated pair-wise correlation analysis. Coefficient of correlation of 0.885 ($p < 0.001$) for UBC, 0.973 ($p < 0.001$) for β -actin and 0.936 ($p < 0.001$) for GAPDH were observed, indicating that the amplification profiles of all three housekeeping genes were stable. Therefore all three were used for standardising the expression levels (mRNA levels) of the target genes. The difference in Ct values of the gene of interest with the housekeeping genes was the basis for the relative expression analysis. The amount of mRNA of the target genes in the unknown sample was normalised to the housekeeping genes and then it was expressed relatively to a control sample included in the run. The relative quantification analysis was performed using the REST software (Pfaffl *et al.* 2002) which is based on the method of analysis described by Pfaffl (Pfaffl 2001).

4.3.2 TaqMan Genotyping

The TaqMan technology is also used for allelic discrimination of a gene variant. The genotyping of all the gene variants investigated in the present thesis was performed using the TaqMan technology. The method involves the inclusion of two TaqMan probes specific for each variant's allele and labelled with different fluorescent reporter

molecules. The allele-specific probes each contain a short sequence complementary to the allele and the surrounding sequence being investigated, a fluorescent reporter dye (labelled either VIC or FAM for each allele) at the 5' end, and a non-fluorescent quencher at the 3' end. During the PCR cycle, the pair of forward and reverse primer pair anneal to the target sequence DNA, along with the respective allelic probe. The DNA polymerase (AmpliTaq Gold DNA Polymerase, Applied Biosystems) replicates the disassociated DNA strands up to the allele-specific probe. If the probe is annealed to the correct allele for which it is fully complementary, then the 5' to 3' exonuclease activity of polymerase acts and cleaves the fluorescent dye molecule attached to the 5' end of the probe. Therefore as the amplification of the target sequence increases during the PCR cycles, so does the emission of VIC or FAM fluorescence depending on the genotype of the DNA sample. The ABI prism 7900HT sequences detection system (Applied Biosystems, Cheshire, UK) is able to detect the fluorescence in each sample post-PCR and determine the levels of VIC and/or FAM and thus determine the genotype of each DNA sample. In this way the Taqman method allows the high-throughput genotyping in 384-well plates.

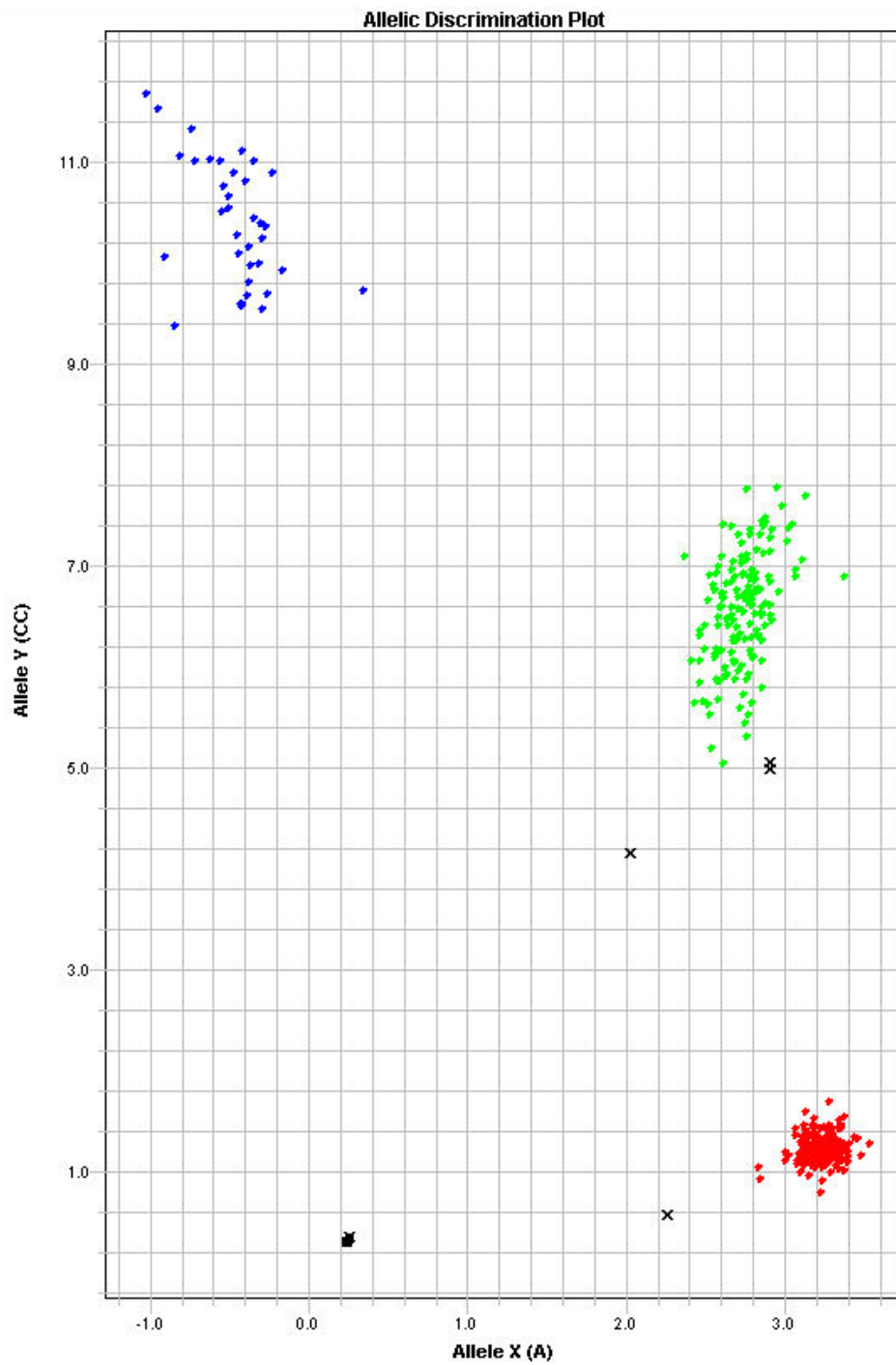
Protocol: The 96-well working arrays of standardised DNA were used to create 384-well plates of standardised DNA for genotyping with the TaqMan method. Using the Beckman Coulter Biomek 2000 Robot (Beckman-Coulter, High Wycombe, UK), DNA was transferred from four 96-well DNA plates to one Thermofast 384-well PCR plate (ABgene, Surrey, UK) and down-diluted to a 1.25 ng/ μ l DNA concentration with a final volume of 4 μ l. A data sheet detailing the samples layout in the plate and the unique plate identifier code was prepared and the plate was left to dry out overnight, and then stored at room temperature in a sterile paper bag.

Forward and reverse oligonucleotides and their respective labelled probe pairs were ordered using the 'Assay by Design' online service provided from Applied Biosystems (www.appliedbiosystems.com). A master mix consisting of 2.5 µl TaqMan Genotyping Master Mix (Applied Biosystems, Cheshire, UK), 0.125 µl of 40x Assay by Design, 2.375 µl Sigma dH₂O per sample was prepared and a 5 µl aliquot was added to each well using an 8-channel pipette. A clear plastic lid (ABgene, Surrey, UK) was applied to seal the plate and prevent excess evaporation and the plate was spun-down. Then the plate was placed on the Thermohybrid (Basingstoke, UK) and the following PCR profile was run: 95⁰C for 10 min, 95⁰C for 15s and 60⁰C for 1min for 40 cycles.

Allelic discrimination analysis: After the completion of the PCR run, the plate was "read" on the ABI prism 7900HT sequences detection system, and the SDS v2.1 (Applied Biosystems) software was used for the allelic discrimination. More specifically, the SDS v2.1 assigns genotypes automatically to each well of the plate by detecting the VIC or FAM fluorescence intensity. For example, in a homozygote DNA sample for the allele corresponding to the FAM probe, only this colour fluorescence will be detected and the software will call the sample homozygous for the respective allele. In a heterozygote DNA sample the machine will detect both probe's colours and thus will call it heterozygote. Figure 4 shows an example of the allelic discrimination plot produced by the software. The wells emitting only FAM fluorescence are shown on the top left corner of the plot and correspond to homozygotes for the mutant allele (CC) of that variant, those emitting both VIC and FAM are clustered in the middle of the plot and correspond to the heterozygotes (AC), and finally the wells emitting only VIC fluorescence are clustered at the bottom right corner of the plot and correspond to the wild-type homozygotes (AA). The software creates also a text output file with the genotypes assigned automatically to each well of the plate. This text file was converted

from 384-well to four 96-well plates in Microsoft Excel, and merged with the study database.

Figure II-4. Allelic discrimination plot.



5. TAGGING SNPS – HAPLOTYPE ANALYSIS

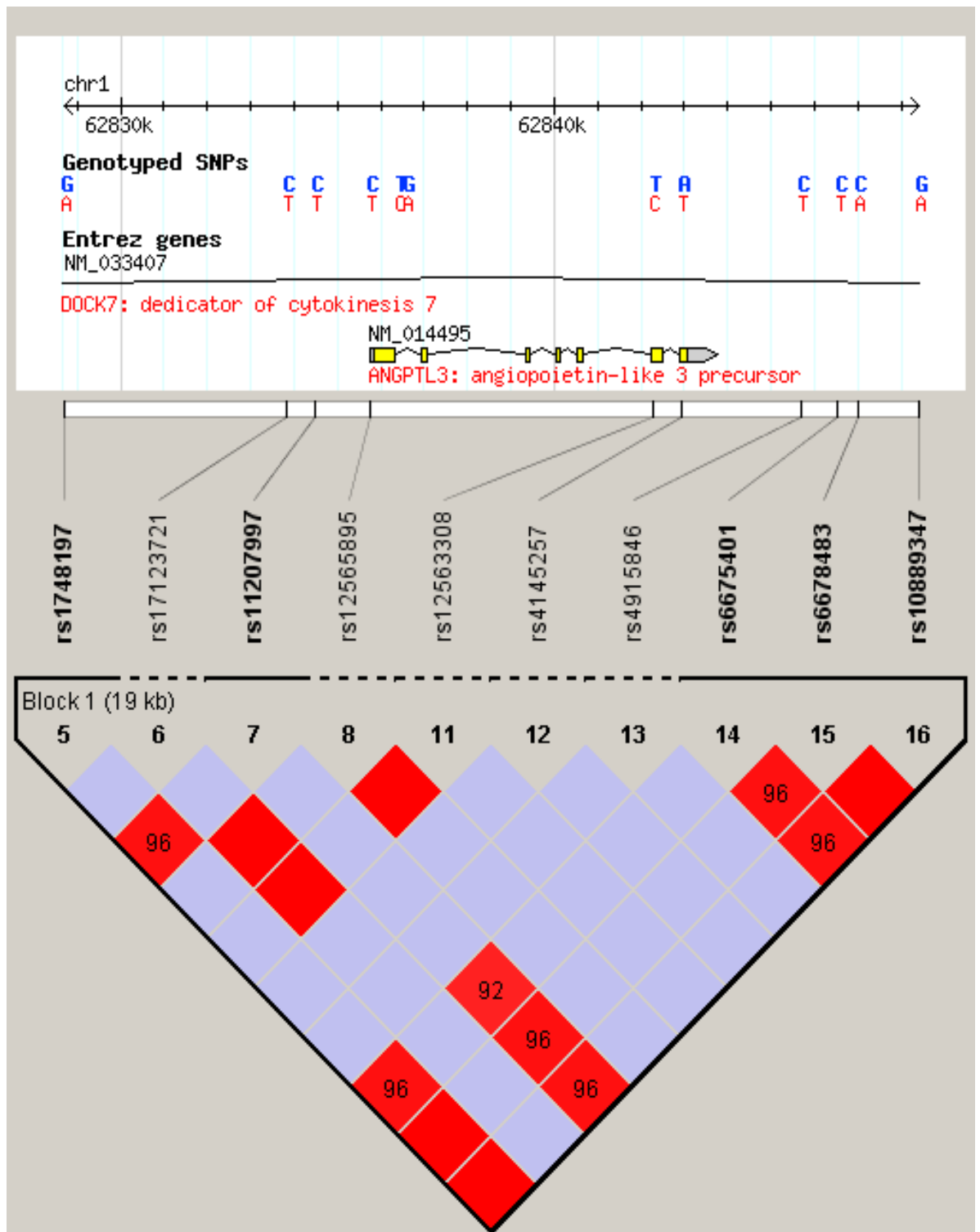
Having the technology for high throughput genotyping, genetic studies are now focusing in studying the whole variation across a gene of interest or across a greater genomic region, instead of single candidate variants. It is possible to identify the genetic variation without genotyping every SNP in a chromosomal region. This can be achieved with the genotyping of “tagging” SNPs and the subsequent haplotype mapping. The tagging SNPs are SNPs accounting for the whole variation in a specific genomic region. The selection of such SNP-markers is based on the linkage-disequilibrium of genetic variants in a chromosome region, which is essentially the non-random association of alleles at two or more *loci*. Due to this phenomenon several variants of a chromosome area are “linked”, and therefore have a high probability to exist and be inherited together in individuals of a particular ethnic group. The pattern of linkage disequilibrium varies across the genome (Reich *et al.* 2001), nonetheless studies suggest that discrete regions of high linkage disequilibrium, i.e. linkage disequilibrium blocks, exist and are characterised by limited haplotype diversity (Cardon & Abecasis 2003; Alper *et al.* 2006). Thus, there is no need to genotype all the variants located in a linkage disequilibrium block; instead, genotyping one of these variants accounts for -or “tags”- the variation of the whole block. This way, selecting and genotyping only a set of tagging SNPs -one SNP for each block of linkage disequilibrium- is sufficient for identifying the whole variation of that chromosome area and inferring its common haplotypes (Johnson *et al.* 2001).

5.1 GENOME VARIATION AND LINKAGE DISEQUILIBRIUM DATABASES

The HapMap Project: The project is a multi-country effort among Japan, US, Canada, Nigeria, China and UK to provide researchers with information on genes affecting health and disease. The information generated by the project was released into the public domain. The aim of the project was to determine the common genetic variants that occur in human beings, to describe where these variants are located in the human DNA, and how they are distributed among people within populations and among different populations. The project has genotyped over six million SNPs in trios of two parents and an adult child from the Centre d'Etude du Polymorphisme Humain (CEPH) samples, the Yoruban (West African) samples (YRI), the Japanese samples (JPT), and the Chinese samples (CHB). The data browser built by this project provides information on SNP genotype frequencies, the genome architecture and linkage disequilibrium blocks, as well as recombination rates. The HapMap data can be accessed at <http://www.hapmap.org/>. All data can be downloaded to and analysed with a specially designed software, called Haploview.

Haploview: Haploview is designed to provide a comprehensive set of tools for haplotype analysis (Barrett *et al.* 2005). Haploview currently provides marker quality statistics, linkage disequilibrium haplotype block analysis, population haplotype frequencies, single marker association statistics, tagging SNPs selection and visualisation of the results in a user-friendly format. As shown in Figure 5, the linkage disequilibrium plot generated by Haploview shows the extent and pattern of the degree of linkage disequilibrium between the SNP-markers with the background colour denoting a scale of logarithm of odds (LOD) score for linkage disequilibrium.

Figure II-5. An example of Haploview linkage disequilibrium plot with a selected set of tagging SNPs.



Legend: This figure shows a linkage disequilibrium (LD) plot generated by Haploview. On the top of the picture there is a schematic presentation of the gene of interest, showing also the position of the selected SNPs in this genomic region. In the large triangle, below the rs numbers of the selected SNPs, each square's color denotes the degree of linkage disequilibrium between the SNPs found at the end of the line of squares starting from this particular square. E.g The degree of linkage disequilibrium between the SNPs rs1748197 and rs10889347 is very high as denoted by the bright red color of the square, which means that these two SNPs are in almost complete linkage disequilibrium. In the case of the rs4915846 and rs4145257, the blue color of the square denotes a low degree of linkage disequilibrium between them.

Haploview is fully compatible with data downloaded from the HapMap project and the Perlegen Genotype Browser and can analyze thousands of SNPs in thousands of individuals. Haploview is available for download from: <http://www.broad.mit.edu/mpg/haploview/>.

Genome Variation Server (GVS): The GVS database provides a quick access to all genotype data found in both the dbSNP and HapMap databases but also from several other genome projects. The current version of the GVS database contains 4.5 million variations with corresponding genotype data. The GVS includes a set of analysis tools which provides the researcher with data on linkage disequilibrium blocks in the chromosome area of interest, and the set of tagging SNPs needed for identifying the variation in a region of interest, based on the combined genotype data of several genome projects. The GVS also provides visualisation tools like linkage disequilibrium plots. The GVS database is hosted by the SeattleSNPs Program for Genomic Applications (PGA) and is available online at <http://gvs.gs.washington.edu/GVS/>.

5.2 HAPLOTYPE DATA ANALYSIS

THESIAS: The objective of the THESIAS program is to test the haplotype effects in association studies with unrelated individuals. This program is based on a maximum likelihood model (Tregouet & Tiret 2004) and is linked to a stochastic version of the EM algorithm (Tregouet *et al.* 2004). Thus, THESIAS allows the simultaneous estimation of haplotype frequencies and of their associated effects on the phenotype of interest. Quantitative, qualitative, categorical and survival analysis as well as covariate-adjusted haplotype effects and interactions analysis can be carried out.

6. HUMAN CELL CULTURE

Cell culture was performed in a specially-built tissue culture suite, which is a protected environment with air filtration and two door locks before entry. Gloves and cell culture dedicated laboratory coats were worn at all times. Sterility was maintained by handling all open culture media, culture-ware and liquids within a class II microbiological safety cabinet with unidirectional laminar flow (Envair UK Ltd). Surfaces and equipment for use within the laminar flow hoods were cleaned with 70% ethanol solutions. All solutions and materials used in the laminar flow hoods had been previously sterilised by autoclaving. Cell contaminants, such as media used for growth, were removed to 1% Virkon-containing vessel and stored for at least twenty-four hours before disposal. Galaxy R CO₂ incubators (Wolf Laboratories) humidified and set to 5% CO₂, 37°C were used for cell incubation. The cells cultured in these conditions were Normal Human Dermal Fibroblasts (NHDF) from juvenile foreskin for the purposes of the work described in the “Fourth result chapter” (pages 317-354).

NHDF cells were cultured first in T-75 and then transferred in T-175 tissue culture flasks (Sarstedt, Nümbrecht, Germany). The NHDF cells were purchased from PromoCell GmbH (Heidelberg, Germany) and were cultured in fibroblast growth medium lacking ascorbic acid (FGM –AA) (PromoCell GmbH, Heidelberg, Germany) supplemented with 2% Foetal Calf Serum (FCS).

6.1 GROWING OF HUMAN CELLS

Each flask of cultured cells was viewed everyday under the inverted microscope and when it reached >80% confluence, the cells were split into new flasks. First the media was removed by aspiration, the monolayer of cells was washed with magnesium

and calcium free phosphate buffer saline (PBS) for at least 30 seconds to remove any serum containing medium, which contains trypsin inhibitors. The cells were detached using the Sigma-Aldrich detach kit for fibroblasts (Sigma-Aldrich, Steinheim, Germany). In more detail, the PBS was removed by aspiration and a minimal volume of trypsin, which digests the cell adhesion proteins, was added (i.e. 4 ml for a T-175 flask). The trypsin solution was incubated with the cell monolayer for 2 min at room temperature and then 2 ml of trypsin inhibitor (TNS), provided with the kit, were added. The cell suspension was transferred to a sterile 15 ml conical centrifuge tube and centrifuged at 1,000 rpm for 5 min. After discarding the supernatant, the cells were diluted in 10 ml of fibroblasts growth medium. 40% of the cells harvested (i.e. 4 ml of the re-suspended cells in medium) were seeded into a new T-175 flask where 22 ml of fibroblast growth medium were also added. The rest (60%) of the cells harvested were used for DNA and RNA and all other required measurements, according to the experiment carried out. The number of cells was calculated in a 1 in 10 dilution by the cell counter Sysmax CDA-500 (Norderstedt, Germany) in order to estimate the population doublings using the following formula:

$$PD = [\ln(\text{number of cells harvested}) - \ln(\text{number of cells seeded})] / \ln 2$$

6.2 FREEZING OF HUMAN CELLS

Cells were frozen for long-term storage in a way that prevented senescence and reduced the risk of contamination. For this purpose, the cryoprotective agent dimethylsulfoxide (DMSO), was used in conjunction with medium and the cells were stored at -70°C or lower. DMSO properties include the decrease of the cells' freezing point and the gradual freezing process of the cells. These properties reduce the risk of

ice crystal formation and cell damage. From the cells harvested a small portion (~100,000 cells) was re-suspended in growth medium containing 10% DMSO (v/v), mixed thoroughly and stored in 2 ml cryovials. These cryovials were then placed in a special case that allows the gradual freezing of the cells in a -70°C freezer overnight. The next day the cryovials were moved into liquid nitrogen for long-term storage.

6.3 MEASUREMENT OF CELL CULTURE APOPTOSIS AND NECROSIS

Assay principle: The percentages of apoptosis and necrosis of the cultured cells were assessed using the Annexin-V-FLUOS-Staining Kit (Roche Diagnostics GmbH, Penzberg, Germany) and flow cytometry. This method is based on the translocation of phosphatidylserine at the cell surface during the early stages of apoptosis (Creutz 1992; Fadok *et al.* 1992). The phosphatidylserine moves from the inner part of the plasma membrane to the outer layer, and becomes exposed at the external surface of the cell, where it can be specifically recognised by macrophages (Fadok *et al.* 1992). The recognition and phagocytosis of apoptotic cells protects organisms from the exposure to cellular compounds leading to inflammation, which mostly accompanies necrosis. Annexin V is a Ca^{2+} -dependent phospholipid-binding protein with a high affinity for phosphatidylserine. Thus it can be used as a probe for phosphatidylserine translocation to the outer part of the cell membrane and therefore for the detection of apoptotic cells (Vermees *et al.* 1995). On the other hand, necrotic cells also expose phosphatidylserine due to the loss of membrane integrity, and need to be differentiated from the apoptotic cells. This can be achieved with the use of propidium iodide, a DNA stain which is used for dye exclusion tests. Necrotic cells lose their integrity completely and leak, exposing their DNA molecules to external factors. Propidium iodide (PI) stains the exposed DNA

of necrotic cells allowing the discrimination of necrotic cells from the apoptotic ones. Annexin V-Fluorescein and PI staining emit at different wavelengths (i.e. Annexin V-Fluorescein at 518 nm and PI at 617 nm), thus a specific and easy discrimination of the two cell states can be performed with the use of flow cytometry.

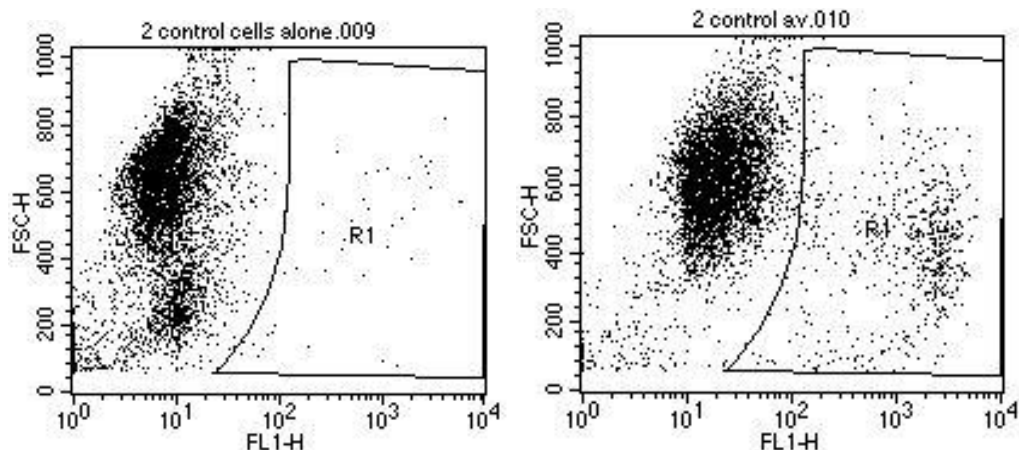
Procedure: Before each experiment, an Annexin-V-FLUOS labeling solution a PI labeling solution and a combination of Annexin-V-FLUOS and PI labeling solution were prepared according to the manufacturer's protocol. In the next step $\geq 6 \times 10^5$ cells were washed with PBS and distributed in 3 different sterile tubes. These were centrifuged at 1,000 rpm for 5 min and the three cell pellets were re-suspended in 100 μ l of the pre-prepared Annexin-V-FLUOS labeling solution, 100 μ l of the pre-prepared Proidium iodide labeling solution and 100 μ l of the pre-prepared Annexin-V-FLUOS/Proidium iodide labeling solution. After incubation at room temperature for 15 min, 0.5 ml Incubation Buffer per 10^6 cells was added and the cells' fluorescence was analyzed on the flow cytometer.

Flow cytometry: a FACSCalibur (Becton-Dickinson) flow cytometer using 488nm excitation with a 530nm filter for fluorescein detection and a 585nm filter for PI detection. Electronic compensation of the instrument was performed before each measurement. A FACSCalibur flow cytometer (Becton-Dickinson, Franklin Lakes, USA) was used for the flow cytometry analysis. The excitation wavelength was set at 488 nm, with a 530nm filter for green fluorescence (Annexin V-Fluorescein) detection and a 585nm filter for red fluorescence (PI) detection. The emitted fluorescence was collected on FL1 and FL2 channels, respectively. In each measurement, a total of 5000 cells were analyzed. Data were acquired and analysed with the Cellquest Pro software (Becton Dickinson Biosciences, Oxford, UK).

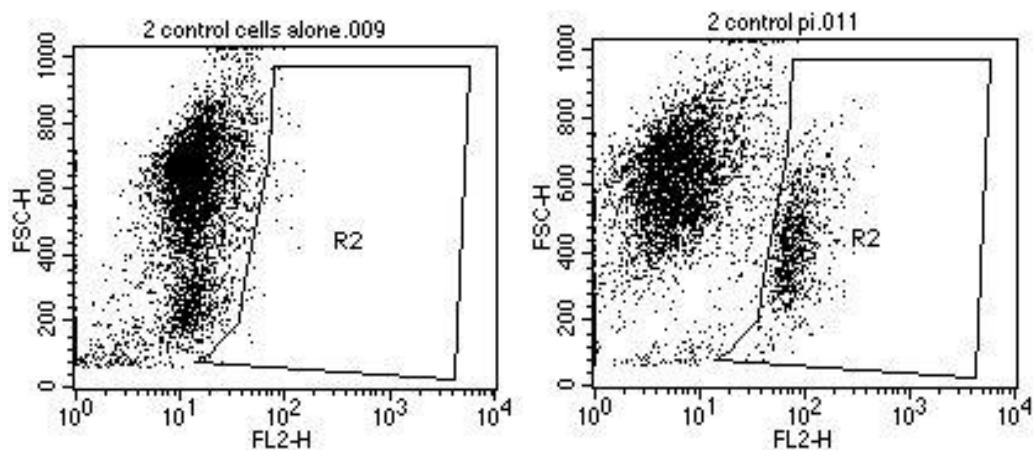
To exclude cellular debris from the analysis and to establish the cells' size, forward (indicating the size of cells) and side (indicating the granularity of cells) scatters were used. Since for the detection of apoptotic and necrotic cells a dual labeling was used, there was a need for electronic compensation of FL2 (detecting the PI fluorescence), in order to exclude overlapping of the two emission spectra. Thus for each sample a measurement with Annexin-V-Fluorescein labeling alone and a Propidium iodide labeling alone were acquired before analysing the cells' with dual labeling, as shown in figures 6A and 6B, respectively. The compensation level was increased to the point that the cells incubated with Annexin V-Fluorescein only did not emit fluorescence detected by the FL2 and *vice versa*.

Figure II-6. A) Cells from the same flask with (on the left) and without (on the right) Annexin V-Fluorescein labeling. The cells shifted into the gate R1 are Annexin V-Fluorescein positive i.e. apoptotic cells. B) Cells from the same flask with (on the left) and without (on the right) PI labeling. The cells shifted into the gate R2 are PI positive i.e. necrotic cells.

A)



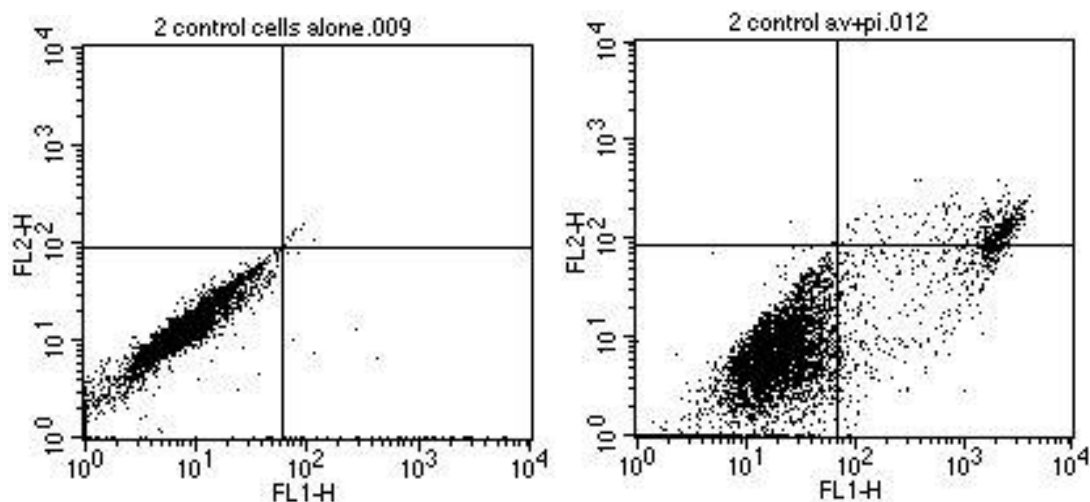
B)



FSC-H: forward scatter (indicating cell size); FL1-H: green fluorescence (Annexin V-Fluorescein) collected in channel 1. FL2-H: red fluorescence (PI) collected in channel 2.

The percentage of apoptotic and necrotic cells was determined with the dual labeled cell samples. Plots of FL1 against FL2 revealed the Annexin V-Fluorescein positive (apoptotic) and PI positive (necrotic) cells as shown in figure 7. The events accumulating at the bottom right quadrante represent the early apoptotic cells, events at the top right quadrante represent the late apoptotic cells and events at the top left quadrante represent the necrotic cells. The cells at the bottom left quadrante are not stained with either probe, thus these are the viable cells. The percentage of early or late apoptotic and necrotic cells were calculated from the events counted in each of the quadrantes of the FL1-FL2 plot.

Figure II-7. Plots of FL1 against FL2 showing the distribution of the cells according to their fluorescent signals. The left plot shows cells which have not been stained, and the right plot shows cells with the double staining of Annexin V-Fluorescein and PI.



FL1-H: green fluorescence (Annexin V-Fluorescein) collected in channel 1. FL2-H: red fluorescence (PI) collected in channel 2.

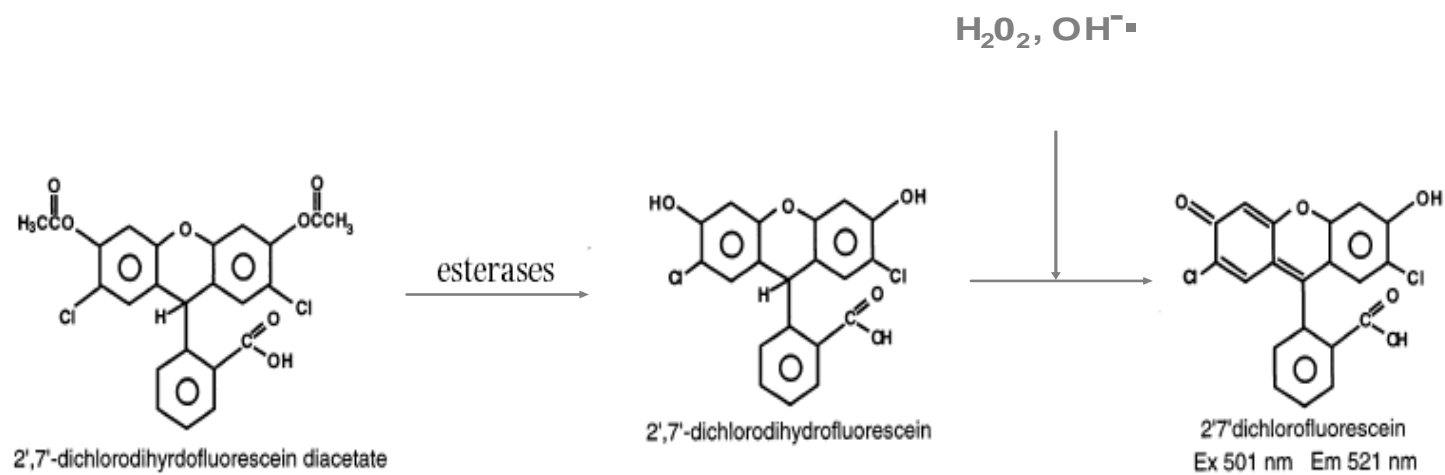
6.4 MEASUREMENT OF INTRACELLULAR REACTIVE OXYGEN SPECIES

Assay principle: Intracellular ROS content was measured using the fluorescent probe 2',7'-dichlorodihydrofluorescein (H₂DCFDA) (Invitrogen, Molecular Probes, Inc., Eugene, USA). Chemically reduced and acetylated forms of 2',7'-dichlorofluorescein (DCF), such as the H₂DCFDA, are widely used as cell-permeate indicators for a large range of ROS (e.g. hydrogen peroxide, peroxy radical and peroxy nitrite anion) (Oyama *et al.* 1994; Jakubowski & Bartosz 2000). These derivatives passively diffuse into cells, where the intracellular esterases cleave off the diacetate group and this yields a charged form of the dye (H₂-DCF) which is better

retained by the cells compared to the parent compound. In the presence of cellular ROS, H₂-DCF is rapidly oxidised to the highly fluorescent DCF (figure 8) (Keston & Brandt 1965; Cathcart *et al.* 1983). The fluorescence produced can be detected by a flow cytometer using excitation sources and filters appropriate for fluorescein.

Procedure: The H₂DCF-DA indicator was reconstituted in 100% ethanol shortly before performing the measurement to avoid any photo-oxidation. Before applying the ROS measurements to the cell experiments, the optimal working concentration and incubation time was determined empirically. The cells harvested after trypsinisation were washed with PBS, collected by centrifugation at 1000 rpm for 5 min, re-suspended in PBS buffer containing the H₂DCFDA at a 10µM concentration and incubated for 10 min at room temperature (15–25°C). Then the buffer was removed and cells were returned to pre-warmed PBS to recover for approximately 10-15 min. The fluorescence intensity was determined in a sample of cells with and one without prior exposure to the fluorescent dye. A sample of cells incubated with 5-(and-6)-carboxy-2',7'-dichlorodihydrofluorescein diacetate (carboxy-DCFDA) (from Molecular Probes, Invitrogen, Oregon, USA) was used as positive control.

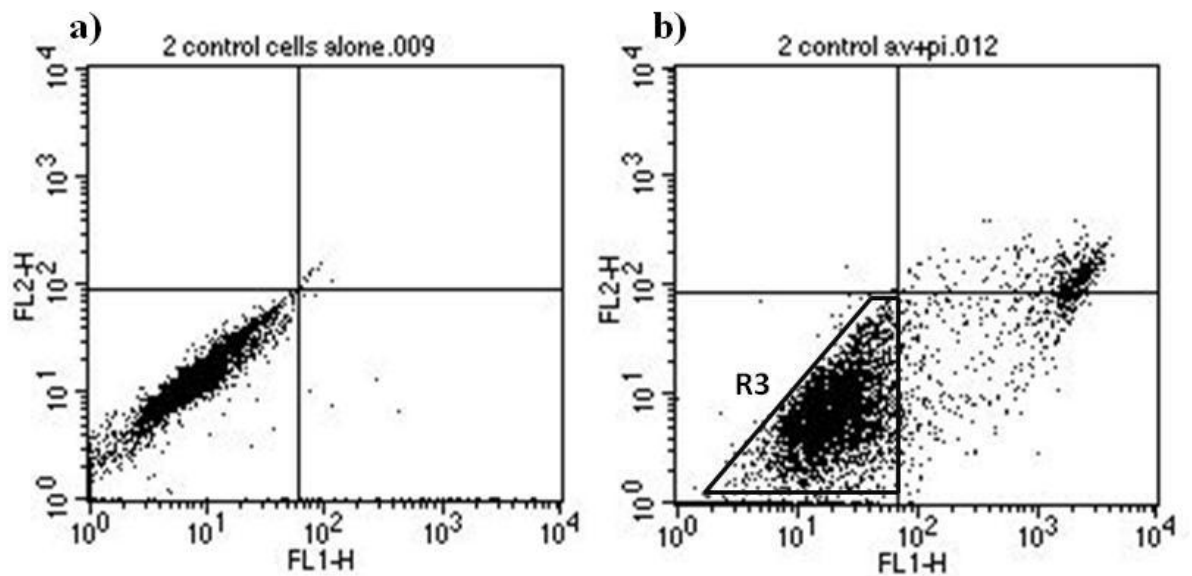
Figure II-8. Measurement of cellular ROS with H₂DCFDA.



Flow cytometry: The samples were then analysed on the FACSCalibur (Becton-Dickinson) flow cytometer using 488nm excitation with a 530nm filter for fluorescein detection (green fluorescence). The emitted fluorescence was collected on FL1 channel. In each measurement, a total of 5000 cells were analyzed. Data were acquired and analysed with the Cellquest Pro software (Becton Dickinson Biosciences, Oxford, UK).

As previously described for the Annexin V-Fluorescein / PI staining, cellular debris was excluded from the analysis using the forward and side scatters. In addition the ROS cellular content was determined only in viable cells. The apoptotic and necrotic cells, as detected with Annexin-V/PI staining from the same cell samples, were excluded from the measurement of ROS content. More specifically, using cell samples stained with Annexin V-Fluorescein and PI, the viable cells could be detected in the respective FL2-to-FL1 plot, as shown in figure 9. Thus, for each sample of cells incubated with H₂DCFDA the viable cells were gated in the FL2-to-FL1 plot and only these cells were used for the quantification of fluorescence intensity.

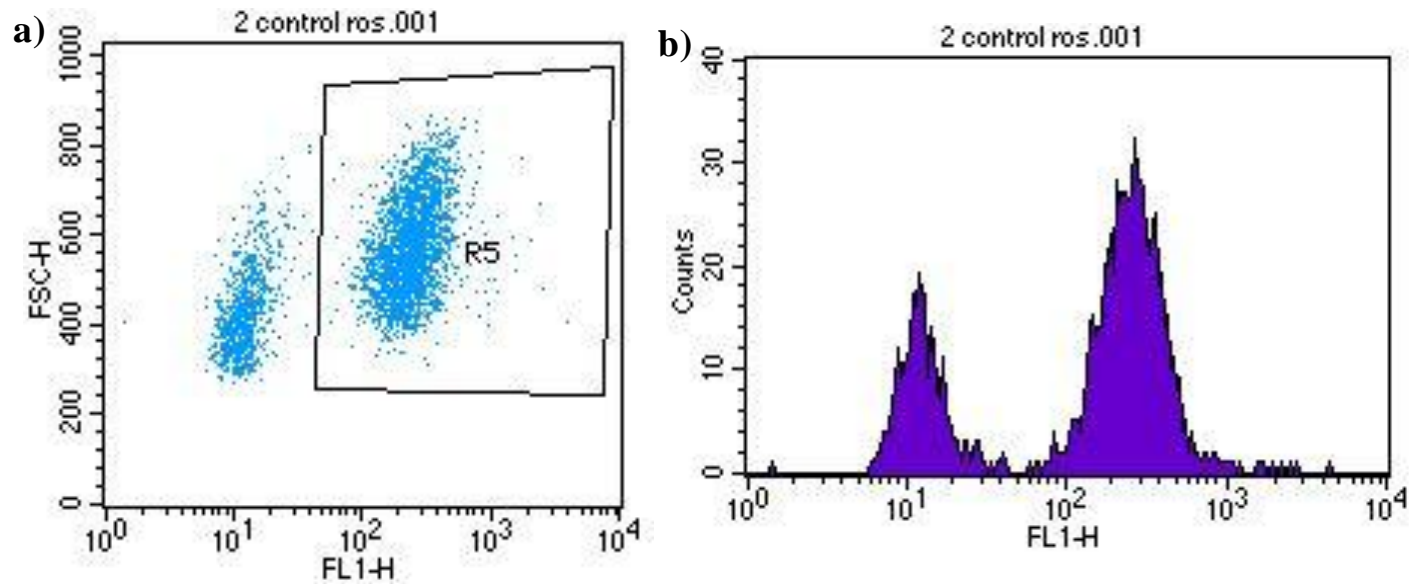
Figure II-9. FL2-to-FL1 plot of cells: a) without staining, b) with double staining of Annexin V-Fluorescein staining and PI. In panel b, the cells at the bottom left quadrante are not stained with either probe, thus these are the viable cells, while the cells shifting to the lower right or the two upper quadrantes are apoptotic or necrotic. The viable cells in the lower left quadrante of panel b were gated (R3) and only these were then used for the ROS measurement.



FL1-H: green fluorescence (Annexin V-Fluorescein) collected in channel 1. FL2-H: red fluorescence (PI) collected in channel 2.

After having determined the viable cells only in the samples incubated with H₂DCFDA, then their fluorescence intensity was measured at FL1. In the forward-to-FL1 scatter plot (figure 10a), the number of cells shifted on the FL1 axis, which are the cells emitting fluorescence due to H₂DCFDA oxidation, was calculated. Then a histogram of the fluorescence of these cells was drawn in order to calculate the fluorescence intensity emitted by those cells (figure 10b). The fluorescence intensity was calculated as the delta between the mean fluorescence intensity in the channel of the treated cells stained with dye and that of the same cells without dye staining. Thus, the ROS content is estimated by the FL1 fluorescence intensity [as calculated in figure 10b by the distance between the peaks of the slopes of cells with and without fluorescence emission] multiplied by the number of viable cells emitting this fluorescence [as calculated in figure 10a by the number of cells shifting on the FL1 axis].

Figure II-10. a) Plot showing the cells shift on the FL1 axis due to the green fluorescence emission from the H₂DCFDA dye oxidation by intracellular ROS . b) Histogram of the fluorescence emitted by cells with oxidised H₂DCFDA dye.



FSC-H: forward scatter (indicating cell size); FL1-H: green fluorescence (Anexin V-Fluorescein) collected in channel 1.

III. FIRST RESULT CHAPTER: “TELOMERE LENGTH MEASUREMENT”

1. SELECTION OF A METHOD FOR QUANTITATIVE ANALYSIS OF MEAN TELOMERE LENGTH

Until recently, the traditional method of measuring telomere length in samples of total human genomic DNA was the mean terminal restriction fragment (TRF) length estimation with Southern blotting. However, this method has certain drawbacks; it requires large amounts of DNA (3-5 µg per sample) and time (3-5 days per assay) (personal communication with Scott Brouillette, March 2007). These drawbacks render very difficult, and sometimes impossible, the application of this method in large clinical/population studies, or large-scale experiments, or experiments with specific cell types where the number of samples is large and the available amount of DNA restricted. Another important disadvantage is that TRF analysis also measures the highly variable sub-telomeric region which may cause artificial inter-individual variability in the mean telomere length estimation. The sub-telomeric region includes restriction site polymorphisms or length polymorphisms and this may confound the identification of primary factors accounting for inter-individual variation in the mean length of the true telomeric repeat sequence.

Recently, methods that allow multiple samples to be compared for their relative content of pure telomeric repeats have been developed (Lansdorp *et al.* 1996; Bryant *et al.* 1997; Nakamura *et al.* 1999). However, the quantitative PCR-based method introduced by Cawthon in 2002 is the simplest, more rapid and the only one allowing a high throughput processing of large numbers of DNA samples without requiring viable cells as starting

material (Cawthon 2002) compared to the other recent methods. This high throughput PCR-based method appears to be valid and fast and requires considerably less DNA compared to TRF analysis, thus it widens the possibilities for research in the field of telomere biology.

PCR-based methods, previous to Cawthon's method, had been designed for the quantification of telomere lengths in specific chromosome arms, using primers for that specific chromosome region. These methods were complex and did not provide the researcher with a global estimate for telomere length. Amplifying the pure telomeric hexamer repeats has always been a problem due to the repetitive nature of telomeric sequences and the generation of primer dimer-derived products. Cawthon (Cawthon 2002) managed to overcome this problem and design a set of primers which specifically amplified telomeric hexamer repeats (TTAGGG) without generating primer-dimer products (Figure 1). Each primer when it is hybridised to telomeric sequences is designed such that every sixth base is a mismatch (red arrows) and a full-match at the last five bases of the 3'-end (blue arrows) in order to allow DNA polymerase to extend. The last six bases on the 5'-end of each primer cannot base pair with the telomere sequence when the rest of the primer is optimally hybridised. The complements of these 5'-sequences are generated at the 3'-ends of all products that are completed in each cycle of the PCR, thereby blocking those 3'-ends from initiating DNA synthesis in the middle of telomere amplification products in subsequent cycles. When the primers are hybridised to the other primer, even with the strongest possible hybridization as shown in the lower part of Figure 1, then four consecutive paired bases are followed by two mismatched bases (purple arrows) which prevents DNA polymerase from acting to extend the 3'-end of each primer. This eliminates the possibilities for primer-dimer formation, which can confound the estimation of PCR

The quantification of telomere repeats with the quantitative PCR method is based on the principle that longer telomeres have more potential primer-annealing sites, thus there will be an increase in fluorescence, and a decrease in the number of cycles needed to reach a given threshold, compared to a shorter telomere. According to Cawthon (Cawthon 2002), the relative telomere length for each DNA sample is determined as the factor by which the sample differed from a reference DNA sample in its ratio of telomere repeat number to single gene copy (SCG) number. For each sample two quantitative PCRs, one for the telomere repeats and one for a SCG, are required. The SCG provides the sample-to-sample normalisation for the copies of the genome included in the sample. Thus the T/S ratio is equal to one when the tested DNA has the same amount of telomere repeats per genome as the reference DNA. The result is then normalised by using a reference DNA in every run, as a calibrator.

Below, I describe the adaptation –including optimisation and validation- of Cawthon’s method in our laboratory in order to use it for the purposes of the present thesis.

2. ADPTATION OF CAWTHON'S PCR METHOD IN OUR LABORATORY

2.1 APPLICATION ON THE ROTORGENE MACHINE

The Rotor-Gene[®] real-time PCR machine (Corbett Research Ltd, Cambridge, UK) was bought by our laboratory and used for telomere length estimation. This machine is the most suitable for applications such as the telomere length quantification for the following reasons. The Rotor-Gene employs a unique centrifugal rotary design instead of the microplate which is employed in common PCR machines. PCR tubes are placed into a rotor which spins tubes past a single excitation light source and a single detector, in a chamber of moving air. This means that there is minimal optical and temperature variation between tubes, enabling high precision in real-time PCR quantification. In addition, as the rotor spins continuously at 400 rpm, high-speed data acquisition is possible (Corbett Rotor-Gene 6000 manual, Version 1.7, <http://www.qiagen.com/corbett/support/default.aspx>). This unique design eliminates the well-to-well variability, increasing the accuracy of measurements. In the case of methods attempting to detect small differences as the telomere measurement, accuracy is a key advantage.

In addition, this machine offers the possibility to perform high resolution melting post-PCR, which allows the identification of the PCR product. With the temperature increase during high resolution melting, the double-stranded DNA disassociates at a certain temperature characteristic for same length and base content PCR products. Therefore, when the PCR generates only a specific product, during high resolution melting analysis the

entire amount produced will melt/disassociate at a specific temperature. This way the PCR specificity can be ensured after each run.

Finally, this machine offers the possibility to perform a comparative quantification analysis of the real-time PCR data, which is the most advantageous method of analysis, since it accounts for the differences in the efficiency of every reaction and does not require performing a standard curve in each run.

2.2 OPTIMISATION OF TELOMERE AND SINGLE COPY GENE PCRS

Telomere PCR optimisation: The primer concentrations and the reaction conditions for the telomere PCR were determined empirically, using the protocols described by Cawthon (Cawthon 2002) and Brouillette (Brouillette *et al.* 2007) as a guide.

The primers for the SCG PCR were adapted from Cawthon's protocol:

Telomere primer 1 (forward):

GGTTTTGAGGGTGAGGGTGAGGGTGAGGGTGAGGGT

Telomere primer 2 (reverse):

TCCCGACTATCCCTATCCCTATCCCTATCCCTATCCCTA

A crucial step in optimising a PCR is the determination of the best primer concentrations. These concentrations were determined using 16 different combinations, as shown in table 1, in order to detect the lowest primer concentration giving the highest

fluorescence, the lowest nonspecific amplification and take-off of the amplification at the earliest cycle.

Table III-1. The combinations of different primer concentrations that were used for the telomere PCR optimisation:

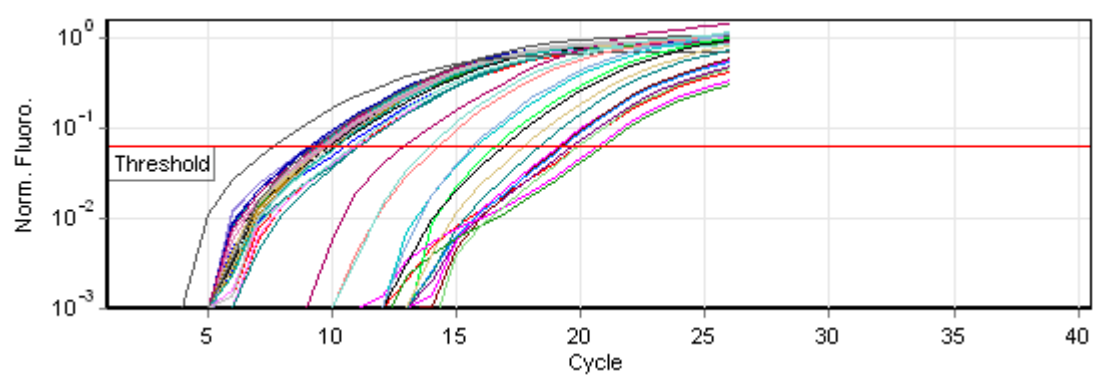
Telomere primer 2 (reverse) concentration (nM)		A (300)	B (600)	C (900)	D (1200)
Telomere primer 1 (forward) concentration (nM)	I (135)	135/300	135/600	135/900	135/1200
	II (270)	270/300	270/600	270/900	270/1200
	III (540)	540/300	540/600	540/900	540/1200
	IV (810)	810/300	810/600	810/900	810/1200

A duplicate of a sample and a no-template control was run for each of the above primer combinations.

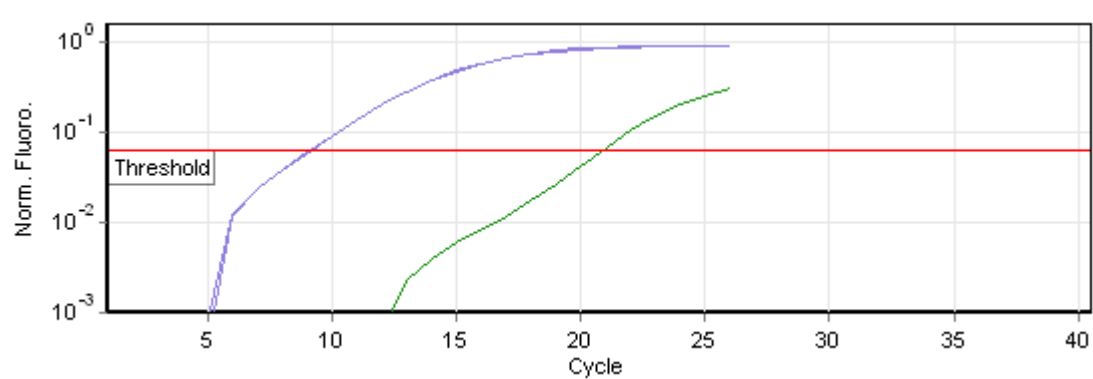
The minimum non-specific amplification, the maximum fluorescence and the earliest take-off (the first point to be 80% below the peak fluorescence level) were achieved with the combination of 135nM of telomere primer 1 and 900nM of telomere primer 2 as shown in figure 2.

Figure III-2. A) The amplification plot generated from the telomere PCR when testing the primer combinations of table 1. B) Amplification plot showing only the duplicate and the NTC of the 135nM / 900nM primer combination.

A)



B)



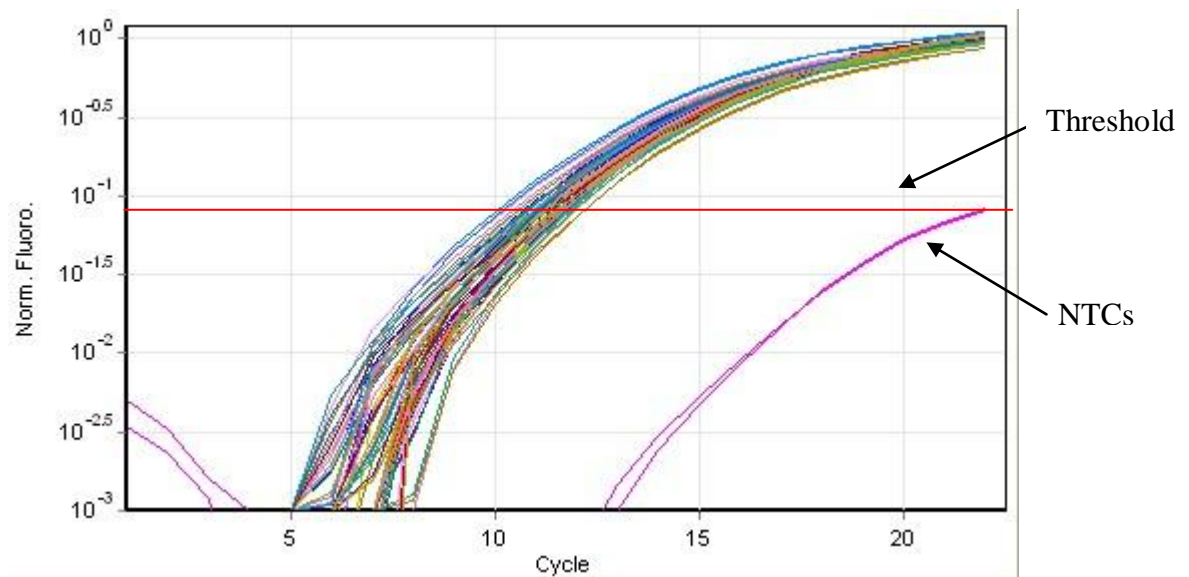
A variety of ready-to-use quantitative PCR mixes was also tested in order to achieve the best PCR quality. Also, after testing different amounts of template (10ng, 20ng, 30ng and 40ng), it was shown that the 30ng of template are the optimal amount. Regarding the cycling profile, a higher annealing temperature of 60°C, which could theoretically increase

the specificity of the PCR, was tested, but it did not prove to ameliorate the efficiency nor the specificity of the PCR. Thus the 58°C suggested by Cawthon was adapted in the end.

The telomere PCR assay was finally optimised at the following conditions. The final reaction volume was 25 µl consisting of 1 x SYBR Green, 1 x qPCR mix (2x SensiMix NoRef DNA kit, Quantace, London, UK), 30 ng of template, telomere primer 1 at 135nM concentration and telomere primer 2 at 900nM. The cycling profile was: 95°C incubation for 10 min, followed by 22 cycles of 95°C for 15 sec and 58°C for 120 sec.

As shown in figure 3, under these PCR conditions, the exponential phase of the telomere reaction begins very early (5-8 cycles), the maximum fluorescence reaches a satisfactory level and the no-template controls (NTCs) amplification level remains much lower than that of the DNA samples.

Figure III-3. A representative amplification plot of the optimised telomere PCR.



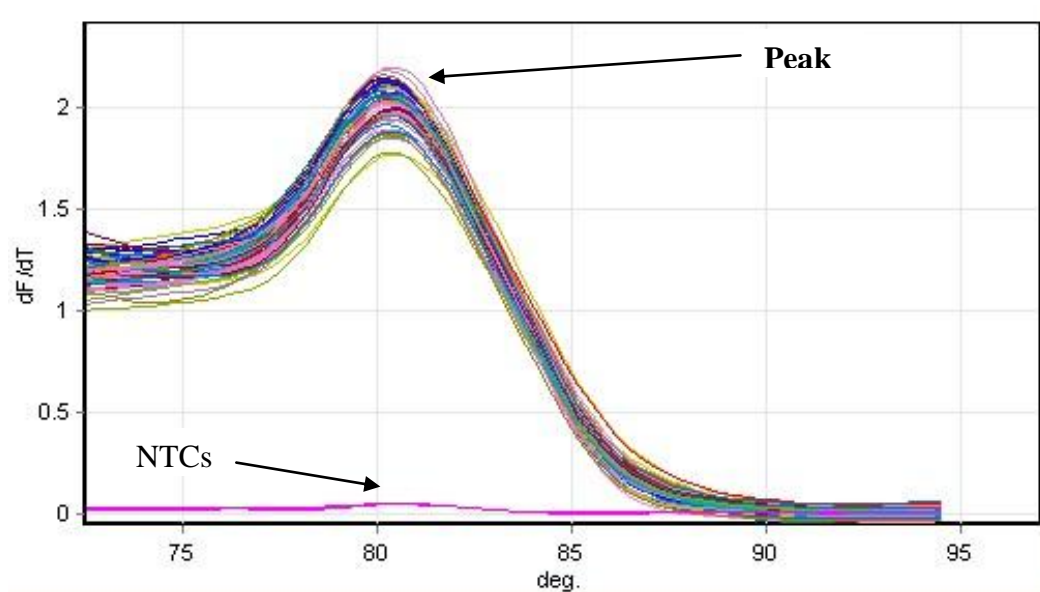
High resolution melt (HRM) analysis: High resolution melt (HRM) analysis is a "closed-tube" technique for characterization of PCR products. The HRM technique detects different PCR product based on different melting temperatures (T_ms). The PCR products are differentiated according to their dissociation behaviour as they transit from double stranded DNA (dsDNA) to single stranded DNA (ssDNA) with increasing temperature (White & Potts 2006).

Prior to performing a HRM analysis, a target sequence must first be amplified by PCR in the presence of a dsDNA intercalating fluorescent dye (e.g. SYBR Green *or* LC Green). The dye does not interact with ssDNA but actively intercalates with dsDNA and fluoresces brightly in this state (White & Potts 2006). Initially, the fluorescence is high in a melt curve analysis because the sample starts as dsDNA, but the fluorescence decreases as the temperature is raised and DNA dissociates (melts) into single strands. The midpoint of the melt phase, at which the rate of decrease in fluorescence is greatest, defines the temperature of melting (T_m) of the particular DNA fragment. PCR products can be discriminated according to their sequence, length, GC content and strand complementarity (White & Potts 2006). HRM is also used to detect single base sequence variations such as SNPs or to discover unknown genetic mutations (Gundry *et al.* 2003).

In order to ensure the specificity of the telomere PCR, the melting profile of the PCR product is always examined, after the PCR reaction is completed, on the Rotor-gene machine by high resolution melting (72-95°C). As shown in figure 4, the melting curve of the telomere PCR product has only a single peak at ~80.5⁰ C indicating that there is a specific in length (76bp) and base consistency PCR product. The NTCs appear to have

generated a negligible amount of PCR product, indicating that there no contamination and/or primer-dimer formation occurred during PCR.

Figure III-4. Melting curve of telomere PCR product.



SCG PCR optimisation: As single copy gene, Cawthon suggests the use of the acidic ribosomal phosphoprotein PO (*36B4* or *RLP0*), which encodes acidic ribosomal phosphoprotein PO and is located on chromosome 12. I tested two single copy genes, the *36B4* and the glyceraldehyde-3-phosphate dehydrogenase gene (*GAPDH*), which is widely used as a housekeeping gene.

The primers and PCR conditions used for the *36B4* were adapted from Cawthon's protocol (Cawthon 2002) and for *GAPDH* from Martin-Ruiz's version of Cawthon's protocol (Martin-Ruiz *et al.* 2004):

36B4 primer u (upstream):

CAGCAAGTGGGAAGGTGTAATCC

36B4 primer d (downstream):

CCCATTCTATCATCAACGGGTACAA

GAPDH primer f (forward):

AAATCCCATCACCATCTTCC

GAPDH primer r (reverse):

GCTGAGTACGTCGTGGAGTC

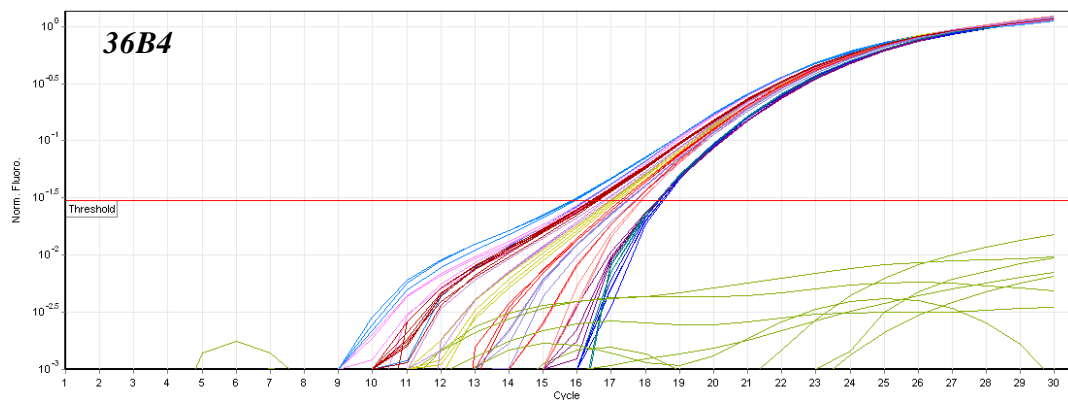
Both SCG PCRs displayed optimal performance at the conditions described in Cawthon's and Martin-Ruiz's protocols. The exponential phase of both gene's PCR reaction began early enough, the maximum fluorescence reached a satisfactory level and the NTCs amplification level remained much lower than that of the DNA samples (figure 5). In addition, both SCG's PCR produced a single product of the expected length as shown by the melting curves in figure 6. The melting temperature of the 74bp product of the *36B4* PCR was ~81°C and that of the 210bp product of the *GAPDH* PCR was ~84.5°C, as expected (figure 6).

In order to select the best SCG for the telomere length assay, the inter-assay variability in estimating the relative amount of *36B4* or *GAPDH* copies was tested. The relative amounts of *36B4* and *GAPDH* copies in respective PCR runs were measured in duplicate for ten randomly selected DNA samples on two consecutive days. There was a

significant linearity between the estimates of *36B4* and *GAPDH* relative concentration obtained on the two different days. However, this linearity was higher for the *36B4* estimates ($R^2=0.79$, $p=0.001$ for *36B4* vs. $R^2=0.53$, $p=0.001$ for *GAPDH*, figure 7).

Figure III-5. A) The amplification plot of *36B4* PCR. B) The amplification plot of *GAPDH* PCR.

A)



B)

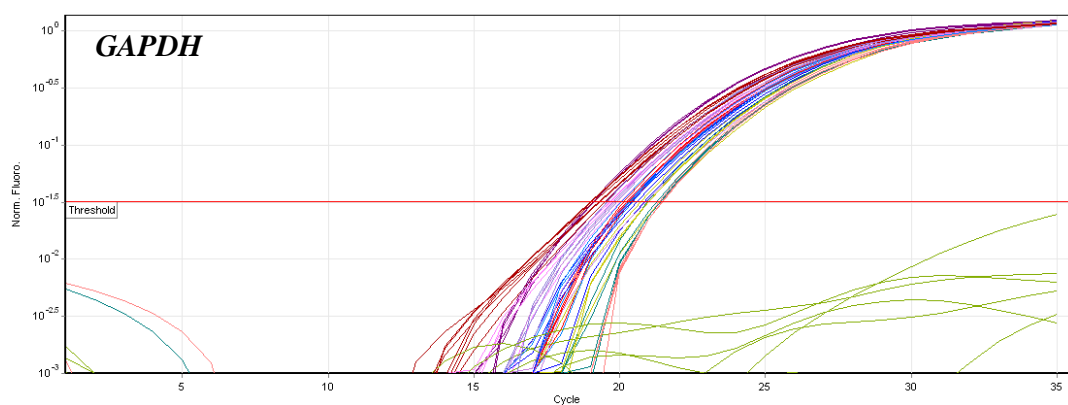
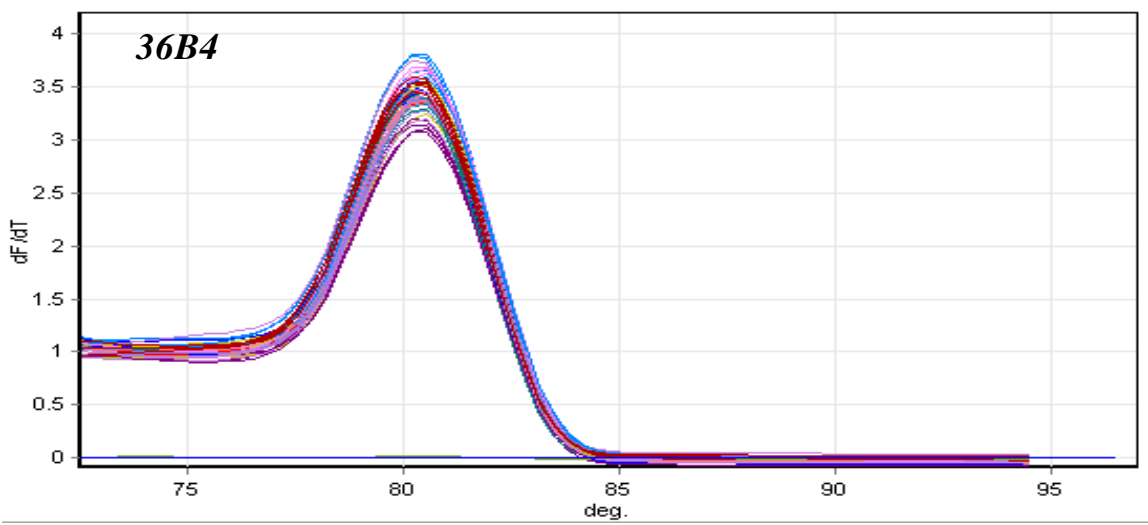


Figure III-6. A) Melting curve of *36B4* PCR product. B) Melting curve of *GAPDH* PCR product.

A)



B)

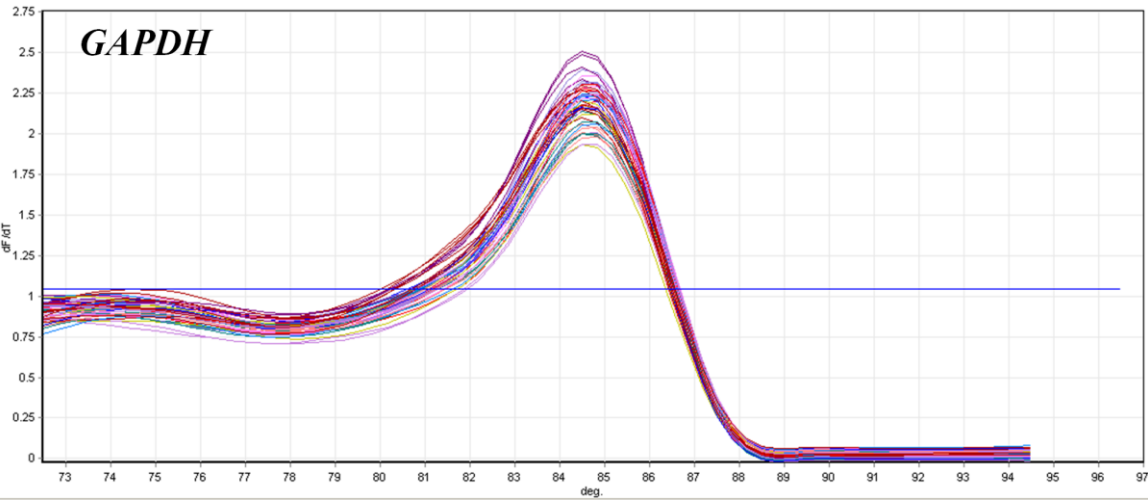
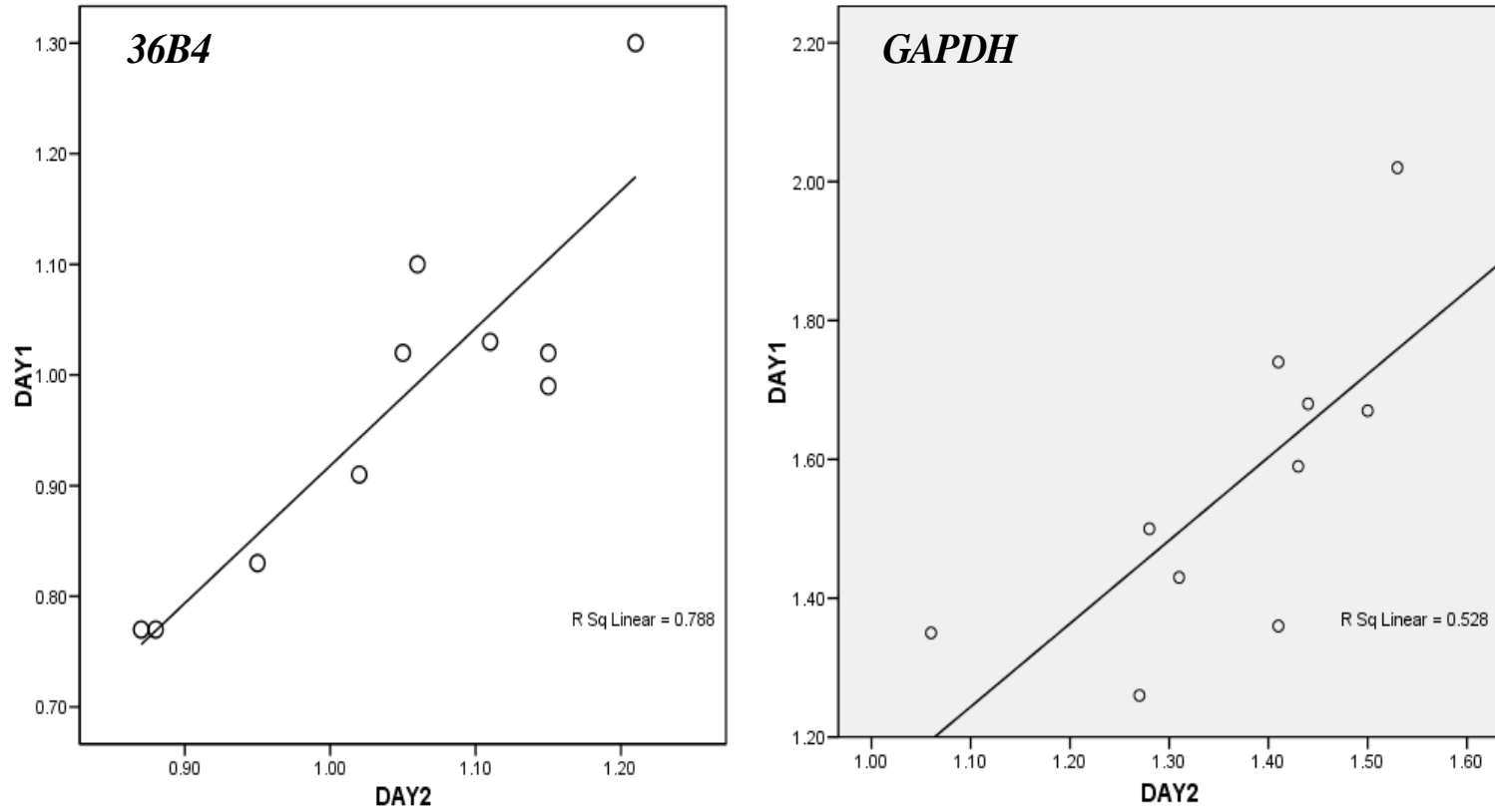


Figure III-7. Linear regression graph between the telomere length estimates of the same 10 samples measured on two consecutive days.



Since the use of *36B4* offers a greater reproducibility to the method, it was chosen as the best SCG. The primer concentrations for the *36B4* PCR were optimised at 300/500 nM and the cycling profile as: 95°C incubation for 10 min, followed by 30 cycles of 95°C for 15 sec and 58°C for 60 sec. The final reaction volume was optimised at 25 µl consisting of 1 x SYBR Green, 1 x qPCR mix (2x SensiMix NoRef DNA kit, Quantace, London, UK), 30 ng of template and the respective primer concentrations.

2.3 METHOD OF ANALYSIS OF QUANTITATIVE PCR DATA

Next, the best method of analysis of the raw data from each of the telomere and SCG PCRs had to be chosen. The methods of relative quantification include the method of the standard curves, the $\Delta\Delta C_t$ method, the Pfaffl method and the comparative quantification (CQ).

The standard curve method: In this method, a standard curve for each of the telomere and the SCG PCR is run with the unknown samples and the relative concentration in each run is calculated based on the standard curve (Cawthon 2002). This method is based on the consistency of the dilution series generating the standard curve. The major disadvantage of this method is the need of a standard curve in each run, which reduces the number of samples analysed per run.

The $\Delta\Delta C_t$ method: This method is very commonly used in quantitative PCRs. Assuming that the efficiency of each PCR reaction is 100%, and thus the PCR product is doubled in each cycle, the formula $2^{-\Delta\Delta C_t}$ gives, relative to a calibrator, the concentration of

PCR product in each reaction (Livak & Schmittgen 2001). The $\Delta\Delta C_t$ is determined as following:

$\Delta C_t = C_t$ (calibrator) - C_t (unknown sample) and $\Delta\Delta C_t = \Delta C_t$ (telomere) - ΔC_t (SCG) (Livak & Schmittgen 2001).

The disadvantage of this method is the assumption that the amplification efficiency is 100% in all PCR runs, which is not true in most cases.

The Pfaffl method: Pfaffl (Pfaffl 2001) introduced in 2001 a new method of analysis for relative quantification which takes into account the efficiencies of the two PCR runs (for example the telomere and the SCG PCR run). In order to estimate the efficiency of each PCR, a standard curve is run at least once. The relative quantification of telomere repeats is calculated as following:

Telomere repeats per SCG copy =

Efficiency of telomere PCR $^{\Delta C_t(\text{telomere})}$ / Efficiency of SCG PCR $^{\Delta C_t(\text{SCG})}$ (Pfaffl 2001)

The disadvantage of this method is that, although it does not assume that the two different PCRs (telomere and SCG) are 100% efficient, it does assume that the amplification efficiency of each sample's reaction within a PCR run is always the same.

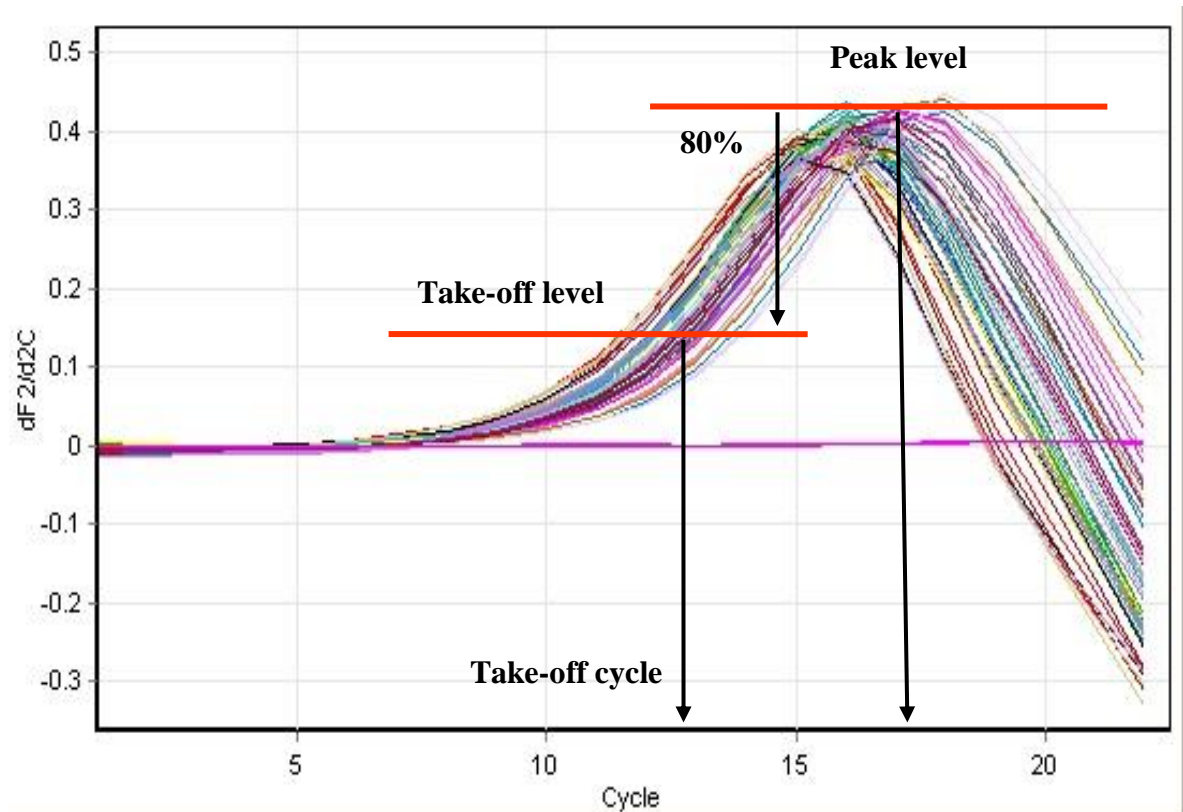
The comparative quantification analysis (CQ): The Rotor-Gene 6000 software from Corbett Research Ltd, Cambridge, UK offers an new alternative method of analysis for relative quantification. The method first determines the “take-off” value for each sample. To calculate the take-off point, the second derivative of the raw data is taken in order to identify the peak reaction velocity. This is the peak of the exponential reaction and

occurs shortly after the take-off of the reaction. The take-off point cannot be determined exactly, but is estimated by finding the first point to be 80% below the peak level (figure 8). Based on the take-off point and the reaction efficiency, the method calculates the relative concentration of each sample compared to the calibrator (reference DNA sample). The following steps are taken to calculate the relative concentrations:

- 1) The take-off points of each sample are calculated by examining the second derivative peaks.
- 2) The average increase in raw data, four points following the take-off, is calculated and used to estimate the amplification efficiency.
- 3) Outlier amplifications are removed to account for noise in background fluorescence.
- 4) The non-outlier amplifications are averaged to become a run “average amplification”.
- 5) The average take-off point is calculated for all replicates of the calibrator (reference DNA sample).
- 6) The relative concentration for a sample is calculated as:

$$\text{Amplification}^{(\text{Calibrator Take-Off} - \text{Sample Take-Off})}$$

Figure III-8. Plot of the second derivative of the amplification.



The quantity of telomere repeats is calculated as the relative concentration in the telomere PCR of each experimental sample. Similarly the relative quantity of the SCG is calculated as the relative concentration in the SCG PCR of each experimental sample. The samples are run in duplicates and the average relative concentration of each duplicate is considered. The ratio of these relative concentrations (T/S ratio) is the relative telomere length and should be proportional to the average telomere length.

T/S ratio = relative concentration of Telomere repeats / relative concentration of Single copy gene copies.

The advantage of this method is that the amplification efficiency of every sample within a run is estimated, and based on that, the relative concentration of each sample is calculated compared to a reference DNA (calibrator) included in every run. Importantly, the amplification efficiency of the reference DNA sample is also estimated and taken into account when each unknown sample's relative concentration is normalised to that of the reference DNA. Thus, no assumption of equal or constant efficiencies in each PCR reaction is made, and no standard curve is required in each run. This way the accuracy of the method and the number of samples included in each run are maximised. Nevertheless, this CQ method of analysis is only suitable for ratio comparisons and in order to detect a trend without allowing an absolute quantification as the standard curve method would allow. The restriction of the method is that it is based on the use of the same sample in each run as calibrator otherwise the results would not be comparable between runs.

However, since the CQ method can serve the purposes of the present studies (i.e. the comparison of T/S ratios) and given its advantages regarding the measurements' accuracy and cost-efficiency, the CQ was chosen as the method of analysis for all telomere assays in the present thesis.

Finally, in each run of 32 samples, a reference sample and a no-template control, all in duplicate, were included. If the duplicate T/S ratio values of a sample differed more than 6%, the sample's measurement was repeated in duplicate in another run in order to obtain a more accurate and reliable estimate of telomere length. The specificity of all PCRs was determined by melting curve analysis. All analyses were processed blinded to case-control status of samples.

3. VALIDATION OF THE ADAPTED PCR METHOD IN OUR LABORATORY

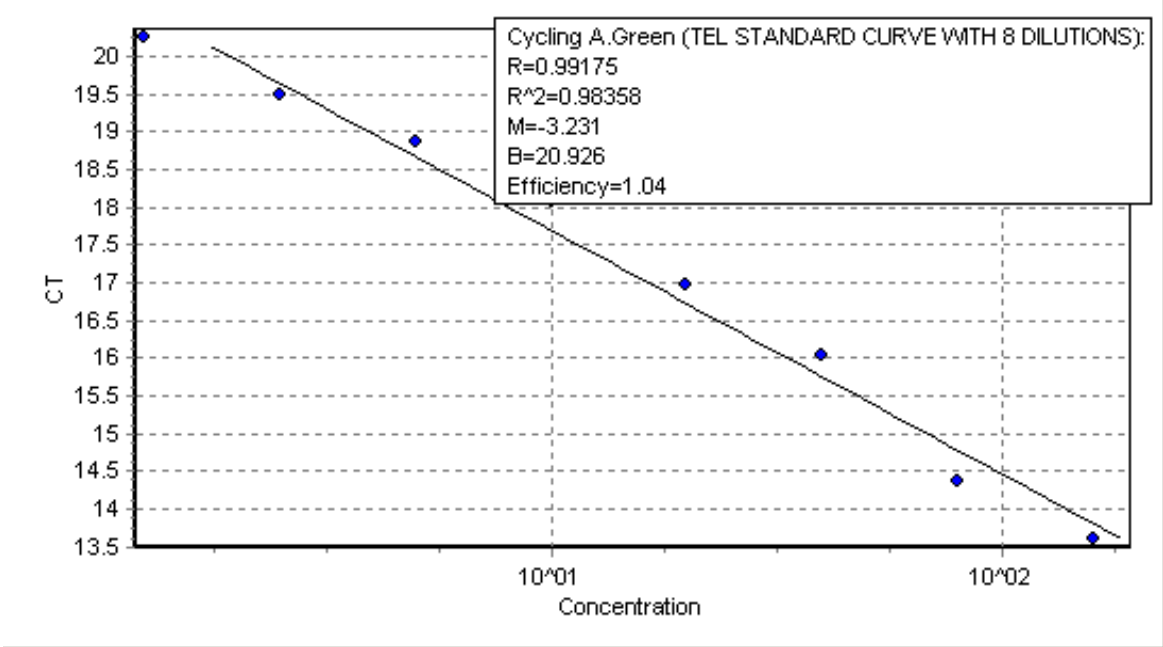
3.1 QUALITY CONTROL – STANDARD CURVES

In order to ensure the validity and accuracy in determining the relative concentration of the PCR product in quantitative PCRs, such as the one for the telomere and SCG estimation, a standard curve needs to be performed. The criterion is the linearity between the template concentration series and the relative copies of PCR product measured in a standard curve analysis.

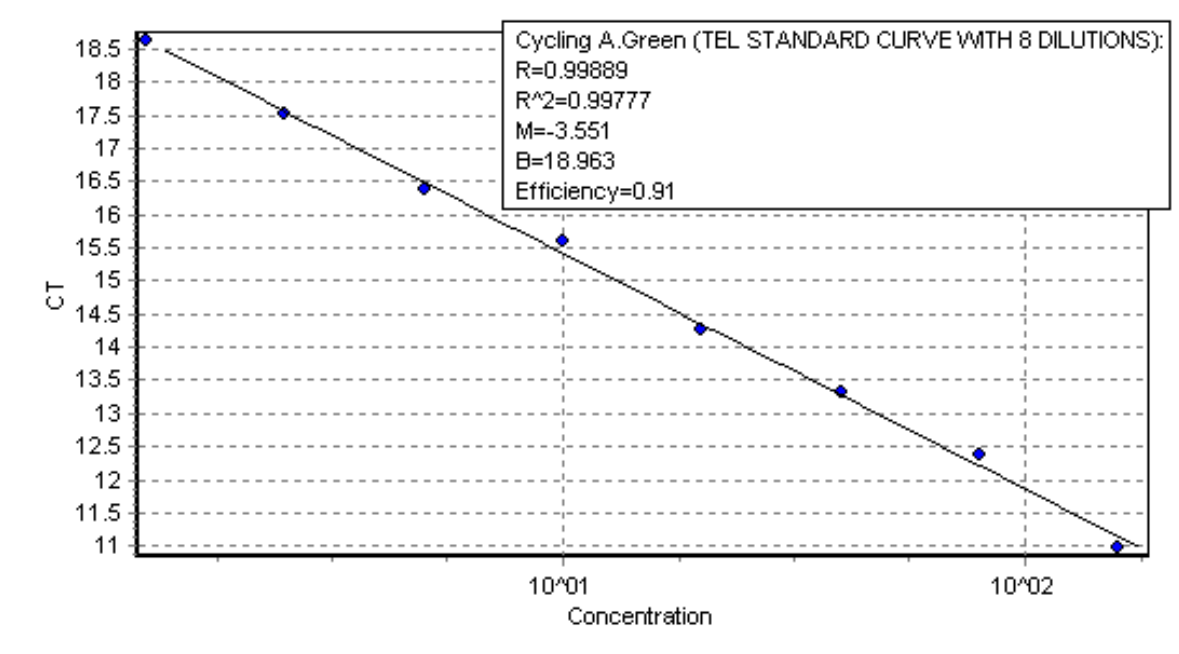
Thus, a dilution series (1.25 ng/μl - 160 ng/μl, two-fold dilution, eight points) was run after optimization for both the telomere and the *36B4* SCG PCRs. For both assays, linearity ($R^2 > 0.98$) over this range of input DNA was observed (figure 9A and 9B, respectively). Furthermore, both PCRs displayed greater than 91% efficiency, as calculated from the slope of the respective standard curves.

Figure III-9. Standard curves of A) Telomere PCR and B) SCG (36B4) PCR.

A)



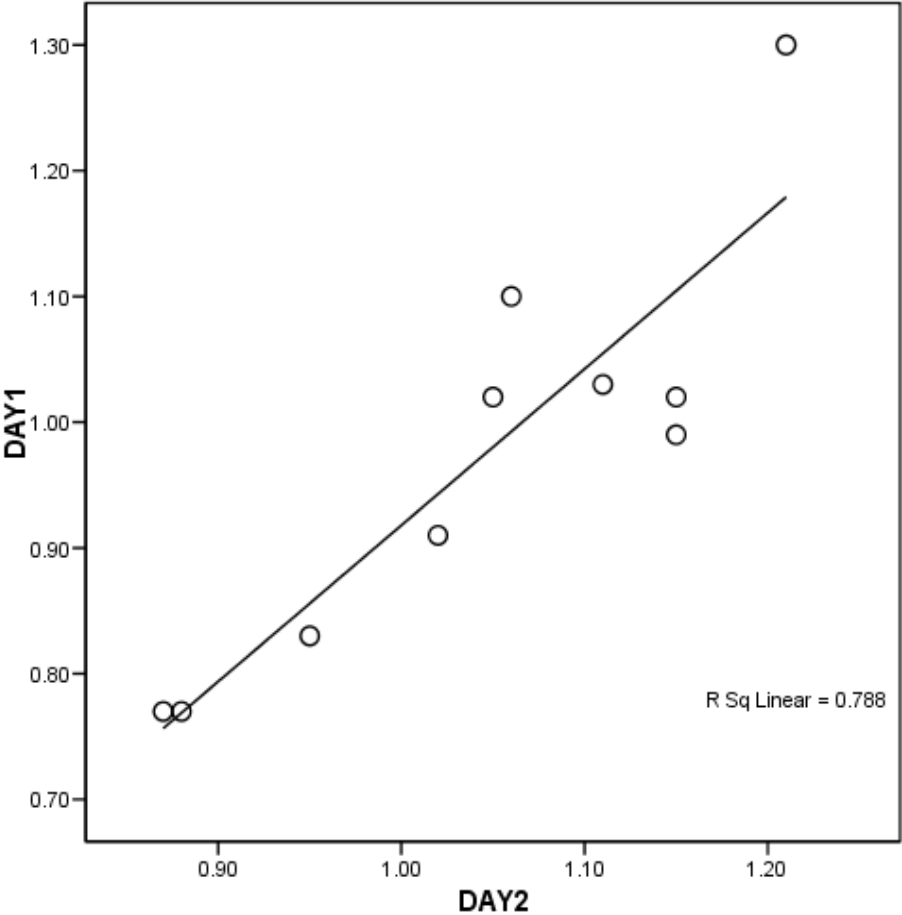
B)



3.2 REPRODUCIBILITY OF THE METHOD

In order to test the reproducibility of the method, ten randomly chosen DNA samples were run in duplicate on two consecutive days. There was a significant linearity between the mean telomere length measurements obtained on the two different days in linear regression analysis ($R^2=0.79$, $p=0.001$, figure 10). Moreover, the reproducibility was also assessed with Spearman's non-parametric test of pair-wise correlation that looks at the ranking of each sample. The correlation of the lengths' ranking as measured on the two different days was significant (Spearman coefficient=0.82, $p=0.004$). The coefficient of variation of the telomere length estimates in the repeated measurements of the same sample was 5.6%, which is similar to the 5.8% inter-assay coefficient of variation observed by Cawthon (Cawthon 2002).

Figure III-10. Linear regression graph between the telomere length estimates of the same 10 samples measured on two consecutive days ($R^2=0.79$, $p=0.001$).



3.3 COMPARISON WITH THE TRADITIONAL METHOD FOR TELOMERE LENGTH MEASUREMENT

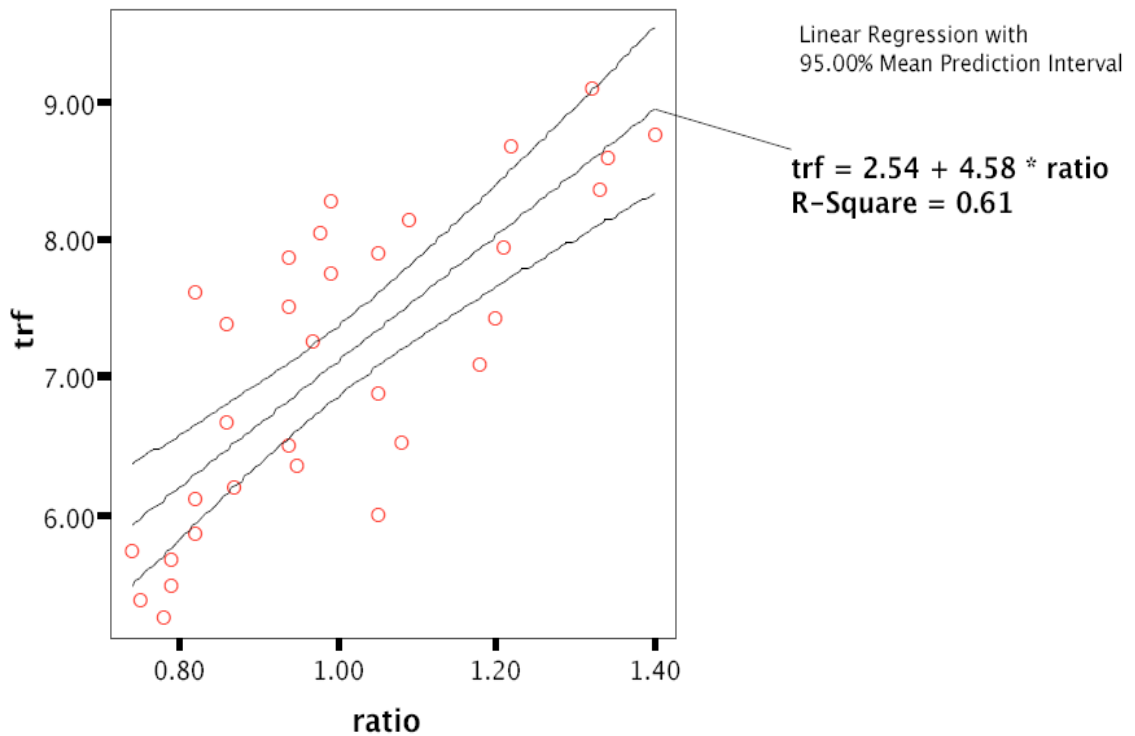
To validate the telomere length assay, 32 DNA samples of subjects aged 24 to 54 years from the Cardiovascular Sciences Department, Leicester University DNA bank were measured in duplicate with the quantitative PCR method in our laboratory. These T/S ratios were then compared to measurements obtained by the conventional TRF analysis in Leicester University, as previously described (Samani *et al.* 2001). The DNA samples from Leicester University DNA bank and their TRF estimates were kindly provided by Professor Nilesh Samani and Dr Scott Brouillette.

A significant positive correlation between the telomere length measurements obtained with the two different methods was found by linear regression analysis ($R^2=0.61$, $p<0.0001$, figure 11). A certain deviation from the telomere length as estimated by TRF analysis was expected. The PCR-based method measures the length of pure telomeric repeat sequences. Subtelomeric regions mainly constitute of degenerated telomeric sequences which also contain stretches of pure telomeric sequences (Blackburn 2001; De Boeck *et al.* 2009). Thus the PCR-based method measures the pure telomere length, probably along with a small portion of subtelomeric sequences. In contrast TRF analysis utilises probes that hybridise to a range of subtelomeric sequences (Baird 2005), thus the resulting measurement includes the highly variable length of the subtelomeric region.

Nevertheless, the level of linearity between the measures obtained by the PCR method as adapted in our laboratory (T/S ratios), and the measures obtained by TRF was similar to that observed by Cawthon ($R^2=0.68$) (Cawthon 2002) and Brouillette ($R^2=0.65$)

(Brouillette *et al.* 2007). Thus, the PCR method as adapted in our laboratory can be considered valid.

Figure III-11. Correlation of the PCR-based method with the conventional TRF analysis.



trf: mean telomere length in kilobases as measured by TRF analysis.

ratio: mean telomere length expressed as T/S ratio as determined by the PCR-based method.

4. ADAPTION OF ABSOLUTE QUANTIFICATION OF TELOMERE LENGTH USING THE PCR METHOD

The PCR method for telomere length determination estimates the relative amount of telomeric repeats per genome relatively to that of a reference DNA sample and does not give an absolute value (e.g. bp). The only way to translate the relative telomere estimation by the PCR method, i.e. the T/S ratios, to bp was through their correlation to the respective TRF values. More specifically, the correlation observed between the T/S ratios of the PCR method and the TRF values in the set of 32 samples, was described by a regression function [$TRF(bp) = 2.54 + 4.58 \times T/Sratio$] (see “First result chapter”, paragraph 3.3, page 173). This function was used later in order to translate the T/S ratios measured in the present thesis study samples to bp values. However, this translation could only give a rough estimate of the corresponding bp values. The R^2 of the regression was 0.61, which meant that only a proportion of variability in the T/S ratio data set was accounted for by this regression model. In addition, with this relative determination of telomere length by the PCR method, the results in our study samples were not directly comparable to those of other laboratories. Thus, it was considered important to try improving the method from a relative to an absolute quantification, since an estimate of absolute telomere length in bp would be far more useful. This became feasible with a modification of the PCR method introduced by O’Callaghan et al. (O’Callaghan *et al.* 2008). I tried to adapt this method in our laboratory.

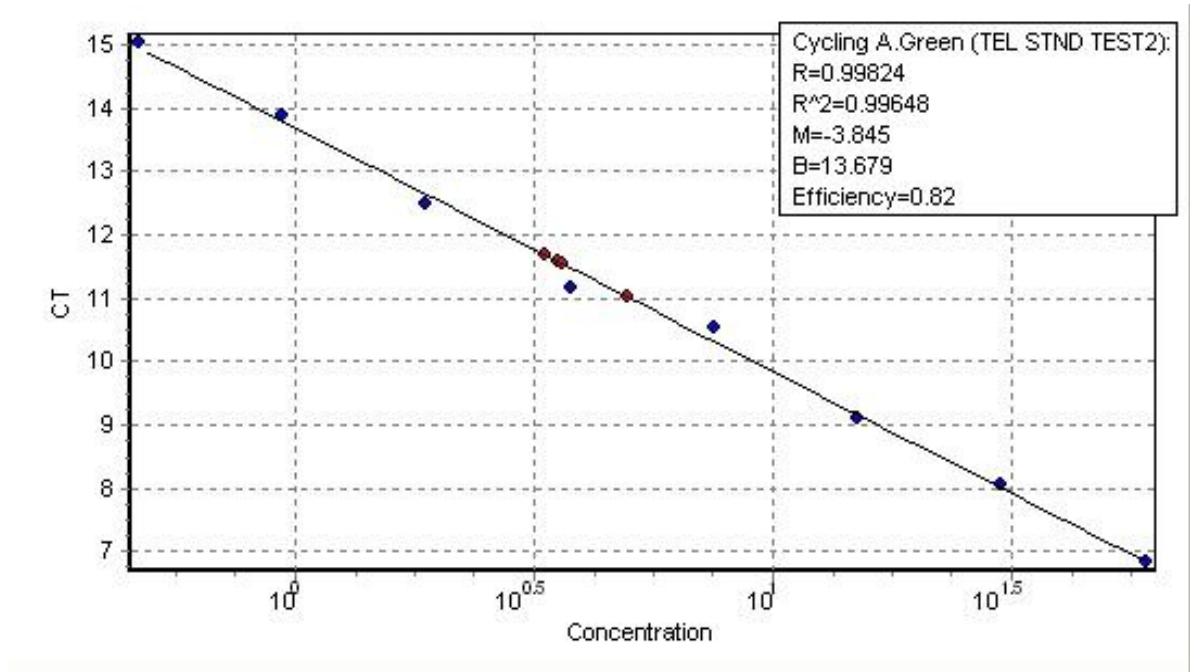
4.1 PRINCIPALS OF ABSOLUTE QUANTIFICATION USING THE PCR METHOD

The original version of the PCR method estimated the telomeric repeats per genome in the tested DNA sample compared to a reference DNA. More specifically, in a telomere PCR, the amount of telomeric repeats of a sample relative to a reference DNA are calculated, and then in a SCG PCR, the copies of the SCG relative to the reference DNA are also calculated. The ratio of these two relative concentrations gives the estimate of telomere length.

T/S ratio = relative concentration of Telomere repeats / relative concentration of Single copy gene copies.

In order to modify this method to an absolute quantification, O'Callaghan (O'Callaghan *et al.* 2008) suggested performing the calculation of the telomere repeats or the SCG copies relative to standard synthesised oligonucleotides. By replacing the reference DNA in the telomere PCR with an oligonucleotide of known telomere repeats, and also in the SCG PCR with a synthesised oligonucleotide mimicking the genomic SCG (*36B4*) sequence, an absolute quantification of the telomere length can be carried out. Thus, a synthesised 84 bp oligonucleotide containing 14 TTAGGG repeats was used as calibrator in the telomere PCR, and a synthesised 75 bp oligonucleotide containing the SCG genomic sequence was used as a calibrator in the SCG PCR.

Figure III-12. Telomere PCR standard curve with a dilution series (2.4 - 0.01875 pg/ μ l, two-fold dilution, eight points) of the synthesised 84 bp oligonucleotide.

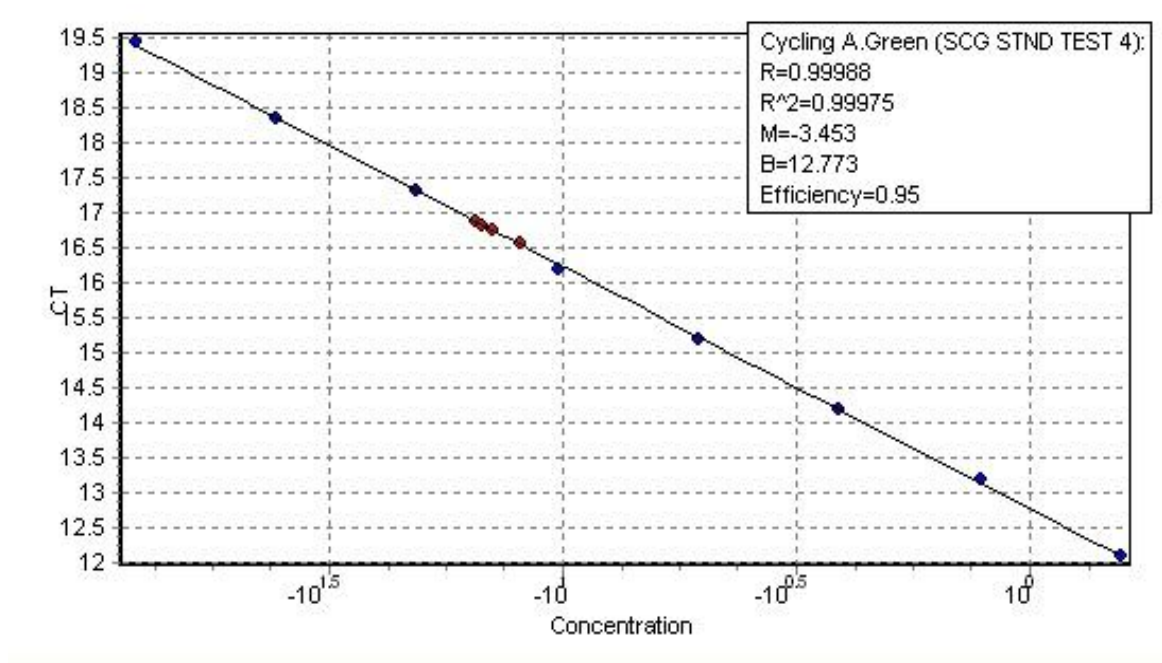


Red points: represent DNA samples at the concentration used in the telomere assay.

Blue points: represent the dilution series of the synthesised oligonucleotide

Using the standard curve of figure 12, the concentration of 0.2pg/ μ l was chosen for the telomere synthesised calibrator. For this concentration the synthesised oligonucleotide contained a similar number of telomere repeats to that contained in an average DNA sample.

Figure III-13. SCG PCR standard curve with a dilution series (0.0032 - 0.000025 pg/ul, two-fold dilution, eight points) of the synthesised 75 bp oligonucleotide.



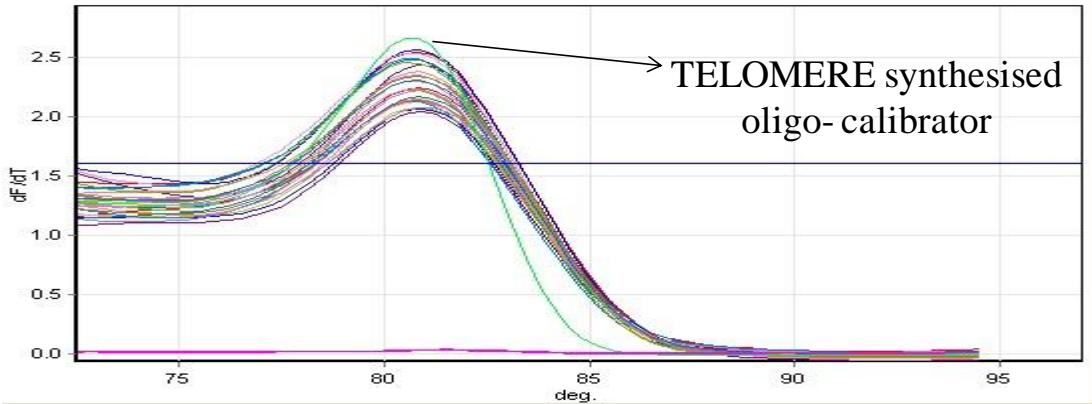
Red points: represent DNA samples at the concentration used in the telomere assay.
 Blue points: represent the dilution series of the synthesised oligonucleotide.

Using the standard curve of figure 13, the concentration of 0.0004pg/μl was chosen for the SCG synthesised calibrator. For this concentration the synthesised oligonucleotide contained a similar number of SCG copies to that contained in a DNA sample.

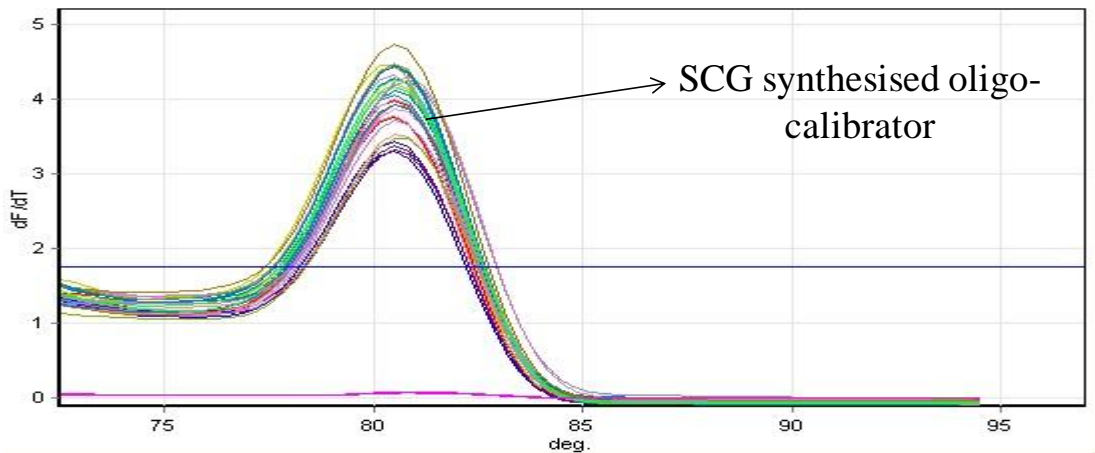
Next, the specificity of the PCR product generated when using as template the synthesised telomere calibrator and the SCG synthesised calibrator had to be determined. Thus, high resolution melting analysis was performed after the telomere and the SCG PCR respectively, using the synthesised calibrators in the optimised concentrations and various DNA samples.

Figure III-14. Melting curves including the synthesised calibrators and DNA samples of: A) the telomere PCR products and B) the SCG PCR products.

A) Telomere PCR melting curve:



B) SCG PCR melting curve:



As shown in figure 14A the melting profile of the PCR product generated when using as template the synthesised telomere calibrator is similar to that of DNA samples; although the melting curve is more sharp, probably due to the greater variation in telomeric repeat sequences of the DNA samples compared to a synthesised oligonucleotide.

Similarly, when using the SCG synthesised oligonucleotide as template the PCR product is the same as that generated by DNA samples, as indicated by the melting curves of figure 14B.

4.3 CALCULATIONS FOR THE ABSOLUTE TELOMERE LENGTH QUANTIFICATION

In each of the telomere and the SCG quantitative PCRs I had to calculate the absolute amount of telomere repeats and SCG copies according to the synthesised calibrators used:

Telomere PCR: The telomere repeats in the unknown sample is calculated relatively to the synthesised oligonucleotide according to the following formula:

Telomere repeats in the unknown sample =

Amplification^(Calibrator Take-Off—Sample Take-Off) x Telomere repeats contained in the synthesised oligonucleotide used as calibrator.

Each reaction contained 5pg (0.2 pg/μl reaction concentration x 25μl reaction volume) of this synthesised 84 bp oligonucleotide, thus the number of template molecules is: $[(5 \times 10^{-12} / MW) / \text{x Avogadro's number}]$ molecules.

Thus, the amount of telomeric hexamer repeats in bp contained in the 5 pg of this oligonucleotide in each reaction is:

$$[(5 \times 10^{-12} / \text{MW}) / \text{Avogadro's number}] \times 84 \text{ bp} = 9.48 \times 10^6 \text{ kb.}$$

Therefore the value of the relative concentration of the unknown sample in the telomere PCR multiplied by the **9.48x10⁶ kb** of telomeric repeats contained in the calibrator, gives the absolute measure of telomeric repeats in the unknown sample.

SCG PCR: The diploid genome copy number in the unknown sample is calculated relatively to the synthesised oligonucleotide according to the following formula:

Diploid genome copy number in the unknown sample =

Amplification $\left(\frac{\text{Calibrator Take-Off}}{\text{Sample Take-Off}} \right) \times \text{SCG copy number contained in the synthesised oligonucleotide used as calibrator.}$

Each reaction contained 0.01pg (0.0004pg/μl reaction concentration x 25μl reaction volume) of this synthesised 75 bp oligonucleotide, thus the number of template molecules is: $[(0.01 \times 10^{-12} / \text{MW}) \times \text{Avogadro's number}]$ molecules or SCG copies.

Therefore the value of the relative concentration of the unknown sample in the SCG PCR multiplied by the **2.64x10⁵** of SCG copies gives the absolute measure of aploid genome copies in the sample. Since this method will be used for human DNA samples, this final number has to be divided by two in order to give the absolute estimate of diploid genome copies.

In the end, the T/S ratio calculated by the CQ analysis when using the synthesised oligonucleotides as calibrators will have to be multiplied by $[9.48 \times 10^6 \text{ kb} / (2.64 \times 10^5 / 2)]$ in order to give the absolute estimate of telomere length per diploid genome in bp.

Using these synthesised calibrators and performing after the CQ analysis the above calculations, I measured in a set of 25 DNA samples the absolute estimate of telomere length per diploid genome. The results ranged from 95-165 kb, which was in accordance with the values reported by O'Callaghan (O'Callaghan *et al.* 2008). . This estimate refers to the sum of the 92 telomeres of 46 chromatids contained in diploid cells of G₀ phase, since lymphocyte DNA was used. In addition, O'Callaghan reported that the values obtained by the absolute quantification were consistently ~7 kb shorter compared to the TRF values for the same DNA samples. This discrepancy is expected when considering that the TRF overestimates mean telomere length since it also measures the sub-telomeric region (Baird 2005). Taking this into account, the range of telomere lengths observed here (90-165 kb) is close to the mean telomere lengths estimated by TRF analysis that have been reported in the literature (Demissie *et al.* 2006; Tentolouris *et al.* 2007; Hunt *et al.* 2008).

Finally, in order to ensure the validity of this modified method I tested its reproducibility. Thirteen randomly selected DNA samples were measured in duplicate on two consecutive days and subsequent linear regression analysis showed that the repeated measurements correlated significantly ($R^2=0.64$, $p=0.001$).

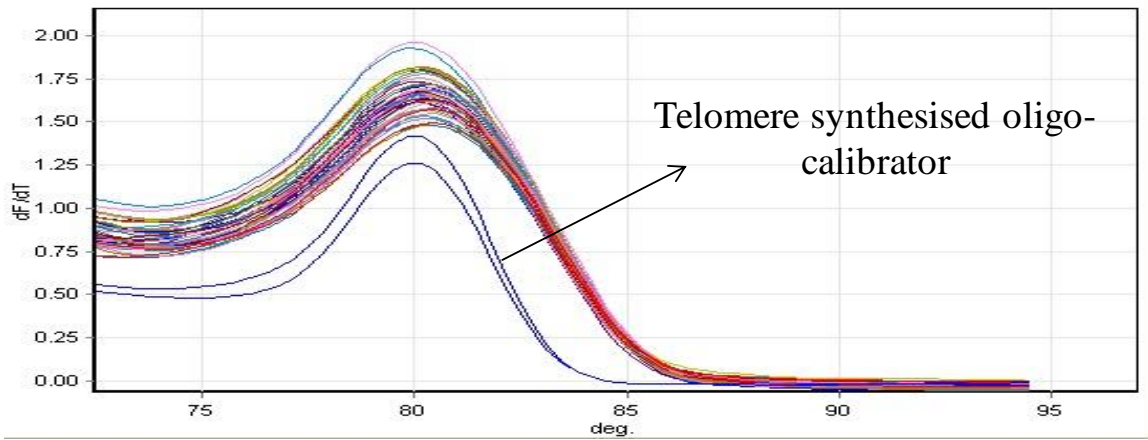
4.4 PROBLEMS IN THE APPLICATION OF THE ABSOLUTE QUANTIFICATION

After the validation of this modified PCR method for absolute quantification, it was used for the telomere length determination in familial hypercholesterolaemia (FH) study samples, in parallel to the original relative quantification. This was achieved by adding in each PCR run the reference DNA and the respective synthesised calibrator. However, both the synthesised calibrators, and especially the SCG one, displayed a much less than optimal amplification and melting profiles, while all the DNA samples displayed normal profiles. This indicated that the problem in these reactions was with the quality of the template. The reactions having as template the synthesised oligonucleotides had generated lower maximum fluorescence and their PCR products had low melting curves (Figure 15). Taking these into account, it was concluded that the synthesised oligonucleotides had been degraded, which was probably due to their very low concentration.

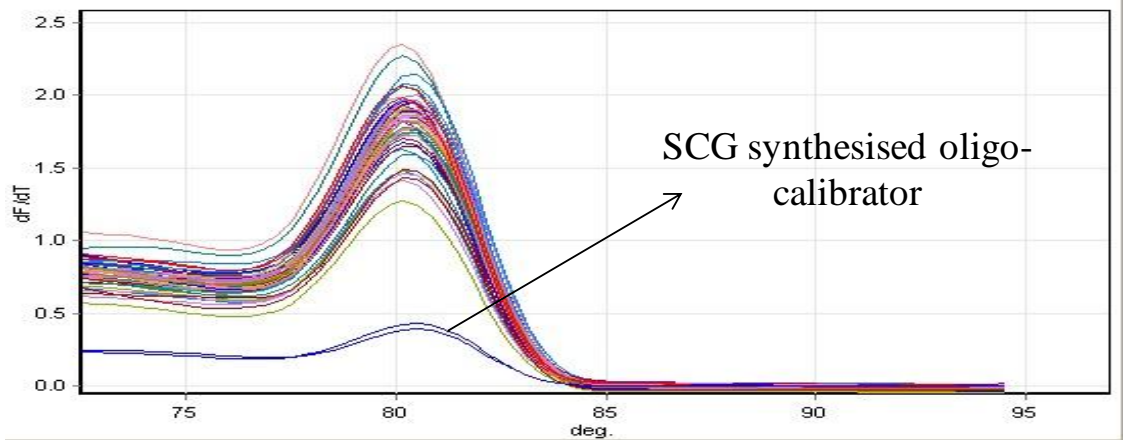
I also examined the possibility of self-annealing (possibly forming homo-duplexes or hairpins) of these synthesised oligonucleotides, since they contained self-complimentary sequences. To prevent the self-annealing from happening, the synthesised oligonucleotides before the PCR reaction were incubated for two minutes at 70⁰ C with 5% dimethyl sulfoxide [(CH₃)₂SO] (DMSO), a polar aprotic solvent which inhibits secondary structures (Quijada *et al.* 1997). However, this did not resolve the problem, and the less than optimal cycling and melting profiles appeared again with the synthesised oligonucleotides.

**Figure III-15. Melting curves of FH DNA samples and the synthesised calibrators of:
A) Telomere PCR products and B) SCG PCR products.**

A) Telomere melting curve



B) SCG melting curve



Considering that the most possible explanation was that the oligonucleotides were degraded, these were stored in aliquots of high concentration up until their use; once diluted into the necessary concentration for the PCR reaction, the leftover was discarded. Nevertheless, this handling did not prove sufficient to prevent the degradation problem. With the synthesised oligonucleotides being often degraded and thus generating less PCR product for the same template concentration, any calculation of the telomere length based on these calibrators would be biased and false. For this reason, I considered this modification of the original PCR method unreliable and thus it was not used for acquiring estimates of telomere length in the present thesis.

An alternative to overcome this problem and yet acquire an estimation of telomere length in kb using the qPCR method is to use a DNA sample of known telomere length in kb as the standard according to which all samples are normalised and calculated. However, since the measurement of the standard's DNA telomere length in kb will be provided by TRF, the estimate will include the subtelomeric length. This means that while qPCR only measured the pure telomeric sequences the translation into kb using the length of the standard DNA will produce an overestimation of the true telomeric length. Nonetheless, the unknown samples' telomere lengths will be comparable since they are normalised to the same reference DNA. This alternative of using a DNA sample of known telomere length in kb has been recently used by other researchers (Martin-Ruiz *et al.* 2004; Collerton *et al.* 2007; Terry *et al.* 2008) and can provide a good estimate of the telomere length measured by qPCR in kb.

5. ADAPTION OF MULTIPLEX MONOCHROME QUANTITATIVE PCR (MMQPCR) FOR TELOMERE LENGTH MEASUREMENT

In 2009, while the present thesis was in progress, Cawthon published a further improved multiplex version of the PCR method (Cawthon 2009), suggesting that this assay was more accurate, and also offered the possibility of higher throughput at lower cost. In the original quantitative PCR method, for each sample the telomere repeats were calculated in a telomere PCR reaction and the SCG copies in a another PCR reaction for the SCG. This way the relative to a reference DNA T/S ratios were calculated. Multiplexing the two different PCR reactions required for the measurement of telomere length would eliminate the inter-assay variation due to DNA pipetting, since both PCRs would occur in the same reaction for each DNA sample. Multiplexing the assay, and thus decreasing the reactions needed in half, also increases the throughput and lowers the cost, since this uses less reagents, DNA template and less set-up time is needed. A further advantage of Cawthon's multiplex assay is that it does not require the use of two fluorescent dyes for the detection of the two different PCR products, but it is based on the use of a single fluorescent DNA-intercalating dye. This adds to the simplicity of the method and the lowering of the cost. Therefore, I tried to adopt this improved version of the PCR method in our laboratory.

5.1 PRINCIPLES OF THE MMQPCR METHOD

The crucial problem that Cawthon had to overcome, in order to design a multiplex reaction for measuring the relative copy numbers of two different DNA target sequences with the use of a single DNA-intercalating dye, was the accumulation of the fluorescent signal from both the PCR products. The design of such a multiplex reaction was based on the theory that the fluorescent signal generated from the first, more abundant target sequence (telomere repeats) would be collected at early cycles, when the signal from the second, less abundant target sequence (SCG) would still be at baseline. The fluorescent signal generated from the second target sequence (SCG) are collected at a much higher temperature than the melting temperature of the first PCR (telomere) product, which would become single-stranded and consequently its fluorescent signal would reach the baseline (Cawthon 2009). For this theory to be applied successfully, it is required that the multiplex reaction involves two target sequences of rather different abundance. Since this is the case for the telomere repeats and the SCG in a DNA sample, multiplexing the two respective PCRs is feasible.

The collection of each of the PCR products at different temperature levels, with the parallel melting of the first PCR product, is achieved through the design of the two sets of primers. Firstly, both sets of primers are designed to generate short length PCR products. Secondly, GC-clamps are added on both ends of the PCR product generated from the less abundant target sequence i.e. the SCG, in order that its melting temperature is raised much higher than that of the telomere PCR product (Cawthon 2009). The set of primers for two different SCGs, albumin (ALB) and hemoglobin beta (HBB):

ALBu (upstream):

CGGCGGCGGGCGGCGGGCTGGGCGGaaatgctgcacagaatccttg

ALBd (downstream):

GCCCGGCCCGCCGCGCCCGTCCCGCCGaaaagcatggtgcctgtt

Expected PCR product: 98bp.

HBBu (upstream):

CGGCGGCGGGCGGCGGGCTGGGCGGcttcatccacgttcaccttg

HBBd (downstream):

GCCCGGCCCGCCGCGCCCGTCCCGCCGgaggagaagtctgccgtt

Expected PCR product: 106bp.

Specifically for the telomere target sequence, Cawthon designed a new set of primers (TELg and TELc) which would ensure the generation of a short, fixed-length product. New set of telomere primers:

TELg (forward):

ACACTAAGGTTTGGGTTTGGGTTTGGGTTTGGGTTAGTGT

TELC (reverse):

TGTTAGGTATCCCTATCCCTATCCCTATCCCTATCCCTAACA

Expected PCR product: 79bp.

The TELg is able to anneal on genomic telomere sequences and initiate DNA synthesis, whereas the TELc primer anneals to genomic telomeres but cannot initiate DNA synthesis due to a mismatched base at its 3' terminus (figure 16A). In following cycles, TELc can hybridise along extensions of the TELg primer but can only initiate DNA synthesis when hybridised in a certain configuration shown in figure 16B, where the 3' terminal base of TELc is fully matched. In this way a single, fixed-length PCR product is generated. Moreover, when the primers anneal to each other as shown in figure 16C, TELg and TELc have multiple mismatches, including at their 3' terminal bases, and thus primer dimer formation is inhibited.

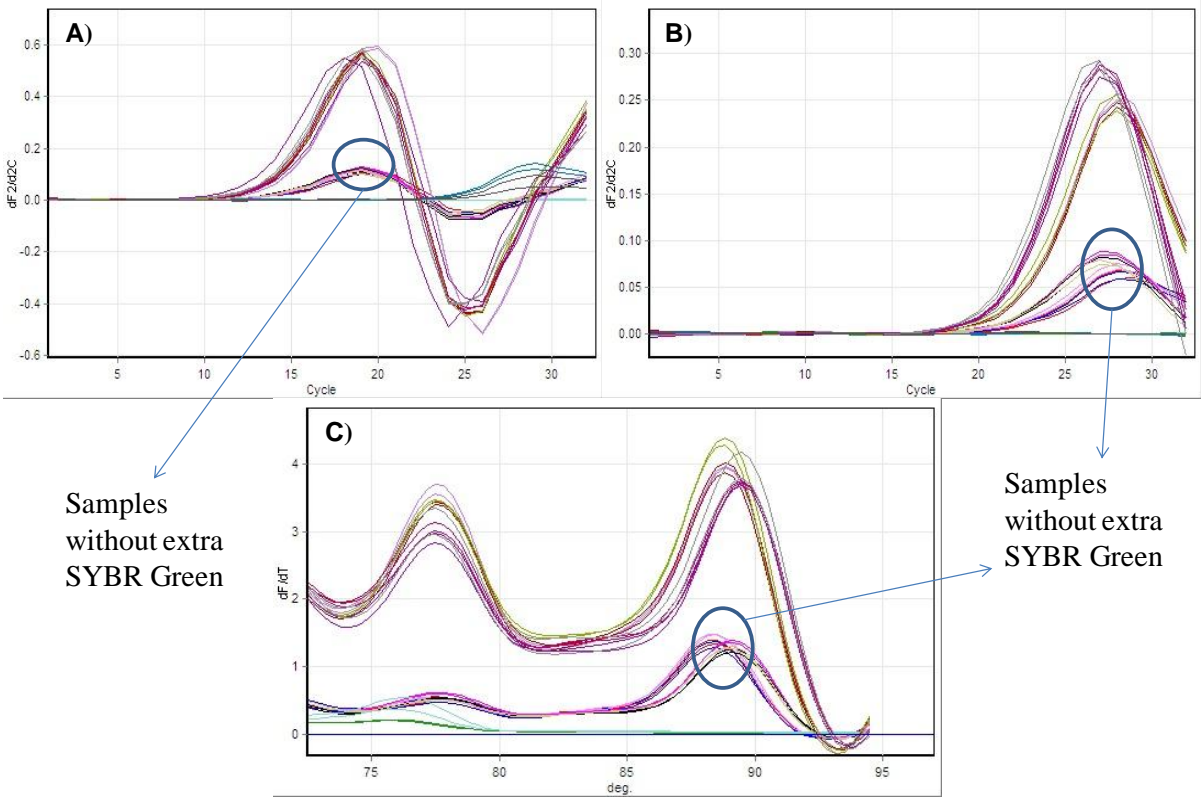
5.2 MMQPCR OPTIMISATION

The reagents and the reaction conditions for the multiplex reaction were empirically determined using the protocol described by Cawthon (Cawthon 2009). The following parameters of the protocol were tested and changed:

Reagents and template of the qPCR reaction mix: The ready-to-use SensiMix qPCR mix (2x SensiMix NoRef DNA kit, Quantace, London, UK) which was used as for the original version of the method, was also used for the MMQPCR. Nevertheless, additional reagents were added to the ready-to-use qPCR mix in order to achieve a better quality and efficiency in the multiplex reaction. Since the SCG primers contained GC-clamps, the use of a reagent that reduces the formation of secondary structure caused by GC-rich regions would improve the amplification of these DNA sequences. Betaine has been suggested to be such a reagent (Henke *et al.* 1997), thus after testing it was added to the final multiplex qPCR mix. Moreover, I assumed that the amount of fluorescent dye contained in the ready-to-use PCR mix might not be sufficient, since the multiplex reaction includes two PCR reactions and the generation of two PCR products. Thus, I tested whether the reaction required extra amount of fluorescent DNA-intercalating dye (i.e. 2x or 3x instead of 1x SYBR Green in the final reaction). The results in figure 17 showed that the extra amount of SYBR Green was necessary in order to have a satisfactory level of maximum fluorescence (i.e. 2x SYBR Green in the final reaction).

Another important point of the optimization is to determine the minimum amount of DNA template needed in order to achieve a good PCR quality. Thus 20ng and 30ng of template were tested and it was shown that 20ng is sufficient.

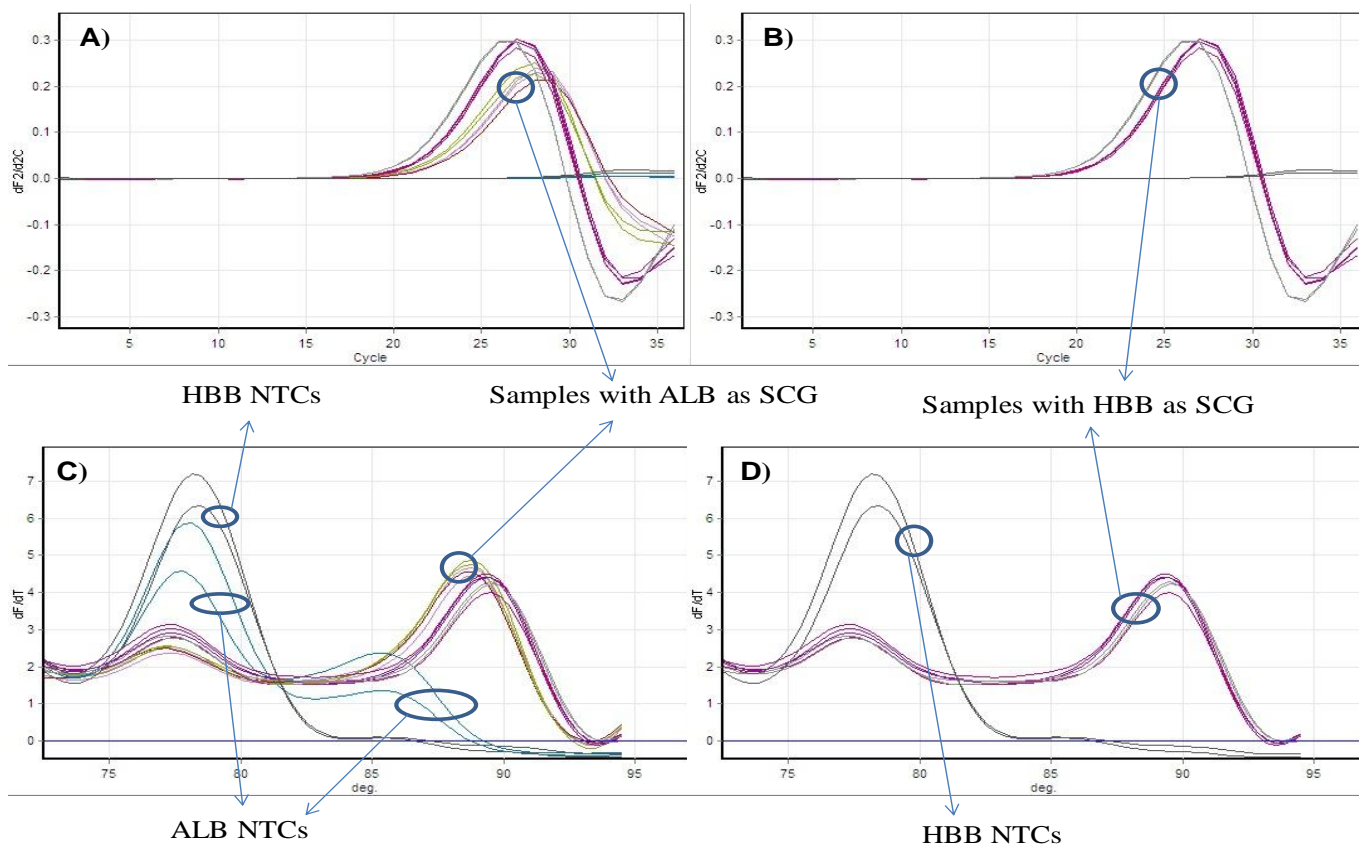
Figure III-17. DNA samples run with and without extra SYBR Green added in their PCR reaction mix. A) Second derivative of the amplification from the channel collecting the telomere PCR fluorescence. B) Second derivative of the amplification from the channel collecting the SCG PCR fluorescence. C) Melting curve of the multiplex PCR products. The melting profile of the MMQPCR consists of two curves of which, the one at lower temperatures corresponds to the melting of the shorter, telomere PCR product, and the other at the higher temperatures corresponds to the longer SCGs products.



Selection of the SCG: Both the ALB and the HBB single copy genes were tested in order to select the best SCG. As shown in figures 18A and 18B, the HBB amplification had a higher peak and earlier take-off compared to that of the ALB. Examining the melting profiles of the two single copy genes in figures 18C and 18D, it is evident that there is no non-specific amplification generated from the HBB primers. This can be concluded from the flat NTCs of the HBB PCR reaction. Also the HBB amplification seem to compete less with the formation of the telomere PCR product compared to the multiplex reactions with the ABB as SCG. This can be concluded from the lower first melting peak in the melting profile of the reactions with ABB as SCG compared to that with the HBB.

Although the differences were not great, the HBB was chosen as the best SCG.

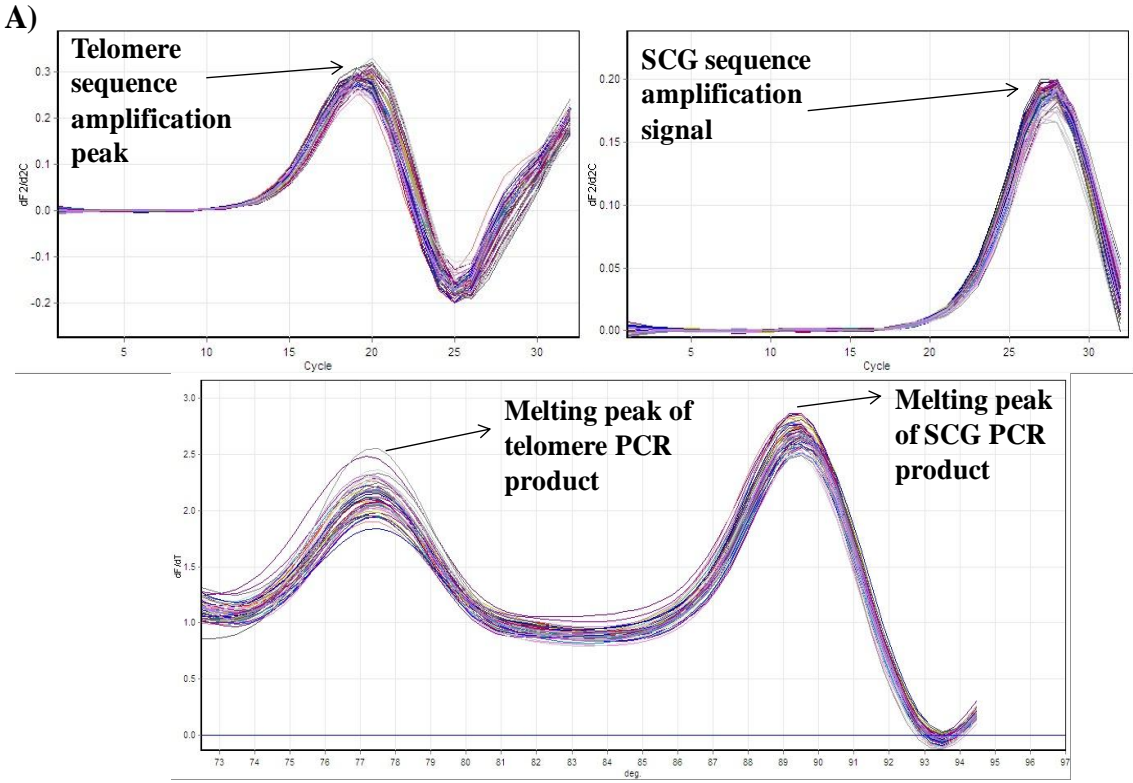
Figure III-18. DNA samples run with ALB or HBG as SCG. A) Second derivative of the amplification from the channel collecting the SCG PCR fluorescence. Samples with ALB and HBB as SCGs are included. B) Second derivative of the amplification from the channel collecting the SCG PCR fluorescence. Samples with HBB only as SCGs are included. C) Melting curve of the multiplex PCR products including samples with ALB and HBB as SCGs. D) Melting curve of the multiplex PCR products including only samples with HBB as SCGs.



Optimisation of the cycling conditions: Higher annealing temperatures in the amplification cycles for both the telomere and the SCG templates were tested (i.e. 50°C instead of 49°C at stage 2 and 63°C instead of 62°C at stage 3). Theoretically, more strict annealing temperatures potentially increase the specificity of the PCR, which could improve the separation of the two target sequences' amplification.

Both the combinations of cycling conditions resulted in optimal amplification and melting profiles as shown in figure 19. The exponential phases of the two target sequences amplification were well separated, with a six to seven cycles difference between them, and the melting curve consisted of two clear peaks as expected by the telomere and the SCG PCR products, respectively. Therefore, the decision of which combination of cycling conditions is the best was based on which one leads to higher reproducibility of measurements. Nineteen randomly selected samples were measured on two consecutive days using both cycling profiles. Linear regression analysis showed that the cycling conditions as in Cawthon's protocol (Cawthon 2009) lead to a higher linearity between repeated measurements of telomere length, compared to the profile with the higher annealing temperatures (figure 20). Thus, the cycling profile as suggested by Cawthon was chosen.

Figure III-19. Amplification and melting profiles of the MMQPCR products with: A) Cycling conditions as suggested by Cawthon. B) Cycling conditions with higher annealing temperatures.



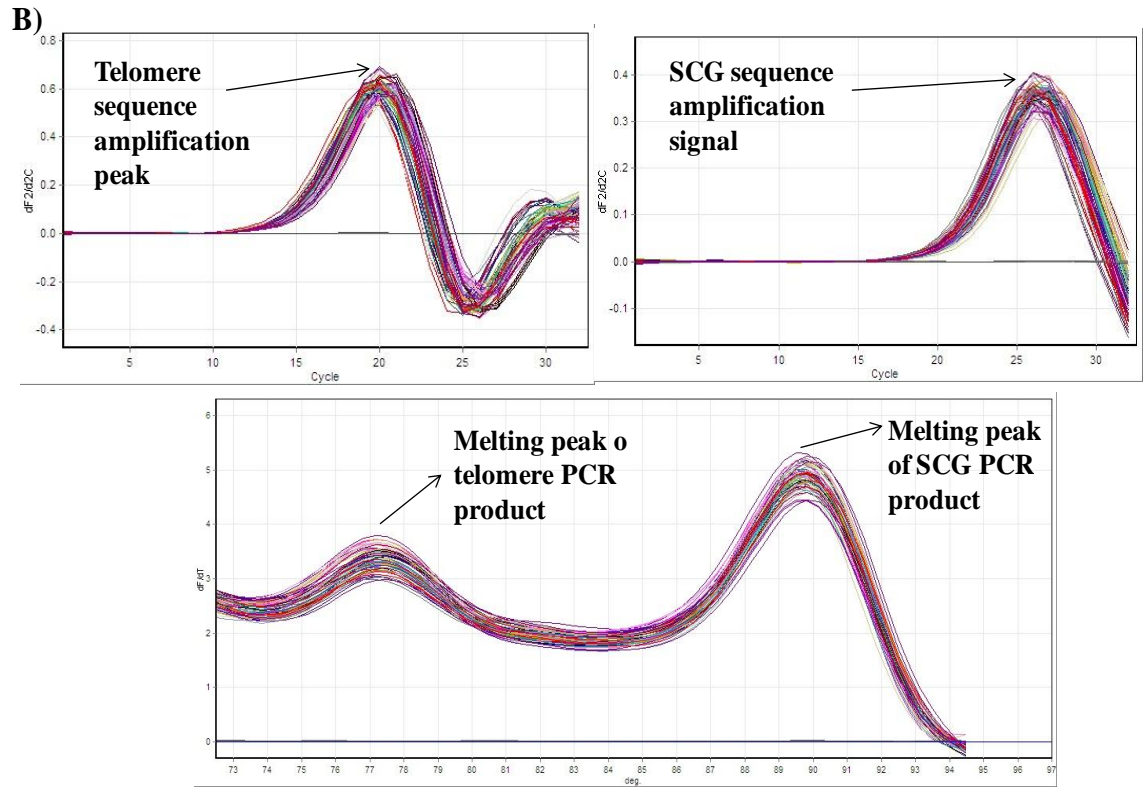
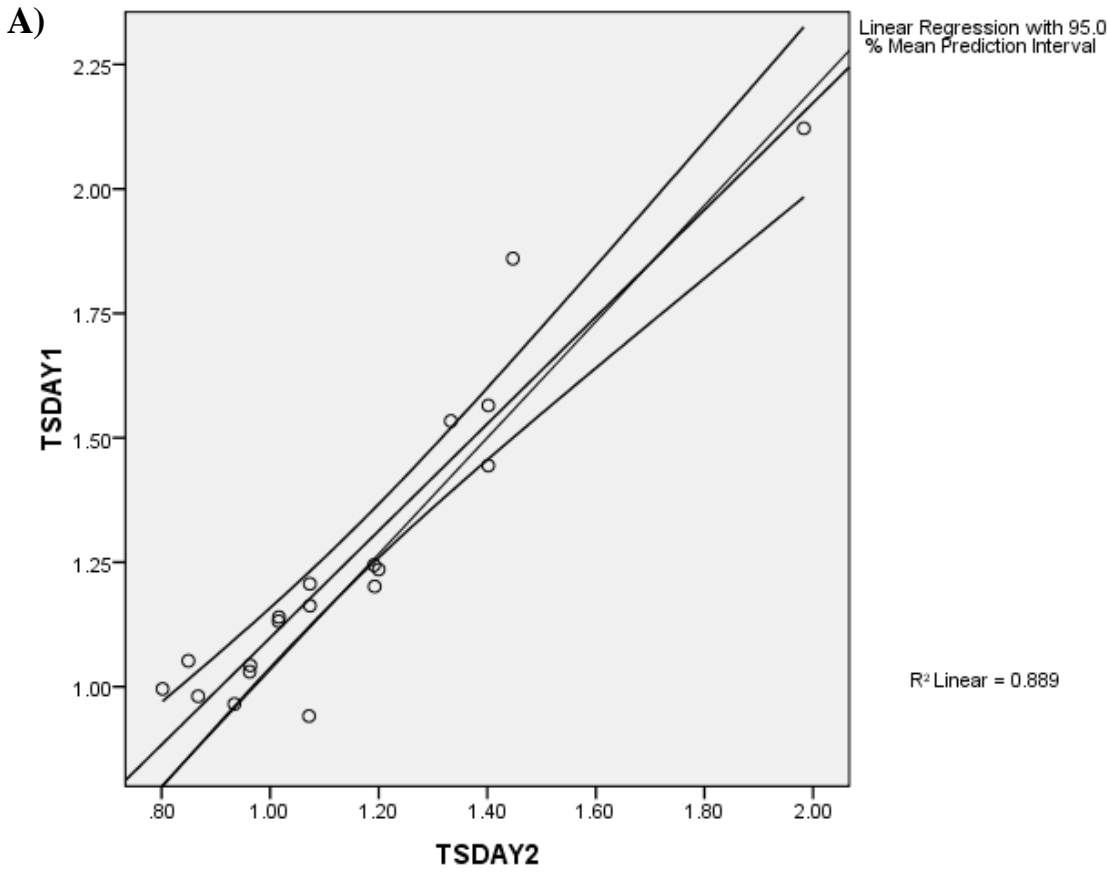
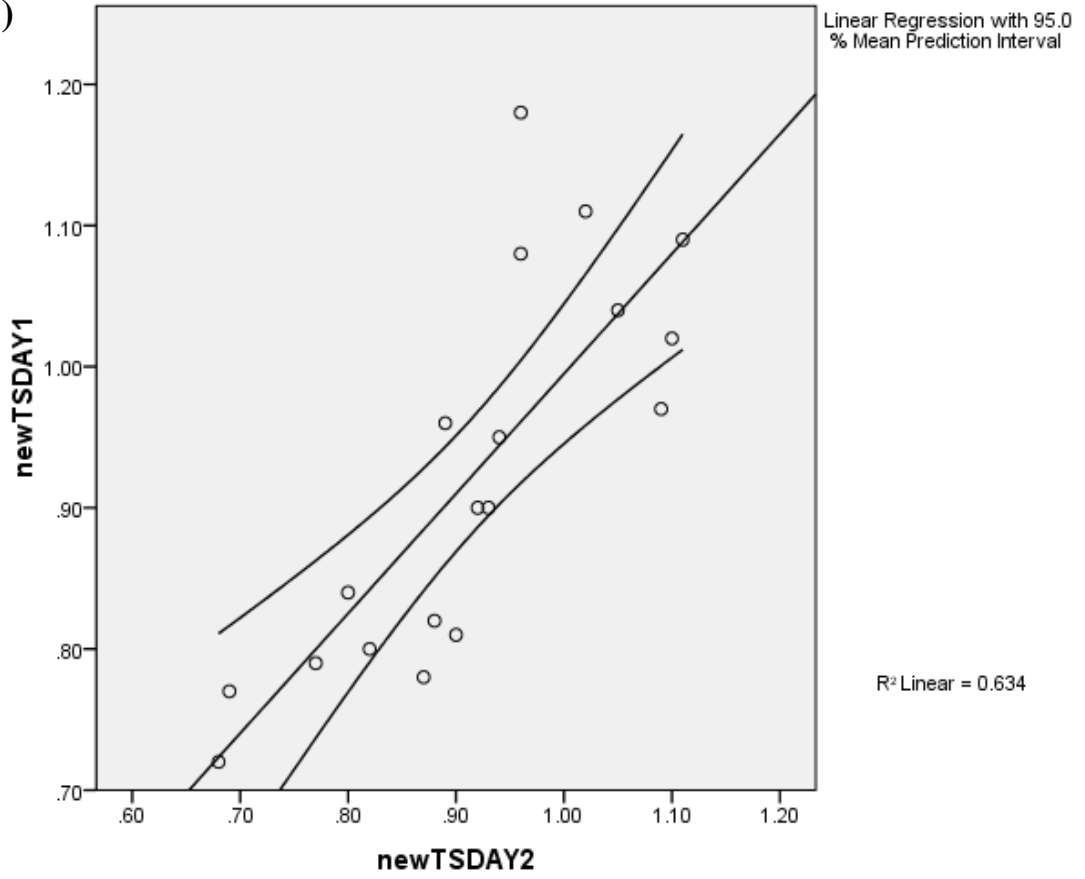


Figure III-20 Linear regression graphs between the telomere length estimates (T/S ratios) of the same 19 DNA samples measured on two consecutive days. A) Cycling conditions as suggested by Cawthon. B) Cycling conditions with higher annealing temperatures.



B)



Final MMQPCR conditions: The MMQPCR assay was finally optimised at the following conditions. A final reaction with volume of 25µl consisting of 2x SYBR Green, 1x qPCR mix (2x SensiMix DNA kit, Quantace), 1M of Betaine (Sigma, Aldrich, UK), 20 ng of template, telomere primers Telc and Telg at 900nM and HBB primers at 500nM. With a cycling profile of:

Stage 1 (1 cycle): at 95°C for 15 min.

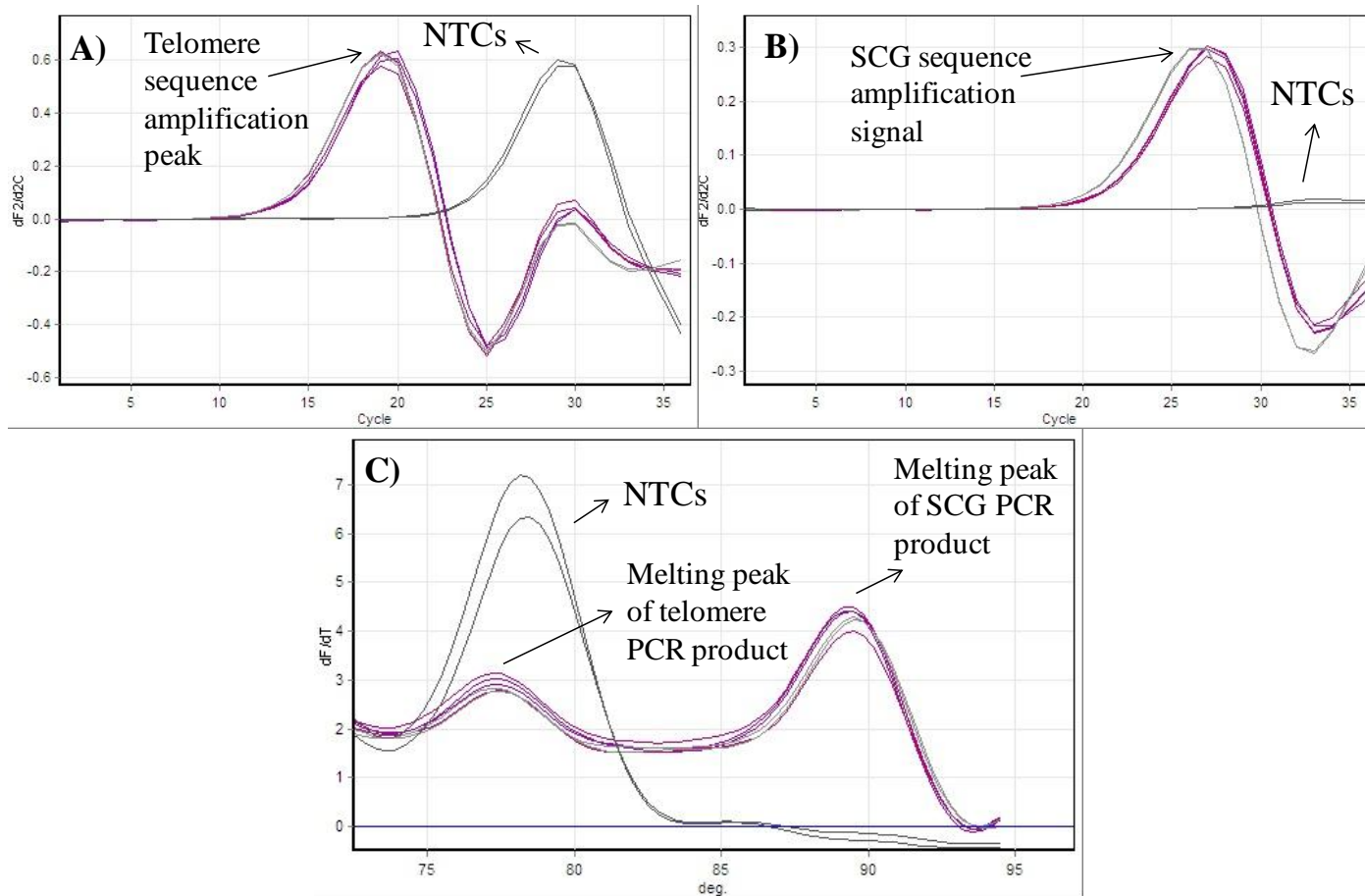
Stage 2 (2 cycles): at 94°C for 15 s and at 49°C for 15 s.

Stage 3 (32 cycles): at 94°C for 15 s, at 62°C for 10 s, at 74°C for 15 s and signal acquisition at channel A (collecting the telomere PCR amplification signal). This was then followed by 10 s at 84°C and 15 s at 88°C with signal acquisition at channel B (collecting the SCG PCR amplification signal).

Figure 21A shows the signal from channel (A) which collects the telomere amplification fluorescence and 21B the signal from channel (B) recording the fluorescence from the SCG amplification. The telomere amplification takes-off very early at 15-16 cycles, while the SCG amplification take-off level is approximately at 22-23 cycles. This means that the exponential phase of each target sequence's amplification is well separated from the other target sequence. Both reach a satisfactory level of maximum fluorescence, while the NTCs amplification level remains much lower than that of the DNA samples. In figure 21B, the NTCs during the cycles of the telomere's amplification exponential phase remain flat, and only in later cycles come up. This means that any non-specific amplification involving the telomere primers happens later when it does not interfere with the measurement of the telomere PCR product fluorescence. Regarding the specificity of

the two amplifications in this multiplex PCR, the melting, in figure 21C, shows that there are only two amplicons produced of the expected length. The two distinct peaks during melting indicate a specific telomere product of 79bp melting at $\sim 77.5^{\circ}\text{C}$ and the specific SCG product of 106bp which melts at $\sim 89.5^{\circ}\text{C}$. The NTCs appear to have generated a negligible amount of SCG primer product. The telomere primer-generated amplification in the NTCs is produced after the genomic telomere sequences' amplification has reached the plateau phase, which is evident in the fluorescence plot of figure 21A.

Figure III-21. A) Amplification signal of the telomere MMQPCR in channel (A), B) Amplification signal of the HBB (SCG) MMQPCR in channel (B), and C) Melting profile of both the MMQPCR products.



5.3 VALIDATION OF MMQPCR ADAPTION

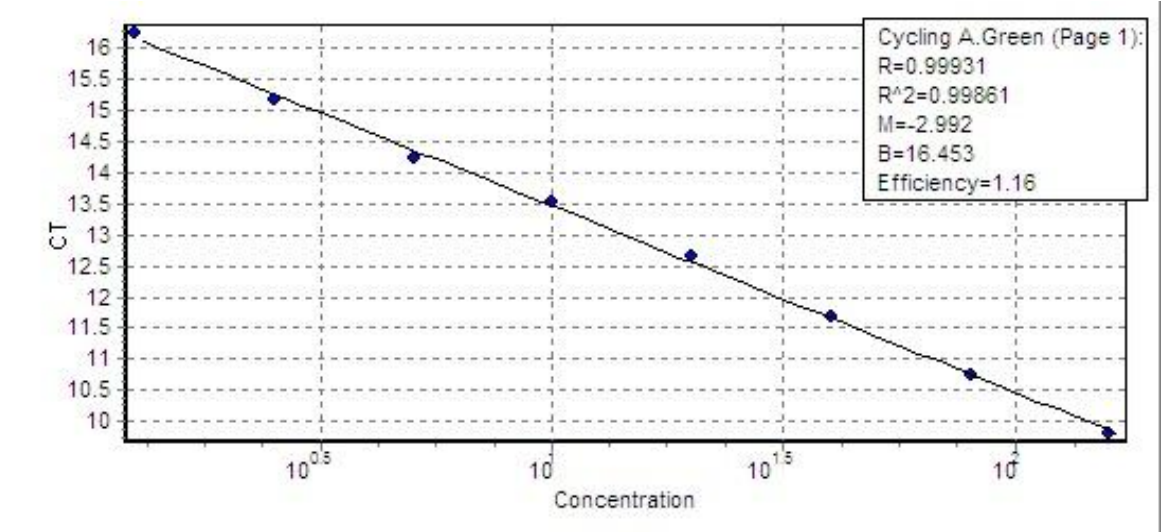
5.3.1 Quality Control – Standard Curves

In order to ensure the validity in determining the relative concentration of the two PCR products in MMQPCR a standard curve analysis for a dilution series was performed. In this case, the linearity between the template concentration series and the relative copies of telomere and SCG PCR product, as measured in parallel in a MMQPCR reaction, was tested.

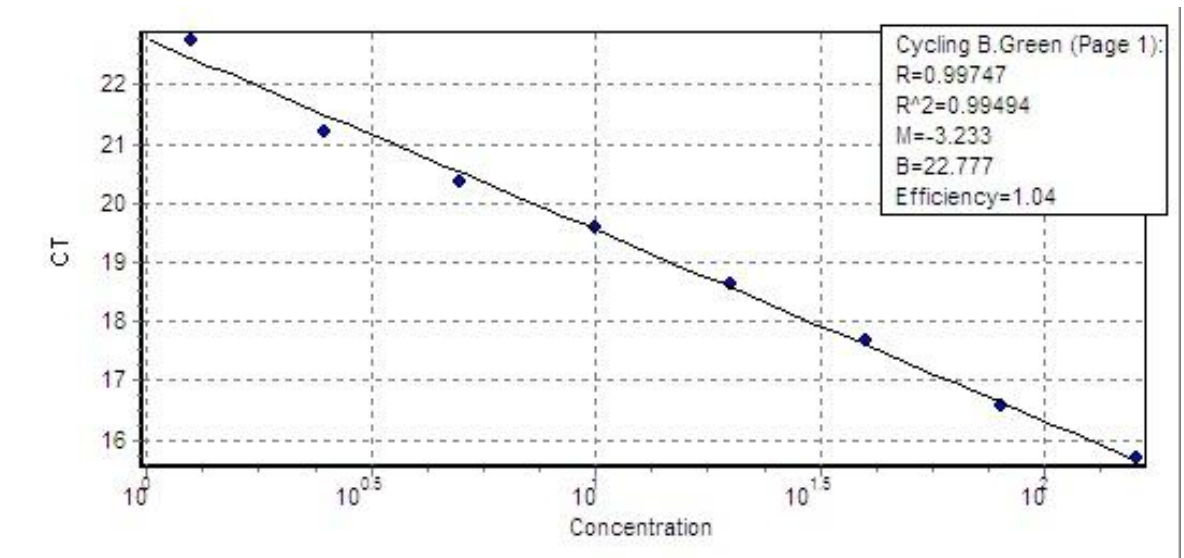
Thus, a dilution series (1.25 ng/μl - 160 ng/μl, two-fold dilution, eight points) was run after optimization of the MMQPCR. The relative concentrations of both PCR products –the telomere repeat copies and the SCG copies- as measured in the same multiplex reaction, linearity ($R^2 > 0.99$) over this range of input DNA was observed (figure 22A and 22B, respectively). Furthermore, both target sequences' amplification displayed ~100% efficiency, as calculated from the slope of the respective standard curves.

Figure III-22. Standard curves of A) Telomere PCR and B) SCG (*HBB*) PCR.

A)



B)



5.3.2 Reproducibility of the MMQPCR method

Nineteen randomly chosen DNA samples were measured on two consecutive days with the MMQPCR assay as optimised in our laboratory. A significant linearity between the mean telomere length measurements obtained on the two different days was observed in linear regression analysis as shown in figure 20A ($R^2=0.89$, $p<0.001$). Moreover, the reproducibility was also assessed with Spearman's non-parametric test of pair-wise correlation; and the correlation of rankings of the two repeated measures was found significant correlation (Spearman coefficient= 0.89 , $p<0.001$). The coefficient of variation of the telomere length estimates in the repeated measurements of the same sample was 4.5%, which is slightly better compared to that of the original qPCR method. This inter-assay coefficient of variation was higher compared to the 3.13% observed by Cawthon with the MMQPCR assay, however Cawthon's assays also displayed a 5.22% intra-assay variability (Cawthon 2009), which is eliminated when the samples are run on a rotor as in the present experiments.

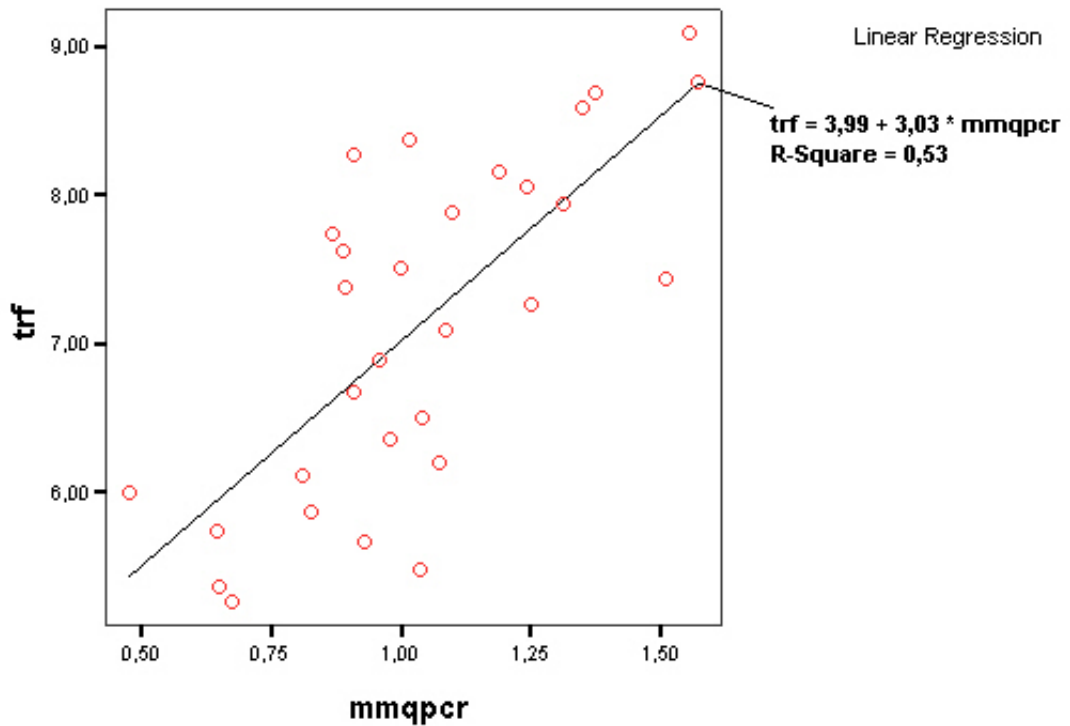
5.3.3 Comparison with the traditional TRF method for telomere length measurement

To validate the assay, the 32 DNA samples of subjects (aged 24 to 54 years) from the Cardiovascular Sciences Department, Leicester University DNA bank (see "First result chapter", paragraph 3.3, page 173) were also measured in using the MMQPCR method as adapted in our laboratory. The T/S ratios obtained were then compared to the TRF values obtained by the conventional TRF analysis in Leicester University, as previously described (Samani *et al.* 2001).

Linear regression analysis showed a significant positive correlation between the TRF values and T/S ratios measured with the MMQPCR assay ($R^2=0.53$, $p<0.0001$,

figure 23). As described also in paragraph 3.3 of this result chapter (174) a certain deviation from the telomere length as estimated by TRF analysis is expected. However this correlation of the TRF values with the T/S ratios measured using the MMQPCR was weaker than that observed with the T/S ratios measured using the original qPCR method ($R^2=0.63$). One possible explanation could be that the MMQPCR assay is more accurate than the original qPCR method, thus it measures more accurately the length of pure telomeric sequences and this increases the deviation from the TRF values which also measure the highly variable sub-telomeric region. Nonetheless, the correlation of MMQPCR telomere lengths with those obtained by TRF analysis was also weaker compared to that observed by Cawthon ($R^2=0.844$). Cawthon on the other hand performed this comparison using a greater number of samples (95 vs. 32 samples used in the present thesis) (Cawthon 2009).

Figure III-23. Correlation of the MMQPCR with the conventional TRF analysis.

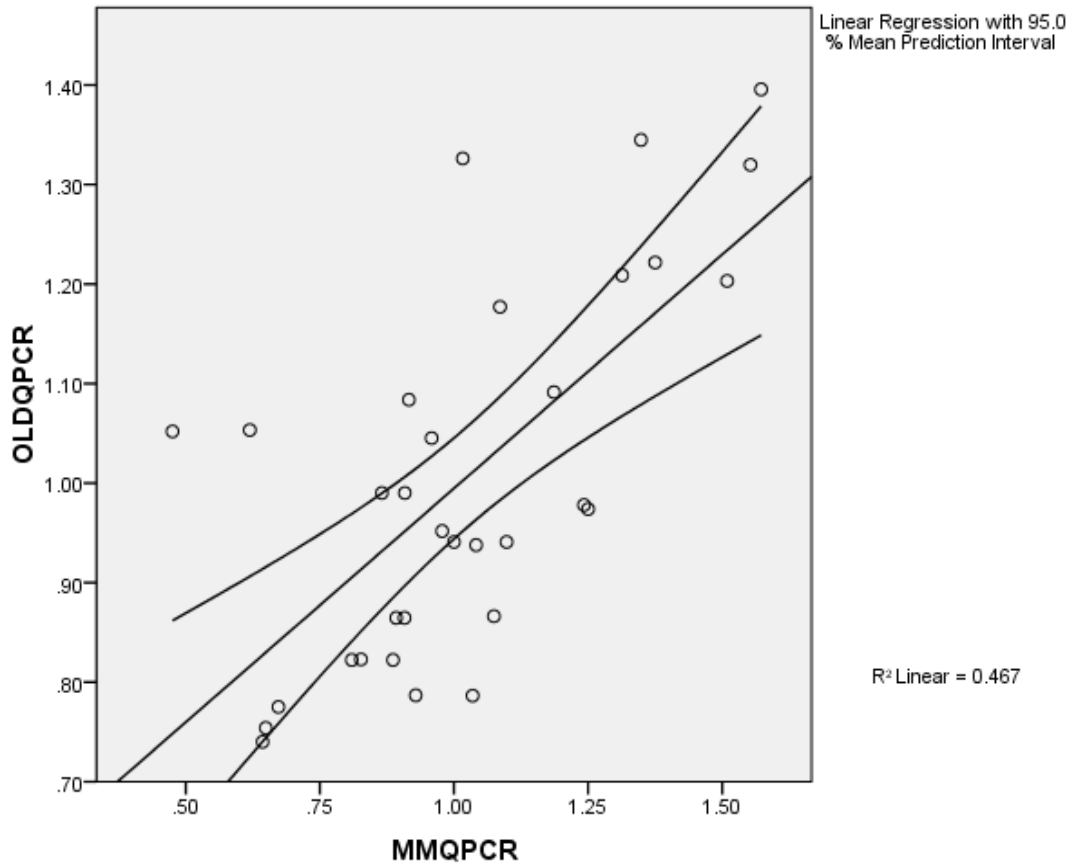


trf: mean telomere length in kilobases as measured by TRF analysis.

mqpcr: mean telomere length expressed as T/S ratio determined by the MMQPCR.

Then, I tested the correlation between the T/S ratios obtained with the original qPCR method and the MMQPCR using the same 32 DNA samples of the Leicester University DNA bank. Linear regression analysis showed that these T/S ratios correlated significantly ($R^2=0.47$, $p<0.001$, figure 24), although this association was not very strong, as it would be expected.

Figure III-24. Correlation of the MMQPCR with the original qPCR method.



This not so strong correlation between the T/S ratios estimated with the original qPCR assay and the MMQPCR is puzzling, since both assays measure the mean copy number per genome of pure telomeric repeat sequences. Unfortunately, Cawthon in his article has not examined this correlation in order to compare.

Nevertheless, the MMQPCR as adapted in our laboratory can be considered reliable since it is highly reproducible and valid taking into account that its measurements correlate significantly with those obtained by the original qPCR assay and with those obtained by TRF analysis. Moreover, this assay has certain advantages compared to the original qPCR. It requires less DNA template, which is very important

in the case of large study samples where the available DNA is restricted. Also, it requires fewer reactions per sample which reduces significantly the cost and time required.

The reproducibility and reliability of the method can be improved by using a set of three DNA samples as references, instead of one, as standards according to which all unknown samples are normalised. Thus, three DNA samples of known telomere length can be used as internal standards in each batch of samples for calculating the T/S ratios. Then the T/S ratio of each standard DNA will be divided by the average T/S ratio for the same DNA sample measured in ten runs, in order to obtain a normalising factor. The average normalizing factor for all three DNA standards can then be used to correct the measured T/S ratio of each unknown DNA sample. This modification for minimizing the inter-assay variability has been used in the study of Lin et al (Collerton *et al.* 2007; Lin *et al.* 2010). In addition, if these three reference DNA samples used as standards are DNA samples of known telomere length in kb as measured by TRF, then a very good estimate of the unknown samples' telomere length in kb can be obtained using the MMQPCR method.

IV. SECOND RESULT CHAPTER: “TELOMERE LENGTH IN CARDIOVASCULAR DISEASE AND T2D DIABETES PATIENTS”.

1. TELOMERE LENGTH IN CORONARY HEART DISEASE PATIENTS

1.1 INTRODUCTION

The first aim of the present thesis was to test the hypothesis that CVD and T2D is associated with shorter mean telomere length. The main disease representing CVDs is CHD, with the major endpoint of MI. There is growing evidence of an association between telomere length and CHD (Serrano & Andres 2004), where age- and sex-adjusted mean LTL of CHD patients was ~300 base pairs (bp) shorter than that of healthy subjects, and this difference was not accounted for by other CHD risk factors in a study of 203 cases and 180 controls. In the same study, the risk of MI for subjects in the lowest quartile of LTL was ~3 times higher compared with subjects in the highest quartile (Brouillette *et al.* 2003). Most importantly, prospective studies have supported the causative role of telomere length in the development of CHD (Brouillette *et al.* 2007; Fitzpatrick *et al.* 2007). The prospective West of Scotland Primary Prevention Study (WOSCOPS) with 484 CHD patients and 1058 controls revealed that individuals in the middle and the lowest tertiles of LTL were at higher risk of developing CHD compared to those in the highest tertile (Brouillette *et al.* 2007).

In this chapter, I examine the association of telomere length with CHD in cases of different disease aetiology, including both the common polygenic form of CHD and for the first time, CHD caused by monogenic familial hypercholesterolaemia (FH).

While, in general, CHD has a multifactorial origin, in some rare cases it has a monogenic cause such as FH. FH is an autosomal co-dominant disorder which leads to high levels of LDL-cholesterol and if untreated to early CHD (Thorogood *et al.* 2009). Heterozygous FH has been estimated to affect about one in 500 of the British population (Neil *et al.* 2000). I also aimed at investigating whether telomere length would be predictive of post-operative mortality, by examining a sample of CHD cases consisting of patients undergoing a first elective coronary artery bypass graft (CABG) surgery.

For pragmatic reasons, most of the population studies are using LTL (LTL), measured in DNA samples extracted from whole blood. Wilson *et al.* (Wilson *et al.* 2008) have shown that LTL is a good predictor of vascular wall telomere length. Thus, in the present thesis shorter LTL was taken as a surrogate marker of telomere length in vascular wall tissue.

1.2 METHODS

1.2.1 Subjects

Hypercoagulability and Impaired Fibrinolytic function MECHANISMS predisposing to myocardial infarction (HIFMECH) study. The HIFMECH study consists of 598 male survivors of a first myocardial infarction aged <60 years (excluding patients with familial hypercholesterolaemia and insulin-dependent diabetes mellitus) and 653 population-based control subjects of the same age and region, recruited from four centers in Europe: Stockholm in Sweden and London in England were designated North Europe and Marseille in France and San Giovanni Rotondo in Italy were designated South Europe. In all, a total of 598 post-infarction patients and

653 controls were included in the study. Patients and control subjects were examined in parallel in the early morning after an overnight fast. Post-infarction patients were investigated 3 to 6 months after the acute event. Blood samples were obtained from the antecubital vein after an overnight fast, collected into citrate (3.8% citrate, 0.129 mol/L) and centrifuged at 2500g for 30 minutes at 4°C. Detailed description of the study can be found in the study of Juhan-Vague et al. (Juhan-Vague *et al.* 2002).

The HIFMECH investigators include: Stockholm: A Hamsten (co-ordinator), S Boquist, C-G Ericsson, P Lundman, A Samnegård, A Silveira, P Tornvall. London: J Yudkin, V Mohamed-Ali, A Holmes. Marseille: I Juhan-Vague, MF Aillaud, PE Morange, MC Alessi, P Ambrosi, I Canavy, F Paganelli, R Didelot, J Ansaldi, M Billerey. San Giovanni Rotondo: G Di Minno, M Margaglione, D Cimino, N Dello Iacono, A Cimino, G Gaeta, C Blasich, G Pucciarelli. London: SE Humphries, E Hawe, L Ahn Luong Leiden: V van Hinsbergh, T Kooistra. Milan: E Tremoli, C Banfi, L Mussoni.

CABG study sample. The CABG patients were drawn from the coronary artery surgery inflammation study (CASIS) and are described in detail in the study of Brull et al. (Brull *et al.* 2001). All patients undergoing elective first time CABG at the Middlesex Hospital, London, UK, between October 1999 and September 2000 were invited to participate. Subjects undergoing additional surgical procedures (such as valvar surgery or aneurysmectomy), subjects with evidence of a preexisting inflammatory state or unstable coronary artery disease, and subjects who suffered potentially confounding infective postoperative complications or circulatory failure requiring inotropic support were excluded. Aspirin was omitted routinely 10 days before surgery. Blood samples were drawn preoperatively. These were centrifuged immediately (3500g, 10 minutes), and plasma and cells were separated and frozen at -

20°C. In the end this CABG group included in total 439 individuals (20 % women) having different ethnic origin (83% Caucasians, 8% Asians, 2% Afro-Caribbean, 2% of other ethnicity and 5% of unknown origin). The CASIS principle investigators include: HE Montgomery, J Sanders, and SE Humphries.

FH study samples. Two independent groups of FH patients were recruited from London hospitals. The first FH sample included 410 definite FH adult patients (47.7% women) recruited by one of the six outpatient hospital lipid clinics participating in the Simon Broome Familial Hyperlipidaemia Register Group and Scientific Steering Committee (FH-SB group). The second group of 94 FH patients was recruited from the Royal Free Hospital, London (FH-RF group).

The diagnostic criteria for familial hypercholesterolaemia were defined as a total cholesterol concentration above 7.5 mmol/l (treated or untreated), or LDL cholesterol above 4.9 mmol/l, together with the presence of tendon xanthomas either in the patient or in a parent, child, grandparent, sibling, uncle, or aunt (Scientific Steering Committee 1991). Patients with known diabetes, renal, or thyroid disorders were excluded. Clinical CHD was defined as patients with a definite MI (new Q waves and/or ST elevation and/or new T wave inversion persisting in more than two leads together with creatine kinase > 400 iu/l or other equivalent enzyme changes) or having undergone coronary artery bypass grafting, percutaneous transluminal coronary angioplasty, having angina with an ischaemic resting ECG, or an abnormal angiogram CHD. Using these criteria, CHD was documented in 104 of the 211 men and in 55 of the 199 women with mean ages of onset of 43.1 and 46.5 years, respectively (Neil *et al.* 2004) among the FH-SB patients. The mean age of the FH-RF patients was 57.7 years (SD=14.6) and 17 of them suffered from CHD.

All studies had been designed and carried out according to the Helsinki declaration and received approval from the ethics committee of the respective recruitment centers/hospitals. All patients gave written informed consent. The principle investigators of the FH-SB study group, which is part of the Simon Broome Familial Hyperlipidaemia Register Group FH patient sample, include: A Neil and SE Humphries. The principle investigators of the FH-RF study group include: & D Nair and SE Humphries.

1.2.2 Phenotypic variables

Details on lifestyle factors (i.e. smoking, alcohol consumption, and physical activity), personal and family medical history, medication and physiological measurements [i.e., height, weight, BP] were acquired using standardised questionnaires and protocols (Brull *et al.* 2001; Neil *et al.* 2004) by each study's principle investigators.

1.2.3 Measurement of leukocyte telomere length

Leukocyte DNA was extracted by the salting-out method, as described in the "General methods" paragraph 2.1 (pages 109-112). Telomere length was measured in these DNA samples using the validated qPCR-based method, which is thoroughly described in the "First result chapter", paragraphs 1, 2 and 3 (pages 149-174). The coefficient of variation in repeated measurements was 5.6%. The corresponding telomere length in bp was calculated from the T/S ratio measured in each sample using the linear regression line between measures obtained by both the qPCR-based method and the conventional TRF analysis for the same set of 32 samples, as described in the "First result chapter", paragraph 3.3 (page 173).

To assess the validity of the method, variability in telomere and SCG PCR amplification efficiency was compared between the three studies. Values were comparable, and the standard deviations overlapped, rendering the T/S ratios obtained in different runs comparable. To ascertain that inter-assay variability did not interfere with the results, T/S ratio measurements were repeated for 32 randomly selected samples from the FH group without CHD and 32 region-matched controls from the HIFMECH study in two runs including samples from both studies. LTL was longer in the FH group (9.41 kb, SD=6.20) compared to the UK controls (8.49, SD=5.10; $p=0.059$) for this sub-set of samples, as reported for the total group.

1.2.4 Statistical analysis

Statistical analysis was performed using Stata (version 10, StataCorp Texas). Analysis was restricted to Caucasians in order to maintain ethnic homogeneity in the sample. LTL, BMI, triglycerides, insulin, homocysteine, C-reactive protein and systolic blood pressure were not normally distributed, and thus log-transformed data were used for the analysis. For all transformed variables, geometric means with approximate standard deviation (SD) are presented in tables. Results on telomere lengths are presented as geometric means with 95% confidence intervals (CIs). The comparison between cases and controls for the variables presented in table 1 was performed with conditional logistic regression models in HIFMECH matching for age and centre. For the FH study, mean values were compared by t test. For the association of telomere length with lifestyle parameters, p values were obtained from analysis of covariance models, and the regression estimates were used to obtain adjusted mean values. Adjustment was made for age, centre and exercise in HIFMECH, age in CABG and age and gender in FH.

The comparison between CHD cases and controls is also presented as odds ratios obtained from conditional logistic regression models using telomere length as a categorical variable, after dividing into tertiles. The tertiles of telomere length were constructed using the combined case-control group with the age-adjustment made within the separate groups. In the end a random effects meta-analysis of the odds ratios in each study was performed. Statistical significance was taken as $p < 0.05$.

1.3 RESULTS

1.3.1 General characteristics of study subjects

Mean LTL was successfully determined in 559 cases and 520 controls of the HIFMECH study, 413 cases of the CABG study and 461 FH patients in total (367 FH-SB and 94 FH-RF patients). The characteristics of these subjects are shown in Table 1, and they did not differ significantly from that of the whole group for any of the parameters. In both the HIFMECH and the FH studies, there were the expected significant differences between CHD cases and controls in risk factors such as BMI, diastolic blood pressure, cholesterol, triglyceride levels and where available inflammatory [i.e. CRP and interleukin 6 (IL6)] factors.

Table IV-1. Characteristics of study subjects.

	HIFMECH			CABG	FH - SB			FH - RF		
	Controls	Cases	<i>p</i>		- CHD	+ CHD	<i>p</i>	- CHD	+ CHD	<i>p</i>
Number	559	520		413	222	145		77	17	
%women	(0)	(0)	-	(20.8)	(56.8)	(33.8)	<0.001	(61.3)	(47.1)	0.28
Age (yrs)	51.5 (5.5)	51.9 (5.4)	-	64.9 (92.2)	44.3 (13.4)	56.1 (10.3)	<0.001	51.9 (14.3)	58.7 (14.0)	0.08
BMI*	26.1 (3.2)	27.1 (3.3)	0.001	28.2 (4.5)	23.8 (4.0)	25.1 (3.4)	0.005			
SBP*	127.8 (14.4)	127.7 (16.9)	0.75		123.7 (15.6)	130.6 (19.7)	<0.001			
DBP	84.0 (8.4)	81.7 (10.2)	<0.001		77.3 (9.1)	79.3 (11.3)	0.06			
TC	5.52 (0.97)	5.40 (1.18)	0.06	4.71 (1.03)	6.91 (1.30)	6.35 (1.31)	<0.001	8.76 (1.50)	10.11 (2.77)	0.02
TG*	1.44 (0.61)	1.88 (0.77)	<0.001		1.24 (0.56)	1.46 (0.69)	0.001	1.52 (0.68)	2.16 (1.24)	0.03
LDL				2.53 (0.88)	4.80 (1.28)	4.21 (1.23)	<0.001	6.34 (1.48)	7.65 (2.68)	0.05
HDL				1.23 (0.35)	1.38 (0.35)	1.28 (0.36)	0.01	1.47 (0.40)	1.10 (0.29)	0.005
GLU				6.19 (2.05)	4.82 (0.59)	5.07 (0.59)	<0.001			
Insulin*	37.8 (24.3)	49.3 (34.5)	<0.001							
HC*	8.27 (2.59)	8.55 (3.36)	0.03		10.54 (3.45)	11.57 (3.20)	0.005			
CRP*	1.23 (1.40)	2.22 (2.55)	<0.001	2.29 (2.77)	1.16 (1.34)	1.42 (1.59)	0.10			
IL-6	1.24 (0.78)	1.97 (1.33)	<0.001	4.55 (3.12)	1.58 (1.14)	2.18 (1.34)	<0.001			
Unadjusted LTL‡	8.04 (7.88-8.20)	7.90 (7.77-8.03)	0.34	6.85 (6.69-7.01)	9.82 (9.51-10.13)	9.04 (8.68-9.40)	0.001	9.82 (9.30-10.34)	9.04 (7.99-10.09)	0.001

Means with standard deviation are presented for each variable unless otherwise stated.

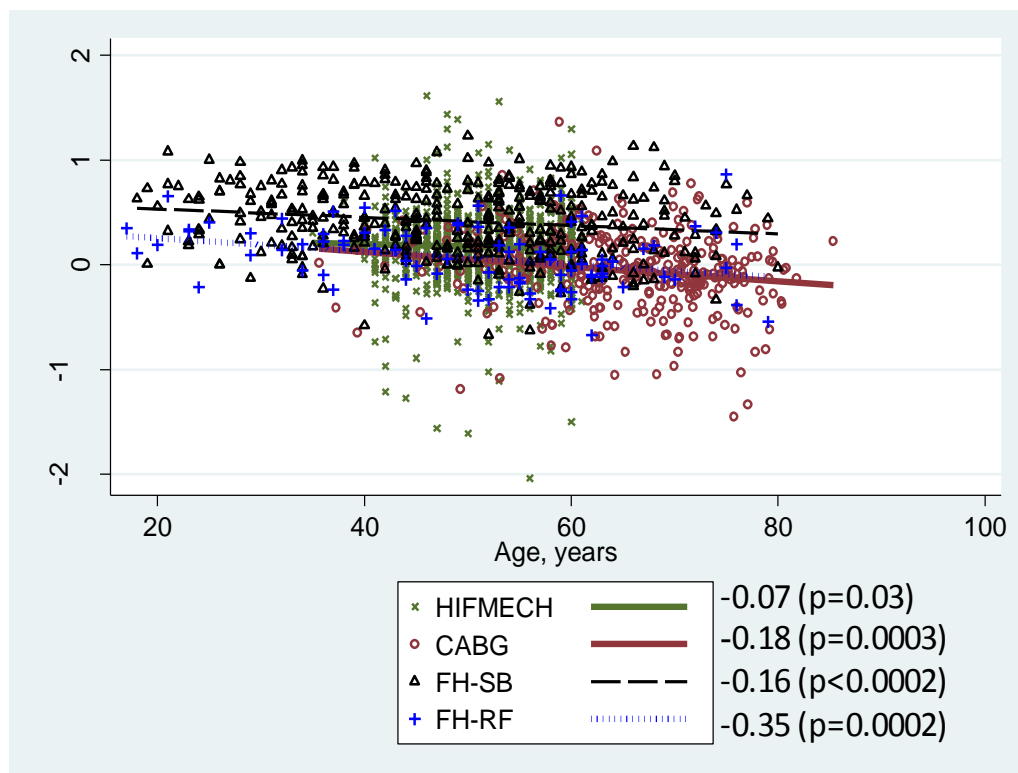
*data were log-transformed and geometric means (approx SD) are presented, ‡ Data were log-transformed and the geometric means with 95% confidence intervals (95%CI) was then used to calculate the corresponding telomere length in kb.

BMI: Body mass index in kg/m², SBP: systolic blood pressure in mmHg, DBP: diastolic blood pressure in mmHg, TC: total cholesterol in mmol/l, TG: triglycerides in mmol/l, HDL: high density lipoprotein in mmol/l, GLU: Glucose in mmol/l, INS: insulin in (mU/l), HC Homocysteine in mmol/l CRP: C reactive protein in (mg/l), IL-6: interleukin 6 in pg/ml, LTL: leukocyte telomere length in kb.

1.3.2 Age and gender differences in telomere length

As shown in figure 1, LTL correlated negatively with age in all three study samples, HIFMECH ($r=-0.07$, $p=0.03$), CABG ($r=-0.18$, $p=0.0003$), FH-SB ($r=-0.16$, $p<0.0002$) and FH-RF ($r=-0.35$, $p=0.0002$). No significant gender difference was found in the CABG group (0.95 kb in men vs. 0.93 kb in women, $p=0.74$), whereas among FH patients, men had significantly shorter telomeres than women (9.23 kb in men vs. 9.82 kb in women, $p=0.01$ for the FH-SB group and 6.93 kb in men vs. 7.57 kb in women, $p=0.02$ for the FH-RF patients). Therefore, telomere length was adjusted for age in all further analysis and for age and gender in analysis concerning the FH groups.

Figure IV-1. Decrease of telomere length with age in each study sample.



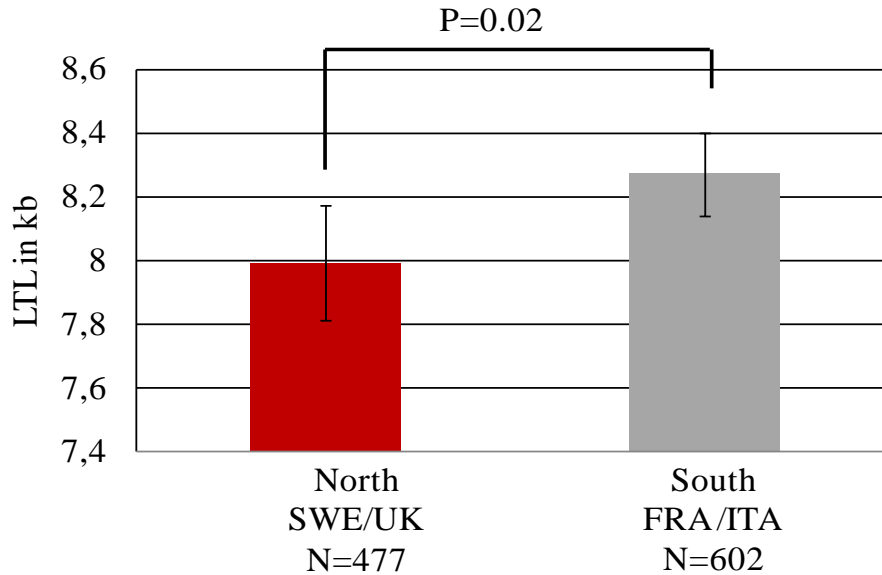
1.3.3 Lifestyle-related differences in telomere length

Smoking and alcohol intake did not have a significant effect on telomere length ($p>0.4$). However, it appeared that the less active subjects had longer telomeres in the combined HIFMECH cohort after adjustment for case–control status (sedentary: 7.90 (7.75-8.05) $n=399$, moderate active: 7.99 (7.81-8.17) $n=399$, active: 7.53 (7.29-7.77) $n=183$ and fit: 7.58 (7.26-7.89) $n=93$, $p=0.005$). When cases and controls were examined separately, no significant association between LTL and level of exercise was found. Nevertheless, in order to avoid any possible confounding effect in the rest of the analysis in HIFMECH, telomere length was also adjusted for exercise level.

1.3.4 Geographical differences in telomere length

Age, exercise and case–control status adjusted telomeres were significantly longer in subjects from the South compared to the North of Europe in HIFMECH [7.99 kb (7.81-8.17) vs. 8.27 kb (8.14-8.40), $p=0.02$] (Figure 2); a difference corresponding to approximately 280 bp. All further analysis in HIFMECH was also adjusted for geographical region.

Figure IV-2. Comparison of mean leukocyte telomere length (kb) between North and South of Europe in HIFMECH study.



Geometric mean of age, exercise and status adjusted leukocyte telomere length (LTL) in kb and 95% confidence intervals are presented.

1.3.5 The effect of CHD risk factors on telomere length

As shown in table 2, in the FH-SB subjects, BMI and triglyceride and glucose correlated positively with telomere length ($r=0.26$, $p<0.0001$, $r=0.11$, $p=0.03$ and $r=0.14$, $p=0.006$ respectively) but these effects were not consistent across studies. Insulin levels displayed a negative correlation with telomere length in HIFMECH cases ($r=-0.15$, $p=0.005$) only but not the controls. Homocysteine has been previously shown to increase the amount of telomere length loss per population doubling in endothelial cells through a redox-dependent pathway (Xu *et al.* 2000). Thus its correlation with LTL was also tested,

but no significant effect was observed. No association was found between telomere length and diabetes, hypertension or hyperlipidaemia in the HIFMECH and the CABG cohorts.

Table IV-2. Partial Pearson correlation coefficients of telomere length with classical risk factors.

	HIFMECH				CABG		FH	
	Controls		Cases		<i>r</i>	<i>p</i>	<i>r</i>	<i>p</i>
	<i>r</i>	<i>p</i>	<i>r</i>	<i>p</i>				
BMI (kg/m²)	-0.07	0.09	-0.07	0.13	0.03	0.63	0.26	<0.0001
SBP (mmHg)	-0.01	0.76	0.04	0.35			-0.06	0.29
DBP (mmHg)	-0.02	0.60	-0.02	0.73			-0.08	0.13
TC (mmol/l)	-0.02	0.61	-0.03	0.56	-0.01	0.86	-0.03	0.54
TG (mmol/l)	-0.004	0.93	-0.07	0.15			0.11	0.03
HDL (mmol/l)					-0.02	0.8	-0.03	0.54
Glucose (mmol/l)					-0.06	0.38	0.14	0.006
Insulin (mU/l)	-0.008	0.87	-0.15	0.005				
Homocysteine (mmol/l)	-0.03	0.53	-0.06	0.16			0.02	0.77

Partial Pearson correlation coefficients *r* was adjusted for age, center and exercise in HIFMECH, age in CABG and age and gender in FH and further adjusted for case-control status when cases and controls are pooled.

BMI: Body mass index, SBP: systolic blood pressure, DBP: diastolic blood pressure, TC: total cholesterol, TG: triglycerides HDL: high density lipoprotein.

BMI, triglyceride, insulin, homocysteine, CRP, SBP and homocysteine were log-transformed for tests.

1.3.6 Polygenic CHD case–control differences in telomere length

i) HIFMECH

Age, exercise and region adjusted LTL was significantly shorter in premature MI cases [7.85 kb (7.72-7.98)] compared to controls [8.04 kb (7.88-8.20), $p=0.04$] (Figure 3). The difference corresponded to approximately 190 bp.

ii) CABG

The CABG cases were compared to region-matched controls from the HIFMECH study. Due to the geographical differences observed in LTL between South and North of Europe, the North Europe controls from the HIFMECH study were used in order to match the UK recruited CABG cases. LTL, adjusted to the age of 65 years, was significantly shorter in CABG cases [6.89 kb, (6.74-7.04)] compared to the North region HIFMECH controls [7.99 kb (7.39-8.59), $p=0.003$] (Figure 3), but also compared to all HIFMECH controls [7.72 kb (7.62-7.82), $p<0.0001$].

After 6 years follow-up of the CABG patient sample, 40 deaths were recorded. Interestingly, subjects who died in these 6 years had shorter telomeres [6.66 kb (6.20-7.12)] compared to those who survived [6.94 kb (6.78-7.10), $p=0.28$], but this difference was not significant.

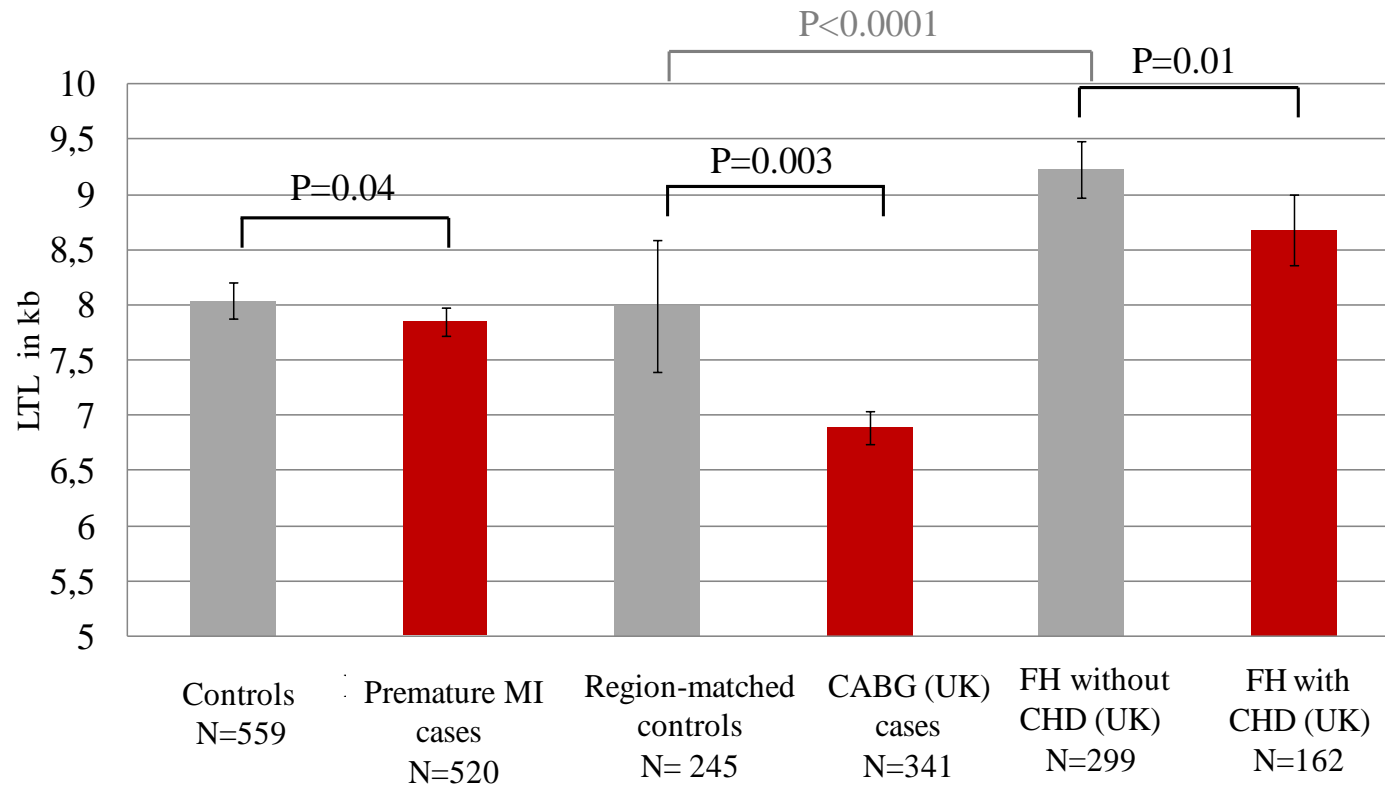
1.3.7 Monogenic CHD case–control differences in telomere length

Since both FH patient samples were recruited from UK according to the same diagnostic criteria, they were combined for the comparison of LTL between those with and without CHD in order to increase statistical power. In the combined FH cohort, age, gender

and study adjusted LTL was shorter in those with CHD [8.68 kb (8.36-9.0)] compared to those patients without CHD [9.23 kb (8.97-9.49), $p=0.01$] (Figure 3). The difference between those with and without CHD was also examined in each FH patient sample separately. The same trend towards shorter telomeres in those with CHD was observed [FH-SB: 9 kb (8.64-9.36) vs. 9.46 kb (9.17-9.75), $p=0.09$ and FH-RF: 6.84 kb (6.43-7.25) vs. 7.53 kb (7.20-7.86), $p=0.15$].

In addition, telomere length was compared between the combined FH patients without CHD and region-matched controls from HIFMECH. LTL, adjusted to males at the age of 51.6 years, was longer in FH patients compared to the region-matched controls [8.81 kb (8.49-9.14) vs. 7.85 kb (7.58-8.13), $p<0.0001$].

Figure IV-3. Comparison of telomere length between CHD cases and controls.

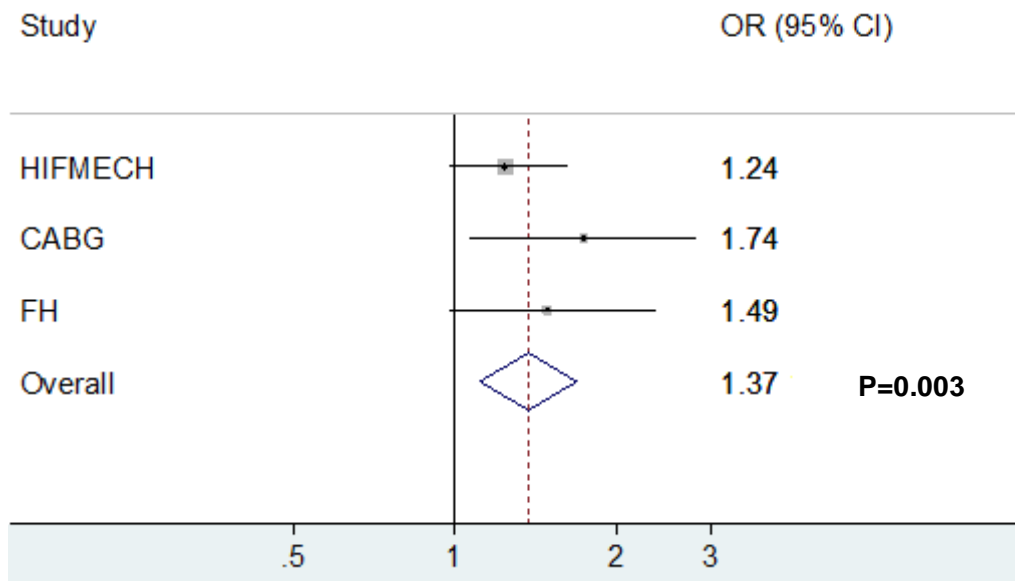


Geometric mean of LTL in kb and 95% confidence intervals are presented. In HIFMECH, telomere length is adjusted for age, region and exercise, in CABG for age and in FH study, for age and gender.

1.3.8 Overall association of CHD with telomere length / meta-analysis

To better illustrate the association of CHD with short telomeres, the present study samples were divided in tertiles of LTL. In each of the three case-control designs the subjects with LTL in the lowest tertile, i.e. shorter telomeres, displayed higher odds ratio for CHD when compared to subjects in the middle and the highest tertile of LTL [HIFMECH: 1.24 (95%CI: 0.95-1.62), CABG: 1.74 (95%CI: 1.07-2.81), FH: 1.49 (95%CI: 0.95-2.36)]. A meta-analysis of the three case-control studies showed that being in the lowest tertile of LTL is significantly associated with 37% higher odds ratio for CHD compared to those in the middle and highest tertiles of LTL [1.37 (95%CI: 1.11-1.69), $p=0.003$] (Figure 4).

Figure IV-4. Odds ratio (OR) for CHD when having LTL in the lowest tertile / meta-analysis.



1.4 Discussion

The results of this chapter showed that premature MI male patients, CHD patients undergoing CABG and FH patients with CHD have shorter age-adjusted LTL compared to subjects without CHD. These observations confirm that shortened telomeres are linked to CHD and extend this association to those with monogenic and polygenic forms of CHD. Using the correlation between telomere length and age, the decline in telomere length can be approximately estimated at 14 bp per year in HIFMECH and 34 bp per year in the FH studies. From these values, the difference in mean LTL between CHD cases and controls (190 bp in HIFMECH and 550 bp in FH) corresponds to a biological age equivalent to 14 older for the polygenic CHD cases and 16 years older for the monogenic CHD cases compared to controls. This is in accordance with Brouillette *et al.* (Brouillette *et al.* 2003) who found that premature MI cases had 300 bp shorter LTL than controls, which corresponded in average to a biological age gap of 11 years.

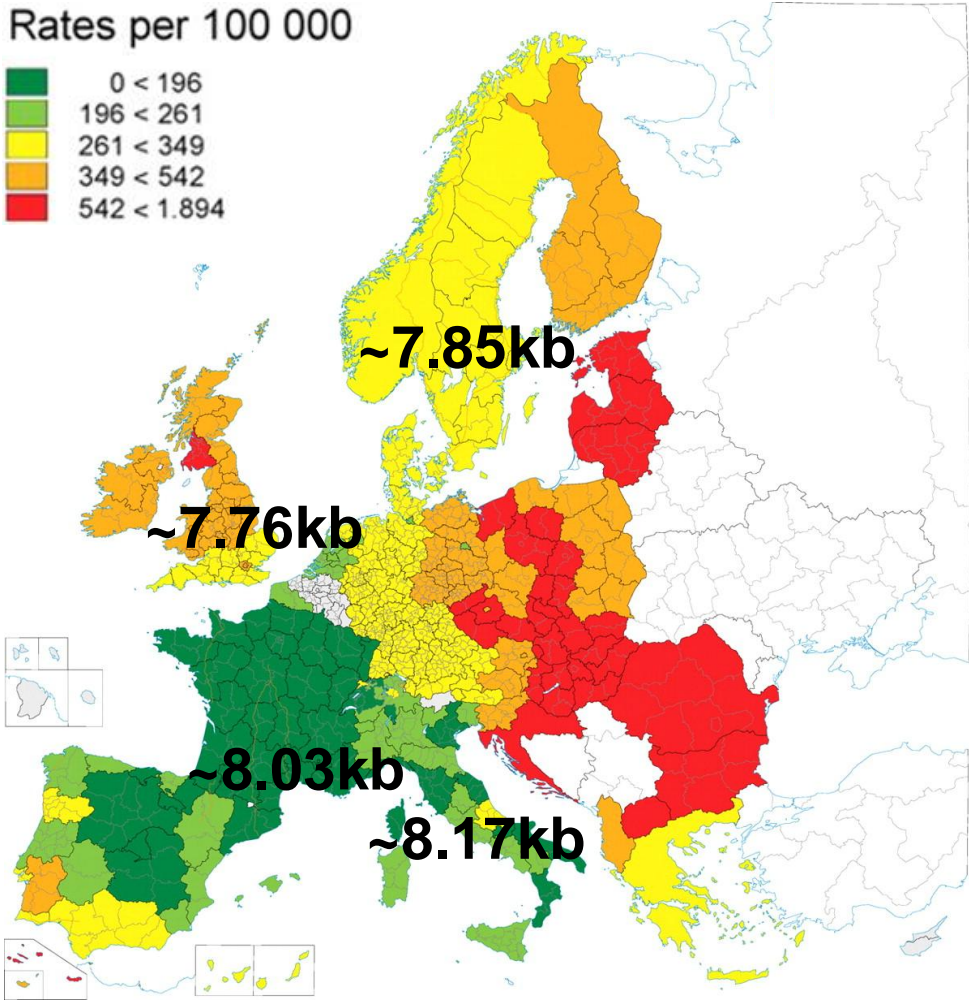
These data, coupled with those of others (Brouillette *et al.* 2003; Brouillette *et al.* 2007; Fitzpatrick *et al.* 2007; Farzaneh-Far *et al.* 2008; Mukherjee *et al.* 2009), suggest that shorter LTL, is a marker for CHD and MI. Since LTL has been shown to strongly correlate with vascular wall telomere length (Wilson *et al.* 2008), it can be concluded the association of CHD with shorter LTL, reflects the common underlying abnormality of excessive vascular wall ageing in patients developing CHD. This raises the possibility for telomere length to prove useful in identifying individuals at particularly high risk of CHD, who may benefit from earlier or more intensive treatment (Spyridopoulos *et al.* 2004). However, because telomere length is highly variable between subjects of different ethnicity (Salpea *et al.* 2009) and ages (Aviv 2008), and, so far, the data on the rate of shortening are scarce, it

is not yet possible to establish a cut-off value in order to distinguish patients who may benefit from early use of medication.

In the present study samples, there were a few significant correlations between classical risk factors and LTL. The inverse correlation with insulin in HIFMECH cases could possibly reflect the inverse association of LTL with insulin resistance, although it was not significant in HIFMECH controls. Unfortunately, data on insulin levels were not available in the other studies. In the FH patients, unexpected positive correlations with BMI, triglycerides and glucose were observed; however these findings were not replicated in the other three study samples. The fact that no consistent correlation with risk factors, such as HDL levels, BMI and smoking, were observed throughout the four studies is in contrast to other published reports (Valdes *et al.* 2005; Chen *et al.* 2009; Lee *et al.* 2011). In each particular study presented here, the absence of a significant correlation can be due to lack of power resulting from a relatively small sample size. Given these data, we cannot confirm the correlations observed nor refute those reported in other studies.

Worthy of remark are the geographical differences observed in the multicenter European study employed here (HIFMECH), with telomeres being approximately 280 bp longer in the South (San Giovanni Rotondo, Italy and Marseille, France) compared to the North of Europe (Stockholm, Sweden and London, UK) At the same time, the regions having longer telomeres have also been repeatedly shown to have lower CHD risk (Iacoviello *et al.* 2001) and CVD-related mortality rates (Muller-Nordhorn *et al.* 2008) compared to the North, where mean telomere length was found to be shorter.

Figure IV-5. Color-illustrated age-standardised mortality from CVD among men of the age group 45–74 years in Europe (Muller-Nordhorn *et al.* 2008) and age-adjusted mean LTL (kb) in each of the four recruitment centers (Stockholm, Sweden; London, UK; Marseille, France; San Giovanni Rotondo, Italy) in HIFMECH.



As illustrated in figure 5, there appears to be an agreement between the region-specific mortality from CVD across Europe with the differences seen in telomere length, supporting the association of telomere length with the development and possibly the prognosis of CVD. However, more data on telomere length in the different European countries is needed to confirm this.

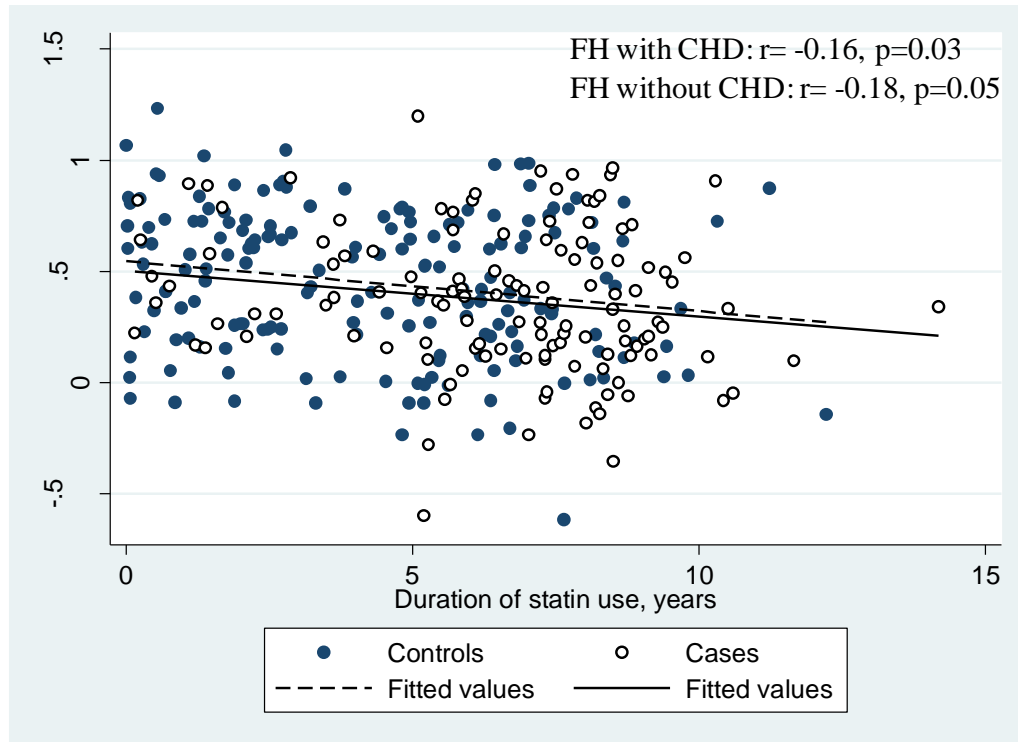
In the present study LTL was, for the first time, evaluated in FH patients. The patients suffering from CHD had roughly 550 bp shorter telomeres than FH patients without CHD, broadening the association of short telomeres with CHD to also monogenic forms. This finding is important as it shows that short telomeres reflect an essential feature of CHD pathogenesis, common in both polygenic and monogenic forms, which probably is the accelerated vascular wall ageing. Interestingly, the differences observed with the CHD cases of monogenic aetiology, in this case FH, are greater than the difference in telomere length observed with cases of polygenic CHD aetiology in the present study and that of Brouillette et al.

Of particular interest is the observation that FH patients, which have not developed CHD, had an estimated 960 bp longer telomeres than healthy controls after adjustment for age and gender. A possible explanation could be that the FH patients without CHD, being recruited in this study, are the “survivors”, and the FH patients with shorter telomere length had died earlier, most likely from CHD. Another possibility is that the prolonged statin treatment, prescribed to FH patients early in life, is responsible for the longer telomere length observed in these subjects. Evidence supporting this hypothesis comes from studies showing that statin administration attenuates telomere shortening. Satoh et al. showed that in a culture of endothelial progenitor cells subject to oxidative stress (by inhibiting the

cellular detoxification of peroxides), intensive lipid lowering treatment with atorvastatin led to the prevention of endothelial progenitor cells telomere shortening (Sato *et al.* 2009). Moreover, Mahmoudi *et al.* showed that atorvastatin treatment reduced telomere shortening in vascular smooth muscle cells cultured with a free radical-generating agent (Mahmoudi *et al.* 2008). Regarding the possible mechanism of this effect, Mahmoudi *et al.* (Mahmoudi *et al.* 2008) showed that statin treatment reduced telomere shortening in their experiments by markedly enhancing DNA repair. Also, Spyridopoulos *et al.* showed *in vitro* that statins induce an increase in expression of the important telomere capping protein TRF2, (Spyridopoulos *et al.* 2004), which potentially stabilises the structure of telomeres preventing their shortening. The direct relevance of this to patients has yet to be confirmed.

Considering the protective effect of statins against telomere shortening as shown in the above studies, it is possible that the longer telomere length in the FH patients free of CHD compared to healthy subjects could be a consequence of the prolonged statin treatment that these patients have received. While a proof of this hypothesis would require the availability of follow-up measurements of telomere length in subjects on statins or not, the observed significant negative correlation between telomere length and duration of statin use in the FH-SB group renders this explanation less likely (Figure 6).

Figure IV-6. Correlation between telomere length and duration of statin use in FH patients.



Nonetheless, it will be of great interest to evaluate telomere length and rate of attrition in larger samples of FH patients, in order to examine whether the observed longer telomeres is a chance finding or not and investigate the underlying mechanism.

In conclusion, it is now strongly confirmed that short telomeres length is a marker of CHD along with its complications, such as MI. The present data in three different case-control studies support this concept and provide the first data on the association of short telomeres with CHD among FH patients.

2. LEUKOCYTE TELOMERE LENGTH IN TYPE 2 DIABETES PATIENTS

2.1 INTRODUCTION

The first aim of the present thesis included the comparison of telomere length between diabetes patients and controls. T2D is also an age-related disease, where cell senescence plays a major role in its pathogenesis, and at the same time consists a major feature of its complications (Sampson *et al.* 2006).

Conditions preceding T2D (like prediabetes and metabolic syndrome) (Hansel *et al.* 2004; Su *et al.* 2008), and the disease itself (Sampson *et al.* 2006), are characterised by increased oxidative stress, and consequent high oxidative DNA damage. The high levels of ROS in the above mentioned conditions may be a result of hyperglycaemia which leads to an increased input of reducing equivalents into the mitochondrial electron transport chain and a consequent higher production of reactive oxygen species (ROS) as byproducts (Nishikawa *et al.* 2000; Brownlee 2001). Moreover, it is likely that in these hyperglycaemic conditions the catabolism of glucose is increased leading to an increased production of reducing equivalents and thus to a high NADPH-to-NADP ratio which in turn enhances the NADPH oxidases activity and the consequent ROS formation (Raddatz *et al.* 2011). Finally, either of the above scenarios in combination with a less effective antioxidant cell defence (decreased superoxide dismutase and/or glutathione peroxidase activity) may underlie the observed increase in ROS levels in prediabetes, metabolic syndrome or diabetes itself. With telomeric DNA being particularly prone to oxidative DNA damage, the high

ROS levels in the above conditions presumably lead to accelerated telomere erosion (Petersen *et al.* 1998; Serra *et al.* 2000).

Therefore, it is hypothesised that accelerated telomere erosion in conditions predisposing to diabetes, eventually leads to extensive and premature senescent phenotypes in multiple cell types, including beta cells, the consequent apoptosis of which hastens the onset of diabetes.

The data on T2D and telomere length are scarce, with only a few small studies published with up to 80 subjects, showing that T2D patients have shorter telomeres than controls (Adaikalakoteswari *et al.* 2005; Sampson *et al.* 2006; Uziel *et al.* 2007). Therefore, the aim of this work was to examine the association of telomere length with the presence of T2D in a large cohort.

2.2 METHODS

2.2.1 Subjects

University College London Diabetes and Cardiovascular disease Study (UDACS): The UDACS is a cross-sectional sample of diabetes patients designed to study the association between common genetic variants and biochemical risk factors implicated in coronary heart disease (CHD) in patients with diabetes. One thousand and eleven subjects were consecutively recruited from the diabetes clinic at University College London Hospitals NHS Trust (UCLH) between the years 2001–2. Diabetes was diagnosed according to the World Health Organization criteria (Alberti & Zimmet 1998). No subjects

requiring renal dialysis were recruited. In the end, the study comprised of 742 T2D and 164 T1D eligible patients. The sample of T2D included three ethnic groups: Caucasians (n=569), South Asians (n=103) and Afro-Caribbeans (n=70), while of the 164 T1D patients the 158 were Caucasians. Ethical approval was obtained from UCL /UCL Hospitals ethics committee and all subjects gave informed consent. Characteristics of patients were originally described by Stephens et al. (Stephens *et al.* 2004). The principal investigator of the UDACS study is Prof Jeffrey Stephens and patients' characteristics have been described in more detail in the study by Stephens et al. (Stephens *et al.* 2004).

European Atherosclerosis Research Study II (EARS II): The EARSII was carried out in 1993. Male students between the ages of 18 and 28 years whose fathers had proven MI before the age of 55 (cases, n=407) and age-matched male controls (n=415) were recruited from 14 university student populations of 11 European countries and were designated in to four regions: Baltic, UK, Middle and South Europe. Only the controls of this study were considered in the present chapter. The study has been approved by ethics committees of collaborating centres and the subjects have given informed consent. Details of the study are described in the “Third result chapter”, paragraphs 1.2.1 (page 257).

Hypercoagulability and Impaired Fibrinolytic function MECHANISMS predisposing to myocardial infarction (HIFMECH): The HIFMECH study consists of 598 male survivors of a first myocardial infarction aged <60 years (excluding patients with FH and insulin-dependent diabetes mellitus) and 653 population-based control subjects of the same age and region recruited from four centers in Europe, designated in to two regions: North Europe and South Europe. Only the controls of this study were considered in the present chapter. The study has been approved by ethics committees of collaborating

centres and the subjects have given informed consent. The study is described in more detail in the paragraph “2.1.2 Methods” of the present chapter.

2.2.3 Measurement of leukocyte telomere length

Described in paragraph 1.2.3 of the present chapter (page 215) and in detail in the “First result chapter”, paragraphs 1, 2 and 3 (pages 149-174).

2.2.4 Statistical analysis

Statistical analysis was performed with SPSS statistical software (version 15.0 for Windows). Baseline characteristics were transformed to a normal distribution where appropriate. To compare telomere length in T2D and controls, mean values were adjusted to an age of 68 years (the mean age in the T2D cases) for all studies. Odds ratios were calculated from logistic regression models using telomere length both as a continuous variable and after dividing into tertiles. The tertiles of telomere length were constructed using the combined case-control group with the age-adjustment made within the separate groups. Partial Pearson correlation coefficients were used to examine the association between telomere length and continuous classical risk factors after adjustment for age (when testing the correlation with age, telomere length was not age-adjusted). Differences in telomere length between ethnic groups and categorical characteristics were tested using analysis of covariance. All models used to test the difference in telomere length were adjusted for age. Results were presented as the geometric mean telomere length (95% CI). Statistical significance was taken as $p < 0.05$.

2.3 RESULTS

2.3.1 Study cohorts – Ethnic/geographical diversity

UDACS T2D cases: Mean LTL was successfully determined in 742 T2D patients. Significant differences were found among the three ethnicities, after adjusting for age ($p < 0.0001$). Afro-Caribbeans had 510 bp longer mean length compared to Caucasians [7.46 (95%CI:7.21-7.71) and 6.94 (95%CI:6.80-7.03), $p < 0.0001$, respectively] and 500 bp longer than South Asians (6.96 (95%CI: 6.78-7.09), $p = 0.004$), while Caucasians' and South Asians' length did not differ significantly ($p = 1.00$) (Figure 7). Due to these ethnic differences, and in order to allow the comparison with the Caucasian controls, only the 569 Caucasian T2D cases were examined in further analysis. The characteristics of T2D patients are typical (Table 3), with a mean age of 68 [24-92] years, a mean age of diabetes onset of 55 (13) years and the majority of them (59.4%) being males. The duration of T2D diabetes was 9 [4-16] years and their BMI 29.3 (5.5) kg/m^2 .

EARSII controls: The control subjects from two different studies were employed in an effort to cover the large age range of the cases (24-92 years for T2D and 21-80 years for T1D patients). LTL was measured in 396 controls from the EARSII study aged between 18 and 28 years recruited from 4 different European regions. In EARSII (Salpea *et al.* 2008) significant differences in telomere length were observed among the geographical regions of Europe, as described in the “Third result chapter”, paragraph 1.3.2 (page 260). Therefore, for the analysis only the 81 UK region controls were used to match the UDACS Caucasian patients which have been recruited in the UK (Table 3).

HIFMECH controls: LTL was also measured in 520 HIFMECH controls with an age range of 40-61 years recruited from the North and the South part of Europe. Again, due to the differences in telomere length found between the South and the North [8.27(4.14) kb vs. 7.99(4.51) kb, $p=0.02$) only the analysis of the 367 controls from the North of Europe was used, matching to the UK Caucasian cases of UDACS (Table 3).

Figure IV-7. Ethnic differences in mean age-adjusted leukocyte telomere length (LTL) of the type 2 diabetes patients.

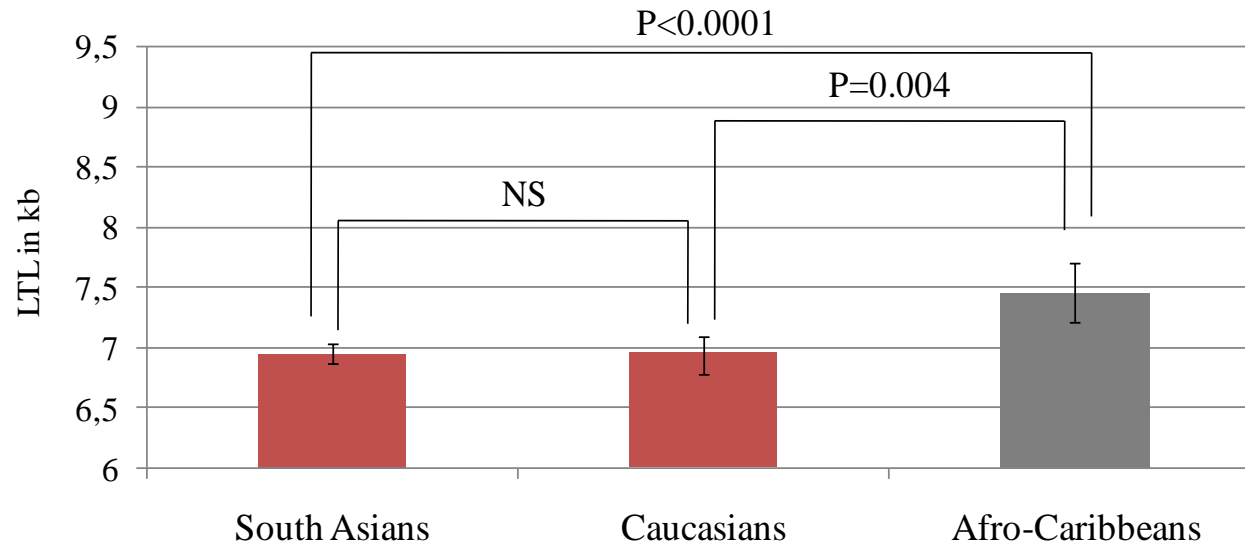


Table IV-3. Characteristics of the Caucasian type 2 diabetes (T2D) cases and controls.

	UDACS T2D cases N=569	EARSII controls N=81	HIFMECH controls N=367
Age (yrs), median [range]⁺	68 [24-92]	21 [18-28]	53 [40-61]
T2D onset age(years)**	55 (13)		
Duration of T2D (years)⁺	9 [4-16]		
% Females (N)	40.6 (231)	0 (0)	0 (0)
% Females >50 yrs (N)	94.4 (218)		
BMI (kg/m²)*	29.3 (5.5)	23.0 (2.4)	25.6 (3.1)
SBP (mmHg)*	140.5 (20.9)	112.6 (9.8)	127.1 (15.3)
DBP (mmHg)*	79.3 (11.4)	66.0 (7.6)	82.8 (8.0)
TC (mmol/l)*	4.96 (1.09)	4.06 (0.70)	5.50 (0.96)
TG (mmol/l)*	1.92 (1.08)	0.93 (0.35)	1.40 (0.60)
HDL (mmol/l)*	1.28 (0.37)	1.17 (0.20)	
Glucose (mmol/l)*	9.8 (4.3)	5.20 (0.37)	
HBA1c (%)*	7.65 (1.61)		
%Hypertension (N)	83.4 (472)	0 (0)	4.2 (15)
%Ex/Current smokers (N)	52.3 (291)	38.3 (31)	60.8 (223)
Hypoglycaemics			
% None (N)	11.2 (63)		
% Insulin (N)	13.1 (74)	0 (0)	0 (0)
% Oral (N)	62.6 (353)		
% Both (N)	13.1 (74)		
% Statin use (N)	31.6 (177)	0 (0)	0 (0)
Unadjusted LTL (kb) ‡	6.94 (6.80-7.03)	9.27 (8.86-9.73)	7.85 (7.67-8.04)

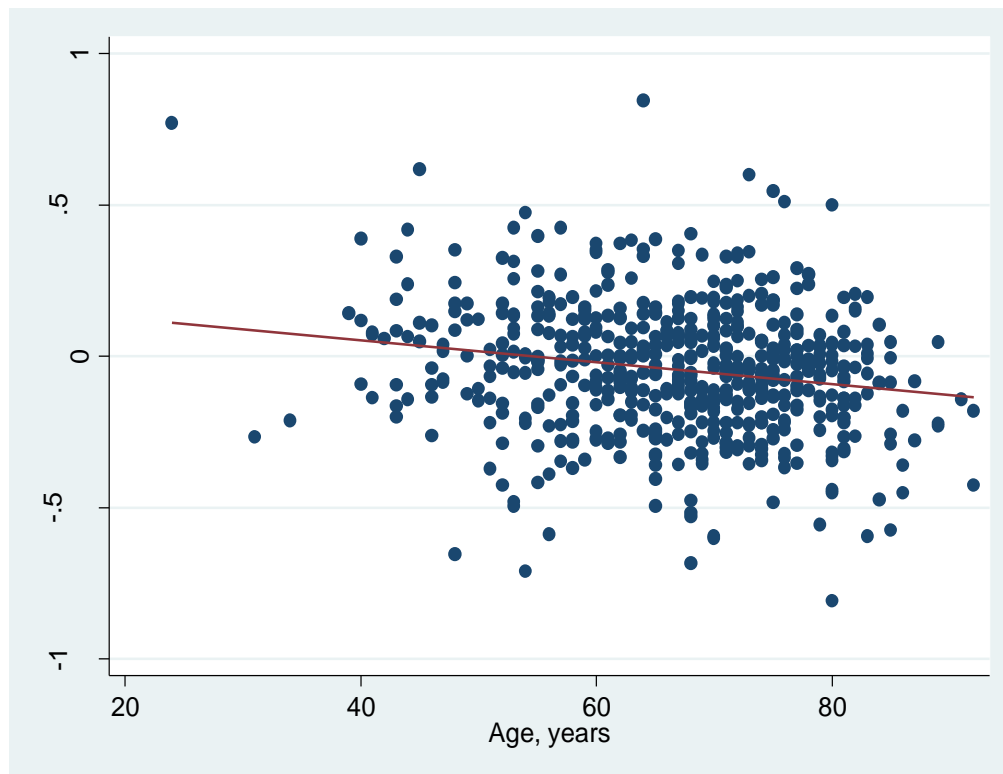
*data were log-transformed and geometric means [(approximate standard deviation (SD))] are presented, ** mean with SD is presented, ⁺ median [IQR] is presented, ‡ Data were log-transformed and the geometric means with 95% confidence intervals (95%CI) was then used to calculate the corresponding telomere length in kb.

TC: total cholesterol, BMI: body mass index, SBP: systolic blood pressure, DBP: diastolic blood pressure, TG: triglycerides, HDL: high density lipoprotein, LDL: density lipoprotein, CRP: C-reactive protein, LTL: leukocyte telomere length.

2.3.2 The effect of T2D risk factors on telomere length

As expected, overall mean telomere length in the T2D diabetes patients showed a significant negative correlation with age ($r=-0.18$, $p<0.0001$, figure 8). Telomere length was therefore age-adjusted in all further analyses.

Figure IV-8. The correlation of telomere length (T/S ratio) with age in Caucasian type 2 diabetes patients.



However, no other classical T2D risk factor was significantly correlated with LTL, including BMI, glucose, triglycerides and BMI (Table 4). Moreover, there was no significant difference in age-adjusted telomere length between males and females, between patients with different smoking history, or between hypertensive and normotensive subjects (Table 5). Interestingly, as also shown in Table 5, there was no significant association with the age of onset or the duration of diabetes, the use of hypoglycaemic drugs or statins (Table 5).

Table IV-4. Partial Pearson correlation coefficients of age-adjusted telomere length with classical risk factors in Caucasian type 2 diabetes patients.

	<i>r</i>	<i>p</i>	<i>N</i>
BMI (kg/m²)	0.02	0.64	563
SBP (mmHg)	0.05	0.27	566
DBP (mmHg)	-0.03	0.51	566
TC (mmol/l)	0.03	0.41	566
TG (mmol/l)	-0.03	0.44	566
HDL (mmol/l)	0.04	0.40	566
Glucose (mmol/l)	-0.02	0.59	566
HBA1c (%)	0.01	0.77	563

BMI: body mass index, SBP: systolic blood pressure, DBP: diastolic blood pressure, TC: total cholesterol, TG: triglycerides, HDL: high density lipoprotein, LDL: density lipoprotein.

Table IV-5. Age-adjusted telomere length by sex, smoking, hypertension status, age of diabetes onset, duration of diabetes and medication use in Caucasian type 2 diabetes patients.

		Telomere length (kb) *	P	N
Sex	Males	6.90 (6.8-7.01)	0.48	338
	Females	6.96 (6.84-7.08)		231
Smokers	Never	6.96 (6.86-7.06)	0.33	341
	Ex/Current	6.88 (6.76-7.01)		205
Hypertension	No	6.88 (6.69-7.07)	0.58	96
	Yes	6.94 (6.85-7.02)		470
Age of onset	<55	6.87 (6.74-7.00)	0.28	259
	>=55	6.97 (6.86-7.1)		310
	0-5	6.86 (6.71-7.01)		150
Duration of diabetes	5-10	6.97 (6.83-7.12)	0.74	159
	10-15	6.95 (6.77-7.13)		100
	>15	6.93 (6.79-7.08)		160
Hypoglycaemic treatment	None	6.88 (6.66-7.12)	0.79	63
	Insulin	6.86 (6.66-7.08)		74
	Oral	6.93 (6.83-7.03)		353
	both	7.01 (6.79-7.23)		74
Statin use	No	6.89 (6.8-6.99)	0.15	384
	yes	7.01 (6.88-7.16)		177

* Data were log-transformed and the geometric mean (95%CI) was then used to calculate the corresponding telomere length in kb.

2.3.3 Case-Control differences

The T2D cases [6.94(6.80-7.03)] displayed shorter age-adjusted LTL compared to the EARSII [8.27(7.62-9.00), $p<0.001$] and the HIFMECH controls [7.58(7.39-7.81), $p<0.001$] as well as the two control samples combined [7.72(7.53-7.90), $p<0.001$] (Figure 9).

Decreasing age-adjusted telomere length was associated with a higher odds ratio for T2D when comparing the cases to the EARSII controls [2.96(2.16-4.06), $p<0.001$], the HIFMECH controls [1.88(1.58-2.24), $p<0.001$] and the combined controls [2.38(1.45-3.89), $p<0.001$] (Figure 10A). To better illustrate this effect the age-adjusted telomere length was divided in tertiles. Subjects in the middle and the lowest tertile of length had significantly higher odds ratio for T2D compared to the highest tertile [1.50(1.08-2.07) and 5.04(3.63-6.99) respectively, $p<0.0001$], with the effect being more pronounced between lowest and highest tertiles (Figure 10B).

Figure IV-9. Type 2 diabetes case-control differences in mean age-adjusted leukocyte telomere length (LTL).

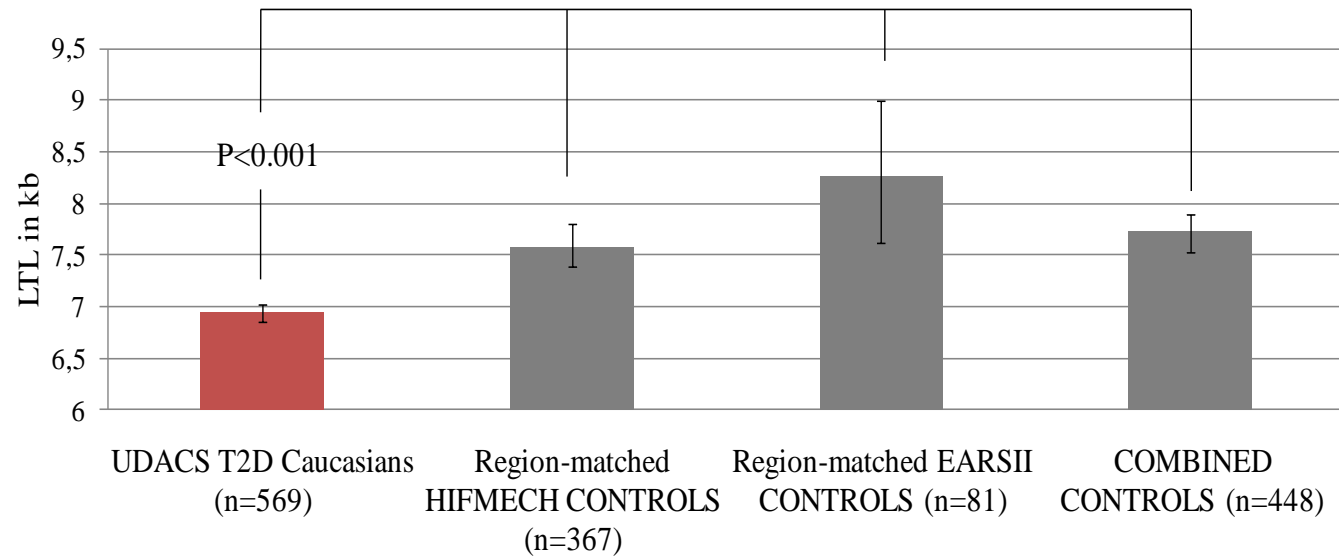
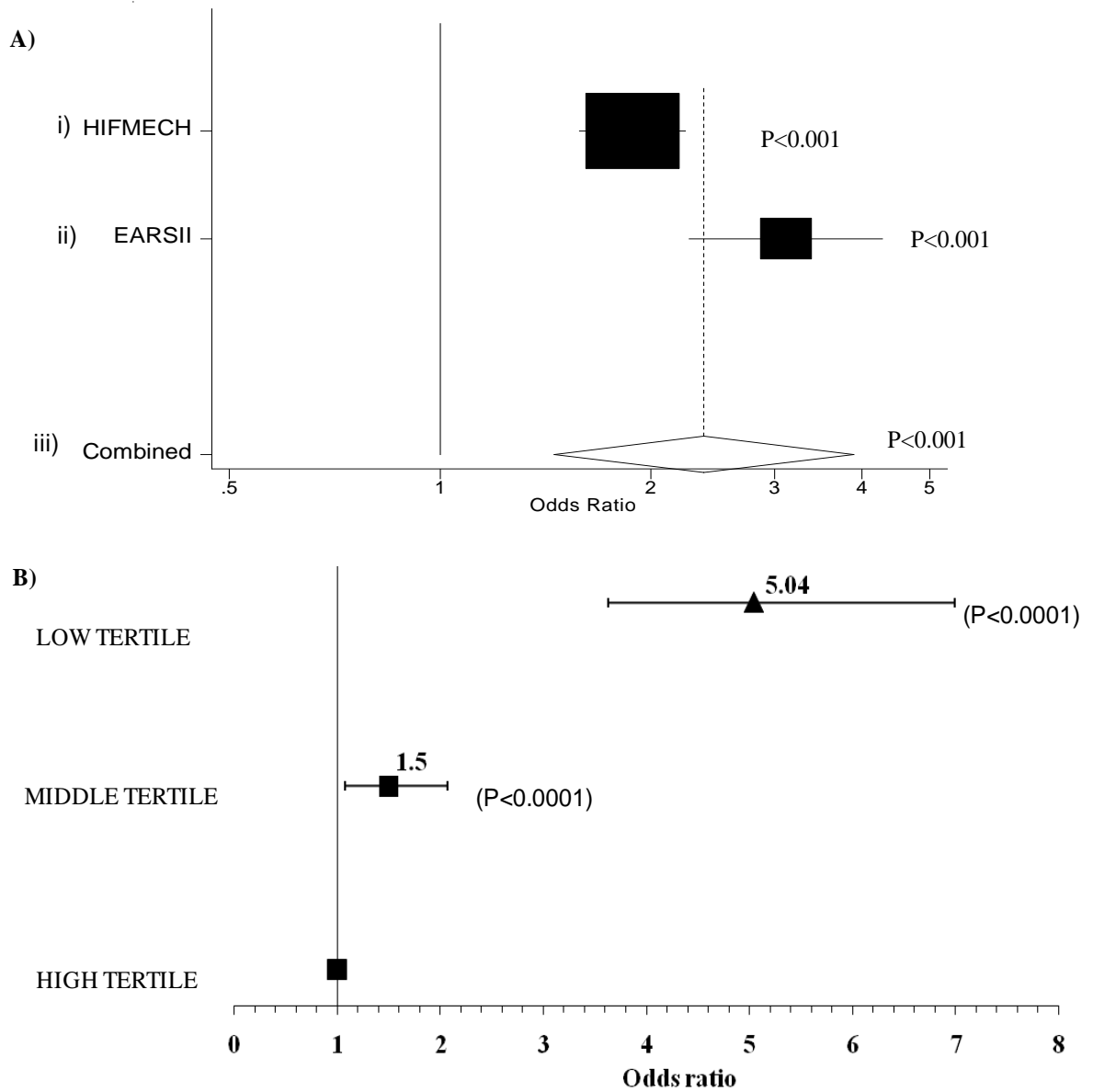


Figure IV-10. A) The odds ratio of type 2 diabetes for one standard deviation decrease in age-adjusted telomere length when comparing the cases with i) the HIFMECH controls, ii) the EARSII controls and iii) the combined controls. B) The odds ratio of type 2 diabetes for each tertile of age-adjusted telomere length when comparing the cases with the combined controls.



2.4 DISCUSSION

The present study is the largest to date to demonstrate that LTL is significantly shorter in T2D compared to controls over a wide age range. T2D patients had on average 780 bp shorter telomeres than healthy individuals, a difference which represents a biological age gap of approximately 24 years. This difference in LTL between T2D cases and controls is greater than the previously reported 500bp difference in Caucasians (Sampson *et al.* 2006) but smaller compared to the 3.1 kb difference found in an Asian Indian cohort (Adaikalakoteswari *et al.* 2005). The discrepancy of the effect size on telomeres might be due to the small sample size of these other studies but also, in the second case, might point to the increased tendency for diabetes in South Asians compared to Caucasians (Adaikalakoteswari *et al.* 2005). Nevertheless, the differences in telomere length of diabetes patients and controls, including the one observed here, are much greater than the ~300 bp difference reported in other studies between coronary heart disease (CHD) patients and controls (Samani *et al.* 2001; Brouillette *et al.* 2003; Brouillette *et al.* 2007; Mukherjee *et al.* 2009). Moreover, in this study decreasing telomere length was associated with more than two fold higher risk for T2D. Having telomeres in the middle tertile of length was associated with 50% higher odds ratio for T2D, while having telomeres in the lowest tertile of length was associated with a fivefold higher odds ratio for T2D. These data suggest an important role of biological ageing in diabetes.

Men have been reported to have shorter telomeres than women of the same age (Bekaert *et al.* 2007). In the present sample, women had longer age-adjusted telomeres than men but this difference was not significant, possibly due to the fact that most of these women were postmenopausal. An oestrogen-responsive element exists in telomerase, the

enzyme that replaces telomeric loss in progenitor cells (Kyo *et al.* 1999); thus hormonal changes may influence telomerase to maintain telomere length in the progenitor cells after menopause.

LTL has been shown to be representative of telomere length in vascular wall cells (Wilson *et al.* 2008) and thus inter-individual differences in LTL probably apply to those of other cell types including pancreatic beta cells. Oxidative DNA damage and up-regulated DNA repair mechanisms have been observed in beta cell in T2D (Tyrberg *et al.* 2002), and an inverse relationship between beta cell volume density and levels of DNA oxidation products has been reported (Sakuraba *et al.* 2002). My data, coupled with these experiments, support the theory that diabetes-related oxidative stress may accelerate local and systemic senescence process, as reflected by telomere dynamics.

A plausible mechanism of the situation in subjects who developed T2D may be that hyperglycaemia in the prediabetic state induces high oxidative stress, which in turn causes oxidative telomeric DNA damage and consequent shortened telomeres, which eventually lead to premature senescence. Evidence supporting the plausibility of this mechanism come from the study of Tarry-Adkins *et al.* who observed short telomeres together with increased markers of oxidative stress and cell senescence in beta cells of low birth weight rats (Tarry-Adkins *et al.* 2009). This theory is also compatible with the beta cell failure in T2D, and also the vascular endothelial and smooth muscle cell senescence which promotes atherogenesis in T2D patients.

Nevertheless, T2D patients' LTL was not associated with any classical risk factors, including glucose and triglycerides. Possibly the oxidative stress conferred by all risk

factors collectively, rather the individual risk factor's effect, is responsible for the short telomeres found in T2D. On the other hand the short telomeres in T2D subjects could be the result of chronic inflammatory responses involved in diabetes development and progression (Bekaert *et al.* 2007). These hypotheses will be investigated in the following result chapter (Result Chapter 3).

Interestingly, measures of diabetes severity such as the age of onset and the duration of the disease were not associated with differences in length. However, T2D in most cases has a silent onset; therefore the age of onset cannot be defined with precision in contrast to other diseases as CHD where specific overt symptoms as stable or unstable angina pectoris or myocardial infarction indicate the disease onset. In addition, I believe that duration of diabetes is not representative of the severity of diabetes in the present cohort, since it was not possible to evaluate whether and for how long glycaemia was effectively controlled with treatment. Uziel *et al.* evaluated arterial and blood mononuclear cell telomere length in diabetic patients and found that glycaemic control attenuated the shortening, but in the present study it was not possible to examine this (Uziel *et al.* 2007). A better indicator of diabetes severity and worsening is probably the complications of the disease as kidney failure, blindness, and cardiovascular disease or the increasing need for hypoglycaemic treatment. Indeed, shorter telomeres were significantly associated with higher odds ratio for coronary heart disease in the studied patients (see data in next paragraph 2.3). Records on other T2D complications were not available.

Another very interesting finding of the present study is the ethnical diversity in telomere length among T2D patients. These data confirm the recent observation of Hunt *et al.* (Hunt *et al.* 2008) that Africans have longer telomeres than Caucasians, but also show

that South Asians have similar telomere length to Caucasians. Hunt et al. showed in their study (Hunt *et al.* 2008) that the rate of age-dependent telomere shortening was faster in Africans than in Caucasians. Such evidence supports the theory that Africans are more likely to be born with longer telomeres and is in accordance with previously reported evidence of a high degree of genetic determination in telomeric length (Graakjaer *et al.* 2004). The ethnic differences seen in telomere length though imply an important genetic component in its determination. The role of genetic predisposition to shorter telomeres in subjects prone to develop diabetes with regard to environmental factors needs further investigation.

Limitations of this study need to be considered. The absence of data on T2D complications other than CHD and increasing need for hypoglycaemic treatment did not allow the association of the disease severity and telomere length to be examined. Moreover, this study does not include any data on telomere loss over time, as all measurements were taken at a certain time point and therefore the rate of telomere attrition in diabetes patients could not be addressed. Finally, no definite conclusions can be made on whether the observed shorter telomeres in patients are a cause or a consequence of diabetes since this is a case-control study.

In conclusion, this study showed that T2D is associated with shorter telomeres in Caucasians. Thus, telomere length might be of use as a marker of biological age, providing a valuable tool in the management of T2D. A prospective evaluation of T2D risk in relation to LTL could shed light on the question of whether telomere shortening is a cause or a consequence of diabetes, and provide an insight to the potential of using telomere length for the risk assessment of T2D development.

3. LEUKOCYTE TELOMERE LENGTH IN TYPE 1 DIABTES PATIENTS

Although, the aetiology of T1D is different to that of T2D, and T1D is not an age-related disease, in both types beta cell failure is the final trigger. Therefore, if the hypothesis that critically short telomeres contribute to the onset of diabetes by eliciting senescent phenotypes in beta cells is true, then in T1D patients mean LTL should also be shorter compared to healthy subjects. In order to test this hypothesis, LTL was measured in the 158 Caucasian T1D cases included in UDACS. The characteristics of the T1D cases are shown in table 6.

For the T1D case-control comparison, both the control samples (EARSII and HIFMECH) which were used for the comparison with the T2D cases were also employed in order to cover their age range of 21 to 80 years. Also, since the T1D subjects were also recruited in London hospitals, the geographical region-matched subjects from EARSII and HIFMECH were only used. Thus, age-adjusted LTL was significantly shorter in T1D cases [7.12 (6.85-7.35)] compared to the EARSII UK controls [8.27(7.62-9.00), $p < 0.001$] and the North region HIFMECH controls [7.58(7.39-7.81), $p < 0.001$], as well as compared to the combined control samples [7.72(7.53-7.90), $p < 0.001$] (Figure 11).

As shown in Figure 10, T1D patients had approximately 500 bp shorter telomeres than healthy subjects, a difference which is smaller compared to the difference between T2D patients and controls, but in agreement with the difference observed in previous smaller studies with T1D (Jeanclos *et al.* 1998; Uziel *et al.* 2007). Thus, it can be speculated that critically short telomeres may contribute to the onset of both types of diabetes by eliciting senescent phenotypes in beta cells.

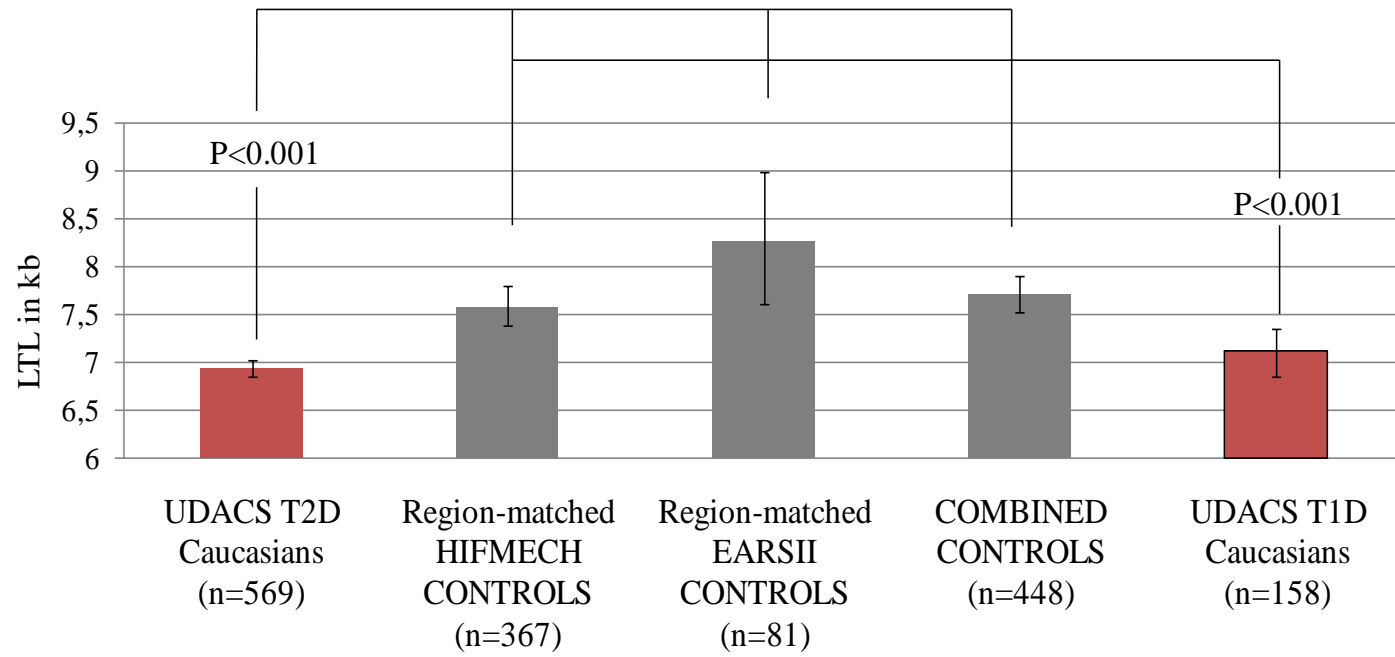
Table IV-6. Characteristics of the Caucasian type 1 diabetes (T1D) cases.

UDACS T1D cases	
N=158	
Age (years), median [range]	48.9 [21-80]
Age of T1D onset (years)	23.3 (12.8)
Duration of T2D (years)⁺	24 [16-33]
% Females (N)	36.7 (58)
% Females >50 years (N)	0
BMI (kg/m²)*	26.0 (4.4)
SBP (mmHg)*	132.9 (16.7)
DBP (mmHg)*	78.2 (10.6)
TC (mmol/l)*	5.17 (0.94)
TG (mmol/l)*	1.05 (0.56)
HDL (mmol/l)*	1.70 (0.56)
LDL (mmol/l)^x	2.85 (0.83)
CRP (mg/l)*	1.09 (0.89)
Glucose (mmol/l)*	8.9 (5.8)
HBA1c (%)*	8.08 (1.33)
% Hypertension (N)	51.6 (81)
% Ex/Current smokers (N)	17.8 (28)
% Insulin use (N)	95.6 (151)
% Statin use (N)	25.3 (40)

*data were log-transformed and geometric means [(approximate standard deviation (SD)] are presented, ** mean with SD is presented, ^x data were square root transformed and square of mean (approx SD) is presented, ⁺median [IQR] is presented.

TC: total cholesterol, BMI: body mass index, SBP: systolic blood pressure, DBP: diastolic blood pressure, TG: triglycerides, HDL: high density lipoprotein, LDL: density lipoprotein, CRP: C-reactive protein, LTL: leukocyte telomere length.

Figure IV-11. Type 1 and type 2 diabetes case-control differences in mean age-adjusted leukocyte telomere length (LTL).



4 LEUKOCYTE TELOMERE LENGTH IN CO-EXISTENCE OF CARDIOVASCULAR DISEASE AND TYPE 2 DIABETES

Based on the “common soil” hypothesis for CVD and T2D, it is relevant to examine whether telomere length partly represents the speculated common abnormalities underlying the pathogenesis of these diseases.

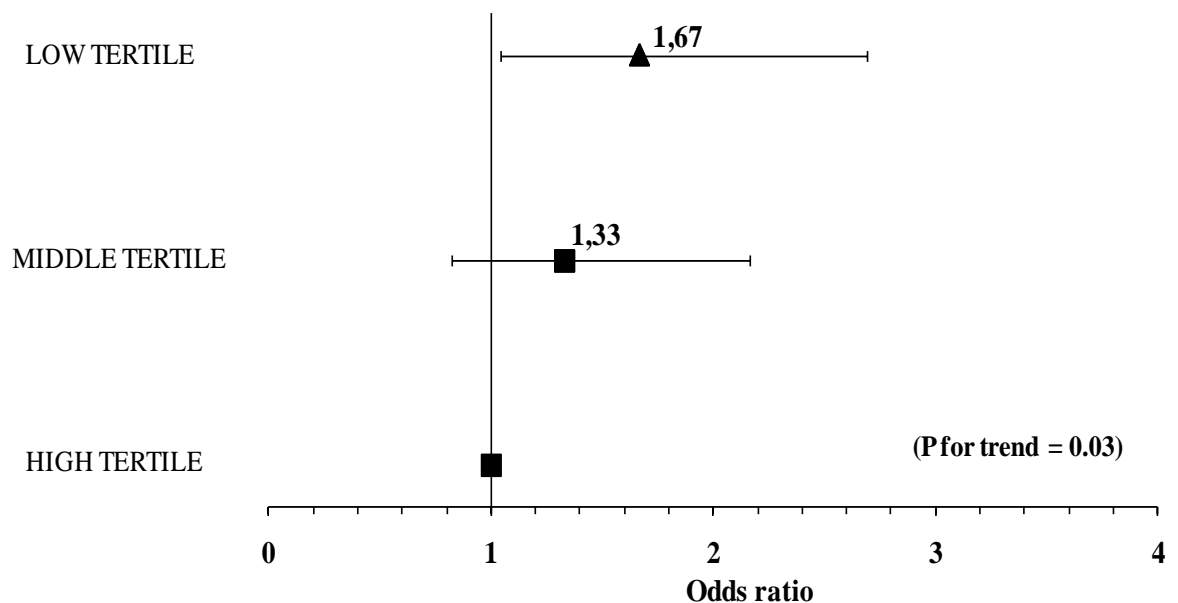
Nevertheless, a very interesting finding, supported by independent studies, is that patients with diabetes or prediabetes exhibiting atherosclerotic manifestations have the shortest telomeres compared to patients with diabetes or CVD alone. Adaikalakoteswari *et al.* found that among T2D patients those with atherosclerotic plaques had shorter telomeres (Adaikalakoteswari *et al.* 2007). The study of Olivieri *et al.* showed that T2D patients with MI had shorter telomeres than T2D subjects free of MI (Olivieri *et al.* 2009).

Among the present T2D patients, there was a trend to higher odds ratio for CHD with decreasing telomere length. Compared to subjects in the highest tertile of telomere length, those in the lowest tertile of telomere length had an odds ratio for CHD of 1.67 (1.04-2.69), and those subjects in the middle tertile of telomere length had an odds ratio for CHD of 1.33 (0.82-2.16), $p=0.03$ (Figure 12).

When the association of telomere length with the presence of diabetes was examined among subjects with already developed CHD (i.e. HIFMECH and CABG patients), no significant differences were detected. This might be due to a greater tissue ageing manifestation in patients with CVD which does not allow the discrimination between T2D and non-T2D patients. Nonetheless, Satoh *et al.* showed that CHD patients

with metabolic syndrome had shorter telomeres than CHD patients without metabolic syndrome (Sato *et al.* 2008).

Figure IV-12. The odds ratio of coronary heart disease for each tertile of age-adjusted telomere length among patients with type 2 diabetes.



In conclusion the above observations, collectively, suggest that substantially decreased telomere length, either caused by the common risk factors between CVD and diabetes and/or genetic predisposition to short telomeres, possibly reflects greater tissue ageing and greater prevalence of senescent phenotypes in various tissues, including the vascular wall and pancreatic islets.

V. **THIRD RESULT CHAPTER: “DETERMINANTS OF SHORT
TELOMERES IN CARDIOVASCULAR DISEASE AND DIABETES”.**

The results of the previous chapter showed that short telomeres characterise CVD and T2D. Thus, the aim of this chapter was to examine how these short telomeres arise in those predisposed to or already with CVD and/or T2D. Shorter telomeres can be attributed to short length inherited at birth and/or high rate of shortening during life. The rate of shortening may be determined by the balance between oxidative stress and antioxidant defence and the level of consequent telomeric DNA damage. In addition, the rate of shortening may be also influenced by sustained inflammatory response possibly through enhanced cell turnover. It is important to shed light on the mechanisms leading to short telomeres, since they may contribute to the development of age-related diseases such as CVD and T2D through their effect on telomeres.

1 ASSOCIATION OF FAMILY HISTORY WITH TELOMERE LENGTH

1.1 INTRODUCTION

As described in the “Introduction”, paragraph 6.2 (page 94), telomere length is documented to have a strong hereditary component (Graakjaer *et al.* 2004). This may imply that the observed short telomeres in CVD and T2D patients can at least be partly attributed to inherited short telomeres in those predisposed to premature onset of these diseases. Since family history of premature CVD and T2D is a well-established independent risk factor for

their development (Barrett-Connor & Khaw 1984; Morris *et al.* 1989; Myers *et al.* 1990; Evans *et al.*), this leads to the hypothesis that family history of these diseases may be due to a familial predisposition to short telomeres in the offspring, and through this is leading to premature development of age-related diseases.

In order to examine this hypothesis, it was investigated whether family history of CHD is associated with shorter LTL in healthy subjects compared to controls of the same age and whether this effect is independent of classical risk factors, across Europe. Employing the EARS II, LTL was compared between healthy young men with or without paternal history of premature MI.

1.2 METHODS

1.2.1 Subjects

EARSII: The EARS II was carried out in 1993. Male students between the ages of 18 and 28 years whose fathers had proven MI before the age of 55 (cases, n=407) and age-matched male controls (n=415) were recruited from 14 university student populations from 11 European countries: Tallinn in Estonia (cases/controls, 32/36), Helsinki (32/33) and Oulu (23/23) in Finland were designated Baltic; Glasgow (31/31), Belfast (33/33) and Bristol (22/23) in United Kingdom (UK); Aarhus in Denmark (30/30), Hamburg in Germany (32/32), Ghent in Belgium (32/32), and Zurich in Switzerland (36/36) were designated Middle Europe; Lisbon in Portugal (18/18), Reus in Spain (30/33), Naples in Italy (30/30), and Athens in Greece (26/25) were designated South Europe. The subjects were presumed to have been born in the country where they were studying. Details of

lifestyle i.e. smoking, alcohol consumption, medication and physical activity, personal and family medical history, and physiological measurements [i.e. height, weight, BP, waist and hip circumferences] were established using standardised questionnaires and protocols. BMI was calculated as weight/height². The study has been approved by ethics committees of collaborating centres and the subjects have given informed consent. The principle investigators of this study are listed in Appendix I (page 368).

1.2.2 Biochemical measurements

Blood samples were handled according to specified instructions and were sent to Nancy (France) for storage. They were then dispatched to the different laboratories for specific analyses. The shipment of blood aliquots was done in dry ice. All fasting lipids, glucose and insulin were measured after 12-h overnight fasting. Plasma total cholesterol, HDL cholesterol and triglycerides were measured in Glasgow, UK according to the Lipid Research Clinics Manual of Laboratory Operations standardised to the Centres for Disease Control, Atlanta, GA, USA. Blood glucose was measured after protein removal by glucose dehydrogenase method and insulin level by radioimmunoassay (RIA). The reliability of laboratory performance was assessed by undertaking a repeat blinded analysis of one blood sample in every 20. The correlation between the repeated measurements was $r > 0.95$. More details on the design of EARS I and II studies are described in the article published by “The EARS Group” (Group 1994).

1.2.3 Measurement of leukocyte telomere length

The method is described in paragraph 1.2.3 of the “Second result chapter” (page 215) and in detail in the “First result chapter”, paragraphs 1, 2 and 3 (pages 149-174).

1.2.4 Statistical analysis

Statistical analysis was performed using the SAS statistical software (version 9.1). The differences in the clinical characteristics between cases and controls were tested by a Chi² test, for lifestyle factors which were categorical, and by a general linear model adjusted for age and region, for continuous phenotypes. The mean LTL (T/S ratios), triglycerides and homocysteine were not normally distributed (positive skewness), and thus log transformed data were used for tests and correlations, while geometric means (95% CI) are presented in the tables. Differences in LTL between European regions were tested by a general linear model adjusted for age and case-control status. Differences between cases and controls in LTL were calculated by a general linear model adjusted for age and region. Homogeneity of the case-control difference across regions was tested by introducing the corresponding interaction term in the general linear model. Partial Pearson's correlation coefficients between LTL and continuous classical CHD risk factors, calculated separately in cases and controls, were adjusted for age and region. For this purpose, region was introduced as 3 dummy variables. Homogeneity of the associations in cases and controls was tested by use of a general linear model where the interaction term: “status X telomere length”, was introduced. Since all interactions were non-significant, cases and controls were pooled to calculate partial Pearson's correlation coefficients further adjusted for case-control status. The association between LTL and categorical lifestyle factors (physical activity, alcohol and tobacco consumption) were calculated separately in cases and controls

by a general linear model adjusted for age and region. After having verified that there was no interaction between status and categorical factors, cases and controls were pooled to calculate the overall associations further adjusted for case-control status.

1.3 RESULTS

1.3.1 Study cohort

Mean LTL was successfully determined in 369 cases and 396 controls. The cases and the controls did not differ significantly in any physiological or lifestyle characteristics. Total cholesterol was higher in cases than in controls. No significant differences were found in the other biochemical measurements (Table 1).

1.3.2 Geographical differences

There was a significant difference in mean LTL across the geographical regions of Europe after adjustment for age and paternal history of MI ($p < 0.0001$). Shorter mean length was found in the Baltic [7.94 (7.49-8.49)] and South [7.62 (7.21-8.08)] regions and the longest in the Middle of Europe [10.28 (9.68-10.97)] (Figure 1, Table 2).

Table V-1. Characteristics at recruitment in EARSII cases and controls.

	Cases (n=369)	Controls (n=396)	P
Age (years)	22.7 (0.1)	22.7 (0.1)	0.92
BMI (kg/m²)	23.4 (0.1)	23.3 (0.1)	0.64
Waist/hip ratio	0.852 (0.002)	0.852 (0.002)	0.99
SBP (mmHg)	117.4 (0.5)	117.4 (0.5)	0.95
DBP (mmHg)	73.3 (0.5)	73.1 (0.5)	0.75
TC (mmol/l)	4.53 (0.04)	4.30 (0.04)	<0.001
HDL (mmol/l)	1.19 (0.01)	1.19 (0.01)	0.98
TG(mmol/l)^a	0.91 (0.88 - 0.95)	0.91 (0.87 - 0.94))	0.72
Glucose (mmol/l)	5.16 (0.02)	5.17 (0.02)	0.53
Insulin (mU/l)	10.1 (0.2)	10.6 (0.2)	0.15
Homocysteine (μmol/l)^a	10.15 (9.82 - 10.49)	10.31 (9.98 - 10.64)	0.50
Alcohol consumption >median (>8g/day) (%)	46.9%	42.2%	0.19
Smokers (%)	26.4%	25.6%	0.80
Physical activity (%)			
Low	9.9%	8.4%	
Moderate	72.3%	76.3%	0.78
Heavy	14.8%	15.3%	

Means (standard error) after adjustment for age and region are presented.

^aTG and homocysteine were log-transformed for tests and geometric means (95% CI) are presented.

BMI: body mass index, SBP: systolic blood pressure, DBP: diastolic blood pressure, TC: total cholesterol, HDL: high density lipoprotein, TG: triglycerides.

Figure V-1. Distribution of leukocyte telomere length in each European region for the combined cohort.

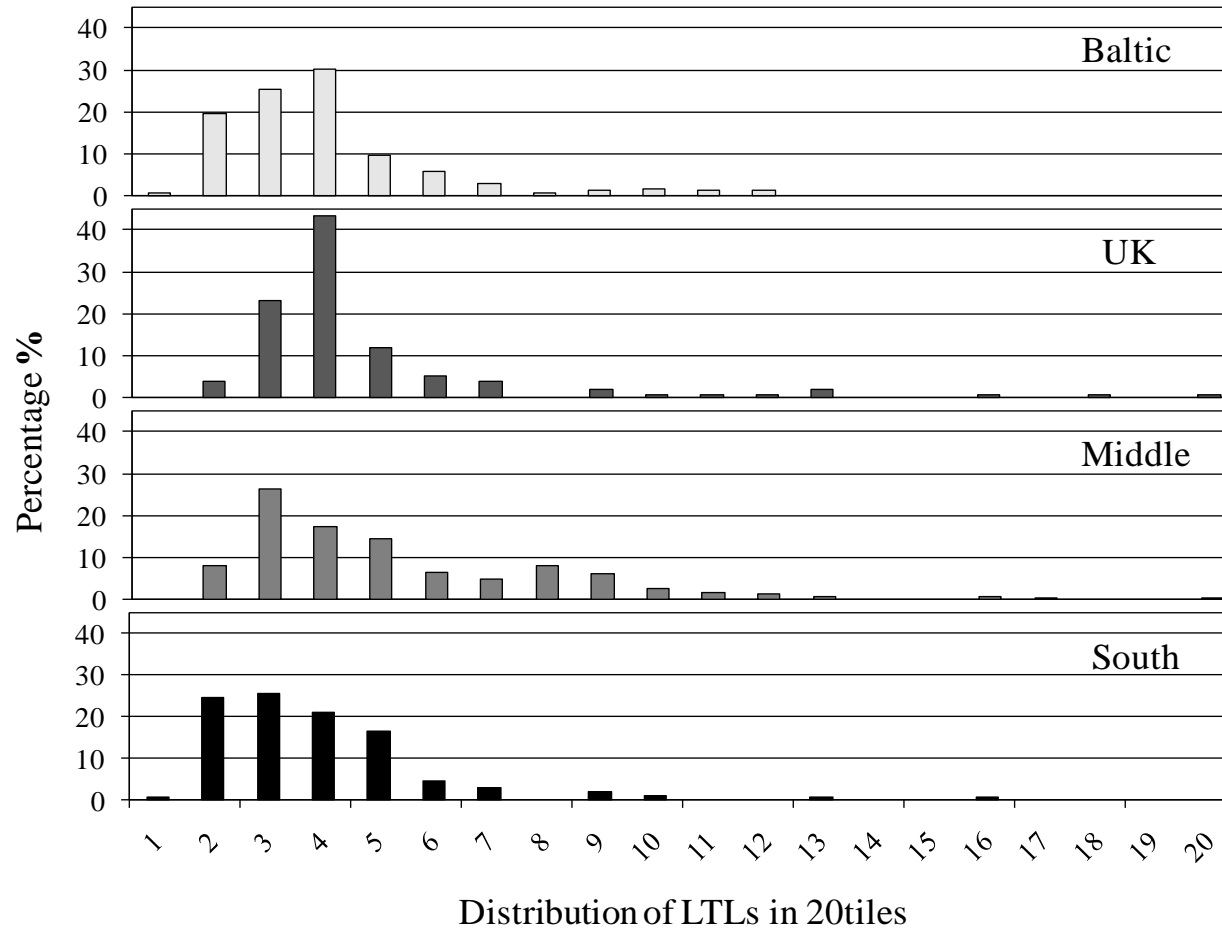


Table V-2. Geometric mean (95% CI) of telomere length (T/S ratio) in cases and control across the Europe.

	Telomere length in combined cases and control	Telomere length in cases	Telomere length in controls	P value for the case-control difference
Overall (369 cases/396 controls)	8.86 (8.54-9.14)	8.49 (8.13-8.91)	9.04 (8.68-9.50)	0.05
Baltic (85 cases / 88 controls)	7.94 (7.49-8.49)	6.94 (6.39-7.53)	9.18 (8.36-10.10)	<0.0001
UK (69 cases / 81 controls)	9.64 (8.91-10.42)	10.05 (9.00-11.29)	9.32 (8.45-10.37)	0.27
Middle (121 cases / 122 controls)	10.28 (9.68-10.97)	10.23 (9.36-11.15)	10.37 (9.55-11.33)	0.82
South (94 cases / 105 controls)	7.62 (7.21-8.08)	7.58 (6.98-8.22)	7.72 (7.12-8.36)	0.78

Mean T/S ratio for the combined cohort in each region was adjusted for age and paternal history. Mean T/S ratio in cases and controls were adjusted for age in each region, and further adjusted for region for the overall results. The geometric means with 95% confidence intervals (95%CI) of T/S ratios were then used to calculate the corresponding telomere length in kb.

Tests of homogeneity for the case-control differences among regions: $p < 0.001$.

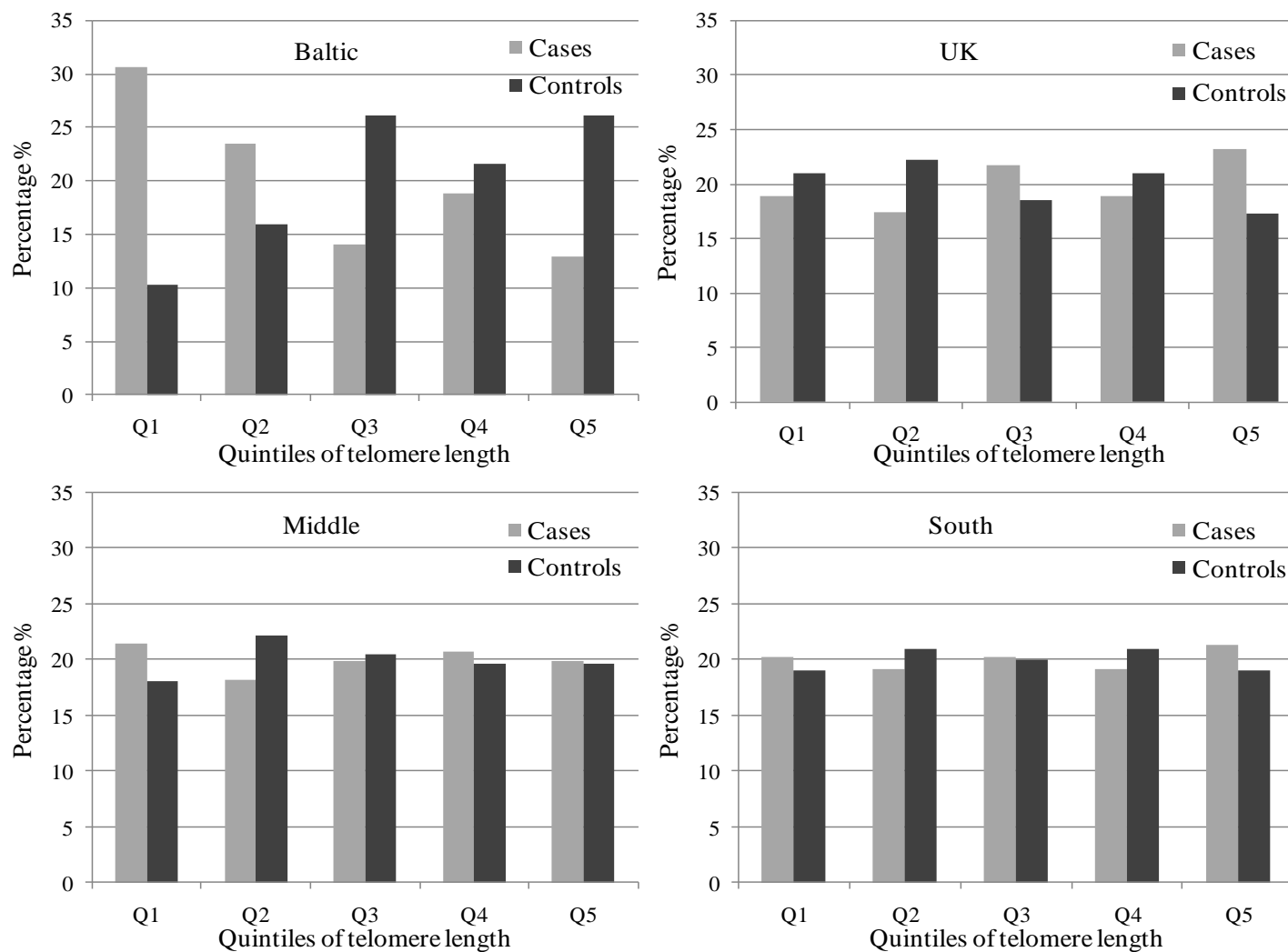
P-value for the difference in mean telomere length across regions: $p < 0.0001$.

1.3.3 Case-control differences

Overall, cases had borderline significantly shorter mean length than controls after adjusting for age and region [8.49 (8.13-8.91) vs. 9.04 (8.68-9.50)], $p=0.05$, Table 2). This difference corresponds to 550 bp approximately. When each geographical region was considered separately, only in Baltic was mean LTL significantly shorter (~2.24 kb) in cases compared to controls [6.94 (6.39-7.53) vs. 9.18 (8.36-10.10)], $p<0.0001$, Table 2).

The length was categorised in region-specific quintiles, in order to illustrate the length's distribution and minimise misclassification. It appeared that the greater difference between the percentages of cases and controls was seen in the lowest quintile of length in the Baltic region (Figure 2).

Figure V-2. Distribution of telomere length in each European region for the cases and the controls.



1.3.4 Association of mean telomere length with classical risk factors and paternal age at birth.

LTL was not significantly correlated with age ($r=0.01$, $p=0.79$) and this was probably due to the very narrow age range (18-28 yrs) of the present young cohort. The correlation of LTL with classical risk factors and homocysteine levels was tested here, as in all the other study samples used in the present thesis. There was a weak but significant positive correlation of LTL with HDL cholesterol ($r=0.10$, $p=0.005$) and glucose ($r=0.21$, $p=0.0001$) levels and also weak but significant negative correlation with waist/hip ratio ($r=-0.09$, $p=0.02$), and homocysteine concentration ($r=-0.10$, $p=0.01$), after adjustment for age, region and case-control status (Table 3). These correlations, apart from the one with glucose, were not consistent in cases and controls, although for all of them the test of homogeneity for the effect in cases and controls was not significant. When adjusted for HDL, glucose, waist/hip ratio, and homocysteine levels the association between length and case-control status remained highly significant in the Baltic and non-significant in the other regions. The significance in the geographical differences did not change after these adjustments. No significant association of LTL with smoking, alcohol consumption or physical activity was found in cases, controls or the combined cohort (data not shown).

According to previous studies (De Meyer *et al.* 2007), paternal age at birth may have an effect on the child's telomere length. The paternal age at birth was calculated from the age of the offspring and the fathers' age at recruitment in the control group. There was no significant correlation between father's age at birth and child's LTL ($r=0.02$, $p=0.08$, Table 3). Such data were insufficient for the cases, since one third of their fathers had already died at the time of recruitment.

Table V-3. Partial Pearson correlation coefficients of telomere length with classical risk factors.

Risk factors	r	P	r	P	r	P
	in cases	in cases	in controls	in controls	in cases and controls pooled	in cases and controls pooled
Age	0.10	0.06	-0.07	0.14	0.01	0.79
BMI	-0.12	0.02	-0.02	0.69	-0.07	0.05
Waist/hip ratio	-0.08	0.12	-0.11	0.04	-0.09	0.02
SBP	0.09	0.11	0.04	0.45	0.06	0.12
DBP	-0.03	0.60	-0.03	0.59	-0.04	0.30
TC	-0.07	0.17	-0.04	0.48	-0.05	0.19
HDL	0.16	0.003	0.05	0.30	0.10	0.005
TG	-0.08	0.16	-0.03	0.62	-0.05	0.19
Glucose	0.26	<0.001	0.18	0.0004	0.21	<0.001
Insulin	-0.07	0.17	0.06	0.29	-0.02	0.66
Homocysteine	-0.15	0.007	-0.04	0.40	-0.10	0.01

Pearson partial correlation coefficient r was adjusted for age and region and further adjusted for case-control status when cases and controls are pooled.

Tests of homogeneity of the association of telomere length with waist/hip ratio, HDL cholesterol, glucose and homocysteine between cases and controls were non-significant.

BMI: body mass index, SBP: systolic blood pressure, DBP: diastolic blood pressure, TC: Total cholesterol HDL: high density lipoprotein, TG: Triglycerides.

1.4 DISCUSSION

This study demonstrated a borderline significant association of shorter LTL and paternal history of premature MI in a large multicentre European study and a highly significant association in the Baltic region. Specifically, overall the offspring of premature CHD patients had on average ~550 bp shorter telomeres than individuals of the same age free of paternal history. This difference is greater than the ~300 bp difference between coronary artery disease patients and controls of 42-72 years of age, reported by Samani *et al.* (Samani *et al.* 2001), or the ~300 bp difference between MI patients and controls of 40-53 years of age, reported by Brouillette *et al.* (Brouillette *et al.* 2003). Although, the effect is of modest statistical significance, it is likely that the true size of the effect is larger when taking into account that the present cohort consists of young healthy men of a very narrow age range (18 to 28 years) having just paternal history as discriminator between cases and controls. Moreover, the effect observed here is diluted since only half the genetic information of an offspring is inherited from the CHD prone father, with the mother's non-risk telomeres contributing to 50% of the measured length.

The present data composed the first documentation of a geographical diversity in LTL across Europe. Students from the Baltic countries and the South of Europe had shorter telomeres (~7.94 kb and ~7.62 kb respectively) while students from the Middle of Europe had the longest (~10.28 kb). A geographical diversity in LTL across Europe was also observed in the HIFMECH study. Comparison between the HIFMECH and the EARSII sample is difficult considering the broad definition of the geographical regions in these two studies. In HIFMECH the South region displayed longer telomeres compared to the North region of Europe (see "Second result chapter", paragraph 1.3.4, page 220). Nevertheless,

the region considered as South in HIFMECH lies between the geographical regions considered as Middle and South in EARSII, and thus the data appear broadly consistent.

The association of the length with paternal MI history also displayed a geographical diversity. Young men from the Baltic countries whose fathers suffered an early MI had ~2.24 kb shorter telomeres than men of the same age free of paternal history. This difference was highly significant, while this was not the case for the other regions. The strong association seen in the Baltic cannot be attributed to particularly short mean length in that region, since the length was as short in the South, but rather to greater differences between cases and controls. A possible explanation of this discrepancy could be that the Baltic population differs genetically from the rest of Europeans. In support of this, the frequency of various genetic polymorphisms (e.g. *PPAR γ* Pro12Ala, *MTHFR* C677T, *LPL HindIII*, *LPL* S447X) is also different in the Baltic compared to the rest of Europe (Gudnason *et al.* 1998; Humphries *et al.* 1998; Poirier *et al.* 2000). The strong association of short length with paternal history of MI in the Baltic compared to the rest of Europe may also be attributed to the effect of an adverse environment on the LTL of fathers in this region.

Of the clinical, biochemical and lifestyle risk factors measured, HDL cholesterol and glucose were positively correlated with the LTL, while waist/hip ratio and homocysteine displayed a negative correlation. Although the correlations with HDL, waist/hip ratio and homocysteine were as expected, the correlation with glucose was unexpectedly positive. This positive correlation with glucose was consistent in EARSII cases and controls and was also observed in the FH subjects examined in the previous chapter. The FH and EARSII subjects are younger and with low glucose levels compare to

the other study samples, where no correlation between LTL and glucose was detected. Thus the observed correlation might reflect a difference in the metabolism of younger subjects with normal glucose tolerance. This finding deserves further investigation in additional patient and population samples, as well as *in vitro* experiments. Nevertheless, the association of short telomeres and paternal history did not change appreciably after adjusting for waist/hip ratio, HDL, glucose and homocysteine levels, indicating that it is not mediated by them. Another factor which was shown in previous studies (De Meyer *et al.* 2007) to have an effect on the offspring telomere length is paternal age at birth. However, no such association was observed in this study, even though the range of paternal age at birth was relatively wide (31 ± 12 yrs).

So far, the influence of CHD paternal history in the EARS I and II studies was mainly expressed in terms of differences in the lipid profile (e.g. cholesterol and triglyceride levels) (De Backer *et al.* 1999; Tiret *et al.* 2000). The present study demonstrates a potential biomarker attributing to the family history-related risk independently of biochemical or lifestyle factors. In addition, most candidate gene studies with the EARS II sample, apart from the HindIII and S447X variants in the lipoprotein lipase gene (*LPL*), found no differences in genotype frequencies between cases and controls (Gudnason *et al.* 1998; Humphries *et al.* 1998; De Backer *et al.* 1999; Poirier *et al.* 2000). Thus, telomere length offers a novel insight into the genetic basis of family history, constituting a possible inherited and early expressed risk factor for CHD.

Limitations of this study need to be considered. Although other studies have used leukocyte DNA to examine the relationship of telomere length with CHD risk (Samani *et al.* 2001; Brouillette *et al.* 2003; Brouillette *et al.* 2007), telomeres display tissue-specific

lengths and rates of loss, so it is not firmly established whether inter-individual differences seen in LTL apply to other cell types and especially the vascular tissue. However it is clear that, in comparison to other persons, those who exhibit relatively short or long length in one type of a proliferative somatic cell, respectively express relatively short or long telomeres in other somatic cells (Martens *et al.* 1998). A possibility of a certain degree of degradation due to storage of the leukocyte DNA for a long period of time should be considered, although telomeres are rather stable complexes of GC-rich double stranded DNA and should maintain their structure when diluted DNA is frozen. The evaluation of telomere length in leukocyte DNA samples stored for as long as the EARSII samples (~14 years) has been previously performed in the West of Scotland Primary Prevention Study (WOSCOP) study (Group 1992; Brouillette *et al.* 2007). The estimates of LTL reported in WOSCOP were lower in average than those in EARS II, as it would be expected due to the different mean age of the two study cohorts.

To summarise, the data suggest that, in young men, the biological expression of a paternal history of premature CHD, primarily in the Baltic, is at least in part mediated through inherited short telomeres, independently of the CHD classical risk factors examined. The outcome of the present study, coupled with that of twin studies showing that epigenetic/environmental effects on length are relatively minor during life (Graakjaer *et al.* 2004), support the theory that in individuals born with relatively short telomeres, vascular cells will reach senescence faster and thus they are predisposed to develop atherosclerosis prematurely.

2 ASSOCIATION OF SYSTEMIC OXIDATIVE STRESS WITH TELOMERE LENGTH

2.1 INTRODUCTION

The rate of shortening after birth is in part genetically determined, but environmental factors, or gene-environment interactions, also exert their effect during life (Huda *et al.* 2007). The factors determining the rate of telomere shortening and the underlying mechanisms are not fully elucidated. There is evidence from *in vitro* studies supporting a role of oxidative stress (Petersen *et al.* 1998; Serra *et al.* 2000; von Zglinicki 2000). The high levels of oxidative stress *in vivo* probably arise from metabolic disorders, like obesity, linked to increased nutrient concentration. Increased nutrient availability (e.g. glucose and free fatty acids) potentially leads to a higher rate of oxidative phosphorylation in the mitochondria and a consequent higher production of reactive oxygen species (ROS) as byproducts, and/or to an enhancement of NADPH oxidase-dependent production of superoxide. Exposure to free radicals or oxidants causes DNA damage and telomere erosion as shown with *in vitro* experiments (Petersen *et al.* 1998; Serra *et al.* 2000; Matthews *et al.* 2006).

In metabolic disorders, such as insulin resistance and obesity, conditions preceding or co-existing with CVD and T2D may result in shorter telomeres in those who develop these age-related diseases. In support of this, shorter telomeres have been observed in circulating epithelial progenitor cells in patients with metabolic syndrome (Satoh *et al.* 2008) and in other conditions of high oxidative stress, such as smoking and obesity (Valdes

et al. 2005). The short telomeres could be the molecular mechanism linking the metabolic disorders to atherosclerosis, diabetes and premature ageing.

In order to examine the role of systemic oxidative stress on LTL, I examined employed T2D patients, since they are considered to be at high oxidative stress and therefore any possible association is more likely to be detected.

2.2 METHODS

2.2.1 Subjects

University College London Diabetes and Cardiovascular disease Study (UDACS). For the purpose of this chapter only the T2D Caucasian subjects were employed. Due to the ethnic differences in LTL observed in result chapter 2, only the 569 Caucasian T2D cases were considered in the present analysis. The UDACS sample of patients has been described in paragraph 2.2.1 of the “Second result chapter (page 234).

2.2.2 Determination of plasma total antioxidant status (TAOS)

Various methods for measuring total antioxidant status (TAOS) exist and all include the generation of a free radical, and the estimation of the antioxidant activity of the test sample against this free radical (Erel 2004). In this study, a modification by Sampson of Laight’s photometric microassay (Sampson *et al.* 2002) was used to measure plasma TAOS.

Plasma TAOS was determined by its capacity to inhibit the peroxidase-mediated formation of the 2,2-azino-bis-3-ethylbenzthiazoline-6-sulfonic acid radical (ABTS⁺). The

relative inhibition of ABTS⁺ formation in the presence of plasma was proportional to the antioxidant capacity of the sample. In each sample, the increase in absorbance at 405nm due to the accumulation of ABTS⁺ was measured with the Labsystems Multiscan Ex microplate reader. The relative inhibition of ABTS⁺ formation in each patient's plasma sample was determined according to a control included in all assays. The control consisted of PBS instead of plasma. Each assay was performed in a 96 well ELISA plate using 2.5µl of plasma. Plasma was specifically used instead of serum in these assays, because serum is obtained after the clotting of blood at room temperature, and ROS may be released by the aggregation of platelets during this process (Leo *et al.* 1997). The UDACS plasma samples were collected within a 12-month period and stored immediately at -80 °C.

The inter-assay coefficient of variation was 10.5% and the intra-assay 4.3%. These figures were derived from repeating the measurement of a single sample 30 times in the same assay for the intra-assay coefficient of variation and in 15 different assays for the inter-assay coefficient of variation. In order to test whether TAOS is a valid measure of oxidative stress, the correlation between plasma TAOS and esterified F2-isoprostane was previously examined and found to be significant ($r=-0.65$; $p=0.003$) (Stephens *et al.* 2006). Since the measures obtain by the two methods correlate, the inter-individual differences in TAOS and/or the correlation to other variables is feasible by using either method.

In general terms, using this method, increased oxidative stress within a sample is negatively correlated with consumption of antioxidants and diminished antioxidant status within that sample.

2.2.3 Leukocyte telomere length measurement

The method is described in paragraph 1.2.3 of the “Second result chapter” (page 215) and in detail in the “First result chapter”, paragraphs 1, 2 and 3 (pages 149-174).

2.2.4 Statistical analysis

Statistical analysis was performed with SPSS statistical software (version 15.0 for Windows). Baseline characteristics were transformed to a normal distribution where appropriate. To examine the associations of age-adjusted LTL and glucose with TAOS, the Spearman’s rho correlation coefficient was calculated. Differences in LTL between tertiles of TAOS were tested using analysis of covariance. All models used to test the difference in LTL were adjusted for age. Partial correlation coefficients were used to examine the association of TAOS with continuous classical risk factors.

2.3 RESULTS

There was a significant positive correlation of the mean length with continuous TAOS measurements overall ($r=0.12$, $p=0.01$, Figure 3) i.e. reduced oxidative stress, as reflected by increased TAOS, correlates significantly with longer LTL. To further examine the effect on telomeres, TAOS measures were categorised in tertiles. Overall, individuals in the low tertile had significantly shorter telomeres compared to those in the middle and the high tertile of TAOS ($p=0.04$) (Table 4 and Figure 4].

Figure V-3. The correlation of age-adjusted telomere length (T/S ratio) with plasma total antioxidant status (TAOS) in Caucasian type 2 diabetes patients.

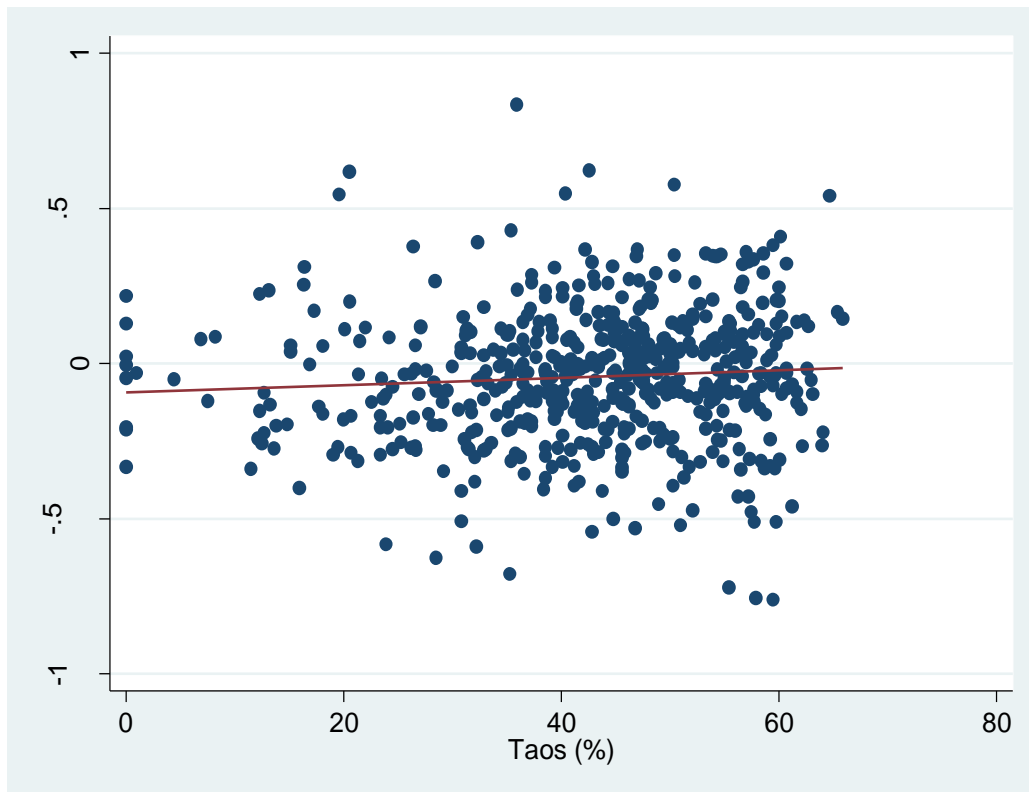
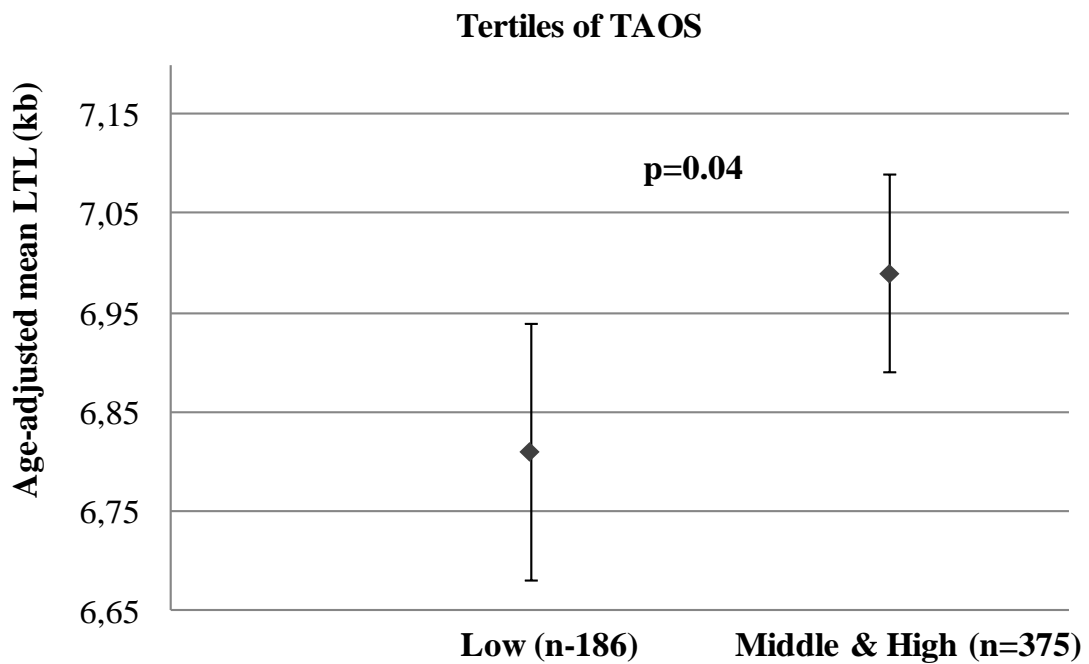


Table V-4. Mean leukocyte telomere length (LTL) in tertiles of plasma total antioxidant status (TAOS) in Caucasian type 2 diabetes patients.

Tertiles of TAOS	Number of patients(N)	Age-adjusted mean LTL (kb)	95%CI	P
Low	186	6.81	6.68-6.94	
Middle	188	6.99	6.9-7.08	
High	187	6.99	6.88-7.1	
Middle & High	375	6.99	6.89-7.09	0.04

Figure V-4. The mean age-adjusted telomere length in tertiles of plasma total antioxidant status (TAOS) measures in Caucasian type 2 diabetes patients. (The error bars represent 95% confidence intervals).



As already shown previously, low levels of TAOS reflect the burden of metabolic disturbances such as low HDL and high TG, glucose and HbA1c (Stephens *et al.* 2006), which are related to prediabetes (or the metabolic syndrome) and diabetes. Specifically, TAOS in UDACS patients correlates positively with plasma HDL-cholesterol and negatively with TG, glucose, and HbA1c concentrations [$r= 0.12, -0.15, -0.11$ and -0.10 , respectively; all $p<0.05$]. Stepwise backward regression showed that glucose and TG concentrations were the strongest independent predictors of plasma TAOS (glucose: $p= 0.004$ and TG: $p= 0.005$). No significant correlations were observed with other risk factors, such as BP, smoking status, other lipid measures, CRP, or BMI.

2.4 DISCUSSION

The results of this chapter demonstrated that high systemic oxidative stress is accompanied by short mean telomere length, at least in peripheral blood cells, suggesting that the shorter telomeres in patients can be partially attributed to high oxidative stress.

Prediabetes (Su *et al.* 2008) and diabetes (Orie *et al.* 2000) are characterised by increased oxidative stress, and in the present patient cohort higher glucose and triglyceride levels were strongly correlated with lower TAOS, which corresponds to higher plasma oxidative status. Plasma TAOS measures the anti-oxidant consumption, which is proportional to oxidative stress generation and represents the net effect of many different compounds and systemic interactions. A typical example of synergism between antioxidants is the ability of glutathione to regenerate ascorbate (Packer *et al.* 1979), and subsequently for ascorbate to regenerate alpha-tocopherol (Stocker *et al.* 1986). Therefore

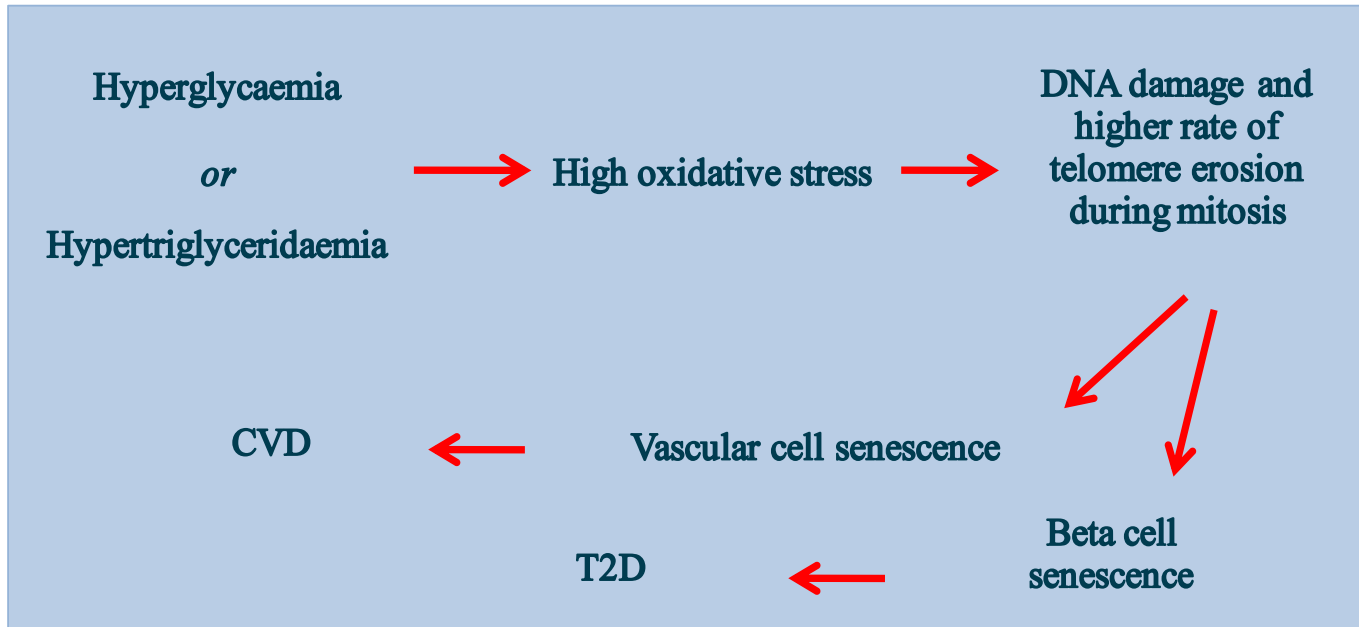
it is possible that plasma TAOS gives more biologically relevant information than that obtained from measuring plasma concentrations of individual antioxidants (e.g. alpha-tocopherol *or* ascorbate). Within the described sample no subject was known to take any form of vitamin supplements.

As initially hypothesised, there was a significant correlation between LTL and measures of oxidative stress, with higher levels of systemic oxidative stress –measured as low TAOS- being associated with shorter telomeres in leukocytes. Thus, the burden of oxidative stress conferred by the metabolic disorders related to diabetes seems to partly determine telomere length in patients, while the risk factors related to these disorders, such as glucose, triglyceride and HBA1c levels did not display individually a significant association with LTL (“Second result chapter”, paragraph 2.3.2, page 241). This observation in plasma is likely to be representative of the processes involved in the development and progress of T2D in other tissues, such as the pancreatic islets and the vascular wall. LTL has been shown to be representative of that in vascular wall cells (Wilson *et al.* 2008), and thus inter-individual differences in LTL probably apply to those of other cell types including beta cells. Oxidative DNA damage and up-regulated DNA repair mechanisms have been observed in beta cells of T2D subjects (Tyrberg *et al.* 2002), and an inverse relationship between beta cell volume density and levels of DNA oxidation products has been reported (Sakuraba *et al.* 2002). The present data, coupled with these experiments, support the theory that hyperglycaemia-induced oxidative stress may accelerate local and systemic senescence process, as reflected by telomere dynamics.

A plausible mechanism of the situation in subjects who developed T2D may be that hyperglycaemia induces high oxidative stress, which in turn causes oxidative telomeric

DNA damage and consequent shortened telomeres, which eventually lead to premature senescence in these cells e.g. pancreatic and vascular wall cells (Figure 5). This theory is compatible with the beta cell failure in T2D and also the vascular endothelial and smooth muscle cell senescence, which promotes atherogenesis in hyperglycaemic patients.

Figure V-5. Proposed mechanism in cardiovascular disease and type 2 diabetes.



3. ASSOCIATION OF VARIATION IN GENES REGULATING REACTIVE OXYGEN SPECIES WITH TELOMERE LENGTH

3.1 INTRODUCTION

In order to further enlighten the effect of ROS on telomere shortening, I also studied the effect of functional variants in genes regulating ROS, as well as gene variants associated with oxidative-induced DNA repair, in determining LTL.

Uncoupling protein 2 (*UCP2*): This ubiquitously expressed protein is a plausible negative regulator of ROS production, since it dissipates the inner mitochondrial membrane electrochemical gradient that drives ATP synthesis and uncouples respiration from oxidative phosphorylation (Casteilla *et al.* 2001). Decreased *UCP2* expression results in increased mitochondrial ROS production, *in vitro* (Duval *et al.* 2002), while animal studies have shown that absence of *UCP2* causes higher oxidative stress (Blanc *et al.* 2003). To maintain homeostasis, *UCP2* expression is induced by elevated oxygen species concentration (Echtay *et al.* 2002). *UCP2* genotype has been associated with T2D and CVD development (Dhamrait *et al.* 2004; Wang *et al.* 2004).

A common functional variant exists in the promoter of human *UCP2* gene (-866G>A, rs659366), with the A allele being associated with lower mRNA levels in adipose tissue, while a non-synonymous SNP leading to an alanine to valine substitution has been identified in exon 4 of the gene (p.A55V, rs660339) (Wang *et al.* 2004). A previous study from our laboratory, demonstrated that the *UCP2*-866G>A variant interacts with smoking to increase oxidative stress in T2D patients (Stephens *et al.* 2008). Given this finding and

the established function of *UCP2*, I hypothesised that these functional variants in the *UCP2* gene will be associated with the stress-induced telomeric DNA damage and therefore with the telomere length of T2D patients, in whom oxidative stress is elevated.

Cytochrome b-245 alpha subunit (*CYBA*): The *CYBA* gene encodes the alpha subunit of cytochrome b-245, which is an essential component of the superoxide-generating vascular NADH/NADPH oxidase (Ushio-Fukai *et al.* 1996). The NADPH oxidase (nicotinamide adenine dinucleotide phosphate-oxidase) is a membrane-bound enzyme complex, which generates superoxide by transferring electrons from NADPH inside the cell across the membrane and coupling these to molecular oxygen to produce the superoxide. Antisense *CYBA* cDNA transfection into rat VSMCs results in decreased cytochrome-b content and superoxide production (Ushio-Fukai *et al.* 1996). With NADPH being a key enzyme of superoxide production in the vasculature, the *CYBA* gene has been implicated in the pathogenesis of atherosclerosis (Alexander 1995). There are two important polymorphisms in the *CYBA* gene, one located in the potential heme-binding sites which changes histidine at position 72 to tyrosine (c.242C>T or p.H72Y, rs4673) and, another located in the 3' untranslated region (UTR), the c.24A>G polymorphism (rs1049254). There are data suggesting that the T allele of the c.242C>T SNP has a protective effect on coronary risk (Inoue *et al.* 1998), whereas the 3' UTR c.24A>G SNP has been associated with reduced ROS generation (Bedard *et al.* 2009).

Angiotensin I-converting enzyme (*ACE*): ACE hydrolyses angiotensin I into angiotensin II (Ang II), which is a potent vasopressor and also inactivates bradykinin, a potent vasodilator. Thus, *ACE* is widely known for its key role in electrolyte balance and blood pressure regulation. Nonetheless, Ang II is a pleiotropic peptide with other important

biological roles; it may induce mitochondrial dysfunction, while ACE inhibitors can attenuate it (de Cavanagh *et al.* 2003; Monteiro *et al.* 2005; Doughan *et al.* 2008). More specifically, the AngII-induced mitochondrial dysfunction was found to be mediated by endothelial cell NADPH oxidase activation and consequent production of superoxide and peroxynitrite production (Doughan *et al.* 2008). The *ACE* gene insertion/deletion (I/D, rs4340) polymorphism is a well-known risk factor of CVD and progression of diabetic nephropathy. In carriers of allele D, the serum level of Ang II is higher, which is associated with increased oxidative stress and subsequent endothelial damage (Molnar *et al.* 2004). Thus, this variant may also affect LTL, through its effect on Ang II levels and in turn on mitochondrial ROS production.

Manganese superoxide dismutase (*MNSOD*): Variation in genes encoding proteins protecting against ROS could also be expected to influence telomere length. The *MNSOD* enzyme has a primary role in antioxidant defence, since it catalyses the dismutation of the superoxide anion (O_2^-) to hydrogen peroxide (H_2O_2) (Soerensen *et al.* 2009), and is localised in the mitochondria (Slot *et al.* 1986). The *MNSOD* gene has a c.47T>C SNP (rs4880), which results in a valine to alanine substitution at position 16 (p.V16A) and is located within the mitochondrial targeting sequence (Rosenblum *et al.* 1996). The C allele, which results in the coding of alanine, has been associated with decreased mortality (Soerensen *et al.* 2009). Thus, it is possible that this SNP has also an effect on LTL.

Glutathione peroxidase 1 (*GPXI*): *GPXI* encodes an enzyme which also has a major role in antioxidant defence. It catalyses the reduction of H_2O_2 to H_2O and is localised both in the mitochondria and the cytoplasm (Esworthy *et al.* 1997). The c.599C>T

(rs1050450), which leads to a proline to leucine substitution at position 200 (p.P200L), has been associated with decreased mortality, most likely by affecting the enzyme's activity (Soerensen *et al.* 2009). Thus, it is possible that this SNP also affects telomere length, through its effect on antioxidant defence, and this way on human survival.

X-ray repair, complementing defective in Chinese hamster 1 (*XRCCI*): *XRCC1* repairs single-strand breaks, typical of those induced by ROS and ionizing radiation. This enzyme stimulates the DNA kinase and DNA phosphatase activities of human polynucleotide kinase at damaged DNA ends, and thereby it accelerates the overall repair reaction (Whitehouse *et al.* 2001). Since telomere loss during replication is also attributed to accumulation of oxidative-induced single-strand breaks (as described in the “Introduction”, page 100), enzymes repairing such breaks are likely to have an effect on the determination of telomere length. The common functional variant in *XRCCI*, p.R399Q (rs25487), will be investigated here for its effect on LTL.

3.2 METHODS

3.2.1 Study sample

The UDACS Caucasian T2D patients (N=569) were genotyped for the eight SNPs described above. The Caucasian patients were only employed, due to the significant ethnic differences observed in LTL, and in order to use a homogenous population for the gene association approach.

3.2.2 Genotyping

SNP genotyping is described in detail in the “General methods”, paragraph 4.3.2 (page 127). Briefly, genotyping was carried-out using TaqMan Assay-by-Design platform (Applied Biosciences, ABI, Warrington UK). Only in the case of the *CYBA* A640G SNP Assay, which failed the Assay-by-Design By Design quality control, the manual design by Source BioScience LifeSciences was employed. Five μ L reactions were performed on 384-well microplates and analysed using ABI TaqMan 7900HT software.

3.2.3 Statistical analysis

Statistical analysis was performed with SPSS statistical software (version 15.0 for Windows). Differences in mean LTL between the SNP genotypes were tested using analysis of covariance. All models used to test the difference in LTL were adjusted for age. In each case of SNP all three possible models (additive, dominant, recessive) were tested and the best fitted one was chosen by the higher R^2 of the test. The differences in TAOS among the SNP genotypes were tested with Kruskal-Wallis or Mann-Whitney U tests. A nonparametric test for trend was also used to examine these differences. Haplotypes were inferred after excluding individuals with missing values using THESIAS

(<http://www.genecanvas.org>). Haplotypes with frequency of less than 2% were excluded from the analysis. Results were presented as the geometric mean LTL (95% CI) for two copies of each haplotype assuming a multiplicative effect and the mean TAOS (95% CI) assuming an additive effect. Statistical significance was taken as $p < 0.05$.

In the present study specific *a priori* hypothesis was tested. Therefore I believe adjustment for multiple comparisons is not necessary. As described in the article by Rothman (Rothman 1990) correction for multiple comparisons is too conservative in hypothesis-deriving analysis such as this and has also been suggested to lead to errors in interpretation (Perneger 1999).

3.3 RESULTS

Among the 569 Caucasian T2D patients, genotype was obtained in 566 (99.5%) for the -866 *UCP2* G>A SNP, in 544 (95.6%) for the *UCP2* p.A55V SNP, in 414 (73%) for the *CYBA* A640G SNP, in 565 (99.3%) for the *CYBA* p.H72Y SNP, in 561 (98.6%) for the *ACE* I/D variant, in 569 (100%) for the *MNSOD* p.V16A SNP, 568 (99.8%) for the *GPXI* p.P200L SNP and 555 (97.5%) for the *XRCCI* p.R399Q SNP (Table 5). Only in the case of *CYBA* A640G SNP the genotype call rate was low, probably due to the lower quality of a manually designed Taqman assay compared to the Assay-by-Design platform used for the other SNPs. The genotype distribution for all variants was as expected from Hardy–Weinberg equilibrium ($p > 0.05$).

Table V-5. Age-adjusted leukocyte telomere length and plasma total antioxidant status (TAOS) measures by the different SNP genotypes in 569 Caucasian type 2 diabetes patients.

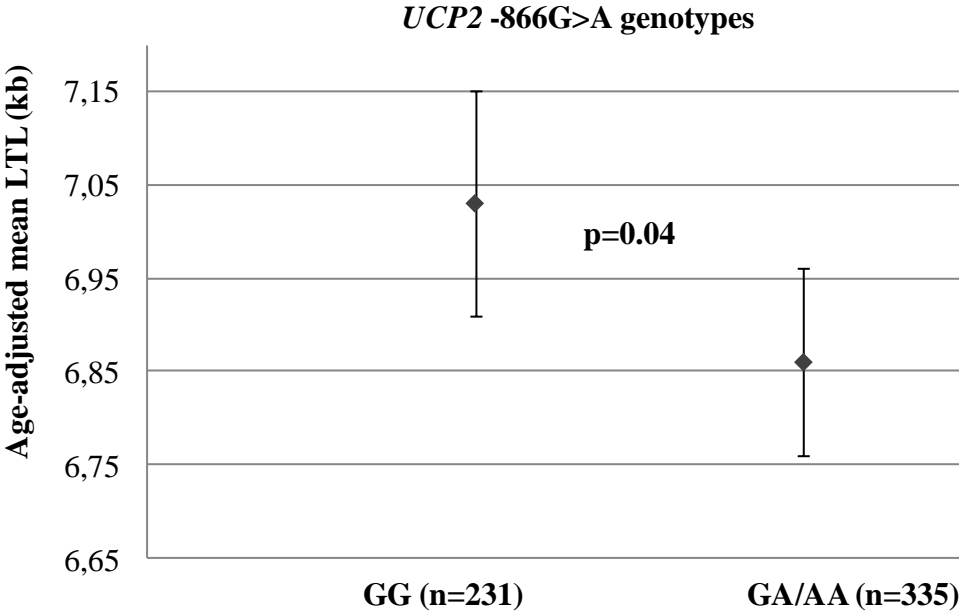
SNP/haplotype	%Genotype/haplotype (N)	Telomere length (kb)*	P	TAOS (%)⁺	P
<i>UCP2 -866G>A</i>					
(rs659366)					
GG	40.8 (231)	7.03 (6.91-7.15)	0.11	45.6 [35.4-54.2]	0.20 (0.08 for trend)
GA	46.5 (263)	6.86 (6.75-6.98)		44.3 [35.7-51.7]	
AA	12.7 (72)	6.84 (6.63-7.06)		42.1 [34.1-48.7]	
GA/AA	59.2 (335)	6.86 (6.76-6.96)	0.04	43.9 [35.4-50.7]	0.17
<i>UCP2 p.A55V</i>					
(rs660339)					
AA	35.5 (193)	7.00 (6.86-7.14)	0.24	45.8 [35.3-54.6]	0.05 (0.03 for trend)
AV	48.4 (263)	6.9 (6.79-7.02)		44.7 [36.5-52.8]	
VV	16.2 (88)	6.8 (6.62-6.99)		41.8 [32.1-48.5]	
AV/VV	64.5 (351)	6.87 (6.78-6.97)	0.15	44 [35.4-50.9]	0.20
<i>UCP2 haplotype: -866G>A/p.A55V‡</i>					
G/A	63.0	6.98 (6.83-7.14)		44.8 [42.4-47.2]	
G/V	4.0	6.89 (6.06-7.91)	0.85	42.0 [30.1-53.9]	0.03
A/V	33.0	6.79 (6.56-7.04)	0.25	39.4 [35.6-43.1]	0.65
<i>CYBA c.640A>G</i>					
(rs1049254)					
AA	28.0 (116)	6.80 (6.66-6.98)	0.61	42.2 [34.6-50.2]	0.39
AG	53.4 (221)	6.85 (6.71-6.94)		42.8 [33.3-51.6]	
GG	18.6 (77)	6.94 (6.71-7.12)		44.5 [37.3-52.8]	
<i>CYBA p.H72Y</i>					
(rs4673)					
HH	41.4 (234)	6.98 (6.85-7.12)	0.28	44.9 [35.9-54.2]	0.37
HY	46.5 (263)	6.85 (6.75-6.98)		43.4 [35.1-50.5]	
YY	11.2 (68)	6.98 (6.75-7.21)		44.9 [38.6-51.0]	

CYBA haplotype:						
A640G/H72Y ‡						
A/H	40.1		6.91 (6.73-7.11)		40.5 [37.9-43.1]	-
A/Y	14.7		6.47 (6.11-6.86)	0.07	40.6 [35.0-46.2]	0.96
G/H	24.5		6.93 (6.68-7.19)	0.91	43.6 [39.7-47.5]	0.26
G/Y	20.8		6.86 (6.53-7.22)	0.81	42.6 [37.3-47.9]	0.49
ACE ID						
(rs4340)						
II	18.2 (102)		7.00 (6.82-7.18)	0.07	44 [35.9-50.3]	0.58
ID	49.9 (280)		6.98 (6.87-7.09)		45.9 [35.4-53.3]	
DD	31.9 (179)		6.79 (6.66-6.93)		44 [35.6-51.7]	
II/ID	68.1 (382)		6.98 (6.89-7.08)	0.02	45.0 [35.4-53.2]	0.41
MNSOD p.V16A						
(rs4880)						
VV	25.5 (145)		6.91 (6.76-7.07)	0.64	42.7 [35.3-51]	0.63
VA	51.0 (290)		6.90 (6.79-7.01)		45 [35.4-53.3]	
AA	23.5 (134)		6.99 (6.84-7.16)		44.8 [36.2-53]	
VV/VA	74.5 (424)		6.93 (6.84-7.02)	0.83	44.9 [35.6-53.2]	0.35
GPXI p.P200L						
(rs1050450)						
PP	43.5 (247)		6.83 (6.72-6.94)	0.01	43.5 [33-51.1]	0.17
PL	45.4 (258)		7.06 (6.95-7.18)		44.8 [36.2-52.1]	
LL	11.1 (63)		6.81 (6.59-7.04)		46.6 [38.6-54.2]	
PL/LL	56.5 (321)		7.01 (6.91-7.12)	0.02	44.9 [36.6-53]	0.17
XRCCI p.R399Q						
(rs25487)						
RR	44.1 (245)		6.95 (6.84-7.07)		44.8 [34.1-53.3]	
RQ	43.6 (242)		6.88 (6.77-7.00)	0.63	43.9 [36.5-51.3]	0.49
QQ	12.3 (68)		6.86 (6.65-7.09)		45.6 [37.3-53.3]	
RQ/QQ	55.9 (310)		6.87 (6.78-6.98)	0.34	44.3 [36.5-51.8]	0.59

*Data were log-transformed and the geometric mean (95%CI) was then used to calculate the corresponding telomere length in kb. ⁺median [IQR] is presented. ‡Data is presented for 2 copies of each haplotype. All haplotypes with frequency <2% are excluded from the analysis.

As shown in table 5 and figure 6, carriers of the *UCP2* -866A allele had ~170 bp (2.4%) shorter mean length than the GG subjects and there was a trend to lower TAOS towards the *UCP2* -866A allele carriers. The effect of the *UCP2* -866A allele on TAOS was statistically significant among smokers of the present cohort, as previously shown by Stephens et al. (Stephens *et al.* 2008). The *UCP2* p.A55V amino acid change was associated with lower TAOS measures, but the effect on LTL was not significant (Table 5). Haplotype analysis using these SNPs in combination failed to detect a statistically significant effect on LTL (Table 5). Significant differences were observed with the *ACE* I/D variant; the homozygotes for the D allele had significantly shorter mean LTL compared to heterozygotes and wild-type subjects ($p=0.02$, Table 5). Moreover, significant differences in LTL were also detected among the different genotypes of the *GPX1* p.P200L variant, with carriers of the minor L allele having significantly longer mean LTL compared to the wild-type subjects ($p=0.02$, Table 5). Nonetheless, this association is not considered robust, since the rare homozygotes had similar LTL to the wild type homozygotes and the heterozygotes had the longest mean LTL. The effect of the *GPX1* p.P200L and *ACE* I/D variants on TAOS was not significant (Table 5). Finally, the *XRCC1* p.R399Q variant did not display any significant effect on LTL.

Figure V-6. The mean age-adjusted telomere length in Caucasian type 2 diabetes patients carrying or not the *UCP2* -866 G>A variant (The error bars represent 95% confidence intervals).



3.4 DISCUSSION

In order to examine in more depth the association of telomere length with oxidative stress, I evaluated the effect of functional variants in genes involved in ROS generation (*UCP2*, *CYBA*, *ACE*) or detoxification (*MNSOD*, *GPXI*) and in a gene involved in the repair of oxidative DNA damage (*XRCCI*). This investigation was carried out in T2D patients, who are under high oxidative stress, and thus the possible effect of gene variants on LTL would be more pronounced.

Among the genes playing a role in ROS generation, functional variants in *UCP2*, an established negative regulator of mitochondrial ROS overproduction (Casteilla *et al.* 2001), and in *ACE*, a gene implicated with mitochondrial dysfunction and consequent ROS production (de Cavanagh *et al.* 2010), displayed association with shorter LTL. The data showed that those carrying the functional promoter variant -866A of *UCP2* have shorter telomeres. The minor allele -866A has been previously shown to interact with smoking to increase oxidative stress (Stephens *et al.* 2008). Considering this, and that in the present diabetes patients plasma oxidative stress was correlated with shorter LTL, it is likely that the observed effect of the A allele on telomeres is due to its association with greater mitochondrial ROS production. On the other hand, it is believed that the association of *UCP2* with T2D is caused by a pancreatic effect of *UCP2* on insulin secretion. *UCP2* is involved in the glucose-induced insulin secretion, through the uncoupling of ATP production from glucose metabolism. The uncoupling of the ATP production from glucose catabolism reduces the ATP production which in turn results in lower ATP/ADP ratio in the pancreatic cell and therefore decreased insulin secretion (Gable *et al.* 2006). This explains the higher risk for diabetes conferred by *UCP2* -866A allele (O'Rahilly 2001),

while this allele has been associated with higher gene expression in the pancreatic β cells (Krempler *et al.* 2002). Thus, the possibility of *UCP2* -866G>A being involved in cell senescence in T2D as reflected by the telomere dynamics here, through a pathway triggered by disturbed insulin secretion, in addition or not to disturbed regulation of ROS, cannot be excluded.

Similarly to the *UCP2* variant, the DD genotype of the *ACE* gene was also associated with shorter LTL. In the case of the *ACE* gene, since the D allele leads to higher Ang II levels and Ang II in turn has been shown to cause mitochondrial dysfunction and high oxidative stress (Molnar *et al.* 2004), it can be inferred that this variant's effect on telomere length is also mediated through an increased mitochondrial ROS generation. By contrast, functional variants in *CYBA*, the gene encoding a key component of the cytoplasmic NADPH-oxidase, did not show any association. Overall, the associations observed of *UCP2* and *ACE* variation but not of *CYBA* variation with LTL or TAOS, suggest that the ROS related to telomere damage and shortening are predominantly of mitochondrial origin.

Regarding the genes involved in the antioxidant defence, variation in the *GPXI*, which encodes the enzyme forming water from the potent oxidant H_2O_2 , demonstrated an association with LTL, with carriers of the rare allele having longer telomeres compared to wild type. This association also supports the hypothesis that genetic predisposition to higher oxidative stress is linked with shorter telomeres. The leucine variant of the *GPXI* p.P200L was associated with lower enzyme activity in two previous studies (Bastaki *et al.* 2006; Ravn-Haren *et al.* 2006) and with no difference in activity in another one (Forsberg *et al.* 2000). Hence, the leucine variant possibly holds a slightly lower activity, which

seems contradictory to the hypothesis that efficient antioxidant enzyme activity contributes to reduced oxidative stress and thus to longer telomeres. However, there is a possibility that moderate levels of ROS have beneficial effects on cellular homeostasis (Droge 2002; Radak *et al.* 2008); or that a more active GPX1 enzyme leads to increased OH⁻ levels due to decreased levels of reduced glutathione. A delicate balance between the advantageous and disadvantageous effects of ROS might exist, and therefore justify the association of the low antioxidant activity variant (leucine variant) with longer telomeres observed here and with lower mortality observed by Sorensen *et al.* (Soerensen *et al.* 2009). It can be speculated that the leucine variant's beneficial effect on survival (Soerensen *et al.* 2009) is partly mediated by its effect on telomere length. On the other hand, variation in the other antioxidant gene, *MNSOD*, which was also associated with mortality in the study of Soerensen *et al.* (Soerensen *et al.* 2009), did not show any association with LTL. Thus more thorough investigation is needed before any conclusions can be made.

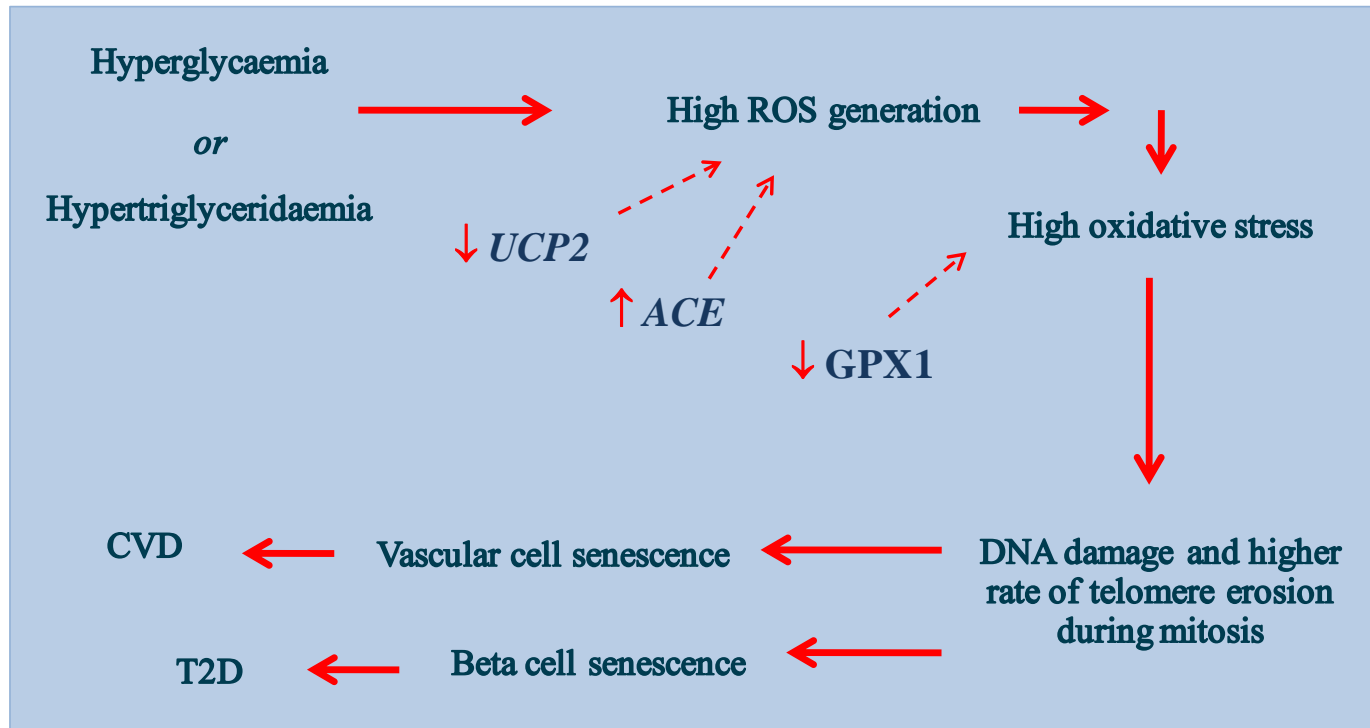
Apart from a trend, there was not any significant association between the functional variants in genes involved in ROS regulation and the plasma antioxidant capacity (TAOS), as measured in the present study. Yet again this may be due to the fact that the loss of the delicate balance in the levels of various ROS and antioxidant molecules is causing telomeric damage, rather than the high levels of any ROS or the low antioxidant defence, as estimated by TAOS. Nevertheless, this may also be attributed to the fact that the single, cross-sectional evaluation of oxidative stress with TAOS is not representative of the accumulated burden of oxidative stress which T2D patients, carrying the respective polymorphisms, experience. Therefore, the genetic variants may be more useful in

providing a better indicator of the oxidative/antioxidant balance on telomeres, especially since genetic variants exert their effect throughout life.

Finally, oxidative damage at telomeric sequences and consequent telomere shortening involves single strand breaks of the telomeric 3' overhang. Oxidative DNA damage and up-regulated DNA repair mechanisms have been observed in the beta cell in T2D (Tyrberg *et al.* 2002). Therefore, it was reasonable to expect genes, which are involved in the repair of oxidative-induced single strand breaks, such as the *XRCC1* (Whitehouse *et al.* 2001), to have an effect on telomere length of individuals with high levels of oxidative stress, such as T2D patients. However, in the present sample of T2D patients, the functional variant in *XRCC1* did not have an effect on LTL.

The present data overall suggest that shorter telomeres in T2D patients can be partly attributed to deregulation of the mitochondrial ROS production and to impaired antioxidant defence. *In vitro* investigation of *UCP2*, *ACE* and *GPXI* regulation will establish the role of these genes in determining the intra-cellular oxygen species levels, the oxidative-induced telomere loss and its consequent effect on cell senescence.

Figure V-7. Proposed mechanism.



4. ASSOCIATION OF SYSTEMIC INFLAMMATION WITH TELOMERE LENGTH

4.1 INTRODUCTION

Regarding the factors which determine the telomere length and the underlying mechanisms of shortening, the evidence presented in the previous chapter coupled with those from *in vitro* studies, support a role of oxidative stress. Nevertheless, chronic inflammatory response might also be responsible for the short telomeres in those with CVD and T2D. Metabolic disorders, like obesity and insulin resistance, subclinical atherosclerosis, as well as overt CVD and T2D, are linked not only to high oxidative stress, but also to an underlying chronic inflammatory response and increased secretion of pro-inflammatory molecules (Pillarisetti & Saxena 2004; Hulsmans & Holvoet 2010). These pro-inflammatory cytokines may lead to a higher rate of telomeric loss, through the stimulation of a sustained cell turnover (Serrano & Andres 2004), or by enhancing the consumption of substrates by the respiratory chain, which in turn leads to higher production of ROS as byproducts (Busik *et al.* 2008).

The aim of the present chapter was to study the association of circulating markers of inflammation with LTL in CVD and T2D patients. The inflammatory markers evaluated here are CRP, a non-specific marker of systemic inflammation, which has been associated with sub-clinical measure of atherosclerosis and a high risk for CHD (Kivimaki *et al.* 2008) and interleukin-6 (IL6), a circulating pro-inflammatory cytokine IL6, which has been associated with higher mortality in epidemiological studies (Gouin *et al.* 2008).

4.2 METHODS

4.2.1 Subjects

For this chapter all the study samples used in previous chapters were employed:

- 1) CHD cases and controls from the HIFMECH study (described in the “Second result chapter”, paragraph 1.2.1, page 212).
- 2) CHD patients from the CABG (described in the “Second result chapter”, paragraph 1.2.1, page 212).
- 3) CHD and non-CHD patients from the FH group (described in the “Second result chapter”, paragraph 1.2.1, page 212).
- 4) T2D patients from the UDACS study (described in the “Second result chapter”, paragraph 2.2.1, page 234).

Analysis in all study samples was restricted to Caucasians in order to maintain ethnic homogeneity in the sample.

4.2.2 Measurement of inflammatory markers

HIFMECH: Core laboratories performed the biochemical determinations on all samples from the entire HIFMECH cohort. CRP was determined with an in-house enzyme immunoassay using rabbit antihuman antibodies (X0293) from Dako Diagnostics (Ely, Cambs, UK), validated against the International Reference Preparation, with an assay range of 0.15 to 48mg/l and with intra-assay and inter-assay coefficient of variation (CV) of <10%. IL-6 was measured by 2-site high sensitivity enzyme-linked immunosorbent assay (ELISA) (R & D Systems, Oxon, UK) with a detection limit of 0.09 pg/ml and intra-assay and inter-assay CVs of 5.3% and 9.2% (Yudkin *et al.* 2004).

CABG: Citrated 4.5-mL blood samples were drawn before and after surgery and immediately centrifuged (3500g, 10 minutes) in order to separate the plasma and freeze it at -20°C until analysis. C-reactive protein was measured on a BN Prospec (Dade Behring). Inter-assay and intra-assay coefficients of variation were <4% and <2%, respectively, with a detection limit of 0.20 mg/l. IL-6 concentration was measured using a commercial assay (R&D Systems) by staff blind to all subject data. Inter-assay and intra-assay coefficients of variation were 5% and 3%, respectively, with a detection limit of 0.70 pg/ml (Brull *et al.* 2003).

FH Simon Broome (SB): A fasting venous blood specimen was taken at the registration visit and CRP and IL6 were measured by the laboratories routinely used by the participating clinics (Neil *et al.* 2003).

UDACS: Blood samples were taken at recruitment and CRP and IL6 was measured at the laboratory routinely used by the diabetes clinics at UCL hospital (UCLH).

4.2.3 Measurement of leukocyte telomere length

The method is described in paragraph 1.2.3 of the “Second result chapter” (page 215) and in detail in the “First result chapter”, paragraphs 1, 2 and 3 (pages 149-175).

4.2.4 Statistical analysis

Statistical analysis was performed using Stata (version 10, StataCorp Texas). LTL and CRP and were not normally distributed, thus log-transformed data were used for the analysis, and geometric means (approx SD) are presented in the tables. In table 6, p values comparing cases and controls for different parameters are from conditional logistic regression models in HIFMECH taking account of matching on age and centre. For the FH study mean values are compared by t-test. Correlations were assessed using

Pearson partial correlations to allow adjustment for age and other covariates. Adjustment was made for age, centre and exercise in HIFMECH, age in CABG and age and gender in FH.

4.3 RESULTS

Table 6 shows the mean values of the two inflammatory markers in each study sample. As expected, the CHD cases have significantly higher levels in both markers compared to controls, apart from CRP levels in FH patients with and without CHD. The values of both markers are also high in the T2D cases. For the CABG sample, only the pre-operative values are presented.

Table V-6. Inflammatory markers in the study samples.

Study sample		Number (% women)	Age (years)	CRP (mg/l)	IL6 (pg/ml)
HIFMECH	CHD controls	559 (0)	51.5 (5.5)	1.23 (1.40)	1.24 (0.78)
	CHD Cases	520 (0)	51.9 (5.4)	2.22 (2.55)	1.97 (1.33)
	p value			<0.0001	<0.0001
CABG	CHD cases	341 (20.8)	64.9 (92.2)	2.29 (2.77)	4.55 (3.12)
FH - SB	FH without CHD	222 (56.8)	44.3 (13.4)	1.16 (1.34)	1.58 (1.14)
	FH with CHD	145 (33.8)	56.1 (10.3)	1.42 (1.59)	2.18 (1.34)
	p value	<0.0001	<0.0001	0.10	<0.0001
UDACS	T2D cases	569 (40.6)	68 (12.3)	1.72 (1.49)	3.50 (2.50)

Table V-7. Partial Pearson correlation coefficients of age-adjusted telomere length with inflammatory markers.

Study sample		CRP (mg/l) (r)	P	IL-6 (pg/ml) (r)	P
HIFMECH	Controls	-0.01	0.77	0.02	0.75
	CHD Cases	0.003	0.95	-0.06	0.25
CABG	CHD cases	0.12	0.03	0.23	<0.001
FH - SB	FH without CHD	-0.01	0.90	-0.03	0.62
	FH with CHD	0.05	0.34	0.07	0.16
UDACS	T2D cases	-0.05	0.21	0.03	0.43

As shown in table 7, a significant correlation of LTL with pre-operative IL6 and CRP levels was observed in CABG patients alone (r=0.23, p<0.0001 and r=0.12, p=0.03, respectively). In all other study samples there was no significant correlation of LTL with either of the inflammatory markers and LTL.

4.4 DISCUSSION

In the four studies presented here, no consistent correlation was found between LTL and inflammatory markers, such as CRP and IL6, although in the CABG patients, a positive correlation of pre-operative IL6 and CRP levels with LTL was found. These findings in CABG patients differ from previous studies showing a negative correlation of LTL with IL6 levels in a community-based population (Fitzpatrick *et al.* 2007) and multiple myeloma subjects (Wu *et al.* 2003), and with CRP in haemodialysis patients (Carrero *et al.* 2008) in another community-based sample (Bekaert *et al.* 2007). However, these associations in CABG patients did not persist postoperatively (data not shown), and also were not replicated in the other CHD cases examined (HIFMECH and

FH). A number of previous studies have also failed to detect a significant correlation of LTL with inflammatory markers, such as CRP, in postmenopausal women (Lee *et al.* 2005; Aviv *et al.* 2006), in individuals with diabetes or impaired glucose tolerance (Sampson *et al.* 2006; Adaikalakoteswari *et al.* 2007; Olivieri *et al.* 2009), as well as in chronic pulmonary disease subjects (Houben *et al.* 2009).

One possible explanation of the unexpected positive association of IL6 with LTL is that in the preclinical phase of disease, systemic inflammation promotes both atherosclerosis and LTL attrition. However, once CHD is established other genetic and environmental factors, possibly influencing the activity of telomerase, have greater influence in determining the rate of telomere shortening.

On the other hand, in any particular study, the absence of a significant correlation can be due to lack of power resulting from the relatively small sample size. Thus, I cannot confirm or refute the reported associations with inflammatory markers, although in general, they appear to be relatively weak. Since no robust association of inflammatory markers and LTL was observed, further investigation on the effect of genes involved in chronic inflammatory response was not performed.

Whether LTL shortening contributes directly to the progression of CHD or T2D at the cellular level cannot be determined from the present results. *In vitro* work with cell cultures being treated with pro-inflammatory molecules may be of help in understanding this phenomenon.

5. FACTORS DETERMINING THE TELOMERE LENGTH CHANGE OVER FOLLOW UP

5.1 INTRODUCTION

The cross-sectional data presented so far in this thesis support an association of short LTL with CVD and T2D; also, apart from the genetically determined telomere length at birth, the data suggest an age- and oxidative stress-related telomere attrition during life time.

However, a single telomere length assessment leaves unclear whether the observed associations are due to shorter length at birth or rather a mere reflection of accelerated telomere attrition during lifetime, or else, a combination of both. As previously mentioned twin and family studies show that telomere length's heritability ranges from 44% to 80% (Slagboom *et al.* 1994; Vasa-Nicotera *et al.* 2005; Njajou *et al.* 2007). On the other hand, data from studies focusing in older twin pairs indicate that non-genetic factors can have significant effects on telomere length during life. The lengths between identical twins were found to be almost as similar as between fraternal male twins over 70 years old (Huda *et al.* 2007). Another study has shown that identical twins who exercised had longer LTL than the identical twin who did not (Cherkas *et al.* 2008), which also suggests a large non-genetic influence.

Thus, longitudinal studies are required to accurately assess telomere attrition, its presumed link with accelerated ageing and its association with oxidative stress and inflammation. For this purpose, it was considered of great importance to examine the change of LTL over time and the factors determining it. Follow up blood samples were obtained for a subset of the UDACS patients and the study of LTL change over time

was performed. Identifying modifiable risk factors which influence telomere length over time, may lead to novel insights into mechanisms which can delay biological ageing.

5.2 METHODS

5.2.1 Study sample

Subjects were a subset of participants in the UDACS study, recruited from the diabetes clinic at UCL Hospitals in 2001–2 (described in the “Second result chapter”, paragraph 2.2.1, page 234). Among these T2D patients, 80 individuals re-attended the diabetes clinic at UCL Hospitals in 2008 and therefore participated in the UDACS follow up. During the follow up, the patients went through physical examination and blood samples were drawn for biochemical analysis and DNA extraction. The collection of data and samples from the 80 UDACS individuals in 2008 was performed by Dr Nikos Gkranias.

5.2.2 Leukocyte telomere length measurement

In this prospective sample of 80 individuals with T2D, mean LTL was measured at baseline, and after the seven years of follow up, using the MMQPCR. LTL was measured in leukocyte DNA samples from these patients extracted from whole blood using the salting out method (Bolla *et al.* 1995). The TL at baseline and follow up of each patient was measured in the same plate to avoid confounding of the LTL change (Δ LTL) assessment due to inter-assay variability. Briefly, the new version of the qPCR-based method, the MMQPCR, differs compared to the original q-PCR in the following points: a) Both the SCG and the telomere PCR are concurrently performed in the same tube, in order to increase accuracy of the estimation of the copies of the genome and the number of telomere repeats in the same sample, b) the SCG employed for this method is

the *HBB* and c) the cycling profile is adapted accordingly for a multiplex qPCR. This version of the qPCR method was also validated with samples measured also with TRF. The coefficient of inter-assay variation of the method was estimated at 5.22%. The method is described in detail in the “First result chapter”, paragraph 5, pages 187-210.

5.2.3 Statistical analysis

Statistical analysis was performed using Stata (version 10, StataCorp Texas). Baseline risk factors were transformed to a normal distribution where appropriate. Partial correlation coefficients were used to examine the association of the percentage % of change in LTL (% Δ LTL) with selected continuous risk factors. All models for baseline LTL included baseline age. Models for change were adjusted for the change in age from baseline to follow-up. Adjusted mean changes were obtained from analysis of covariance models. Δ LTL was determined as the change in LN transformed values which allowed the % Δ LTL to be calculated. Stepwise regression models with change in LN (LTL) as the dependent variable were used in order to identify the independent predictors of the % Δ LTL over the seven-year follow up. The model was validated using 1000 bootstrap samples with the bootstrap inclusion fraction set at 60%. Statistical significance was taken as $p < 0.05$.

5.3 RESULTS

5.3.1 Characteristics of T2D patients with follow up

This subset of UDACS included subjects aged from 35 to 87 years and their characteristics were typical for T2D patients (Table 8). The age-adjusted mean LTL of this subset of patients at baseline was similar to the mean LTL of the whole UDACS (p=0.85).

Table V-8. Characteristics of the total of T2D cases and of the subset participating in follow up.

	UDACS T2D cases N=569	UDACS T2D cases with follow-up N=81	<i>P</i>
Age (yrs) ⁺	68 [24-92]	63 [29-82]	<0.001
Age of T2D onset (yrs)**	55 (13)	50 (13)	<0.001
Duration of T2D (years) ⁺	9 [4-16]	9 (5-15)	0.99
% Females (N)	40.6 (231)	37.0 (30)	0.52
% Females >50 years (N)	94.4 (218)	83.3 (25)	0.01
BMI (kg/m ²)*	29.3 (5.5)	29.3 (4.3)	0.98
SBP (mmHg)*	140.5 (20.9)	138.8 (17.7)	0.30
DBP (mmHg)*	79.3 (11.4)	80.0 (8.3)	0.36
TC (mmol/l)*	4.96 (1.09)	4.91 (1.02)	0.62
TG (mmol/l)*	1.92 (1.08)	1.88 (0.97)	0.77
HDL (mmol/l)*	1.28 (0.37)	1.27 (0.36)	0.92
CRP (mg/l)*	1.72 (1.49)	1.81 (1.68)	0.57
Glucose (mmol/l)*	9.8 (4.3)	10.2 (4.3)	0.61
HBA1c (%)*	7.65 (1.61)	8.13 (1.54)	0.006

*data were log-transformed and geometric means [(approximate standard deviation (SD))] are presented, ** mean with SD is presented, ⁺median [IQR] is presented,

TC: total cholesterol, BMI: body mass index, SBP: systolic blood pressure, DBP: diastolic blood pressure, TG: triglycerides, HDL: high density lipoprotein, LDL: density lipoprotein, CRP: C-reactive protein, LTL: leukocyte telomere length.

5.3.2 Seven-year change in LTL

The patients were categorised in three groups according to their % Δ LTL during the seven-year follow up. A cut-off of 10% Δ LTL was chosen for the grouping of patients, which fell outside the ~5% range of variability expected from the assay (i.e. the 5.22% coefficient variation of the MMQPCR method), and also corresponded to substantial and, thus more meaningful, changes in LTL. A similar approach has been used by other studies assessing the longitudinal change of LTL (Epel *et al.* 2009; Farzaneh-Far *et al.* 2010). Thus the patients were categorised in the following groups of LTL change:

A) “Shortened LTL” group: Included subjects with % Δ LTL $<-10\%$ i.e. greater than 10% decrease in LTL. The percentage of subjects in this group was 2.5% (N=2) and they displayed a reduction in LTL of 21.59% and 11.78%.

B) “Maintained LTL” group: Included subjects with % Δ LTL $<-10\%$ and $<10\%$ i.e. a decrease in LTL smaller than 10% or an increase in LTL smaller than 10%. The percentage of subjects in this group was 8.8% (N=7). The mean change in LTL was a 1.42% decrease (Median: -1.42, Inter-quartile range: -3.74 to 2.70).

C) “Lengthened LTL” group: Included subjects with % Δ LTL $>10\%$ i.e. greater than 10% increase in LTL. The percentage of subjects in this group was 88.8% (N=71). The mean increase in LTL was 54.7% (Median: 54.70, Inter-quartile range: 36.72 to 81.11).

5.3.3 Determinants of longitudinal change in LTL

The % Δ LTL was found to significantly correlate with baseline LTL ($r=-0.22$ $p=0.05$, Table 9 and Figure 8).

The association of % Δ LTL with TAOS, CRP, IL6, HBA1c and the change in HBA1c and BMI over the follow up was examined by including the change in age from baseline to follow-up as a covariate. Baseline LTL was not included, since baseline adjustment has been suggested to induce spurious statistical associations between the different exposures and the resulting change (Glymour *et al.* 2005). Among these variables, low baseline CRP was significantly correlated with a greater increase in LTL ($r=-0.32$ $p=0.005$, Table 9 and Figure 9).

Table V-9. Partial correlation coefficients of baseline LTL and % Δ LTL with selected risk factors.

	Baseline LTL*	% ΔLTL**	N
Baseline LTL		$r=-0.22$, $p=0.05$	80
Baseline IL6	$r=-0.21$, $p=0.06$	$r=-0.09$, $p=0.41$	78
Baseline CRP	$r=0.04$, $p=0.73$	$r=-0.32$, $p=0.005$	78
TAOS	$r=-0.08$, $p=0.46$	$r=-0.07$, $p=0.53$	80
Change in HBA1c	$r=0.07$, $p=0.55$	$r=-0.19$, $p=0.11$	77
Change in BMI	$r=-0.02$, $p=0.86$	$r=-0.01$, $p=0.94$	80
Duration of diabetes	$r=-0.03$, $p=0.80$	$r=-0.19$, $p=0.10$	80

* The model for baseline LTL includes baseline age.

**In the model for % Δ LTL the dependent variable is change and includes as a covariate the change in age from baseline to follow-up.

Figure V-8. Correlation graph of baseline LTL with % Δ LTL (LN change).

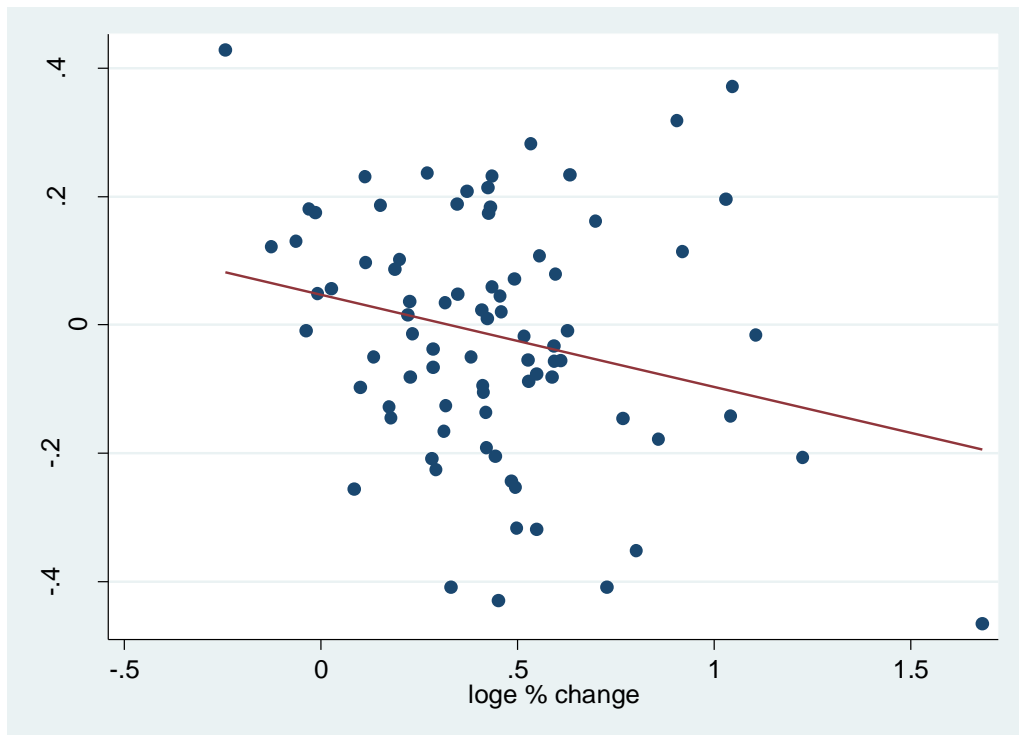
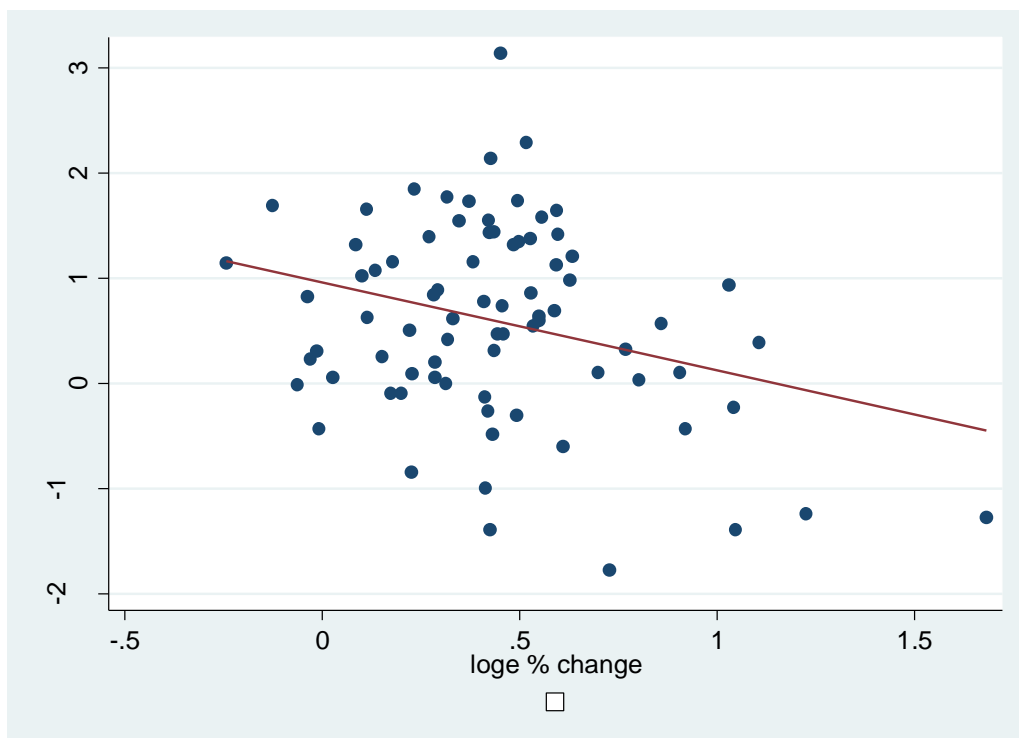


Figure V-9. Correlation graph of CRP with % Δ LTL (LN change).



Then, using a stepwise regression model which also looked at the change in LTL only, without adjusting for baseline, we sought to identify any independent predictor/s of % Δ LTL. Baseline CRP was found to be an independent predictor of % Δ LTL with one SD lower baseline CRP being associated with a 9.8% increase in LTL ($p=0.005$).

Table V-10. Differences in baseline LTL and % Δ LTL by medication and T2D complications.

		Baseline LTL	% ΔLTL
Medication	Anti-inflammatory		
	No (N=13)	6.73 (6.45-7.01)	81.8 (51.8-117.8)
	Yes (N=66)	7.02 (6.88-7.15)	50.3 (39.0-62.6)
	P value	0.08	0.06
	Anti-cholesterolaemic		
	No (N=18)	6.9 (6.64-7.17)	56.7 (34.3-82.7)
	Yes (N=62)	7.0 (6.85-7.14)	54.6 (42.4-67.9)
	P value	0.56	0.88
	Hypoglycaemic		
	No (N=2)	6.96 (6.18-7.74)	51.5 (-4.0-139.3)
	Yes (N=78)	6.97 (6.85-7.1)	55.2 (44.2-66.9)
	P value	0.97	0.92
T2D complications (i.e. cardiovascular event, systemic event, nephropathy or retinopathy)	Any T2D complication		
	No (N=15)	7.32 (6.99-7.64)	53.9 (30.2-81.8)
	Yes (N=65)	6.9 (6.77-7.03)	55.4 (43.4-88.3)
	P value	0.02	0.92

For the % Δ LTL, means with 95% confidence intervals (CI) are presented.

For the baseline LTL, means with 95% confidence intervals are used to calculate the corresponding values in kb based on the regression line between measures obtained by both the MMQPCR-based method and the conventional TRF analysis for the same set of 32 samples, as described in the “First result chapter”, paragraph 5.3.3 (page 206).

Interestingly, a borderline significant association of the change in LTL over follow up with medication was observed, with those under anti-inflammatory drug therapy displaying a greater change in LTL compared to those who did not receive any anti-inflammatory treatment. The treatment with other groups of medication did not have an effect on the follow up change in LTL (Table 10). Nevertheless, information on specific drugs was not available. Also, it was considered possible that the change in LTL might reflect the worsening of the disease, thus the association with T2D complications was tested but no significant differences were found. However, the baseline LTL was shorter in the patients who went on to develop T2D complications during the follow up period ($p=0.02$) (Table 10).

5.4 DISCUSSION

This is the first evaluation of temporal change in LTL, and the factors determining it, in individuals with established T2D. The majority of patients, in the present longitudinal study, displayed a lengthening of their LTL over the seven-year time period. Moreover, short baseline LTL and a low grade of inflammation at baseline were found to be independent predictors of LTL lengthening.

Previous longitudinal studies have also observed lengthening of LTL. In young adults of the “Bogalusa Heart Study”, a biracial population-based cohort, LTL was lengthened in 12% of Caucasians and 14% of African-Americans over the five-year follow up (Aviv *et al.* 2009). In a study of healthy elderly men, telomere lengthening was observed in 24% of subjects over 2.5 years (Epel *et al.* 2009). The “Heart and Soul Study” showed that in 23% of individuals with stable CHD participating in the study, LTL was lengthened over the five-year follow up (Farzaneh-Far *et al.* 2010). In the

present sample of diabetes patients, a greater percentage (89%) displayed an increase in mean LTL. Worthy of remark is that older or diseased study samples display greater percentages of LTL lengthening. It is likely that the study samples displaying highest percentages of LTL lengthening are those with the shorter LTLs at baseline. This is further supported by the consistent association of baseline LTL with its change over time in all relevant studies (Aviv *et al.* 2009; Epel *et al.* 2009; Farzaneh-Far *et al.* 2010).

The purpose of this chapter was also to reveal the determinants of this temporal change in LTL of diabetes patients. Based on the hypothesis that inflammation and oxidative stress are the forces driving the rate of telomere change over time, the effect of TAOS, an estimate of antioxidant defence, and the effect of the inflammatory markers CRP and IL6 was examined. It was also investigated whether duration of diabetes, disease worsening or improvement, as reflected by good or not glycaemic control, and gain or loss of weight play a role. Glycaemic control in diabetes patients has been previously associated with telomere length (Uziel *et al.* 2007), and is widely monitored by the changes in HBA1c (Colman *et al.* 1997). Finally, the effect of baseline LTL was tested, since previous studies have suggested a significant role in predicting telomere length trajectory (Aviv *et al.* 2009; Epel *et al.* 2009; Farzaneh-Far *et al.* 2010). Among the factors examined, short baseline LTL and low baseline levels of CRP showed a significant correlation with the increase in LTL. The low level of inflammation at baseline, as reflected by CRP, was found to be the only independent predictor of LTL lengthening.

First, the present data suggest that LTL may increase in patients with T2D, as a result of a negative feedback mechanism for the regulation of LTL in humans. This mechanism is probably activated in very short telomeres, such as the leukocyte

telomeres of T2D patients. The enzyme telomerase, which is active in hematopoietic stem and progenitor cells, as well as in peripheral blood leukocytes at low levels (Ornish *et al.* 2008), is a good candidate for mediating this mechanism. The change in LTL over time is proportional to the baseline both in individuals who display shortening and lengthening. Regarding the proportional shortening of long telomeres, Aviv *et al.* propose that oxidative stress might be the driving force, since longer telomeres contain more G triplets, which are the targets of free radicals (Aviv *et al.* 2009). However, the proportional lengthening, observed mainly in the present study, cannot be explained by the same mechanism. It can be attributed either to telomerase activation at a very short telomere length, or to the regeneration of blood cells from haematopoietic cells. The addition of new blood cells generated from the stem cell pools, which preserve their mean LTL through an active telomerase, could be the reason for the increase in mean telomere length of blood cells during the follow up period (Aviv *et al.* 2009).

Second, in the present study, the low grade of inflammation was the independent predictor of the lengthening of telomeres in diabetes patients, implying that inflammatory molecules are detrimental to the telomere length regulation. Alternatively, it can be speculated that high levels of inflammation at baseline have already caused exhaustion of stem cell reserves.

Whereas CRP was observed to have an influence on the change of LTL did not also display significant correlation with the cross-sectional measurement of LTL at baseline. This finding suggest that epidemiology of the longitudinal telomere dynamics is different to epidemiology of cross-sectional telomere length estimations (Farzaneh-Far *et al.* 2010). Presumably, the single time point measurements reflect the lifelong effect of environmental factors in combination with the genetic effect, while telomere length trajectory is mainly driven by a negative feedback mechanism for protection of

very short telomeres, or the rate of stem cell turnover during that certain period of time. In support of this is also the association of short baseline LTL, and not of the relative change in LTL, with the development of T2D complications during the follow up.

Finally, the use of anti-cholesterolaemic or hypoglycaemic was not associated with the LTL increase observed in the present T2D patients, while anti-inflammatory treatment was marginally associated with those under treatment showing a smaller increase in LTL. Possibly the patients prescribed anti-inflammatory drugs were those more severely diseased and/or with higher CRP levels at baseline. However, This association should be interpreted with caution, since no information was available on the specific drugs or their effectiveness. Moreover, the possibility that a class of drugs has a beneficial effect on LTL change, as previously suggested for statins (Spyridopoulos *et al.* 2004; Mahmoudi *et al.* 2008; Satoh *et al.* 2009), cannot be excluded based on the present data, since only groups of drugs were examined and any drug-specific effect may have been diluted.

Limitations of this study need to be considered. The small sample size of 80 subjects, the lack of comparison with longitudinal data in controls or patients free of medication question the reliability of the findings of the present study, especially regarding the factors determining the change in LTL,. Unfortunately, data on several key factors, such as oxidative stress measures, inflammatory markers and drug use, were missing at follow up and this limited the ability to identify all the possible factors determining the longitudinal LTL change. On the other hand the fact that the majority of patients displayed a considerable lengthening of LTL and that both the baseline and the follow up samples were measured in the same assays, avoiding bias due to inter-assay variability, offer robustness to the observation of LTL lengthening in T2D patients under treatment.

In conclusion, the present observations suggest a bidirectional regulation of telomere length, and raise the possibility to reverse telomere-dependent ageing. Also, this study raises the potential for LTL to prove useful as a marker for disease improvement. Thus the factors governing telomere dynamics during lifetime deserve further study.

VI. FOURTH RESULT CHAPTER: “IN VITRO INVESTIGATION OF THE DETERMINANTS OF TELOMERE LENGTH DURING AGING”

1. THE EFFECT OF PRO-INFLAMMATORY CONDITIONING AND/OR HIGH GLUCOSE ON TELOMERE SHORTENING OF AGING FIBROBLASTS

1.1 INTRODUCTION

The studies included in the previous chapter aimed at elucidating the determinants of short telomeres in patients with CVD and T2D. It was shown that shorter telomeres, at least in T2D patients, can be partly attributed to mitochondrial production of ROS and impaired antioxidant defence. However, glucose displayed an unexpected positive correlation with LTL in the EARSII and FH subjects, which is in contrast to the hypothesis that hyperglycaemia elicits the high levels of ROS that may cause telomere shortening. Moreover, whether inflammation contributes to the shorter telomeres in CHD or T2D patients was not determined by the cross-sectional data of the previous chapter. Whereas, follow up analysis suggested that low grade of inflammation may favor the lengthening of telomeres, in diabetes patients, implying that inflammatory molecules are unfavorable to telomere length maintenance. In order to shed more light on these mechanisms, I decided to carry out *in vitro* experiments investigating what CVD/T2D risk factors determine telomere shortening during aging at the cellular level.

My hypothesis was that factors having an effect on telomeres may be arising from metabolic disorders, linked to increased nutrient concentration, or chronic

inflammation. Increased nutrient availability (e.g. glucose) potentially leads to a higher rate of oxidative phosphorylation in the mitochondria and/or a consequent higher production of reactive oxygen species (ROS) as byproducts. Also, an increased catabolism of these nutrients is likely to lead to an increase of the NADPH-to-NADP ratio and a consequent enhancement of NADPH oxidase-dependent production of superoxide. The high levels of ROS are known to cause oxidative DNA damage, and therefore to result in greater loss of telomeric sequences during replication as shown *in vitro* (Petersen *et al.* 1998; Serra *et al.* 2000; von Zglinicki 2000). Nevertheless, the data on whether hyperglycaemia elicits an increase in intracellular ROS production are conflicting, with other studies supporting the glucose-induced increase in ROS generation (Nishikawa *et al.* 2000; Piconi *et al.* 2006; Morgan *et al.* 2007) and others which argue that this is true under all circumstances (Martens *et al.* 2005; Busik *et al.* 2008).

Pro-inflammatory cytokines may lead to a higher rate of telomeric loss through the stimulation of a sustained cell turnover, or through an enhancement of substrate consumption by the respiratory chain, which in turn leads to higher production of ROS as byproducts. Interestingly, Busik *et al.* have shown that high glucose alone may not result an augmentation of ROS production, whereas the pro-inflammatory cytokine IL1B may trigger higher glucose consumption by the respiratory chain, and thus to an enhancement of ROS production (Busik *et al.* 2008).

Therefore, my aim was to examine whether high concentration of a basic mitochondrial substrate, such as glucose, and/or pro-inflammatory conditioning with IL1B, cause greater telomere erosion in a well described *in vitro* model of replicative senescence (i.e. telomerase is not expressed), the human skin fibroblast (Goldstein 1990). Interleukin 1 beta (IL1B) was chosen based on its regulatory role in the

atherosclerotic process (Galea *et al.* 1996) and its implication in the failure of β -cells during diabetes development (Maedler *et al.* 2009) but also on the experiment of Busik *et al.* (Busik *et al.* 2008) which showed that IL1B may enhance ROS production. For the *in vitro* modelling of oxidative stress, an inhibitor of γ -glutamyl cysteine synthase, buthionine sulphoximine (BSO), was employed (Kurz *et al.* 2004); γ -glutamyl cysteine synthase is a key enzyme of the glutathione redox-cycle, which is part of the intracellular machinery for peroxide detoxification (Griffith & Meister 1979). The number of copies of mitochondrial DNA per cell was investigated in parallel, since it has been suggested to increase with oxidative stress (Lee *et al.* 2000) and respiratory-function decline during aging (Ames *et al.* 1995).

1.2 METHODS

1.2.1 Cell culture

Materials: Normal Human Dermal Fibroblasts (NHDF) from juvenile foreskin, fibroblast growth medium lacking ascorbic acid (FGM –AA) and fibroblast detach kit were purchased from PromoCell GmbH (Heidelberg, Germany). L-buthionine-[S,R]-sulphoximine (BSO) and L-glucose were from Sigma-Aldrich (Steinheim, Germany). IL1B was purchased from Peprotech (London, UK) and D-glucose from Peprotech (London, UK).

Procedure: First passage cryopreserved NHDF from four genetically distinct donors were grown in FGM –AA for 13 days (up to passage 4). The growth medium was especially made without ascorbic acid, in order to exclude the antioxidant effect of ascorbic acid on the pro-oxidant effect of the treatments applied subsequently in the present experiment. The donors were 3, 14, 2 and 2 years old. For each donor six

independent cultures were initiated and serially passaged under different conditions for 90 days. The six different conditions were: 1) FGM –AA only (control), 2) FGM –AA + 10 μ M BSO (pro-oxidant treatment), 3) FGM –AA + 25mM D-glucose (high glucose treatment), 4) FGM –AA + 1ng/ml IL1B (pro-inflammatory conditioning), 5) FGM –AA + 25mM D-glucose + 1ng/ml IL1B (combination). In addition a culture from each donor was treated with FGM –AA + 25mM L-glucose in order to control for any osmotic effect caused to cells by the high concentration in medium. The medium containing each treatment was changed every three days. The number of population doubling (PD) was calculated using the formula $PD = [\ln(\text{number of cells harvested}) - \ln(\text{number of cells seeded})] / \ln 2$ and the cumulative PD (CPD) by progressively adding the PD in each passage.

1.2.2 Telomere length measurement

At each passage a sample of the cells harvested from each culture was used for total DNA extraction with the PUREGENE DNA kit (Qiagen, West Sussex, UK). The extracted DNA samples were frozen at -20° C until measurement, without repeated freeze–thawing cycles. Mean telomere length was measured in these DNA samples using the validated quantitative PCR-based method as described in the “First result chapter”, paragraph 1, 2 and 3 (pages 149-175).

1.2.3 Mitochondrial DNA (mtDNA) copy number measurement

The DNA samples extracted, as described above from each culture at each passage, were also used for the estimation of the copy number of mtDNA per nucleus, which is representative of the mitochondria number per cell. For this purpose, I set up a quantitative PCR-based method previously described by Xing et al. (Xing *et al.* 2008) for the first time in our lab. The method was validated before applied in the present

experiment. The relative number of mtDNA copies per genomic DNA copies (M/G ratio) was calculated as the ratio of the mitochondrial subunit 1 (*MTND1*) gene copies to the genomic *36B4* (now called *RLP0*) gene copies. These genes are single copy genes for the mtDNA and the genomic DNA respectively. The number of mtDNA copies and genomic DNA copies in each sample was determined in comparison to a reference sample in a *MTND1* and a *36B4* quantitative PCR, respectively. All PCRs were performed on the Rotor-Gene 6000 (Corbett Research Ltd, Cambridge UK). The relative concentrations of PCR products were estimated using the comparative quantification analysis (Rotor-Gene 6000 software, Corbett Research Ltd, Cambridge, UK). The second derivative of the amplification curve was considered in order to identify the peak of the exponential amplification and determine the Take-Off of the reaction. The Take-Off was estimated by finding the first point to be 80% below the peak level. Based on the Take-Off point and the amplification, the software calculated the relative quantity of *MTND1* and *36B4* copies in each sample compared to the reference sample. The same reference DNA was used in all runs to allow comparison of the results in different runs. The *MTND1* and the *36B4* PCRs for each sample were performed in duplicate in the same run in order to increase accuracy. The specificity of all amplifications was determined by melting curve analysis.

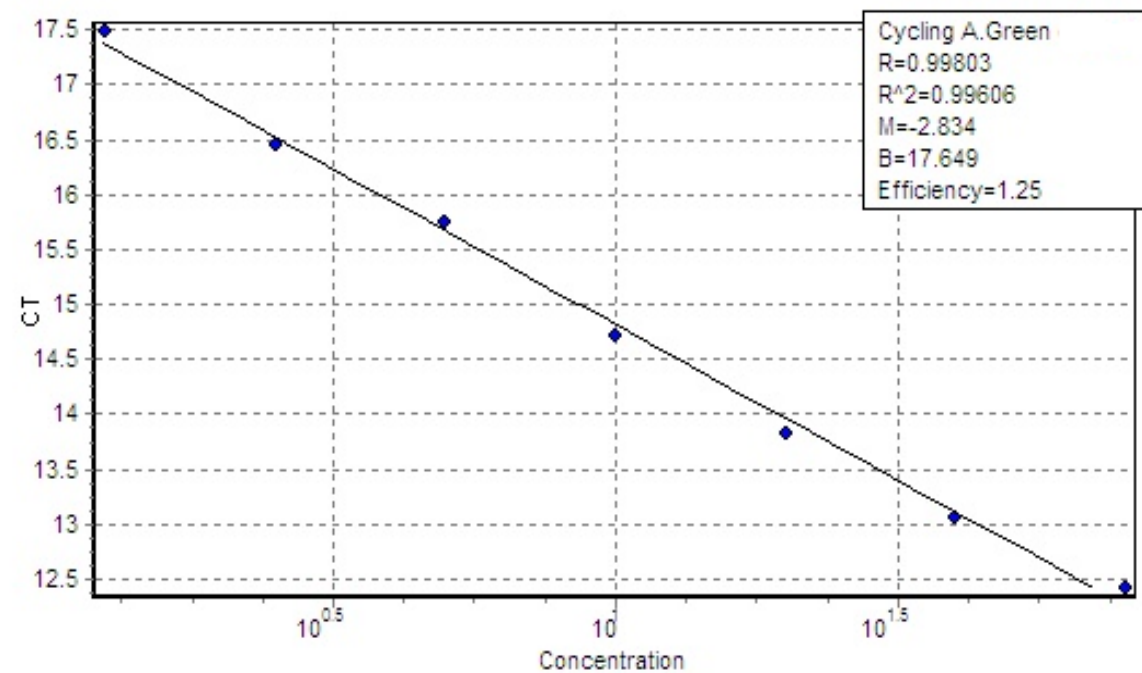
The primers, used for the *MTND1* amplification, were: *MTND1* forward: 5'-TGGGTACAATGAGGAGTAGG-3', *MTND1* reverse: 5'-GGAGTAATCCAGGTCGGT-3' at a 215nM concentration and for the *36B4* these were: *36B4* forward: 5'-CCCTAAAACCCGCCACATCT-3', *36B4* reverse: 5'-GAGCGATGGTGAGAGCTAAGGT-3' at a 300/500nM (forward/reverse) concentration. For both PCRs the cycling profile was 95°C incubation for 10min, followed by 34 cycles of 95°C for 15sec and 58°C for 60sec and the final reaction

consisted of 1xqPCR mix (2x SensiMix NoRef DNA kit, Quantace, London, UK), 30ng of template and the respective primer concentrations at a 25 μ l total volume.

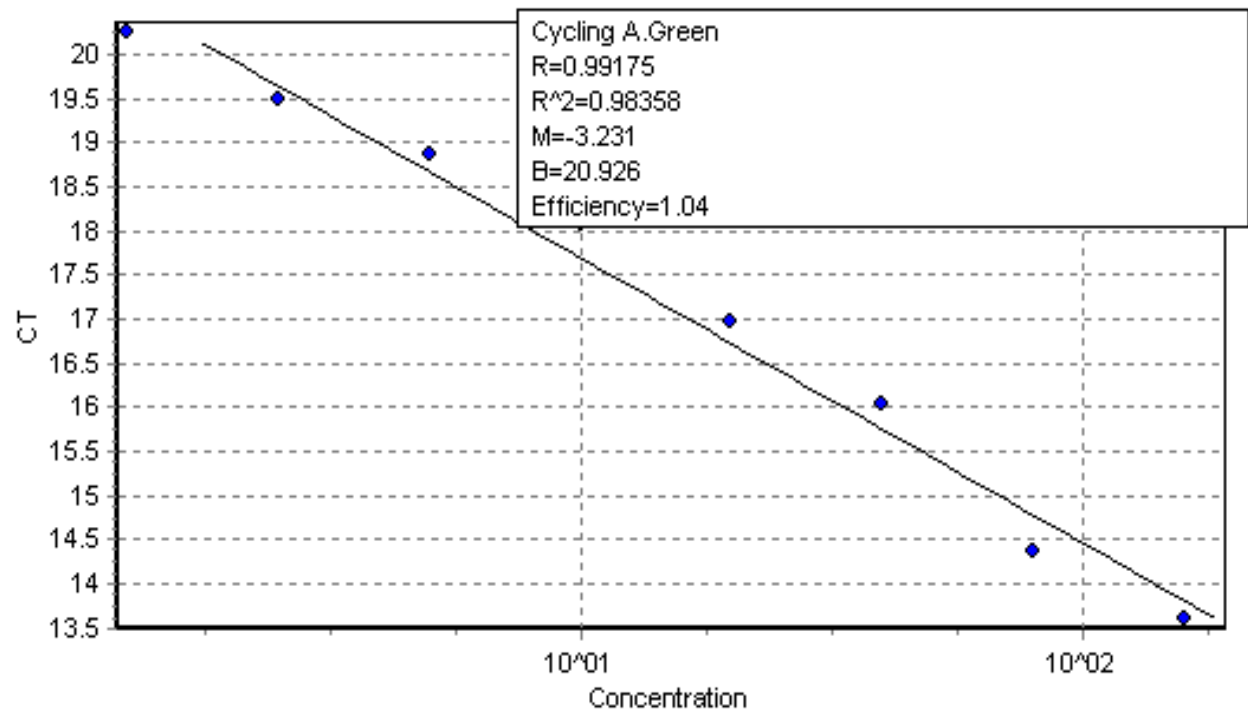
A dilution series (1.25 ng/ μ l - 80 ng/ μ l, two-fold dilution, seven points) was run after optimization for both the *MTND1* and *36B4* PCRs. For both assays, linearity ($R^2 > 0.99$) over this range of input DNA and 100% efficiency was observed (Figure 1 A and B).

Figure VI-1. A) Mitochondrial single copy gene (*MTND1*) PCR standard curve. B) Genomic single copy gene (*36B4*) PCR standard curve.

A)

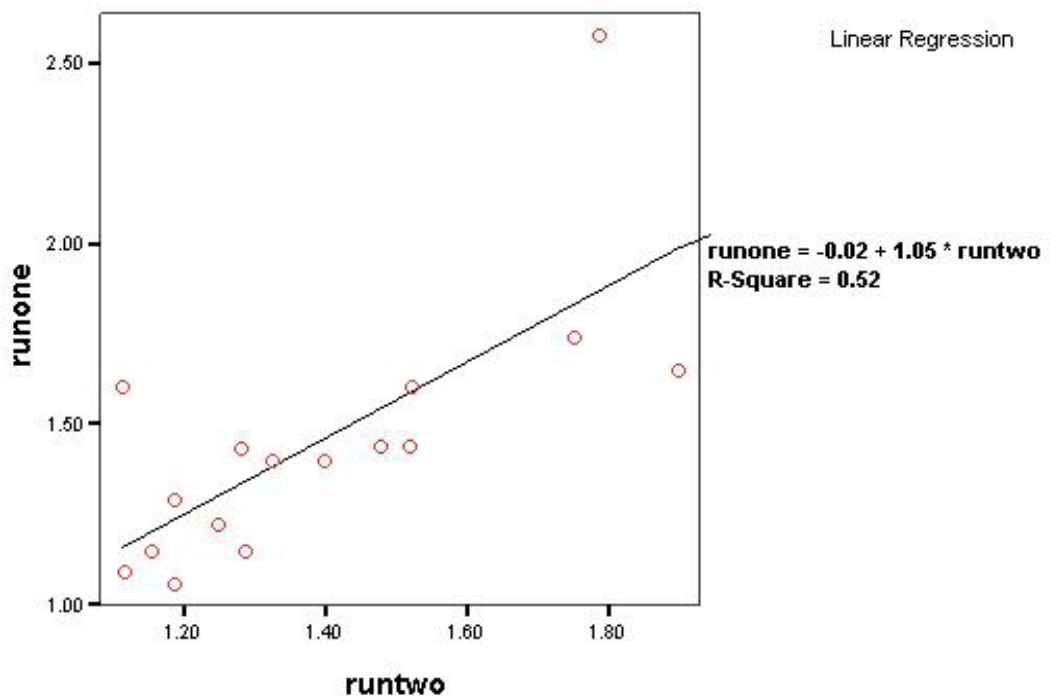


B)



In order to test the reproducibility of the method, 16 randomly chosen samples were run in duplicate on two consecutive days. There was significant linearity between the measurements obtained on the two different days in linear regression analysis ($R^2=0.52$, $p=0.002$, Figure 2). Moreover, the reproducibility was also assessed with Spearman's non-parametric test of pair-wise correlation that looks at the ranking of each sample. The correlation of the mtDNA copy number ranking as measured on the two different days was significant (Spearman rho coefficient= 0.69, $p=0.003$). The coefficient of inter-assay variation in repeated measurements was 7.4%.

Figure VI-2. Linear regression between measurements of mtDNA copy number measurement with the quantitative PCR in 16 samples acquired on two consecutive days ($R^2=0.52$, $p=0.002$).



1.2.4 Quantification of apoptosis

The Annexin-V-FLUOS Staining Kit (Roche Diagnostics GmbH, Penzberg, Germany) was employed for the quantification of apoptosis, and differentiation from necrosis, as described in the “General Methods”, paragraph 6.3 (page 138). NHDF cells from donors 1 and 2 were treated for seven days under the conditions indicated above. A sample from the cells harvested from each culture was stained with Annexin V-Fluorescein and/or PI. The samples were then analysed on the FACSCalibur (Becton-Dickinson).

1.2.5 Measurement of intracellular ROS content

The ROS detection reagent, H₂DCFDA (Molecular Probes, Invitrogen, Oregon, USA), was applied for the measurement of intracellular ROS content, as described in the “General Methods”, paragraph 6.4 (page 142). NHDF cells were treated for seven days under the conditions indicated above. A sample from the cells harvested from each culture was stained with H₂DCFDA. The samples were then analysed on the FACSCalibur (Becton-Dickinson). Apoptotic and/or necrotic cells, as detected with Annexin-V/PI staining, were excluded from the estimation of ROS content.

1.2.6 Gene expression assays

Total RNA was extracted using the RNeasy Mini Kit 250 (Qiagen, West Sussex, UK), as described in the “General Methods”, paragraph 3 (page 115), from samples of each culture before treatment and at two time points during treatment (after six and 45 days of treatment). cDNA was synthesised using the Superscript III Reverse Transcriptase (Invitrogen, Paisley, UK), as described in General Methods (page 116). The level of expression of the telomere reverse transcriptase (*TERT*) and the

mitochondrial transcription factor A (*TFAM*) genes were estimated using TaqMan technology, described in the “General Methods”, paragraph 4.3.1 (page 126), using the respective probes: *TERT* (Hs01082775_m1) and *TFAM* (Hs00162669_m1), Applied Biosystems, Cheshire, UK. The qPCR reactions were performed on the ABI prism 7900HT sequences detection system (Applied Biosystems, Cheshire, UK), in triplicate, and the results were analysed with the S.D.S.2.1 Applied Biosystems software for relative quantification. The BestKeeper software (Pfaffl *et al.* 2004) was used to test the suitability of the three housekeeping genes. The relative expression ratio of the target genes was estimated after standardisation with the three house-keeping, using the REST software as previously described (Pfaffl *et al.* 2002) (Web appendix 2).

1.2.7 Statistical analysis

Statistical analysis was performed with SPSS statistical software (version 17.0 for Windows). Telomere length and mtDNA copy number were log-transformed (natural log) to a normal distribution. The differences in CPD, telomere length and mtDNA copy number among the cultures generated from the four different donors were tested with univariate analysis of variance using the pooled data and adjusting for treatment. The data from the four independent experiments, generated from the four donors, were analysed pooled after adjusting for donor as well as on a per donor basis. The association of the days of treatment with telomere length and mtDNA copy number as well as the association of CPD with telomere length and mtDNA copy number were evaluated using partial correlation coefficients controlling for donor. To assess the effect of each treatment on the telomere length change over time, I used a linear regression model with telomere length as the dependent variable and the days of treatment, the donors and the different treatments as the independent variables. The treatments were introduced in the model as dummy variables by leaving out of the

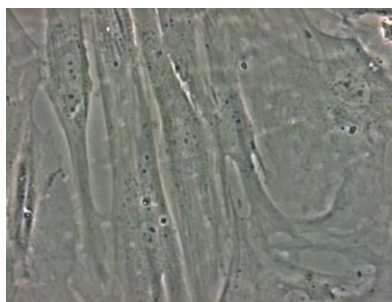
model the dummy variable corresponding to the control. This was done in order to force the comparison of each treatment to the control, since this was my hypothesis. The same model with the CPD or the mtDNA as independent variables was used to test the effect of the treatments on the growth rate (i.e. the CPD change over time) or the change of the mtDNA copy number over time, respectively. In order to examine the effect on telomere length or the mtDNA copy number of each treatment compared to the control adjusting for the CPD, I used the respective linear regression models as described above, by replacing the days of treatment with the CPD in the list of independent variables. The p values from the comparison of each treatment with the control were obtained from the multivariable regression models described above. The percentages of change in telomere length and mtDNA per day or PD, as well as the PD per day presented, were obtained from separate analysis for each treatment regression model adjusted for donor. Statistical significance was taken as $p < 0.05$. Regarding the comparisons between the percentages of apoptotic and necrotic cells, as well as the intracellular ROS content of each treatment with the control, non parametric tests were used due to the small number of measurements. The Kruskal-Wallis test was used for comparisons among all treatments and the Mann-Whitney test for the comparison of each treatment with the control. The relevant data are presented as median with inter-quartile range (IQR) of the measurements from different donors in each of the two independent experiments performed.

1.3 RESULTS

1.3.1 General characteristics of cultures

Fibroblasts were serially passaged for approximately 90 days. The general morphology of fibroblasts in cultures was that of elongated spindle-shaped cells having a branched cytoplasm, which is a normal morphology for skin fibroblasts. This normal morphology was retained in all cultures for the time course of 90 days. Also, no osmotic effect was observed in cultures treated with L-glucose compared to the control cultures. Figure 3 shows pictures of the fibroblast cultures, after 62 days of treatment in each of the experimental conditions, taken with a “Zeiss Axioshop 2” microscope. One of the cultures generated from donor 4, which was treated with the combination of high glucose and IL1B, was contaminated at day 25 of the culture period, thus the measurements from this culture were discarded from all analyses.

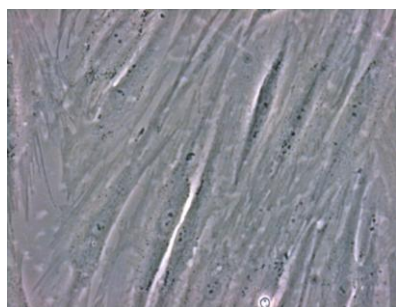
Figure VI-3. Microscope pictures of cultures, after 62 days of treatment in each of the experimental conditions.



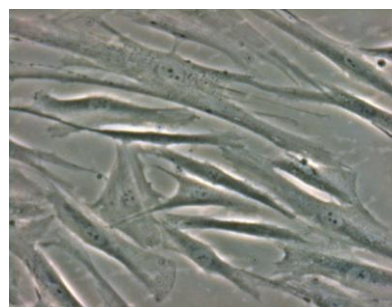
control



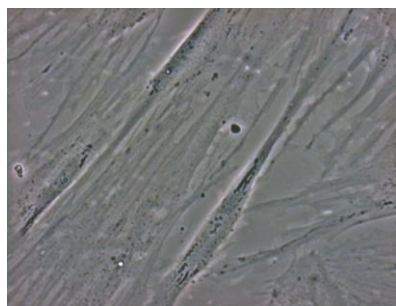
L-glucose



BSO



IL1B+ D-glucose



D-glucose



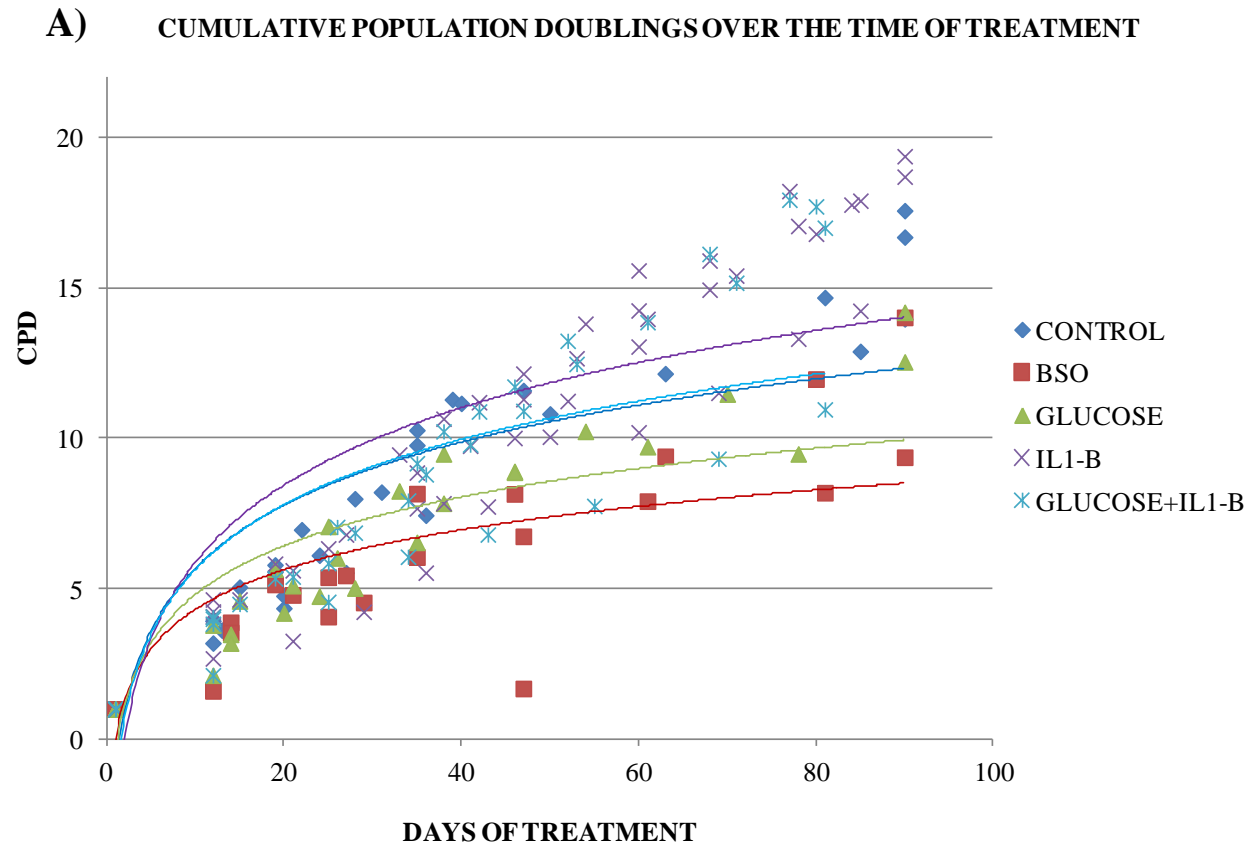
IL1B

1.3.2 Growth rate

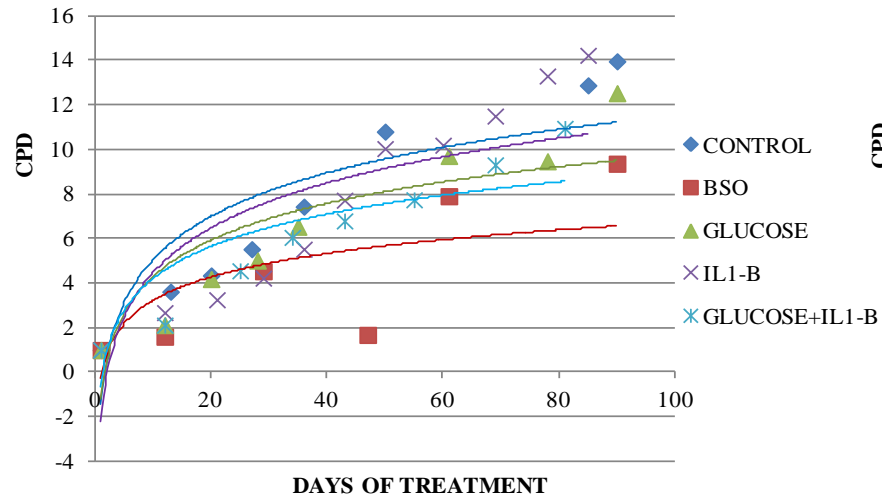
The cultures from the four different donors displayed significantly different growth rate, as reflected by the number of cumulative population doublings (CPD) ($p=0.04$) occurring during the course of the experiment. The rate of growth was also significantly different among cultures with different treatments ($p=0.001$), after adjusting for donor. A lower growth rate was observed in cultures treated with high glucose and BSO compared to the control [Glucose: 0.14 PD/day, $p<0.001$ and BSO: 0.11 PD/day, $p=0.006$ vs. Control: 0.16 PD/day], whereas, cultures treated with IL1B displayed a marginally higher cell turnover compared to the control [IL1B: 0.19 PD/day, $p=0.093$ vs. Control: 0.16 PD/day] (Figure 4A and Table 1).

Similar results were observed when growth curves were plotted separately and the effect of the treatments was compared on a donor per donor basis, as shown in Figure 4B. More specifically, the growth rate under IL1B treatment was significantly higher compared to control in two out of four donors (donor 1: $p=0.03$ and donor 4: $p=0.09$). BSO treatment caused a significantly lower growth rate compared to the control in three out of four donors (donor 1: $p<0.001$, donor 2: $p<0.001$ and donor 3 $p=0.03$) and high glucose in one out of four donors (donor 1: $p=0.05$). The relatively low rates of growth measured (5 to 10 days were needed for a whole PD to occur) is probably due to the fact that the flasks used for the cultures had a very large surface and thus longer time was needed for them to become confluent. Whereas, typically, cultures are grown in 75 cm² or 150 cm² flasks, the largest commercially available flasks of 225 cm² were used in this experiment due to the need to harvest a large number of cells in each passage for the various measurements carried out.

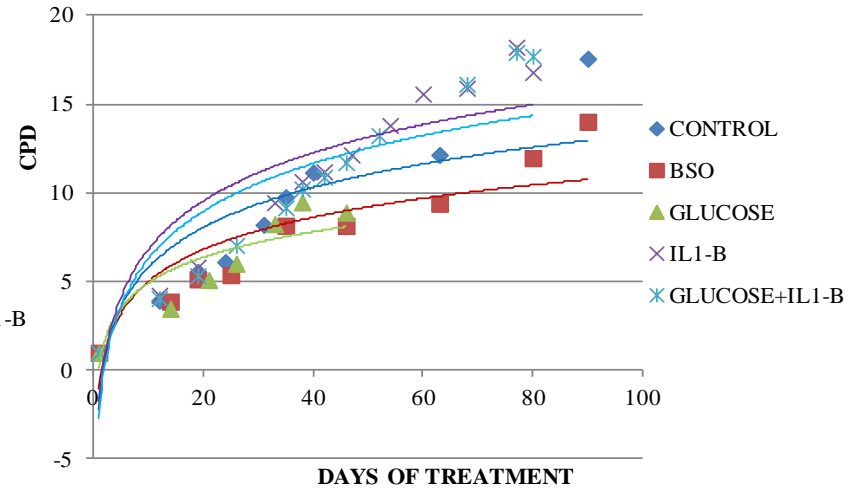
Figure VI-4. The cumulative population doublings (CPD) over the time of culture in each treatment (growth rate). A) In pooled data from all four donors, B) In each of the four donors separately.



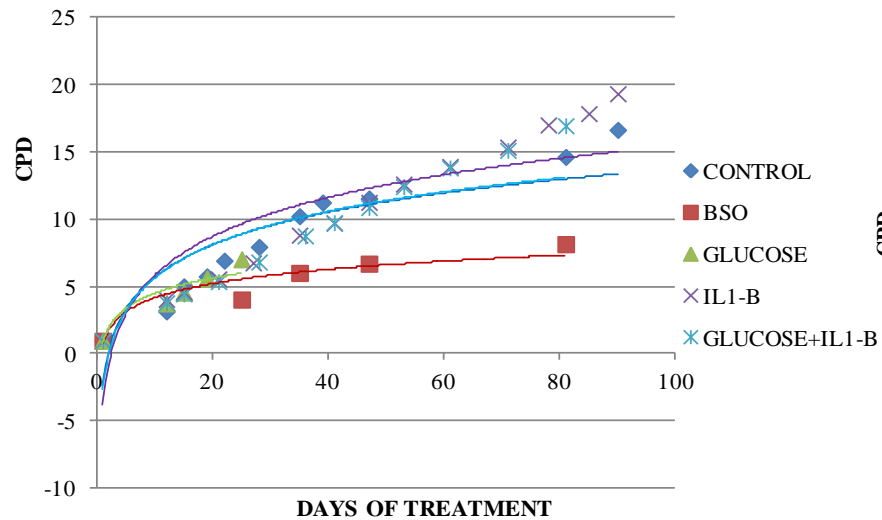
B) CUMULATIVE POPULATION DOUBLINGS OVER THE TIME OF TREATMENT IN DONOR 1



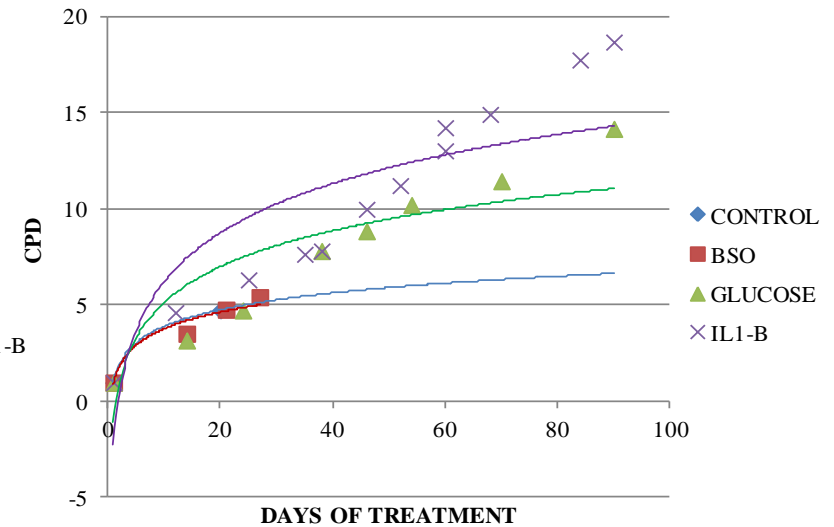
CUMULATIVE POPULATION DOUBLINGS OVER THE TIME OF TREATMENT IN DONOR 3



CUMULATIVE POPULATION DOUBLINGS OVER THE TIME OF TREATMENT IN DONOR 2



CUMULATIVE POPULATION DOUBLINGS OVER THE TIME OF TREATMENT IN DONOR 4



1.3.3 Telomere length

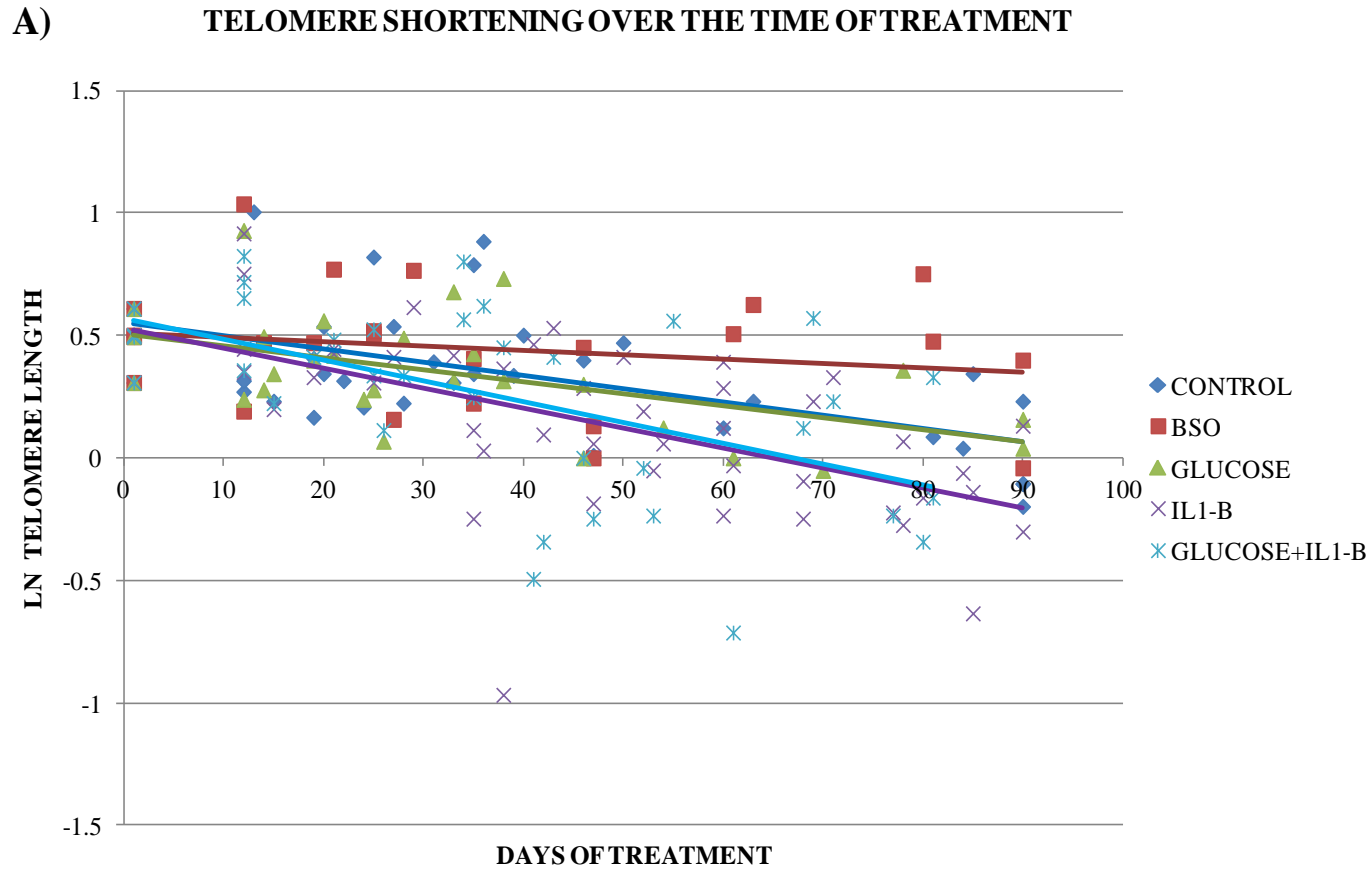
As expected, mean telomere length displayed a strong negative correlation with the number of days of culture ($r = -0.65$, $p < 0.001$) and the CPD ($r = -0.59$, $p < 0.001$) when the data from all treatments were pooled. Mean telomere length differed significantly between the cell cultures from the four different donors ($p = 0.008$). After adjusting for donor, the rate of telomere shortening over the time of treatment was significantly higher in cells treated with IL1B compared to the control [IL1B: $-0.8\%/day$ (95%CI: $-1.1, -0.5$) vs. Control: $-0.6\%/day$ (95%CI: $-0.8, -0.3$), $p = 0.012$] (Figure 5 and Table 1). No significant differences were found with the other treatments compared to control.

The effect of the treatments on telomere length was also compared on a donor per donor basis, and the observed results were similar to the pooled data analysis. A significantly higher rate of telomere shortening was observed in cultures treated with IL1B in two out of the four donors (donor 1: $p = 0.05$, donor 3: $p = 0.01$). Nevertheless, as shown in Figure 5B where the curves of telomere shortening are plotted separately for each donor, the cultures treated with IL1B displayed an accelerated telomere shortening in all donors. Also the combination of treatment with high glucose and IL1B caused a higher rate of telomere shortening compared to the control in donors 1, 3 and 4, which reached the level of significance only in donor 1 ($p = 0.06$).

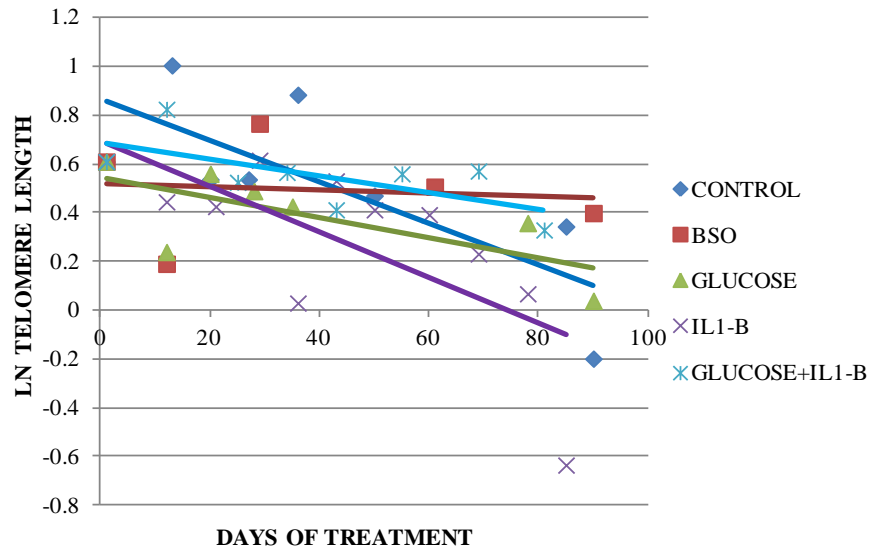
In order to examine whether the effect of each treatment on telomere shortening was caused by their effect on cell turnover, I tested the differences in the decline of telomere length with each treatment, adjusting for CPD. The effect of IL1B on telomere shortening was attenuated only to some extent and retained borderline significance [IL1B: $-4.1\%/PD$ (95%CI: $-5.7, -2.4$) vs. Control: $-2.5\%/PD$ (95%CI: $-4.4, -0.7$), $p = 0.067$] (Figure 6 and Table 1). The respective regression models in each donor

separately also showed that the adjustment for CPD did not change the effect of IL1B on telomere shortening. This effect of IL1B compared to the control remained significant in donors 1 and 3 ($p=0.03$ and $p=0.05$, respectively) as before the adjustment. In addition, the effect of the combination of high glucose and IL1B on telomere shortening remained borderline significant in donor 3 after the adjustment for CPD ($p=0.06$).

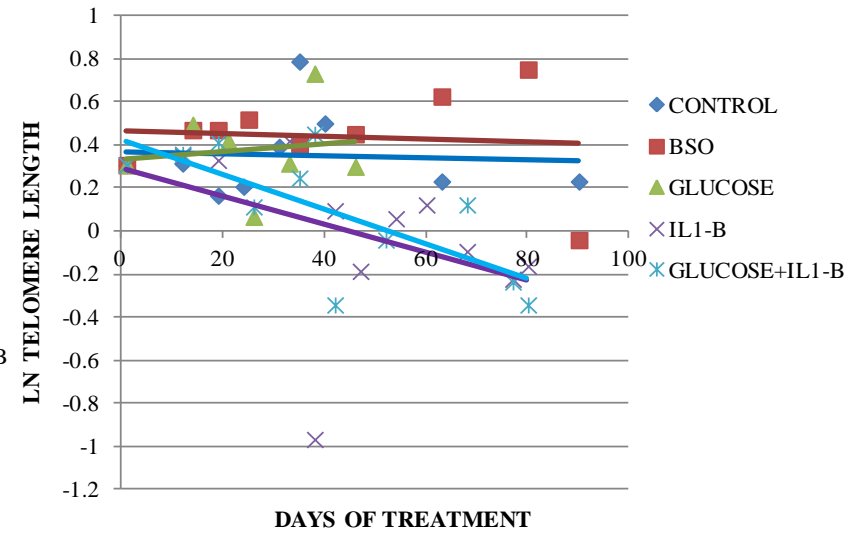
Figure VI-5. The shortening of mean telomere length over time of culture in each treatment. A) In pooled data from all four donors, B) In each of the four donors separately.



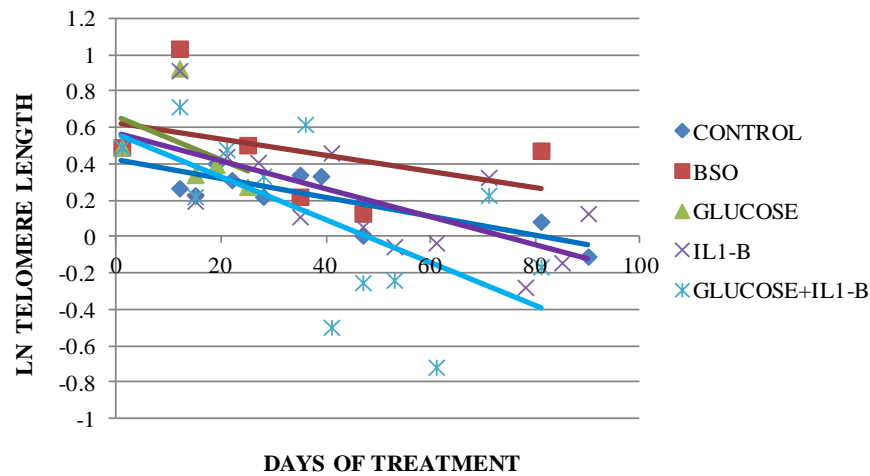
B) TELOMERE SHORTENING OVER THE TIME OF TREATMENT IN DONOR 1



TELOMERE SHORTENING OVER THE TIME OF TREATMENT IN DONOR 3



TELOMERE SHORTENING OVER THE TIME OF TREATMENT IN DONOR 2



TELOMERE SHORTENING OVER THE TIME OF TREATMENT IN DONOR 4

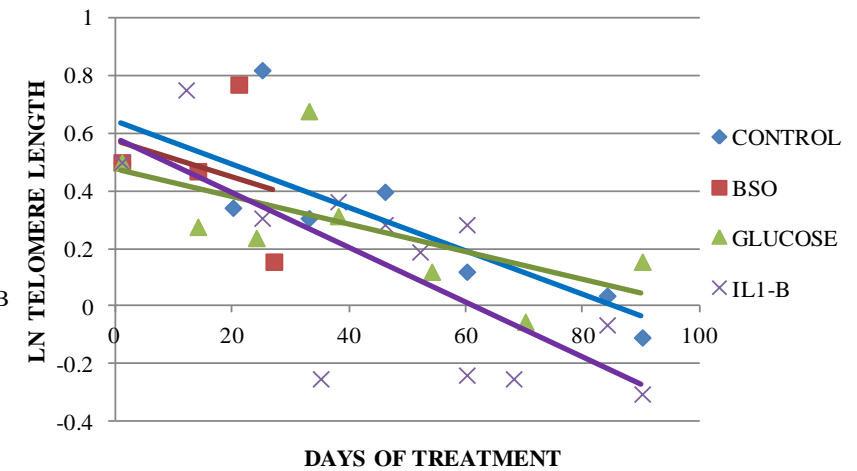
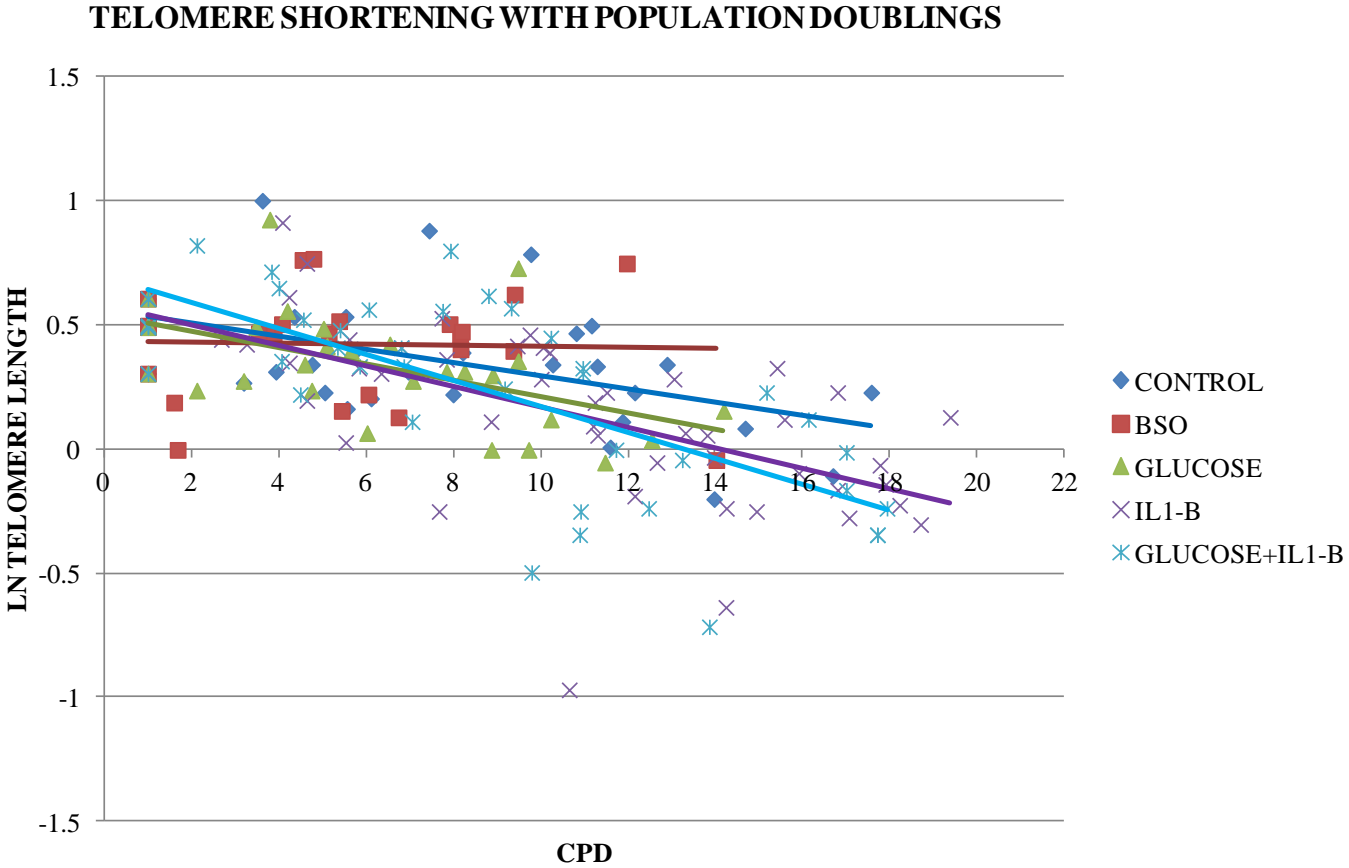


Figure VI-6. The shortening of mean telomere length over the number of cell divisions occurring during the experiment, as reflected by the cumulative population doublings (CPD), in each treatment.

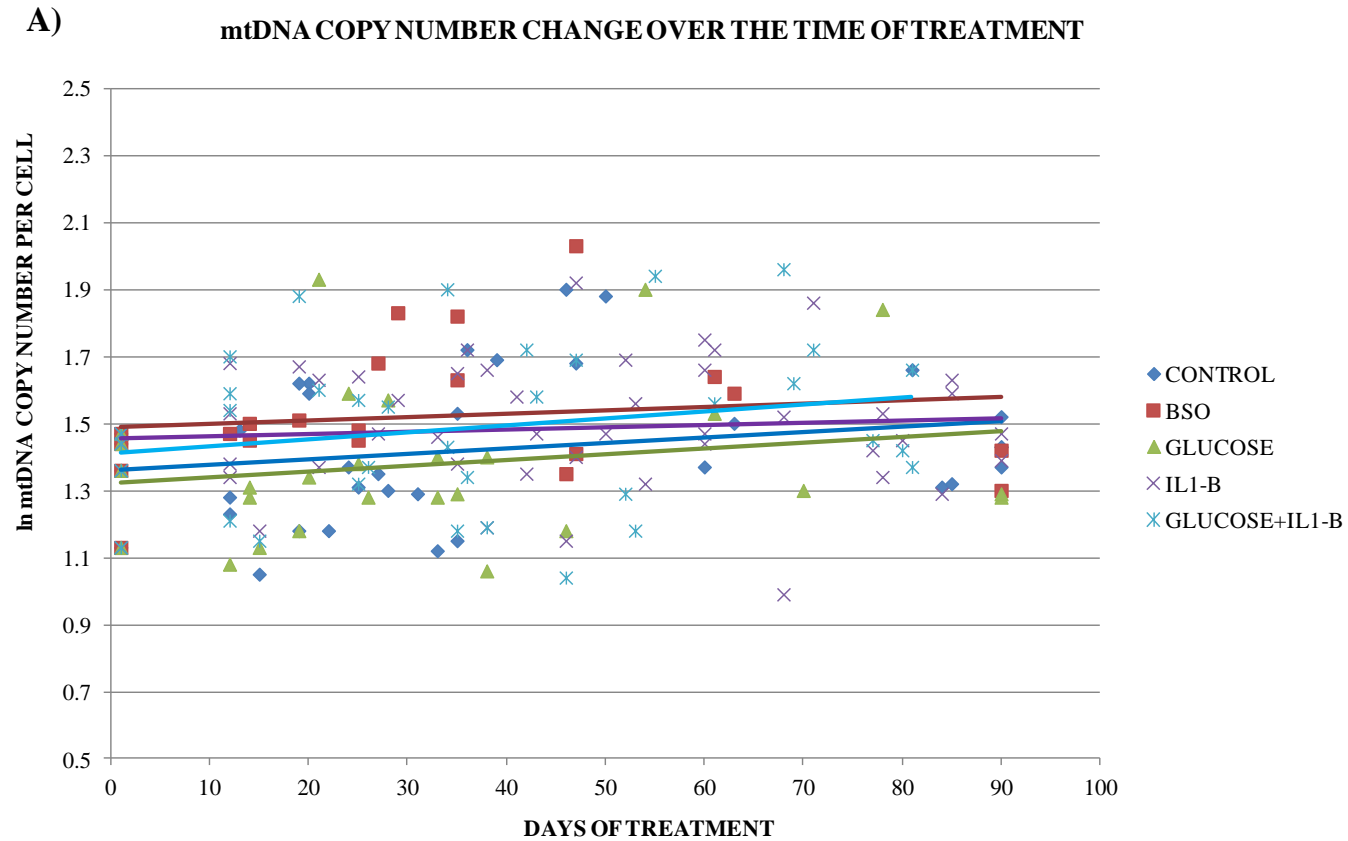


1.3.4 MtDNA copy number per nucleus

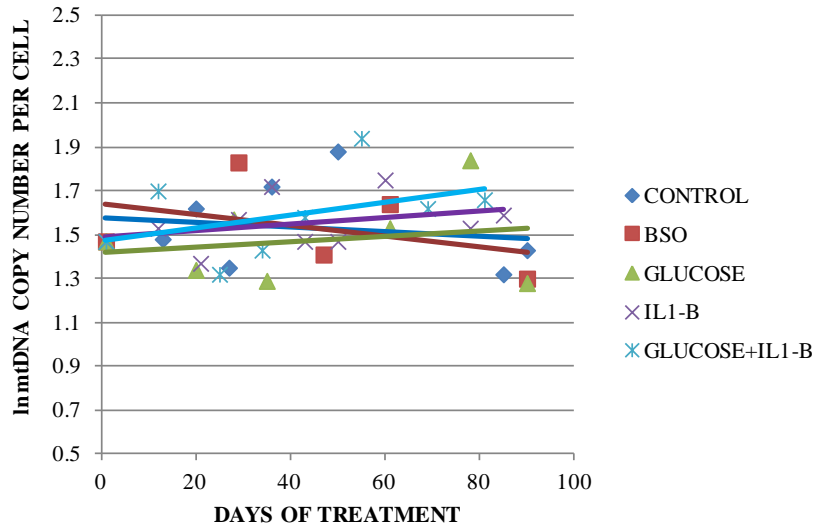
In all treatments, a statistically significant increase in the number of mtDNA copies per nucleus over time was observed ($r= 0.19$, $p= 0.019$). A modest increase in the number of mtDNA copies per nucleus was also observed with the number of cell divisions ($r= 0.16$, $p= 0.056$). The cultures from the four donors displayed significant differences in the number of mtDNA copies per nucleus ($p= 0.041$). After adjusting for donor, treatment with BSO resulted in a greater increase in the number of mtDNA copies per nucleus over the time of culture compared to the control [BSO: 0.2%/day (95%CI:-0.2, 0.6) vs. Control: 0.1%/day (95%CI:-0.1, 0.4), $p=0.047$] (Figure 7 and Table 1). The effect of the treatments on telomere length was also compared on a donor per donor basis. Treatment with BSO resulted in a significantly higher increase in the number of mtDNA copies per nucleus over the time of culture compared to the control in donor 2 ($p=0.02$). This effect was only observed in cultures generated from donor 2, whereas the regression models testing the change in mtDNA copies over the time of culture in the three other donors were not significant. As shown in Figure 7B, where the curves of mtDNA copies change over time are plotted separately for each donor, there is no specific pattern of the treatments effect in all four donors.

The effect of BSO was not altered when adjusting for CPD in both the pooled data analysis [BSO: 2.3%/PD (95%CI:-0.8, 5.6) vs. Control: 1.5%/PD (95%CI:0.0, 3.1), $p=0.042$] (Figure 8 and Table 1) and the the donor per donor analysis (Donor 2: BSO vs control, $p= 0.01$). No other treatment had a statistically significant effect on the number of mtDNA copies per nucleus compared to the control.

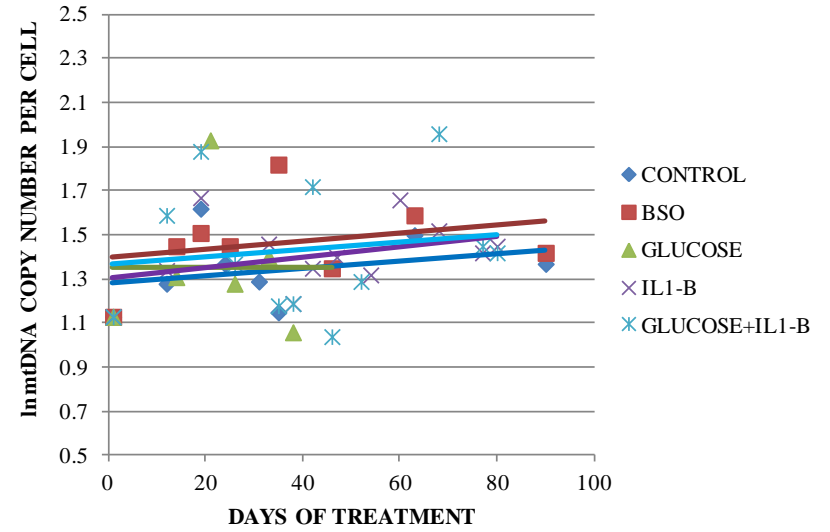
Figure VI-7. The change in the number of mitochondria per cell, as reflected by the copy number of mtDNA per nucleus, over time in each of the treatments. A) In pooled data from all four donors, B) In each of the four donors separately.



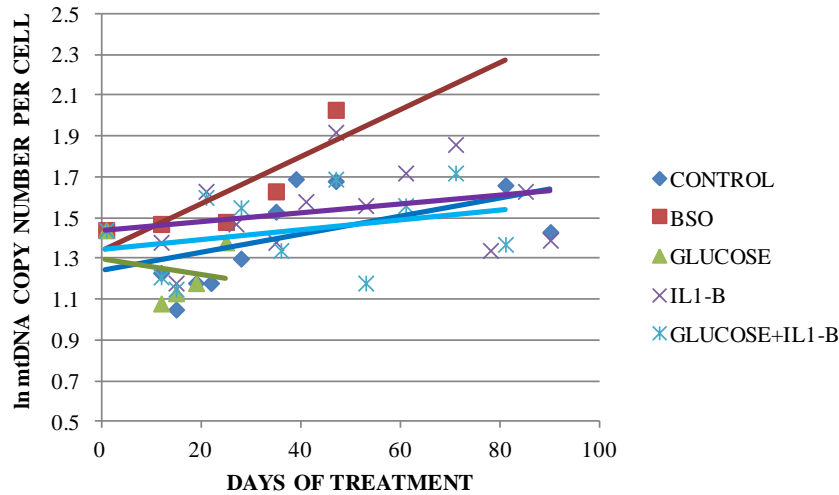
B) mtDNA COPY NUMBER CHANGE OVER THE TIME OF TREATMENT IN DONOR 1



mtDNA COPY NUMBER CHANGE OVER THE TIME OF TREATMENT IN DONOR 3



mtDNA COPY NUMBER CHANGE OVER THE TIME OF TREATMENT IN DONOR 2



mtDNA COPY NUMBER CHANGE OVER THE TIME OF TREATMENT IN DONOR 4

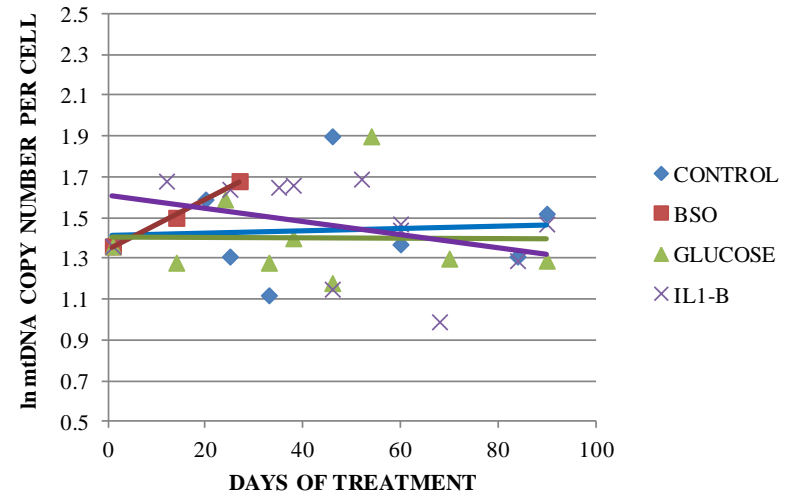


Figure VI-8. The change in the number of mitochondria per cell, as reflected by the copy number of mtDNA per nucleus, over the number of cell divisions occurred during the experiment [cumulative population doublings (CPD)] in each treatment.

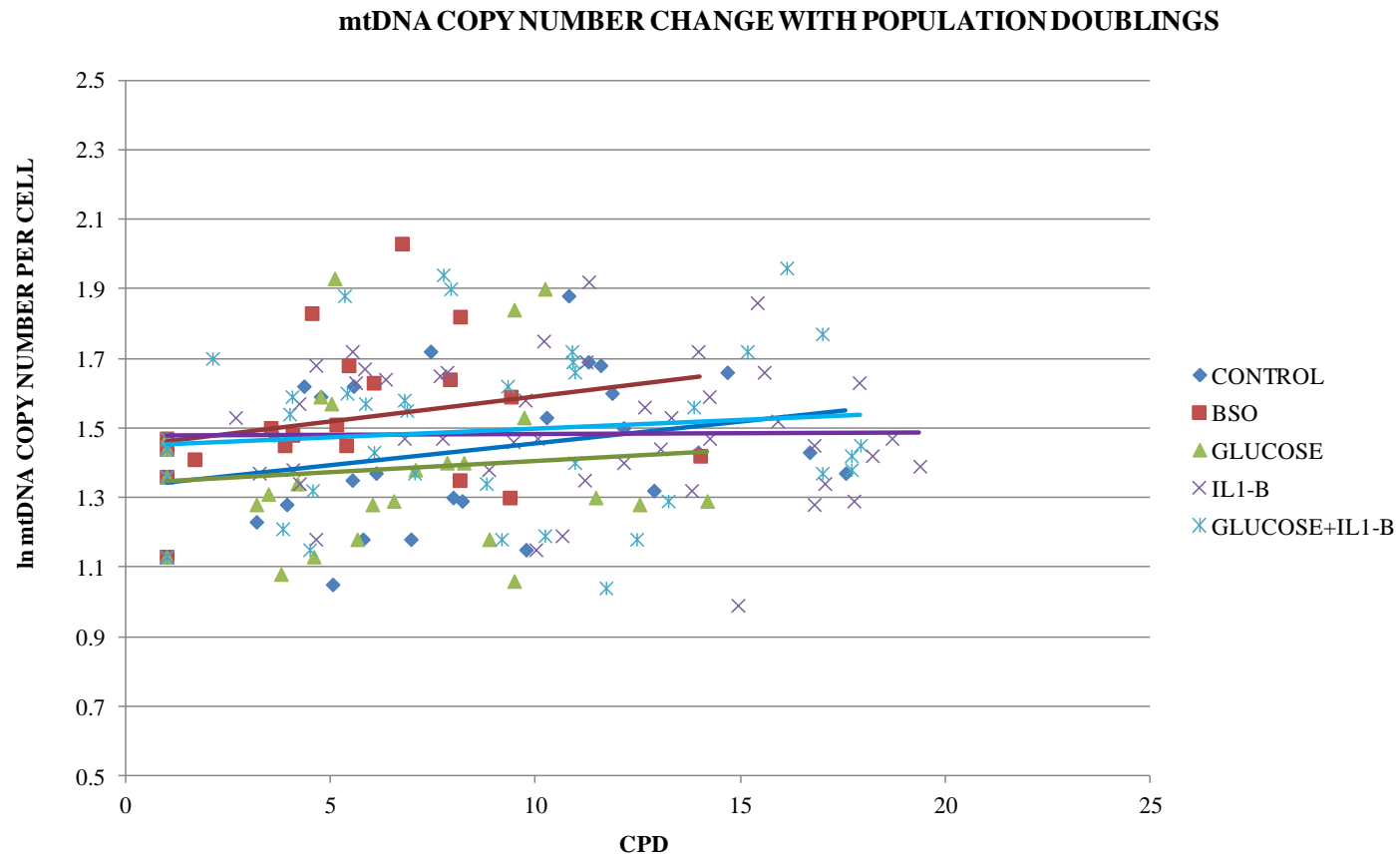


Table VI-1. Percentage changes in mean telomere length and mtDNA copies per nucleus over the time of culture (days) or cell divisions occurred during the experiment (CPD). The primary experimental data on these parameters are presented in Appendix II (page 370).

	Telomere Length				mtDNA				CPD	
	%/day (95%CI)	<i>P</i>	%/CPD (95%CI)	<i>P</i>	%/day (95%CI)	<i>P</i>	%/CPD (95%CI)	<i>P</i>	CPD/day (95%CI)	<i>P</i>
CONTROL	-0.6 (-0.8- -0.3)		-2.5 (-4.4- -0.7)		0.1 (-0.1- 0.4)		1.5 (0.0- 3.1)		0.16 (0.14- 0.18)	
BSO	-0.2 (-0.6- 0.2)	0.112	-0.9 (-4- 2.2)	0.843	0.2 (-0.2- 0.6)	0.047	2.3 (-0.8- 5.6)	0.042	0.11 (0.09- 0.13)	0.006
GLUCOSE	-0.4 (-0.7- 0.0)	0.685	-2.3 (-4.7- 0.0)	0.341	0.1 (-0.4- 0.5)	0.436	0.1 (-2.9- 2.8)	0.442	0.14 (0.13- 0.16)	<0.001
IL1B	-0.8 (-1.1- -0.5)	0.012	-4.1 (-5.7- -2.4)	0.067	0.1 (-0.1- 0.3)	0.210	0.3 (-0.7- 1.4)	0.461	0.19 (0.18- 0.2)	0.093
GLUCOSE+ IL1B	-0.8 (-1.2- -0.4)	0.156	-4.3 (-6.3- -2.4)	0.169	0.3 (0.0- 0.6)	0.136	1.2 (-0.4- 2.9)	0.230	0.18 (0.17- 2.0)	0.926

Percentage changes (%) in telomere length or mtDNA with days or CPD were obtained from separate regression models for each treatment adjusted for donor and are presented with 95% confidence intervals (CI). CPD per days were also obtained from separate regression models for each treatment adjusted for donor and are presented with 95% confidence intervals (CI). P values for the percentage changes (%) over days or CPD were obtained from regression models including all treatments as dummy variables compared to the control, adjusting for donor.

#: percentage change, CPD: cumulative population doublings, mtDNA: mitochondrial DNA, IL1B: interleukin 1B, BSO: buthionine sulphoximine.

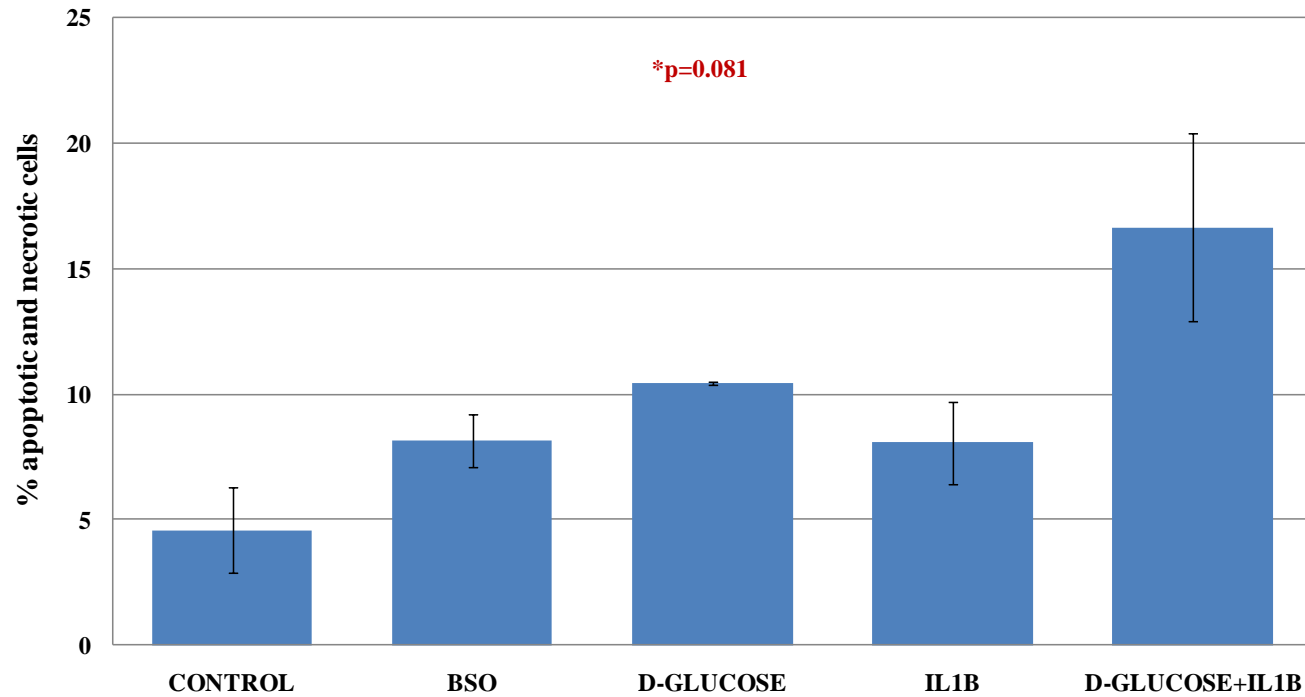
1.3.5 Apoptosis and necrosis

The percentage of apoptotic and necrotic cells was evaluated in duplicate, in cultures of each of the five treatments generated from two of the donors, after a period of seven days. Measurements were obtained from two independent experiments. In both experiments, all treatments displayed higher percentages of apoptotic and necrotic cells compared to the control. The results from one of the independent experiments are presented in figure 9. The difference between the control and each treatment was not statistically significant ($p=0.121$). However, overall there was a borderline significant difference in the percentages of apoptosis and necrosis ($p=0.081$), which appeared to be driven by the effect of the combination of high glucose and IL1B. The pattern was similar in the other independent experiment.

1.3.6 Intracellular ROS production

The intracellular ROS was evaluated in duplicate, in cultures of each of the five treatments generated from two of the donors, after a period of seven days. Measurements were obtained from two independent experiments. Figure 10 shows the results from one of these two independent experiments. BSO induced in fibroblasts a significantly higher production of ROS compared to the control ($p=0.033$). The intracellular ROS content was similar in cells treated with all the other treatments and the control ($p>0.2$). The results of the second independent experiment displayed the same pattern.

Figure VI-9. The percentage of cells at any stage of apoptosis or necrosis in each treatment after 7 days of treatment.

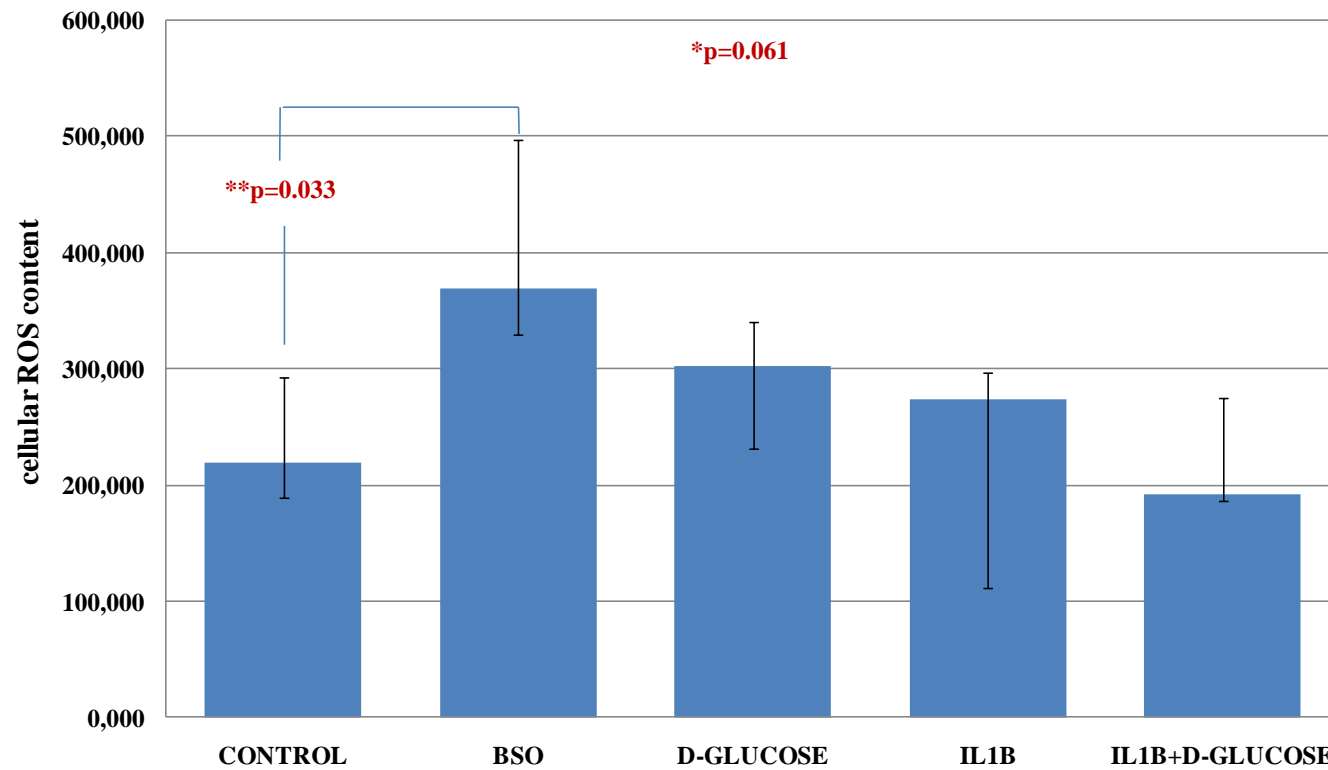


Due to the small number of measurements, normal distribution cannot be inferred. Thus, the graph represents median values, with inter-quartile range as error bars.

*P value obtained from Kruskal-Wallis test.

**Mann-Whitney tests between the percentages of apoptosis and necrosis in each of the treatments compared with the control were non-significant (p=0.121).

Figure VI-10. The intracellular ROS content of viable cells in each treatment after 7 days of treatment.



Due to the small number of measurements, normal distribution cannot be inferred. Thus, the graph represents median values, with inter-quartile range as error bars.

*P value obtained from Kruskal-Wallis test.

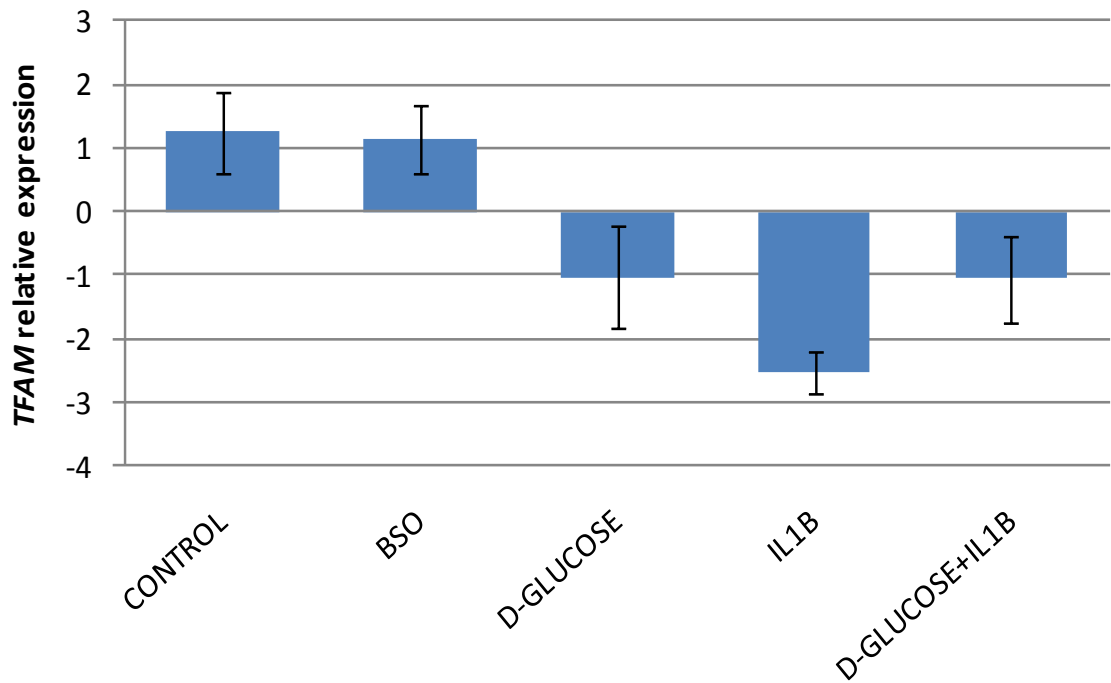
**P value obtained from Mann-Whitney test.

1.3.7 Gene expression

TERT: Human skin fibroblasts do not normally express telomerase (Goldstein 1990). In order, to examine whether telomerase expression was induced by the different treatments, expression levels of *TERT*, the gene encoding the catalytic part of telomerase, were measured in each culture by RT-PCR. No quantifiable expression of *TERT* was detected before applying any treatment, nor at the first days of treatment (six days of treatment), or towards the end of the experiment (45 days of treatment), in any of the five treatments.

TFAM: In order to examine whether the increase in the mtDNA copies in the cells treated with BSO reflected an enhancement of mitochondria proliferation, I examined the expression of *TFAM*, the gene encoding the transcription factor responsible for mitochondria proliferation. *TFAM* mRNA levels from cells before any treatment were used as control, in order to calculate the relative change in expression of *TFAM* after six and 45 days of treatment. The relative expression ratio of *TFAM* fell in the high glucose and IL1B treatments alone and in combination, but overall these differences were not statistically significant (Figure 11).

Figure VI-11. The change in *TFAM* expression levels after 45 days of treatment in each of the five conditions.



Expression ratio was calculated using the REST software.

The change in *TFAM* expression with each of the five treatments was calculated relatively to the levels of *TFAM* expression in each donor before the beginning of treatment.

There were no significant differences in the changes in *TFAM* expression with each of the five treatments.

1.4 DISCUSSION

1.4.1 Discussion of *in vitro* findings

The results of the present experiment suggest that pro-inflammatory conditioning with IL1B, which is implicated in the pathogenesis of both CVD (Galea *et al.* 1996) and T2D (Maedler *et al.* 2009), exacerbates the shortening of telomeres in an *in vitro* model of human cellular aging. This effect of IL1B on telomeres was only in part driven by higher cell turnover. In the present model, IL1B induced a moderate increase in cell turnover, and its effect on telomere shortening was only in part attenuated after adjustment for the number of cell divisions in the cultures. This is further supported by the fact that between the two donors' cultures, where the effect of IL1B on the cells' telomere shortening was more pronounced, only in one donor's cultures IL1B treatment led to an increased cell turnover. Thus, it can be speculated that pro-inflammatory conditioning with IL1B might exacerbate the shortening of telomeres through a still unknown pathway. The trigger of this proposed pathway may be a specific response to IL1B, or part of a general inflammatory response, such as is known to occur in early atherosclerosis and diabetes. Possibly IL1B deregulates the expression or the interplay of proteins essential for the protective structure of telomeres, the "shelterin" complex, such as TRF2 (De Boeck *et al.* 2009). Further experiments are needed to explore the mechanism by which pro-inflammatory conditioning exacerbates the shortening of telomeres employing different inflammatory factors, or testing the reversibility of this phenomenon using anti-inflammatory agents such as aspirin and statins.

The effect of pro-oxidant treatment with BSO was also examined in the present experiment. BSO inhibits glutathione synthesis, a process essential for the intracellular

detoxification of peroxides (Griffith & Meister 1979). As expected, the cultures of fibroblasts treated with BSO exhibited a higher intracellular ROS production compared to control cultures; however, the high ROS levels in these cultures did not result in greater telomere shortening. ROS are known to cause single DNA strand breaks in G-rich overhangs of telomeres, which are prone to oxidative damage and which are considered to lead to greater telomere shortening in each cell division (von Zglinicki 2000). Such telomeric loss does not seem to have occurred here. Instead, the ROS-induced DNA damage appear to have led to a stress-associated, but telomere length-independent, arrest of the cell cycle (Petersen *et al.* 1998). This phenomenon has been described as “stasis”, where the cells are arrested at G1 phase and do not display genomic instability or critically short telomeres (Garbe *et al.* 2009). The occurrence of the phenomenon of “stasis” is evident in the cultures generated from donor 2, where the increase in mtDNA copies was accompanied by a pronounced lowering of the growth rate in cultures treated with BSO compared to the control. In order to verify whether this increase was due to induced proliferation of the mitochondria, in an effort to compensate for the ROS increase (Ames *et al.* 1995), the expression of *TFAM* was examined. *TFAM* is the transcription factor regulating the mitochondria proliferation, and its expression was higher but not significantly so in BSO treated cultures compared to control cells. Thus, the observed increase in mtDNA content probably indicates an oxidative stress-induced cell cycle arrest at G1 phase rather than mitochondrial proliferation, as has been also described by Lee and colleagues (Lee *et al.* 2000). The present findings are also supported by the study of Ksiazek *et al.* (Ksiazek *et al.* 2008), which showed that high glucose-induced increase in ROS production was accompanied by double-stranded DNA breaks mainly localised to

non-telomeric regions of the genome. This provides a rationale for the lack of effect on telomere length and the cell cycle arrest in cultures treated with BSO, which could have been caused by double stranded DNA breaks in non-telomeric regions.

In the present experiment high glucose concentration, alone, did not result in faster telomere shortening. This was not surprising given that glucose did not seem to have a significant effect on ROS levels in the present experiment. My hypothesis was that high glucose, as a substrate for the mitochondrial oxidative phosphorylation, would hasten the input of reducing equivalents into the electron transport chain and would thus increase the ROS production; apparently this did not occur in the present experimental model. The current literature provides conflicting evidence regarding this hypothesis. There are studies showing that hyperglycaemia elicits an increase in intracellular ROS production which is a trigger for pathways responsible for hyperglycaemia-induced cell damage (Nishikawa *et al.* 2000; Piconi *et al.* 2006; Morgan *et al.* 2007). However, other studies have provided data arguing that high glucose induces an increase in ROS generation (Martens *et al.* 2005; Busik *et al.* 2008). The experiments of Busik *et al.* (Busik *et al.* 2008) demonstrated in endothelial cells that glucose consumption, and thus the generation of ROS, increases only when high glucose concentration is combined with pro-inflammatory conditioning with IL1B. However, in the present experiments with fibroblasts, the combination of high glucose and IL1B treatment did not result in higher intracellular ROS content. It is possible that the sensitivity to ROS generation, or the stimulus for higher consumption of nutrients, depends on the type of cell. In addition, although the main source of intracellular ROS in most cell types is the mitochondria (Lee *et al.* 2000), the actual substrate causing greater ROS generation during its catabolism in the mitochondria, might vary. For example, fatty

acids like palmitate have been shown to induce ROS generation in a variety of cells (Schonfeld 1990), thus experiments testing its effect on telomeres would be valuable. Besides the lack of effect on telomere length in high glucose concentration conditions has been observed previously by Ksiazek et al. (Ksiazek *et al.* 2008) where the vast majority of glucose-induced DNA damage was localised to non-telomeric regions of the genome.

The effect of the combination of high glucose and IL1B on telomere shortening was similar to the effect of IL1B treatment alone. High glucose did not result in higher ROS generation even in combination with IL1B, which could have had further aggravated telomere attrition. However, high glucose led to a lower cell turnover which might have caused a greater variation of telomere lengths in cultures treated with the combination. This variation is probably responsible for the decline in telomere length not being significantly different, when compared to the control. The lower growth rate observed in cultures treated with high glucose indicates that a telomere-independent cell cycle arrest must have occurred (Garbe *et al.* 2009).

Limitations of the present study need to be considered. The decline in mean telomere length of each culture was estimated here, but any elongation in specific chromosomes or in telomeres of subpopulations of cells would have diluted the observed effect on the rate of shortening. Human skin fibroblasts are considered a model of replicative senescence since they do not normally express telomerase (Goldstein 1990); thus the telomerase-mediated elongation of telomeres was not expected. In order to verify this in the present experiments, the expression of *TERT* was examined, and was undetectable both before and during the treatment in all cultures. Nonetheless, the possibility of alternative lengthening of telomeres by recombination (ALT), which was shown to occur in endothelial cells treated with BSO

in the study of Kruz et al. (Kurz *et al.* 2004), cannot be excluded. However, Kruz et al (Kurz *et al.* 2004) reported that ALT occurred only at late passages, after ~20 CPD, while in the present experiment the cultures treated with BSO were not grown beyond the 14 CPD, and in general, no cultures were kept beyond the 19 CPD. A possibility which cannot be excluded is that the high ROS levels induced by BSO might have caused single DNA strand breaks or critically short telomere length in a subpopulation of cells in the culture or in specific chromosome arms. In this case the mean length measured in the present study would have been misleading. Thus, there is a possibility that oxidative stress affects the length of single telomeres and in this way leads to early senescence. On the other hand the present measurements show at least, that the mean telomere length does not gradually shorten under high oxidative stress levels, in contrast to high inflammatory status.

In conclusion, the present experiment showed that chronic inflammation, which characterises cardiovascular disease and diabetes before and after their onset, may exacerbate the shortening of telomeres and thus, result in premature senescence contributing to the disease development and/or progression. This observation is of particular importance also in the context of other clinical conditions exhibiting a chronic pro-inflammatory state, such as autoimmune diseases. Worthy of remark is that short telomeres has been observed in patients with T1D (relevant data are presented in the “Second result chapter”, paragraph 3 (page 251) and in previous studies (Jeanclos *et al.* 1998; Uziel *et al.* 2007)), rheumatoid arthritis (Steer *et al.* 2007) and systemic lupus erythematosus (Wu *et al.* 2007).

1.4.2 *In vitro* vs. epidemiological findings

The *in vitro* data of this chapter are not in full agreement with the epidemiological data of the previous chapter. The effect of inflammation on telomere length was not observed in the cross-sectional studies of Result Chapter 2, although the follow up data implied a role of inflammation in telomere length regulation. On the other hand the observed effect of oxidative stress on telomere length of patients in Result Chapter 2 was not supported by the present *in vitro* data; although previous *in vitro* studies have provided convincing data (Petersen *et al.* 1998; Serra *et al.* 2000; von Zglinicki 2000). Finally, the hypothesised role of high glucose on telomere length can be disputed, since both the epidemiological and the *in vitro* data indicate the absence of a detrimental effect.

The discrepancies between the epidemiological and the *in vitro* data of the present thesis could either be attributed to the poor performance of the inflammatory markers used in the epidemiological studies or to the fact that fibroblasts are not, physiologically, the most suitable cell type to use. The leukocyte mean telomere length, measured in the epidemiological studies, may be mainly determined by the hematopoietic stem cells or the differentiated leukocytes' telomere length, thus *in vitro* studies with these types of cells would be valuable. Additionally, the study of stress *stimuli* on the telomere dynamics of vascular endothelial cells or pancreatic cells would be more relevant to CVD and T2D pathogenesis, and thus more enlightening. Last but not least to consider is the selection of the most suitable method for measuring telomere length during *in vitro* experiments. A method which would provide us with the ability to determine the gradual mean telomere length changes -like the qPCR used here- but also with the ability to detect single critically short telomeres would be a valuable tool in similar experiments.

VII. GENERAL DISCUSSION

Telomere length offers a novel insight into the basis of CVD and T2D predisposition, constituting a possibly inherited and early expressed risk factor. The work presented in this thesis explores the role of telomere length in relation to CVD, T2D and their common risk factors, as well as variation in relevant candidate genes. The majority of the work focused on factors associated with CVD and T2D development, such as oxidative stress and inflammation, and their role in determining the length of telomeres.

1. CONCLUSIONS

1.1 THE ROLE OF TELOMERE LENGTH IN CVD

First, the data presented in this thesis showed that short telomere length is a marker of both monogenic and polygenic CVD, along with its complications, such as MI. The association of telomere length with CVD is now strongly confirmed by a large number of studies (Samani *et al.* 2001; Minamino *et al.* 2002; Brouillette *et al.* 2003; Matthews *et al.* 2006; Brouillette *et al.* 2007; Fitzpatrick *et al.* 2007). The evidence so far suggests that in CVD, telomere length probably contributes as a primary abnormality. In support of this are data presented in this thesis showing that family history of CHD is in part inherited through short LTL (Brouillette *et al.* 2008; Salpea *et al.* 2008), most importantly, the prospective studies associating short baseline LTL with the risk to develop CVD (Brouillette *et al.* 2007; Fitzpatrick *et al.* 2007; Zee *et al.* 2009), and also the association of LTL with markers of

subclinical CVD, such as intima-media thickness (Adaikalakoteswari *et al.* 2007; Fitzpatrick *et al.* 2007). What remains to be determined is whether telomere length estimation is of clinical value; meaning whether it adds information for CVD risk estimation over and above the classical risk factors, currently used in risk algorithms. Also, information is needed on the race and ethnicity specific mean lengths and risk-effect size, as well as on the mean length of healthy individuals in various age groups.

1.2 THE ROLE OF TELOMERE LENGTH IN T2D

The data presented in this thesis on T2D, coupled with those from other smaller studies, show that T2D is also characterised by shorter telomeres (Sampson *et al.* 2006; Adaikalakoteswari *et al.* 2007; Olivieri *et al.* 2009; Salpea *et al.* 2009). It is not clear though, from the cross-sectional data available so far, whether the observed shorter telomeres in diabetes are a cause or consequence of the disease. Although the data are scarce, shorter telomeres have also been observed in type 1 diabetes patients here and elsewhere (Uziel *et al.* 2007). The aetiology of the disease in type 1 diabetes is in part different from that in type 2, although in both cases beta cell failure is the final event. Thus, one could speculate that critically short telomeres contribute to the onset of diabetes by eliciting senescent phenotypes in beta cells. However, in the case of type 1 diabetes again the data are cross-sectional, so the possibility that short telomeres are a result of the disease cannot be excluded.

The epidemiology of cross-sectional telomere length estimations is different from the epidemiology of longitudinal telomere dynamics. The cross-sectional coupled with the

follow up data presented in this thesis suggest a bidirectional regulation of telomere length, where the single time point measurements reflect the lifelong effect of environmental factors in combination with the genetic effect, while telomere length trajectory is mainly driven by a negative feedback mechanism for protection of very short telomeres (Farzaneh-Far *et al.* 2010).

Nevertheless, telomere length seems like a useful marker for T2D since it is associated with disease progression or improvement. In the study of Adaikalakoteswari *et al.* telomeres were shorter in patients with impaired glucose tolerance only, compared to controls, and even shorter in T2D patients (Adaikalakoteswari *et al.* 2007). In addition, telomere shortening has been linked to diabetes complications, such as diabetic nephropathy (Verzola *et al.* 2008), microalbuminuria (Tentolouris *et al.* 2007) and epithelial cancers (Sampson & Hughes 2006), while it seems to be attenuated in patients with well-controlled diabetes (Uziel *et al.* 2007). The present thesis' follow up data showed that low baseline levels of CRP and short initial telomere length predicted the increase in telomere length. Thus, telomere length might be of use as a marker of biological age, providing a valuable tool in the management of T2D.

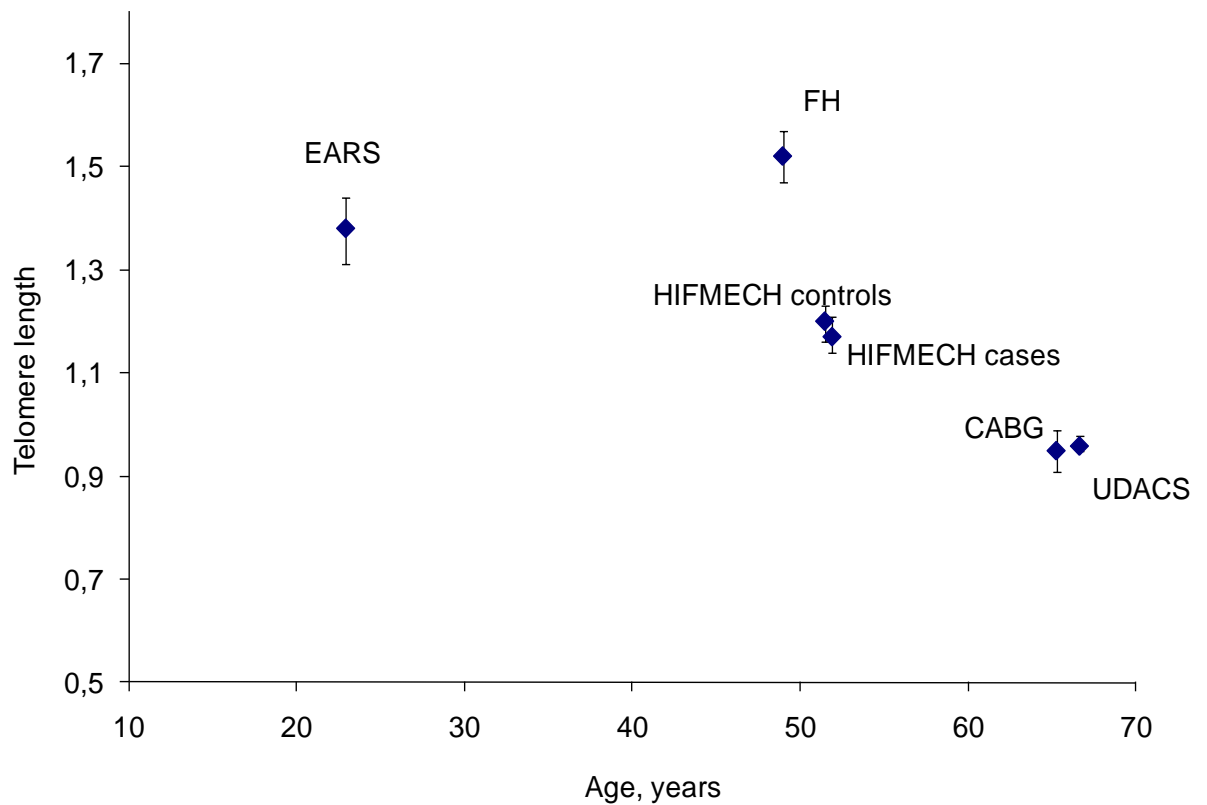
1.3 THE DETERMINANTS OF TELOMERE LENGTH

The inter-individual differences in telomere length are documented to have a strong hereditary component (Graakjaer *et al.* 2004; Andrew *et al.* 2006) and, interestingly, the present thesis showed that paternal history of premature CVD, a major CVD risk factor, is partly expressed through inherited short LTL (Salpea *et al.* 2008). Thus, inheritance must play a major role in determining the telomere length of the embryo. Thereafter, the rate of shortening during life is mainly determined by the environmental factors and gene-environment interactions (Huda *et al.* 2007). Even the *in utero* environment influences the embryo's telomere length (Davy *et al.* 2009; Tarry-Adkins *et al.* 2009; Barnes & Ozanne 2010). Recent population studies with follow up measurements of LTL, as well as the follow up data of the present thesis, suggest that baseline telomere length is associated with the rate of shortening (Chen *et al.* 2009; Nordfjall *et al.* 2009). More specifically, longer telomeres are inclined to faster shortening, whereas very short telomeres are preserved or even lengthened. The latter is possibly the result of stem/progenitor cells sensitization, or that of telomerase activation acting as a negative feedback mechanism for protection. These observations, though, are in contrast with the hypothesis that subjects predisposed to age-related diseases, such as CVD, are born with shorter telomeres (Brouillette *et al.* 2008; Salpea *et al.* 2008). Perhaps the familial predisposition to shorter telomeres is not due to shorter lengths at birth, but rather due to a genetic predisposition to faster shortening. Experiments of *in vitro* ageing are needed in order to investigate whether baseline longer telomeres shorten faster under the effect of stress factors.

Regarding the environmental factors determining telomere length during life, chronological age was shown to play a significant role, as expected. In most of the

individual studies employed in the present thesis, a negative correlation with age was observed. This is also evident in Figure 1, where the mean LTL is plotted against the mean age in each study sample.

Figure VII-1. Mean leukocyte telomere length plotted against mean age in each of the study samples employed in the present thesis.



More interestingly, the data so far suggest a contribution of oxidative stress. The present thesis showed a negative correlation with plasma oxidative stress and variation in

genes regulating reactive oxygen species levels (Salpea *et al.* 2009) and other studies have shown a negative correlation with a lipid peroxidation marker and oxidative DNA damage (Adaikalakoteswari *et al.* 2007; Satoh *et al.* 2008; Olivieri *et al.* 2009). What is not clear yet is which factors, and to what extent, contribute to the high levels of oxidative stress. The inverse correlation of LTL with variables reflecting the glycaemic state of patients in the study of Olivieri *et al.* (Olivieri *et al.* 2009) and the attenuation of telomere shortening in patients with good glycaemic control in the study by Uziel *et al.* (Uziel *et al.* 2007), suggest that hyperglycaemia might be driving the oxidative induced telomere loss in diabetes. However, the *in vitro* experiments and the epidemiological data of the present thesis, both cross-sectional and longitudinal, did not show any effect of high glucose on telomere length. Thus other risk factors, possibly linked to metabolic disorders, might be responsible for the oxidative induced telomere erosion.

To this end, the contribution of inflammation should be discussed. Few studies, including the cross-sectional studies of this thesis, have failed to detect an association with inflammatory markers (Olivieri *et al.* 2009; Salpea *et al.* 2009). Nonetheless, the present thesis' follow up data showed that low grade of inflammation is an independent predictor of telomere elongation and the *in vitro* data showed that pro-inflammatory conditioning aggravates telomere shortening. Thus inflammation seems to be involved in the regulation of telomere length which deserves further investigation. The rate of telomere erosion and consequent uncapping might be regulated by factors affecting the expression of proteins (such as TRF2) essential for the protective shelterin complex (capping), or by factors affecting the activity of the enzyme telomerase. Thus, it is possible that high cellular metabolic rate or high inflammatory response or both might be contributing to vascular or β

cell senescence and decreased proliferative capacity of progenitor cells, not through oxidative stress, but by causing telomere uncapping or deregulation of telomerase expression.

Ultimately, telomeres may offer the molecular mechanism linking the association of metabolic disorders and chronic inflammation with the development of premature ageing (De la Fuente & Miquel 2009) and age-related pathologies (Wilson *et al.* 2005), with telomere length registering the lifelong effect of environmental factors in combination with genetic factors.

2. THE COMMON SOIL HYPOTHESIS

The present thesis and several other studies (Adaikalakoteswari *et al.* 2007; Satoh *et al.* 2008; Olivieri *et al.* 2009) have provided data supporting the “common soil” hypothesis. The observation that patients with diabetes, who also develop atherosclerotic CVD, have the shortest telomeres, suggests that the telomere-represented tissue ageing might provide the molecular basis to the “common soil” hypothesis. In this case, the common factors giving rise to CVD and T2D also determine the shortening of telomeres and the subsequent tissue ageing underlying the pathogenesis of both diseases. Indeed, as the data of the present thesis’ and other studies’ suggest, genetic and environmental factors, common for T2D and CVD, play a role in determining the length of telomeres in patients. Such risk factors are oxidative stress, inflammation and functional SNPs in genes involved in ROS regulation. In order for this hypothesis, of telomere length contribution to the pathogenesis of CVD and T2D, to be confirmed it will require a prospective study design investigating the development of both diseases in the same study sample.

3. FUTURE WORK

Telomere length may prove to be very useful in the management and possibly the prediction of CVD and diabetes, representing the contribution of tissue ageing to their pathology. During the past few years, significant advances have been accomplished in the research field that explores the role of telomeres in CVD and T2D; yet, in my opinion, there are key research question to be answered. The main question is whether telomere length is causally involved in CVD or T2D development, but also whether it can serve as a useful marker for the risk prediction and disease management, representing the premature biological ageing.

Regarding this major research question there are convincing data for CVD but not for T2D. A prospective study where both the risk for CVD and T2D is examined would be the most useful tool for investigating the role of telomere length in risk prediction and the “common soil” hypothesis. Particularly enlightening would be studies with follow up measurements, since it has now become apparent that the trajectory of telomere length is different to its cross-sectional assessment. The few existing follow up studies have provided data suggesting that differentiated somatic cells are likely to have active or reactivated telomerase. In addition, it remains to be confirmed that LTL is a good surrogate measure of beta cells’ telomere length, as it has been shown for the vascular wall cells, before examining whether it is a useful marker for T2D.

To understand the connection of telomere biology with the pathogenesis of CVD and T2D, we need to shed light on how environmental and genetic factors predisposing to these diseases interact with telomere length. Epidemiological studies have shown an

association of CVD and T2D risk factors with LTL (Samani *et al.* 2001; Minamino *et al.* 2002; Brouillette *et al.* 2003; Matthews *et al.* 2006; Brouillette *et al.* 2007; Fitzpatrick *et al.* 2007; Wong *et al.* 2009). Although the role of oxidative stress had been shown in previous studies, the innovation of this thesis is the data provided supporting the role of chronic inflammation in the regulation of telomere length. It would be of great research interest to further investigate how chronic inflammation causes accelerated telomere shortening; whether it inhibits the protective mechanism of telomere elongation, what inflammatory molecules or pathways are involved and whether these interact with molecules of the shelterin complex, the telomerase or whether they exert their effect through an increase in ROS.

On the other hand, a plausible mechanism leading to accelerated telomere shortening is that metabolic disorders related to CVD and T2D, which result in high concentration of certain nutrients, cause the oxidative-induced telomere shortening. Here we studied the role of hyperglycaemia which provided controversial data. The follow up study showed no association of well-controlled hyperglycaemia with telomere elongation, while the cross-sectional studies showed weak positive correlations with LTL and the *in vitro* data argued that high glucose concentration has no effect on telomere shortening. The data in the literature regarding the effect of high glucose levels on ROS production are also controversial. Thus, with the role of glucose being questioned, other nutrients involved in CVD and T2D pathogenesis such as the saturated fatty acids are a plausible candidate for examining their effect on telomere shortening. The possibly detrimental effect of chronic exposure to saturated fatty acids on telomere length is suggested by a study reporting that

omega-3 fatty acids are beneficial for telomere length preservation (Farzaneh-Far *et al.* 2010)

Of particular significance is the role of genetics in determining telomere length and its contribution to premature onset of age-related diseases. In this thesis it was shown that family history of premature CVD is associated with shorter telomeres in the offspring. On the other hand the follow up data of the present thesis and those of other studies support a negative feedback mechanism where short telomeres are preserved or lengthened, and long telomeres are rigorously shortened. Thus the hypothesis that those predisposed to an age-related disease such as CVD are born with shorter telomeres is questioned. In my opinion, it is more likely that some individuals are genetically predisposed to develop conditions which lead to faster telomere shortening (e.g. high levels of oxidative stress), or that they have a genetic defect in the telomere protection mechanism (e.g. lower telomerase activity). As a result of this their telomeres get shorter faster under the burden of adverse environmental effects giving rise to age-related pathologies. The present thesis revealed genes having an effect on the telomere length which are involved in oxidative stress regulation and not in the telomere mechanism. On the other hand, a recent GWA study by Samani *et al.* has shown that the telomerase gene has a significant impact on the determination of telomere length. Therefore, it would be very interesting to study variants in all these candidate genes for association with telomere length in a large prospective cohort, with regard to CVD and T2D risk, in order to assess the significance of their effect. Also, birth cohort studies can prove useful for investigating the association of family history of age-related diseases with telomere length at birth, when the environment has not

yet exerted its effect. The latter is especially interesting regarding the family history of T2D, since there is no previous study examining its association with telomere length.

Last but not least, there is a need to shed more light on the basic biological functions of telomeres, like the mechanism involved in the trigger of cell senescence by telomere length or structure, how this is regulated and the possible interactions of telomeres with other chromosome regions.

4. FUTURE PERSPECTIVES IN TELOMERE RESEARCH

An important aspect of telomere biology is the hypothesis that its role in ageing and age-related diseases onset lies with the exhaustion of stem and progenitor cells causing limited regenerative capacity (Sahin & Depinho 2010). Especially in the era of stem cell therapy, it is mandatory to understand the mechanisms governing telomere dynamics, their interaction with CVD and T2D risk factors and their role in the exhaustion of progenitor cells. What factors determine the progenitor cells' proliferative capacity is crucial for optimizing these new promising regenerative therapies.

Another interesting perspective of telomere research is to manage delay or prevent the telomere-dependent tissue senescence and exhaustion of progenitor cells with pharmacological agents. Telomere biology already offers therapeutic targets in the treatment of cancer, and it may also provide novel therapeutic targets for CVD and T2D. There is already evidence supporting the use of statins (Spyridopoulos *et al.* 2004; Mahmoudi *et al.* 2008; Satoh *et al.* 2009) for preventing telomere attrition, but other agents might be also worth testing, such as the antioxidant agent resveratrol (Li & Forstermann 2009) or the peroxynitrite scavenger ebselen (Brodsky *et al.* 2004). On the other hand, merely identifying modifiable risk factors, which influence the longitudinal change of telomere length, may help us delay tissue ageing and consequently the onset of age-related pathologies. Improving the therapeutic strategies for ageing-related pathologies is very useful for an ageing population, such as that of our contemporary society.

VIII. APPENDICES

APPENDIX I: THE EARSII GROUP

EARS II Project Leader: D. St. J. O'Reilly, UK.

EARS II Project Management Group: F. Cambien, France, G. De Backer, Belgium, D. St. J. O'Reilly, UK, M. Rosseneu, Belgium, J. Shepherd, UK, L. Tiret, France.

The EARS II Group Collaborating Centres and their Associated Investigators:

Austria: H. J. Menzel, Institute for Medical Biology and Genetics, University of Innsbruck, laboratory.

Belgium: G. De Backer, S. De Henauw, Department of Public Health, University of Ghent, recruitment centre.

Belgium: M. Rosseneu, Laboratorium voor Lipoproteïne Chemie/ Vakgroep Biochemie, University of Ghent, laboratory. Denmark: O. Faergeman, C. Gerdes, Medical Department I, Aarhus Amtssygehus, Aarhus, recruitment centre.

Estonia: M. Saava, K. Aasvee, Department of Nutrition and Metabolism, Estonian Institute of Cardiology, Tallinn, recruitment centre.

Finland: C. Ehnholm*, R. Elovainio**, J. Peräsalo, *National Public Health Institute, **The Finnish Student Health Service, Helsinki, recruitment centre.

Finland: Y.A. Kesäniemi*, M.J. Savolainen*, P. Palomaa**, *Department of Internal Medicine and Biocenter, Oulu, **The Finnish Student Health Service, University of Oulu, recruitment centre.

France: L. Tiret, V. Nicaud, O. Poirier, INSERM U525, Paris, EARS data centre, laboratory. France: S. Visvikis, Centre de Médecine Préventive, Nancy, laboratory.

France: J. C. Fruchart, J. Dallongeville, Service de Recherche sur les Lipoprotéines et l'Athérosclérose (SERLIA), INSERM U325, Institut Pasteur, Lille, laboratory.

Germany: U. Beisiegel, C. Dingler, Medizinische Klinik Universitäts-Krankenhaus Eppendorf, Hamburg, recruitment centre and laboratory.

Greece: G. Tsitouris, N. Papageorgakis, G. Kolovou, Department of Cardiology, Evangelismos Hospital, Athens, recruitment centre.

Italy: E. Farinaro, Dept. of Medical Preventive Sciences, University “Frederico II” of Naples, recruitment centre. The Netherlands: L. M. Havekes, IVVO-TNO Health Research, Gaubius Institute, Leiden, laboratory.

Portugal: M. J. Halpern, J. Canena, Instituto Superior de Ciencias da Saude, Lisbon, recruitment centre.

Spain: L. Masana, J. Ribalta, A. Jammoul, A. LaVille, Unitat Recerca Lipids, University Rovira i Virgili, Reus, recruitment centre and laboratory.

Switzerland: F. Gutzwiller, B. Martin, Institute of Social and Preventive Medicine, University of Zurich, recruitment centre and laboratory.

United Kingdom: D. St J. O'Reilly, M. Murphy, Institute of Biochemistry, Royal Infirmary, Glasgow, recruitment centre and laboratory. United Kingdom: S.E. Humphries, P.J. Talmud, V. Gudnason, R.M. Fisher, University College London School of Medicine, London, laboratory.

United Kingdom: D. Stansbie, A. P. Day, M. Edgar, Department of Chemical Pathology, Royal Infirmary, Bristol, recruitment centre and laboratory.

United Kingdom: F. Kee*, A. Evans**, *Northern Health and Social Services Board, **Department of Epidemiology and Public Health, the Queen's University of Belfast, Belfast, recruitment centre.

APPENDIX II: THE PRIMARY DATA PRODUCED BY THE *IN VITRO* EXPERIMENT PRESENTED IN THE FOURTH RESULT CHAPTER.

Treatment	Passage	Donor	Day of treatment	Telomere length-T/S ratio	mtDNA copy number/cell	Cumulative population doublings
CONTROL	4	3	1	1,36	3,1	1
CONTROL	4	2	1	1,64	4,23	1
CONTROL	4	4	1	1,65	3,89	1
CONTROL	4	1	1	1,84	4,35	1
BSO	4	3	1	1,36	3,1	1
BSO	4	2	1	1,64	4,23	1
BSO	4	4	1	1,65	3,89	1
BSO	4	1	1	1,84	4,35	1
D-GLUCOSE	4	3	1	1,36	3,1	1
D-GLUCOSE	4	2	1	1,64	4,23	1
D-GLUCOSE	4	4	1	1,65	3,89	1
D-GLUCOSE	4	1	1	1,84	4,35	1
IL1B	4	3	1	1,36	3,1	1
IL1B	4	2	1	1,64	4,23	1
IL1B	4	4	1	1,65	3,89	1
IL1B	4	1	1	1,84	4,35	1
IL1B+D-GLUCOSE	4	3	1	1,36	3,1	1
IL1B+D-GLUCOSE	4	2	1	1,64	4,23	1
IL1B+D-GLUCOSE	4	4	1	1,65	3,89	1
IL1B+D-GLUCOSE	4	1	1	1,84	4,35	1
CONTROL	6	2	12	1,31	3,43	3,19
CONTROL	6	3	12	1,37	3,59	3,93
BSO	6	2	12	2,82	4,34	
BSO	6	1	12	1,21		1,6
D-GLUCOSE	6	1	12	1,27		2,12
D-GLUCOSE	6	2	12	2,53	2,94	3,79
IL1B	6	1	12	1,56	4,61	2,68
IL1B	6	2	12	2,5	3,97	4,08
IL1B	6	3	12	1,42	3,81	4,24
IL1B	6	4	12	2,12	5,36	4,64
IL1B+D-	6	1	12	2,28	5,48	2,12

GLUCOSE						
IL1B+D-GLUCOSE	6	2	12	2,05	3,35	3,83
IL1B+D-GLUCOSE	6	4	12	1,92	4,65	4
IL1B+D-GLUCOSE	6	3	12	1,43	4,9	4,06
CONTROL	6	1	13	2,73	4,39	3,62
BSO	6	4	14	1,6	4,5	3,54
BSO	6	3	14	1,6	4,27	3,88
D-GLUCOSE	6	4	14	1,32	3,59	3,19
D-GLUCOSE	6	3	14	1,64	3,7	3,48
CONTROL	7	2	15	1,26	2,87	5,05
D-GLUCOSE	7	2	15	1,41	3,1	4,59
IL1B	7	2	15	1,22	3,24	4,64
IL1B+D-GLUCOSE	7	2	15	1,25	3,15	4,49
CONTROL	7	3	19	1,18	5,03	5,56
CONTROL	8	2	19	1,5	3,24	5,79
BSO	7	3	19	1,6	4,51	5,14
D-GLUCOSE	8	2	19	1,49	3,26	5,65
IL1B	7	3	19	1,39	5,33	5,83
IL1B+D-GLUCOSE	7	3	19	1,51	6,53	5,34
CONTROL	7	1	20	1,71	5,07	4,35
CONTROL	7	4	20	1,41	4,91	4,76
D-GLUCOSE	7	1	20	1,75	3,82	4,19
BSO	7	4	21	2,16		4,79
D-GLUCOSE	7	3	21	1,52	6,89	5,1
IL1B	7	1	21	1,53	3,95	3,26
IL1B	8	2	21	1,56	5,08	5,61
IL1B+D-GLUCOSE	8	2	21	1,62	4,95	5,4
CONTROL	9	2	22	1,37	3,27	6,96
CONTROL	8	3	24	1,23	3,92	6,11
D-GLUCOSE	7	4	24	1,27	4,9	4,75
CONTROL	8	4	25	2,27	3,7	
BSO	7	2	25	1,66	4,4	4,07
BSO	8	3	25	1,68	4,26	5,38
D-GLUCOSE	9	2	25	1,32	3,97	7,07
IL1B	7	4	25	1,36	5,17	6,34
IL1B+D-GLUCOSE	7	1	25	1,69	3,75	4,56
IL1B+D-GLUCOSE	7	4	25	1,4	4,79	5,85
D-GLUCOSE	8	3	26	1,07	3,61	6,02

IL1B+D-GLUCOSE	8	3	26	1,12	3,95	7,05
CONTROL	8	1	27	1,71	3,85	5,53
BSO	8	4	27	1,17	5,36	5,44
IL1B	9	2	27	1,51	4,33	6,8
CONTROL	10	2	28	1,25	3,67	7,99
D-GLUCOSE	8	1	28	1,63	4,83	5,02
IL1B+D-GLUCOSE	9	2	28	1,4	4,7	6,86
BSO	8	1	29	2,15	6,22	4,54
IL1B	8	1	29	1,85	4,82	4,23
CONTROL	9	3	31	1,48	3,65	8,21
CONTROL	9	4	33	1,36	3,08	
D-GLUCOSE	8	4	33	1,97	3,58	
D-GLUCOSE	9	3	33	1,37	4,07	8,25
IL1B	9	3	33	1,52	4,32	9,46
IL1B+D-GLUCOSE	8	1	34	1,76	4,19	6,06
IL1B+D-GLUCOSE	8	4	34	2,23	6,69	7,93
CONTROL	10	3	35	2,2	3,17	9,77
CONTROL	11	2	35	1,41	4,62	10,27
BSO	8	2	35	1,25	5,11	6,05
BSO	9	3	35	1,5	6,2	8,16
D-GLUCOSE	9	1	35	1,53	3,65	6,54
IL1B	8	4	35	0,78	5,22	7,67
IL1B	10	2	35	1,12	3,98	8,86
IL1B+D-GLUCOSE	9	3	35	1,28	3,26	9,17
CONTROL	9	1	36	2,42	5,56	7,44
IL1B	9	1	36	1,03	5,59	5,53
IL1B+D-GLUCOSE	10	2	36	1,86	3,8	8,8
D-GLUCOSE	9	4	38	1,37	4,07	7,84
D-GLUCOSE	10	3	38	2,08	2,88	9,48
IL1B	9	4	38	1,44	5,25	7,84
IL1B	10	3	38	0,38	3,29	10,65
IL1B+D-GLUCOSE	10	3	38	1,57	3,29	10,23
CONTROL	12	2	39	1,4	5,43	11,29
CONTROL	11	3	40	1,65		11,16
IL1B	11	2	41	1,59	4,87	9,75
IL1B+D-GLUCOSE	11	2	41	0,61		9,79
IL1B	11	3	42	1,1	3,87	11,2
IL1B+D-	11	3	42	0,71	5,59	10,89

GLUCOSE						
IL1B	10	1	43	1,7	4,33	7,73
IL1B+D- GLUCOSE	9	1	43	1,51	4,84	6,8
CONTROL	11	4	46	1,49	6,7	
BSO	10	3	46	1,57	3,87	8,15
D-GLUCOSE	10	4	46		3,24	8,87
D-GLUCOSE	11	3	46	1,35		8,9
IL1B	10	4	46	1,33	3,17	10,01
IL1B+D- GLUCOSE	12	3	46		2,82	11,72
CONTROL	13	2	47	1,01	5,37	11,59
BSO	9	1	47		4,1	1,68
BSO	9	2	47	1,14	7,6	6,74
IL1B	12	2	47	1,06	6,83	11,3
IL1B	12	3	47	0,83	4,07	12,15
IL1B+D- GLUCOSE	12	2	47	0,78	5,43	10,91
CONTROL	11	1	50	1,6	6,53	10,81
IL1B	11	1	50	1,51	4,34	10,05
IL1B	11	4	52	1,21	5,43	11,24
IL1B+D- GLUCOSE	13	3	52	0,96	3,62	13,24
IL1B	13	2	53	0,95	4,78	12,66
IL1B+D- GLUCOSE	13	2	53	0,79	3,26	12,47
D-GLUCOSE	11	4	54	1,13	6,69	10,23
IL1B	13	3	54	1,06	3,76	13,81
IL1B+D- GLUCOSE	10	1	55	1,75	6,98	7,75
CONTROL	12	4	60	1,13	3,92	
IL1B	12	1	60	1,48	5,75	10,2
IL1B	12	4	60	1,33	4,22	13,05
IL1B	13	4	60	0,79	4,37	14,25
IL1B	14	3	60	1,13	5,27	15,58
BSO	10	1	61	1,66	5,17	7,91
D-GLUCOSE	11	1	61		4,6	9,72
IL1B	14	2	61	0,97	5,6	13,97
IL1B+D- GLUCOSE	14	2	61	0,49	4,74	13,86
CONTROL	13	3	63	1,26	4,46	12,15
BSO	11	3	63	1,87	4,88	9,4
IL1B	14	4	68	0,78	2,69	14,94
IL1B	15	3	68	0,91	4,55	15,91
IL1B+D- GLUCOSE	15	3	68	1,13	7,08	16,13

IL1B	13	1	69	1,26		11,51
IL1B+D- GLUCOSE	11	1	69	1,77	5,04	9,32
D-GLUCOSE	12	4	70	0,95	3,67	11,47
IL1B	15	2	71	1,39	6,41	15,41
IL1B+D- GLUCOSE	15	2	71	1,26	5,58	15,17
IL1B	16	3	77	0,8	4,14	18,22
IL1B+D- GLUCOSE	16	3	77	0,79	4,26	17,93
D-GLUCOSE	12	1	78	1,43	6,31	9,48
IL1B	14	1	78	1,07	4,63	13,31
IL1B	16	2	78	0,76	3,8	17,06
BSO	12	3	80	2,12		11,97
IL1B	17	3	80	0,85	4,27	16,8
IL1B+D- GLUCOSE	17	3	80	0,71	4,15	17,71
CONTROL	15	2	81	1,09	5,25	14,68
BSO	11	2	81	1,61		8,19
IL1B+D- GLUCOSE	12	1	81	1,39	5,28	10,96
IL1B+D- GLUCOSE	16	2	81	0,85	3,93	17
CONTROL	14	4	84	1,04	3,69	
IL1B	15	4	84	0,94	3,62	17,77
CONTROL	13	1	85	1,41	3,73	12,89
IL1B	15	1	85	0,53	4,92	14,24
IL1B	17	2	85	0,87	5,1	17,9
CONTROL	15	4	90	0,9	4,56	
CONTROL	14	1	90	0,82	4,18	13,97
CONTROL	16	2	90	0,9	4,16	16,69
CONTROL	15	3	90	1,26	3,94	17,57
BSO	11	1	90	1,49	3,67	9,37
BSO	13	3	90	0,96	4,13	14,02
BSO	12	2	90	1,28	7,23	
D-GLUCOSE	13	1	90	1,04	3,61	12,54
D-GLUCOSE	13	4	90	1,17	3,64	14,19
IL1B	16	4	90	0,74	4,37	18,7
IL1B	18	2	90	1,14	4,03	19,38
IL1B	18	3	90	1,26	3,59	16,8
IL1B+D- GLUCOSE	13	1	90	1,36	4,04	10,96
IL1B+D- GLUCOSE	17	2	90	0,99	5,88	17
IL1B+D- GLUCOSE	18	3	90	0,71	3,98	17,71

IX. REFERENCES

- Adaikalakoteswari A, Balasubramanyam M , Mohan V (2005). Telomere shortening occurs in Asian Indian Type 2 diabetic patients. *Diabet Med.* **22**, 1151-1156.
- Adaikalakoteswari A, Balasubramanyam M, Ravikumar R, Deepa R , Mohan V (2007). Association of telomere shortening with impaired glucose tolerance and diabetic macroangiopathy. *Atherosclerosis.* **195**, 83-89.
- Agarwal DP (2002). Cardioprotective effects of light-moderate consumption of alcohol: a review of putative mechanisms. *Alcohol Alcohol.* **37**, 409-415.
- Alberti KG , Zimmet PZ (1998). Definition, diagnosis and classification of diabetes mellitus and its complications. Part 1: diagnosis and classification of diabetes mellitus provisional report of a WHO consultation. *Diabet Med.* **15**, 539-553.
- Alexander RW (1995). Theodore Cooper Memorial Lecture. Hypertension and the pathogenesis of atherosclerosis. Oxidative stress and the mediation of arterial inflammatory response: a new perspective. *Hypertension.* **25**, 155-161.
- Allsopp RC , Harley CB (1995). Evidence for a critical telomere length in senescent human fibroblasts. *Exp Cell Res.* **219**, 130-136.
- Allsopp RC, Vaziri H, Patterson C, Goldstein S, Younglai EV, Futcher AB, Greider CW , Harley CB (1992). Telomere length predicts replicative capacity of human fibroblasts. *Proc Natl Acad Sci U S A.* **89**, 10114-10118.
- Alper CA, Larsen CE, Dubey DP, Awdeh ZL, Fici DA , Yunis EJ (2006). The haplotype structure of the human major histocompatibility complex. *Hum Immunol.* **67**, 73-84.
- Ames BN, Shigenaga MK , Hagen TM (1995). Mitochondrial decay in aging. *Biochim Biophys Acta.* **1271**, 165-170.
- Andrew T, Aviv A, Falchi M, Surdulescu GL, Gardner JP, Lu X, Kimura M, Kato BS, Valdes AM , Spector TD (2006). Mapping genetic loci that determine leukocyte telomere length in a large sample of unselected female sibling pairs. *Am J Hum Genet.* **78**, 480-486.
- Angles-Cano E, de la Pena Diaz A , Loyau S (2001). Inhibition of fibrinolysis by lipoprotein(a). *Ann N Y Acad Sci.* **936**, 261-275.
- Aviv A (2002). Telomeres, sex, reactive oxygen species, and human cardiovascular aging. *J Mol Med.* **80**, 689-695.
- Aviv A (2008). The epidemiology of human telomeres: faults and promises. *J Gerontol A Biol Sci Med Sci.* **63**, 979-983.
- Aviv A, Chen W, Gardner JP, Kimura M, Brimacombe M, Cao X, Srinivasan SR , Berenson GS (2009). Leukocyte telomere dynamics: longitudinal findings among young adults in the Bogalusa Heart Study. *Am J Epidemiol.* **169**, 323-329.
- Aviv A, Valdes A, Gardner JP, Swaminathan R, Kimura M , Spector TD (2006). Menopause modifies the association of leukocyte telomere length with insulin resistance and inflammation. *J Clin Endocrinol Metab.* **91**, 635-640.
- Baird DM (2005). New developments in telomere length analysis. *Exp Gerontol.* **40**, 363-368.
- Barnes SK , Ozanne SE (2010). Pathways linking the early environment to long-term health and lifespan. *Prog Biophys Mol Biol.*
- Barrett-Connor E , Khaw K (1984). Family history of heart attack as an independent predictor of death due to cardiovascular disease. *Circulation.* **69**, 1065-1069.

- Barrett JC, Fry B, Maller J, Daly MJ (2005). Haploview: analysis and visualization of LD and haplotype maps. *Bioinformatics*. **21**, 263-265.
- Bastaki M, Huen K, Manzanillo P, Chande N, Chen C, Balmes JR, Tager IB, Holland N (2006). Genotype-activity relationship for Mn-superoxide dismutase, glutathione peroxidase 1 and catalase in humans. *Pharmacogenet Genomics*. **16**, 279-286.
- Baynes JW, Thorpe SR (1999). Role of oxidative stress in diabetic complications: a new perspective on an old paradigm. *Diabetes*. **48**, 1-9.
- Bedard K, Attar H, Bonnefont J, Jaquet V, Borel C, Plastre O, Stasia MJ, Antonarakis SE, Krause KH (2009). Three common polymorphisms in the CYBA gene form a haplotype associated with decreased ROS generation. *Hum Mutat*. **30**, 1123-1133.
- Bekaert S, De Meyer T, Rietzschel ER, De Buyzere ML, De Bacquer D, Langlois M, Segers P, Cooman L, Van Damme P, Cassiman P, Van Criekinge W, Verdonck P, De Backer GG, Gillebert TC, Van Oostveldt P (2007). Telomere length and cardiovascular risk factors in a middle-aged population free of overt cardiovascular disease. *Aging Cell*. **6**, 639-647.
- Benetos A, Okuda K, Lajemi M, Kimura M, Thomas F, Skurnick J, Labat C, Bean K, Aviv A (2001). Telomere length as an indicator of biological aging: The gender effect and relation with pulse pressure and pulse wave velocity. *Hypertension*. **37**, 381-385.
- Bennet A, Di Angelantonio E, Erqou S, Eiriksdottir G, Sigurdsson G, Woodward M, Rumley A, Lowe GD, Danesh J, Gudnason V (2008). Lipoprotein(a) levels and risk of future coronary heart disease: large-scale prospective data. *Arch Intern Med*. **168**, 598-608.
- Billings LK, Florez JC (2010). The genetics of type 2 diabetes: what have we learned from GWAS? *Ann N Y Acad Sci*. **1212**, 59-77.
- Bjorntorp P (1991). Metabolic implications of body fat distribution. *Diabetes Care*. **14**, 1132-1143.
- Blackburn EH (2001). Switching and signaling at the telomere. *Cell*. **106**, 661-673.
- Blackburn EH, Greider CW, Szostak JW (2006). Telomeres and telomerase: the path from maize, Tetrahymena and yeast to human cancer and aging. *Nat Med*. **12**, 1133-1138.
- Blanc J, Alves-Guerra MC, Esposito B, Rousset S, Gourdy P, Ricquier D, Tedgui A, Miroux B, Mallat Z (2003). Protective role of uncoupling protein 2 in atherosclerosis. *Circulation*. **107**, 388-390.
- Bloomgarden ZT (2006). Glycemic treatment in type 1 and type 2 diabetes. *Diabetes Care*. **29**, 2549-2555.
- Bolla MK, Haddad L, Humphries SE, Winder AF, Day IN (1995). High-throughput method for determination of apolipoprotein E genotypes with use of restriction digestion analysis by microplate array diagonal gel electrophoresis. *Clin Chem*. **41**, 1599-1604.
- Bonnefond A, Froguel P, Vaxillaire M (2010). The emerging genetics of type 2 diabetes. *Trends Mol Med*. **16**, 407-416.
- Brien TP, Kallakury BV, Lowry CV, Ambros RA, Muraca PJ, Malfetano JH, Ross JS (1997). Telomerase activity in benign endometrium and endometrial carcinoma. *Cancer Res*. **57**, 2760-2764.
- Brochier ML, Arwidson P (1998). Coronary heart disease risk factors in women. *Eur Heart J*. **19 Suppl A**, A45-52.

- Brodsky SV, Gealekman O, Chen J, Zhang F, Togashi N, Crabtree M, Gross SS, Nasjletti A , Goligorsky MS (2004). Prevention and reversal of premature endothelial cell senescence and vasculopathy in obesity-induced diabetes by ebselen. *Circ Res.* **94**, 377-384.
- Brouillette S, Singh RK, Thompson JR, Goodall AH , Samani NJ (2003). White cell telomere length and risk of premature myocardial infarction. *Arterioscler Thromb Vasc Biol.* **23**, 842-846.
- Brouillette SW, Moore JS, McMahon AD, Thompson JR, Ford I, Shepherd J, Packard CJ , Samani NJ (2007). Telomere length, risk of coronary heart disease, and statin treatment in the West of Scotland Primary Prevention Study: a nested case-control study. *Lancet.* **369**, 107-114.
- Brouillette SW, Whittaker A, Stevens SE, van der Harst P, Goodall AH , Samani NJ (2008). Telomere length is shorter in healthy offspring of subjects with coronary artery disease: support for the telomere hypothesis. *Heart.* **94**, 422-425.
- Brownlee M (2001). Biochemistry and molecular cell biology of diabetic complications. *Nature.* **414**, 813-820.
- Brull DJ, Montgomery HE, Sanders J, Dhamrait S, Luong L, Rumley A, Lowe GD , Humphries SE (2001). Interleukin-6 gene -174g>c and -572g>c promoter polymorphisms are strong predictors of plasma interleukin-6 levels after coronary artery bypass surgery. *Arterioscler Thromb Vasc Biol.* **21**, 1458-1463.
- Brull DJ, Serrano N, Zito F, Jones L, Montgomery HE, Rumley A, Sharma P, Lowe GD, World MJ, Humphries SE , Hingorani AD (2003). Human CRP gene polymorphism influences CRP levels: implications for the prediction and pathogenesis of coronary heart disease. *Arterioscler Thromb Vasc Biol.* **23**, 2063-2069.
- Bryant JE, Hutchings KG, Moyzis RK , Griffith JK (1997). Measurement of telomeric DNA content in human tissues. *Biotechniques.* **23**, 476-478, 480, 482, passim.
- Busik JV, Mohr S , Grant MB (2008). Hyperglycemia-induced reactive oxygen species toxicity to endothelial cells is dependent on paracrine mediators. *Diabetes.* **57**, 1952-1965.
- Cardon LR , Abecasis GR (2003). Using haplotype blocks to map human complex trait loci. *Trends Genet.* **19**, 135-140.
- Carrero JJ, Stenvinkel P, Fellstrom B, Qureshi AR, Lamb K, Heimbürger O, Barany P, Radhakrishnan K, Lindholm B, Soveri I, Nordfors L , Shiels PG (2008). Telomere attrition is associated with inflammation, low fetuin-A levels and high mortality in prevalent haemodialysis patients. *J Intern Med.* **263**, 302-312.
- Carulli L, Rondinella S, Lombardini S, Canedi I, Loria P , Carulli N (2005). Review article: diabetes, genetics and ethnicity. *Aliment Pharmacol Ther.* **22 Suppl 2**, 16-19.
- Casas JP, Shah T, Cooper J, Hawe E, McMahon AD, Gaffney D, Packard CJ, O'Reilly DS, Juhan-Vague I, Yudkin JS, Tremoli E, Margaglione M, Di Minno G, Hamsten A, Kooistra T, Stephens JW, Hurel SJ, Livingstone S, Colhoun HM, Miller GJ, Bautista LE, Meade T, Sattar N, Humphries SE , Hingorani AD (2006). Insight into the nature of the CRP-coronary event association using Mendelian randomization. *Int J Epidemiol.* **35**, 922-931.

- Casteilla L, Rigoulet M, Penicaud L (2001). Mitochondrial ROS metabolism: modulation by uncoupling proteins. *IUBMB Life*. **52**, 181-188.
- Cathcart R, Schwiers E, Ames BN (1983). Detection of picomole levels of hydroperoxides using a fluorescent dichlorofluorescein assay. *Anal Biochem*. **134**, 111-116.
- Cawthon RM (2002). Telomere measurement by quantitative PCR. *Nucleic Acids Res*. **30**, e47.
- Cawthon RM (2009). Telomere length measurement by a novel monochrome multiplex quantitative PCR method. *Nucleic Acids Res*. **37**, e21.
- Celermajer DS, Sorensen KE, Spiegelhalter DJ, Georgakopoulos D, Robinson J, Deanfield JE (1994). Aging is associated with endothelial dysfunction in healthy men years before the age-related decline in women. *J Am Coll Cardiol*. **24**, 471-476.
- Ceriello A, Motz E (2004). Is oxidative stress the pathogenic mechanism underlying insulin resistance, diabetes, and cardiovascular disease? The common soil hypothesis revisited. *Arterioscler Thromb Vasc Biol*. **24**, 816-823.
- Cesare AJ, Reddel RR (2010). Alternative lengthening of telomeres: models, mechanisms and implications. *Nat Rev Genet*. **11**, 319-330.
- Chang E, Harley CB (1995). Telomere length and replicative aging in human vascular tissues. *Proc Natl Acad Sci U S A*. **92**, 11190-11194.
- Chapman MJ, Guerin M, Bruckert E (1998). Atherogenic, dense low-density lipoproteins. Pathophysiology and new therapeutic approaches. *Eur Heart J*. **19 Suppl A**, A24-30.
- Chen W, Gardner JP, Kimura M, Brimacombe M, Cao X, Srinivasan SR, Berenson GS, Aviv A (2009). Leukocyte telomere length is associated with HDL cholesterol levels: The Bogalusa heart study. *Atherosclerosis*. **205**, 620-625.
- Cherkas LF, Hunkin JL, Kato BS, Richards JB, Gardner JP, Surdulescu GL, Kimura M, Lu X, Spector TD, Aviv A (2008). The association between physical activity in leisure time and leukocyte telomere length. *Arch Intern Med*. **168**, 154-158.
- Clarke MC, Figg N, Maguire JJ, Davenport AP, Goddard M, Littlewood TD, Bennett MR (2006). Apoptosis of vascular smooth muscle cells induces features of plaque vulnerability in atherosclerosis. *Nat Med*. **12**, 1075-1080.
- Clarke R, Peden JF, Hopewell JC, Kyriakou T, Goel A, Heath SC, Parish S, Barlera S, Franzosi MG, Rust S, Bennett D, Silveira A, Malarstig A, Green FR, Lathrop M, Gigante B, Leander K, de Faire U, Seedorf U, Hamsten A, Collins R, Watkins H, Farrall M (2009). Genetic variants associated with Lp(a) lipoprotein level and coronary disease. *N Engl J Med*. **361**, 2518-2528.
- Codd V, Mangino M, van der Harst P, Braund PS, Kaiser M, Beveridge AJ, Rafelt S, Moore J, Nelson C, Soranzo N, Zhai G, Valdes AM, Blackburn H, Mateo Leach I, de Boer RA, Goodall AH, Ouwehand W, van Veldhuisen DJ, van Gilst WH, Navis G, Burton PR, Tobin MD, Hall AS, Thompson JR, Spector T, Samani NJ (2010). Common variants near TERC are associated with mean telomere length. *Nat Genet*. **42**, 197-199.
- Colgin LM, Baran K, Baumann P, Cech TR, Reddel RR (2003). Human POT1 facilitates telomere elongation by telomerase. *Curr Biol*. **13**, 942-946.

- Collerton J, Martin-Ruiz C, Kenny A, Barrass K, von Zglinicki T, Kirkwood T, Keavney B (2007). Telomere length is associated with left ventricular function in the oldest old: the Newcastle 85+ study. *Eur Heart J.* **28**, 172-176.
- Collins R, MacMahon S (1994). Blood pressure, antihypertensive drug treatment and the risks of stroke and of coronary heart disease. *Br Med Bull.* **50**, 272-298.
- Colman PG, Goodall GI, Garcia-Webb P, Williams PF, Dunlop ME (1997). Glycohaemoglobin: a crucial measurement in modern diabetes management. Progress towards standardisation and improved precision of measurement. Australian Diabetes Society, the Royal College of Pathologists of Australasia and the Australasian Association of Clinical Biochemists [consensus development conference]. *Med J Aust.* **167**, 96-98.
- Cooperstein CJ (1981). *The Islets of Langerhans.*
- Creutz CE (1992). The annexins and exocytosis. *Science.* **258**, 924-931.
- Dahlof B, Devereux RB, Kjeldsen SE, Julius S, Beevers G, de Faire U, Fyhrquist F, Ibsen H, Kristiansson K, Lederballe-Pedersen O, Lindholm LH, Nieminen MS, Omvik P, Oparil S, Wedel H (2002). Cardiovascular morbidity and mortality in the Losartan Intervention For Endpoint reduction in hypertension study (LIFE): a randomised trial against atenolol. *Lancet.* **359**, 995-1003.
- Davies MJ, Richardson PD, Woolf N, Katz DR, Mann J (1993). Risk of thrombosis in human atherosclerotic plaques: role of extracellular lipid, macrophage, and smooth muscle cell content. *Br Heart J.* **69**, 377-381.
- Davy P, Nagata M, Bullard P, Fogelson NS, Allsopp R (2009). Fetal growth restriction is associated with accelerated telomere shortening and increased expression of cell senescence markers in the placenta. *Placenta.* **30**, 539-542.
- De Backer G, De Henauw S, Sans S, Nicaud V, Masana L, Visvikis S, Gerdes C, Wilhelmsen L (1999). A comparison of lifestyle, genetic, bioclinical and biochemical variables of offspring with and without family histories of premature coronary heart disease: the experience of the European Atherosclerosis Research Studies. *J Cardiovasc Risk.* **6**, 183-188.
- De Boeck G, Forsyth RG, Praet M, Hogendoorn PC (2009). Telomere-associated proteins: cross-talk between telomere maintenance and telomere-lengthening mechanisms. *J Pathol.* **217**, 327-344.
- de Bono DP (1998). Olovnikov's clock: telomeres and vascular biology. *Heart.* **80**, 110-111.
- de Cavanagh EM, Inserra F, Ferder L (2010). Angiotensin II blockade: a strategy to slow aging by protecting mitochondria? *Cardiovasc Res.*
- de Cavanagh EM, Piotrkowski B, Basso N, Stella I, Inserra F, Ferder L, Fraga CG (2003). Enalapril and losartan attenuate mitochondrial dysfunction in aged rats. *FASEB J.* **17**, 1096-1098.
- De la Fuente M, Miquel J (2009). An update of the oxidation-inflammation theory of aging: the involvement of the immune system in oxi-inflamm-aging. *Curr Pharm Des.* **15**, 3003-3026.
- de Lange T (2001). Cell biology. Telomere capping--one strand fits all. *Science.* **292**, 1075-1076.
- De Meyer T, Rietzschel ER, De Buyzere ML, De Bacquer D, Van Criekinge W, De Backer GG, Gillebert TC, Van Oostveldt P, Bekaert S (2007). Paternal age at birth is an

- important determinant of offspring telomere length. *Hum Mol Genet.* **16**, 3097-3102.
- de Pauw ES, Roelofs H, Zwinderman A, van Houwelingen JC, Fibbe WE, de Knijff P, Pearson PL, Tanke HJ (2005). Studying the biological and technical sources of variation in telomere length of individual chromosomes. *Cytometry A.* **65**, 35-39.
- DeFronzo RA (2010). Insulin resistance, lipotoxicity, type 2 diabetes and atherosclerosis: the missing links. The Claude Bernard Lecture 2009. *Diabetologia.* **53**, 1270-1287.
- DeFronzo RA, Tripathy D (2009). Skeletal muscle insulin resistance is the primary defect in type 2 diabetes. *Diabetes Care.* **32 Suppl 2**, S157-163.
- Demissie S, Levy D, Benjamin EJ, Cupples LA, Gardner JP, Herbert A, Kimura M, Larson MG, Meigs JB, Keaney JF, Aviv A (2006). Insulin resistance, oxidative stress, hypertension, and leukocyte telomere length in men from the Framingham Heart Study. *Aging Cell.* **5**, 325-330.
- Dhamrait SS, Stephens JW, Cooper JA, Acharya J, Mani AR, Moore K, Miller GJ, Humphries SE, Hurel SJ, Montgomery HE (2004). Cardiovascular risk in healthy men and markers of oxidative stress in diabetic men are associated with common variation in the gene for uncoupling protein 2. *Eur Heart J.* **25**, 468-475.
- Doughan AK, Harrison DG, Dikalov SI (2008). Molecular mechanisms of angiotensin II-mediated mitochondrial dysfunction: linking mitochondrial oxidative damage and vascular endothelial dysfunction. *Circ Res.* **102**, 488-496.
- Drake TA, Morrissey JH, Edgington TS (1989). Selective cellular expression of tissue factor in human tissues. Implications for disorders of hemostasis and thrombosis. *Am J Pathol.* **134**, 1087-1097.
- Droge W (2002). Free radicals in the physiological control of cell function. *Physiol Rev.* **82**, 47-95.
- Duval C, Negre-Salvayre A, Dogilo A, Salvayre R, Penicaud L, Casteilla L (2002). Increased reactive oxygen species production with antisense oligonucleotides directed against uncoupling protein 2 in murine endothelial cells. *Biochem Cell Biol.* **80**, 757-764.
- Echtay KS, Roussel D, St-Pierre J, Jekabsons MB, Cadenas S, Stuart JA, Harper JA, Roebuck SJ, Morrison A, Pickering S, Clapham JC, Brand MD (2002). Superoxide activates mitochondrial uncoupling proteins. *Nature.* **415**, 96-99.
- Eggen DA, Solberg LA (1968). Variation of atherosclerosis with age. *Lab Invest.* **18**, 571-579.
- Elliott P, Chambers JC, Zhang W, Clarke R, Hopewell JC, Peden JF, Erdmann J, Braund P, Engert JC, Bennett D, Coin L, Ashby D, Tzoulaki I, Brown IJ, Mt-Isa S, McCarthy MI, Peltonen L, Freimer NB, Farrall M, Ruukonen A, Hamsten A, Lim N, Froguel P, Waterworth DM, Vollenweider P, Waeber G, Jarvelin MR, Mooser V, Scott J, Hall AS, Schunkert H, Anand SS, Collins R, Samani NJ, Watkins H, Kooner JS (2009). Genetic Loci associated with C-reactive protein levels and risk of coronary heart disease. *JAMA.* **302**, 37-48.
- Epel ES, Merkin SS, Cawthon R, Blackburn EH, Adler NE, Pletcher MJ, Seeman TE (2009). The rate of leukocyte telomere shortening predicts mortality from cardiovascular disease in elderly men. *Aging (Albany NY).* **1**, 81-88.

- Erel O (2004). A novel automated direct measurement method for total antioxidant capacity using a new generation, more stable ABTS radical cation. *Clin Biochem.* **37**, 277-285.
- Erhardt L (2009). Cigarette smoking: an undertreated risk factor for cardiovascular disease. *Atherosclerosis.* **205**, 23-32.
- Erqou S, Kaptoge S, Perry PL, Di Angelantonio E, Thompson A, White IR, Marcovina SM, Collins R, Thompson SG , Danesh J (2009). Lipoprotein(a) concentration and the risk of coronary heart disease, stroke, and nonvascular mortality. *JAMA.* **302**, 412-423.
- Erusalimsky JD (2009). Vascular endothelial senescence: from mechanisms to pathophysiology. *J Appl Physiol.* **106**, 326-332.
- Esworthy RS, Ho YS , Chu FF (1997). The Gpx1 gene encodes mitochondrial glutathione peroxidase in the mouse liver. *Arch Biochem Biophys.* **340**, 59-63.
- Evans JL, Goldfine ID, Maddux BA , Grodsky GM (2002). Oxidative stress and stress-activated signaling pathways: a unifying hypothesis of type 2 diabetes. *Endocr Rev.* **23**, 599-622.
- Fadok VA, Voelker DR, Campbell PA, Cohen JJ, Bratton DL , Henson PM (1992). Exposure of phosphatidylserine on the surface of apoptotic lymphocytes triggers specific recognition and removal by macrophages. *J Immunol.* **148**, 2207-2216.
- Farzaneh-Far R, Cawthon RM, Na B, Browner WS, Schiller NB , Whooley MA (2008). Prognostic value of leukocyte telomere length in patients with stable coronary artery disease: data from the Heart and Soul Study. *Arterioscler Thromb Vasc Biol.* **28**, 1379-1384.
- Farzaneh-Far R, Lin J, Epel E, Lapham K, Blackburn E , Whooley MA (2010). Telomere length trajectory and its determinants in persons with coronary artery disease: longitudinal findings from the heart and soul study. *PLoS One.* **5**, e8612.
- Ferrannini E, Gastaldelli A , Iozzo P (2011). Pathophysiology of prediabetes. *Med Clin North Am.* **95**, 327-339, vii-viii.
- Finkel T, Serrano M , Blasco MA (2007). The common biology of cancer and ageing. *Nature.* **448**, 767-774.
- Fitzpatrick AL, Kronmal RA, Gardner JP, Psaty BM, Jenny NS, Tracy RP, Walston J, Kimura M , Aviv A (2007). Leukocyte telomere length and cardiovascular disease in the cardiovascular health study. *Am J Epidemiol.* **165**, 14-21.
- Forsberg L, de Faire U, Marklund SL, Andersson PM, Stegmayr B , Morgenstern R (2000). Phenotype determination of a common Pro-Leu polymorphism in human glutathione peroxidase 1. *Blood Cells Mol Dis.* **26**, 423-426.
- Frayling TM (2007). A new era in finding Type 2 diabetes genes-the unusual suspects. *Diabet Med.* **24**, 696-701.
- Freeman DJ, Norrie J, Sattar N, Neely RD, Cobbe SM, Ford I, Isles C, Lorimer AR, Macfarlane PW, McKillop JH, Packard CJ, Shepherd J , Gaw A (2001). Pravastatin and the development of diabetes mellitus: evidence for a protective treatment effect in the West of Scotland Coronary Prevention Study. *Circulation.* **103**, 357-362.
- Gable DR, Stephens JW, Cooper JA, Miller GJ , Humphries SE (2006). Variation in the UCP2-UCP3 gene cluster predicts the development of type 2 diabetes in healthy middle-aged men. *Diabetes.* **55**, 1504-1511.

- Galea J, Armstrong J, Gadsdon P, Holden H, Francis SE, Holt CM (1996). Interleukin-1 beta in coronary arteries of patients with ischemic heart disease. *Arterioscler Thromb Vasc Biol.* **16**, 1000-1006.
- Garbe JC, Bhattacharya S, Merchant B, Bassett E, Swisshelm K, Feiler HS, Wyrobek AJ, Stampfer MR (2009). Molecular distinctions between stasis and telomere attrition senescence barriers shown by long-term culture of normal human mammary epithelial cells. *Cancer Res.* **69**, 7557-7568.
- Gaziano JM, Gaziano TA, Glynn RJ, Sesso HD, Ajani UA, Stampfer MJ, Manson JE, Hennekens CH, Buring JE (2000). Light-to-moderate alcohol consumption and mortality in the Physicians' Health Study enrollment cohort. *J Am Coll Cardiol.* **35**, 96-105.
- Gloyn AL, McCarthy MI (2001). The genetics of type 2 diabetes. *Best Pract Res Clin Endocrinol Metab.* **15**, 293-308.
- Glymour MM, Weuve J, Berkman LF, Kawachi I, Robins JM (2005). When is baseline adjustment useful in analyses of change? An example with education and cognitive change. *Am J Epidemiol.* **162**, 267-278.
- Goldstein BJ (2002). Insulin resistance as the core defect in type 2 diabetes mellitus. *Am J Cardiol.* **90**, 3G-10G.
- Goldstein S (1990). Replicative senescence: the human fibroblast comes of age. *Science.* **249**, 1129-1133.
- Gouin JP, Hantsoo L, Kiecolt-Glaser JK (2008). Immune dysregulation and chronic stress among older adults: a review. *Neuroimmunomodulation.* **15**, 251-259.
- Graakjaer J, Pascoe L, Der-Sarkissian H, Thomas G, Kolvraa S, Christensen K, Londono-Vallejo JA (2004). The relative lengths of individual telomeres are defined in the zygote and strictly maintained during life. *Aging Cell.* **3**, 97-102.
- Grarup N, Sparso T, Hansen T (2010). Physiologic characterization of type 2 diabetes-related loci. *Curr Diab Rep.* **10**, 485-497.
- Greenspon AJ, Schaal SF (1983). The "holiday heart": electrophysiologic studies of alcohol effects in alcoholics. *Ann Intern Med.* **98**, 135-139.
- Greer EL, Dowlatshahi D, Banko MR, Villen J, Hoang K, Blanchard D, Gygi SP, Brunet A (2007). An AMPK-FOXO pathway mediates longevity induced by a novel method of dietary restriction in *C. elegans*. *Curr Biol.* **17**, 1646-1656.
- Greider CW, Blackburn EH (1985). Identification of a specific telomere terminal transferase activity in Tetrahymena extracts. *Cell.* **43**, 405-413.
- Greider CW, Blackburn EH (1989). A telomeric sequence in the RNA of Tetrahymena telomerase required for telomere repeat synthesis. *Nature.* **337**, 331-337.
- Griffith OW, Meister A (1979). Potent and specific inhibition of glutathione synthesis by buthionine sulfoximine (S-n-butyl homocysteine sulfoximine). *J Biol Chem.* **254**, 7558-7560.
- Group TE (1994). The European Atherosclerosis Research Study (EARS): design and objectives. *Int J Epidemiol.* **23**, 465-471.
- Group TWoSCPS (1992). A coronary primary prevention study of Scottish men aged 45-64 years: trial design. The West of Scotland Coronary Prevention Study Group. *J Clin Epidemiol.* **45**, 849-860.

- Gudnason H, Dufva M, Bang DD , Wolff A (2007). Comparison of multiple DNA dyes for real-time PCR: effects of dye concentration and sequence composition on DNA amplification and melting temperature. *Nucleic Acids Res.* **35**, e127.
- Gudnason V, Stansbie D, Scott J, Bowron A, Nicaud V , Humphries S (1998). C677T (thermolabile alanine/valine) polymorphism in methylenetetrahydrofolate reductase (MTHFR): its frequency and impact on plasma homocysteine concentration in different European populations. EARS group. *Atherosclerosis.* **136**, 347-354.
- Gundry CN, Vandersteen JG, Reed GH, Pryor RJ, Chen J , Wittwer CT (2003). Amplicon melting analysis with labeled primers: a closed-tube method for differentiating homozygotes and heterozygotes. *Clin Chem.* **49**, 396-406.
- Hansel B, Giral P, Nobecourt E, Chantepie S, Bruckert E, Chapman MJ , Kontush A (2004). Metabolic syndrome is associated with elevated oxidative stress and dysfunctional dense high-density lipoprotein particles displaying impaired antioxidative activity. *J Clin Endocrinol Metab.* **89**, 4963-4971.
- Hansson L, Zanchetti A, Carruthers SG, Dahlof B, Elmfeldt D, Julius S, Menard J, Rahn KH, Wedel H , Westerling S (1998). Effects of intensive blood-pressure lowering and low-dose aspirin in patients with hypertension: principal results of the Hypertension Optimal Treatment (HOT) randomised trial. HOT Study Group. *Lancet.* **351**, 1755-1762.
- Harle-Bachor C , Boukamp P (1996). Telomerase activity in the regenerative basal layer of the epidermis in human skin and in immortal and carcinoma-derived skin keratinocytes. *Proc Natl Acad Sci U S A.* **93**, 6476-6481.
- Harley CB, Vaziri H, Counter CM , Allsopp RC (1992). The telomere hypothesis of cellular aging. *Exp Gerontol.* **27**, 375-382.
- Harrison D, Griendling KK, Landmesser U, Hornig B , Drexler H (2003). Role of oxidative stress in atherosclerosis. *Am J Cardiol.* **91**, 7A-11A.
- Hausenloy DJ , Yellon DM (2009). Enhancing cardiovascular disease risk reduction: raising high-density lipoprotein levels. *Curr Opin Cardiol.* **24**, 473-482.
- Hayflick L (1965). The Limited in Vitro Lifetime of Human Diploid Cell Strains. *Exp Cell Res.* **37**, 614-636.
- Hayflick L , Moorhead PS (1961). The serial cultivation of human diploid cell strains. *Exp Cell Res.* **25**, 585-621.
- Heid CA, Stevens J, Livak KJ , Williams PM (1996). Real time quantitative PCR. *Genome Res.* **6**, 986-994.
- Heinrich J, Balleisen L, Schulte H, Assmann G , van de Loo J (1994). Fibrinogen and factor VII in the prediction of coronary risk. Results from the PROCAM study in healthy men. *Arterioscler Thromb.* **14**, 54-59.
- Henke W, Herdel K, Jung K, Schnorr D , Loening SA (1997). Betaine improves the PCR amplification of GC-rich DNA sequences. *Nucleic Acids Res.* **25**, 3957-3958.
- Hingorani AD (2001). Polymorphisms in endothelial nitric oxide synthase and atherogenesis: John French Lecture 2000. *Atherosclerosis.* **154**, 521-527.
- Hingorani AD, Shah T, Casas JP, Humphries SE , Talmud PJ (2009). C-reactive protein and coronary heart disease: predictive test or therapeutic target? *Clin Chem.* **55**, 239-255.

- Hiyama K, Hirai Y, Kyoizumi S, Akiyama M, Hiyama E, Piatyszek MA, Shay JW, Ishioka S, Yamakido M (1995). Activation of telomerase in human lymphocytes and hematopoietic progenitor cells. *J Immunol.* **155**, 3711-3715.
- Holland PM, Abramson RD, Watson R, Gelfand DH (1991). Detection of specific polymerase chain reaction product by utilizing the 5'----3' exonuclease activity of *Thermus aquaticus* DNA polymerase. *Proc Natl Acad Sci U S A.* **88**, 7276-7280.
- Hollander W (1976). Role of hypertension in atherosclerosis and cardiovascular disease. *Am J Cardiol.* **38**, 786-800.
- Honig LS, Schupf N, Lee JH, Tang MX, Mayeux R (2006). Shorter telomeres are associated with mortality in those with APOE epsilon4 and dementia. *Ann Neurol.* **60**, 181-187.
- Honjoh S, Yamamoto T, Uno M, Nishida E (2009). Signalling through RHEB-1 mediates intermittent fasting-induced longevity in *C. elegans*. *Nature.* **457**, 726-730.
- Houben JM, Mercken EM, Ketelslegers HB, Bast A, Wouters EF, Hageman GJ, Schols AM (2009). Telomere shortening in chronic obstructive pulmonary disease. *Respir Med.* **103**, 230-236.
- Hsueh WA, Orloski L, Wyne K (2010). Prediabetes: the importance of early identification and intervention. *Postgrad Med.* **122**, 129-143.
- Huda N, Tanaka H, Herbert BS, Reed T, Gilley D (2007). Shared environmental factors associated with telomere length maintenance in elderly male twins. *Aging Cell.* **6**, 709-713.
- Hulsmans M, Holvoet P (2010). The vicious circle between oxidative stress and inflammation in atherosclerosis. *J Cell Mol Med.* **14**, 70-78.
- Humphries SE, Nicaud V, Margalef J, Tiret L, Talmud PJ (1998). Lipoprotein lipase gene variation is associated with a paternal history of premature coronary artery disease and fasting and postprandial plasma triglycerides: the European Atherosclerosis Research Study (EARS). *Arterioscler Thromb Vasc Biol.* **18**, 526-534.
- Humphries SE, Ridker PM, Talmud PJ (2004). Genetic testing for cardiovascular disease susceptibility: a useful clinical management tool or possible misinformation? *Arterioscler Thromb Vasc Biol.* **24**, 628-636.
- Hunt SC, Chen W, Gardner JP, Kimura M, Srinivasan SR, Eckfeldt JH, Berenson GS, Aviv A (2008). Leukocyte telomeres are longer in African Americans than in whites: the National Heart, Lung, and Blood Institute Family Heart Study and the Bogalusa Heart Study. *Aging Cell.*
- Hunt T (2002). Nobel Lecture. Protein synthesis, proteolysis, and cell cycle transitions. *Biosci Rep.* **22**, 465-486.
- Iacoviello L, Arnout J, Buntinx F, Cappuccio FP, Dagnelie PC, de Lorgeril M, Dirckx C, Donati MB, Krogh V, Siani A (2001). Dietary habit profile in European communities with different risk of myocardial infarction: the impact of migration as a model of gene-environment interaction. The IMMIDIET Study. *Nutr Metab Cardiovasc Dis.* **11**, 122-126.
- Inoue N, Kawashima S, Kanazawa K, Yamada S, Akita H, Yokoyama M (1998). Polymorphism of the NADH/NADPH oxidase p22 phox gene in patients with coronary artery disease. *Circulation.* **97**, 135-137.
- Itahana K, Dimri G, Campisi J (2001). Regulation of cellular senescence by p53. *Eur J Biochem.* **268**, 2784-2791.

- Jakubowski W , Bartosz G (2000). 2,7-dichlorofluorescein oxidation and reactive oxygen species: what does it measure? *Cell Biol Int.* **24**, 757-760.
- Jeanclous E, Krolewski A, Skurnick J, Kimura M, Aviv H, Warram JH , Aviv A (1998). Shortened telomere length in white blood cells of patients with IDDM. *Diabetes.* **47**, 482-486.
- Jin P, Gu Y , Morgan DO (1996). Role of inhibitory CDC2 phosphorylation in radiation-induced G2 arrest in human cells. *J Cell Biol.* **134**, 963-970.
- Johnson GC, Esposito L, Barratt BJ, Smith AN, Heward J, Di Genova G, Ueda H, Cordell HJ, Eaves IA, Dudbridge F, Twells RC, Payne F, Hughes W, Nutland S, Stevens H, Carr P, Tuomilehto-Wolf E, Tuomilehto J, Gough SC, Clayton DG , Todd JA (2001). Haplotype tagging for the identification of common disease genes. *Nat Genet.* **29**, 233-237.
- Joost HG (2008). Pathogenesis, risk assessment and prevention of type 2 diabetes mellitus. *Obes Facts.* **1**, 128-137.
- Juhan-Vague I, Morange PE, Aubert H, Henry M, Aillaud MF, Alessi MC, Samnegard A, Hawe E, Yudkin J, Margaglione M, Di Minno G, Hamsten A , Humphries SE (2002). Plasma thrombin-activatable fibrinolysis inhibitor antigen concentration and genotype in relation to myocardial infarction in the north and south of Europe. *Arterioscler Thromb Vasc Biol.* **22**, 867-873.
- Kaeberlein M, Powers RW, 3rd, Steffen KK, Westman EA, Hu D, Dang N, Kerr EO, Kirkland KT, Fields S , Kennedy BK (2005). Regulation of yeast replicative life span by TOR and Sch9 in response to nutrients. *Science.* **310**, 1193-1196.
- Kannel WB , McGee DL (1979). Diabetes and cardiovascular disease. The Framingham study. *JAMA.* **241**, 2035-2038.
- Kannel WB , Vasani RS (2009a). Is age really a non-modifiable cardiovascular risk factor? *Am J Cardiol.* **104**, 1307-1310.
- Kannel WB , Vasani RS (2009b). Triglycerides as vascular risk factors: new epidemiologic insights. *Curr Opin Cardiol.* **24**, 345-350.
- Kapahi P, Zid BM, Harper T, Koslover D, Sapin V , Benzer S (2004). Regulation of lifespan in *Drosophila* by modulation of genes in the TOR signaling pathway. *Curr Biol.* **14**, 885-890.
- Karlseder J (2003). Telomere repeat binding factors: keeping the ends in check. *Cancer Lett.* **194**, 189-197.
- Kenyon C (2005). The plasticity of aging: insights from long-lived mutants. *Cell.* **120**, 449-460.
- Kenyon CJ (2010). The genetics of ageing. *Nature.* **464**, 504-512.
- Keston AS , Brandt R (1965). The Fluorometric Analysis of Ultramicro Quantities of Hydrogen Peroxide. *Anal Biochem.* **11**, 1-5.
- Kim SH, Han S, You YH, Chen DJ , Campisi J (2003). The human telomere-associated protein TIN2 stimulates interactions between telomeric DNA tracts in vitro. *EMBO Rep.* **4**, 685-691.
- Kirkwood TB (1977). Evolution of ageing. *Nature.* **270**, 301-304.
- Kirkwood TB , Austad SN (2000). Why do we age? *Nature.* **408**, 233-238.
- Kivimaki M, Lawlor DA, Smith GD, Kumari M, Donald A, Britton A, Casas JP, Shah T, Brunner E, Timpson NJ, Halcox JP, Miller MA, Humphries SE, Deanfield J,

- Marmot MG , Hingorani AD (2008). Does high C-reactive protein concentration increase atherosclerosis? The Whitehall II Study. *PLoS One*. **3**, e3013.
- Koch WH (2004). Technology platforms for pharmacogenomic diagnostic assays. *Nat Rev Drug Discov*. **3**, 749-761.
- Koh-Banerjee P, Wang Y, Hu FB, Spiegelman D, Willett WC , Rimm EB (2004). Changes in body weight and body fat distribution as risk factors for clinical diabetes in US men. *Am J Epidemiol*. **159**, 1150-1159.
- Kokkinos P, Sheriff H , Kheirbek R (2011). Physical inactivity and mortality risk. *Cardiol Res Pract*. **2011**, 924945.
- Kostrikis LG, Tyagi S, Mhlanga MM, Ho DD , Kramer FR (1998). Spectral genotyping of human alleles. *Science*. **279**, 1228-1229.
- Krauss S, Zhang CY , Lowell BB (2005). The mitochondrial uncoupling-protein homologues. *Nat Rev Mol Cell Biol*. **6**, 248-261.
- Krempler F, Esterbauer H, Weitgasser R, Ebenbichler C, Patsch JR, Miller K, Xie M, Linnemayr V, Oberkofler H , Patsch W (2002). A functional polymorphism in the promoter of UCP2 enhances obesity risk but reduces type 2 diabetes risk in obese middle-aged humans. *Diabetes*. **51**, 3331-3335.
- Krook A, Bjornholm M, Galuska D, Jiang XJ, Fahlman R, Myers MG, Jr., Wallberg-Henriksson H , Zierath JR (2000). Characterization of signal transduction and glucose transport in skeletal muscle from type 2 diabetic patients. *Diabetes*. **49**, 284-292.
- Ksiazek K, Passos JF, Olijslagers S , von Zglinicki T (2008). Mitochondrial dysfunction is a possible cause of accelerated senescence of mesothelial cells exposed to high glucose. *Biochem Biophys Res Commun*. **366**, 793-799.
- Kurz DJ, Decary S, Hong Y, Trivier E, Akhmedov A , Erusalimsky JD (2004). Chronic oxidative stress compromises telomere integrity and accelerates the onset of senescence in human endothelial cells. *J Cell Sci*. **117**, 2417-2426.
- Kyo S, Takakura M, Kanaya T, Zhuo W, Fujimoto K, Nishio Y, Orimo A , Inoue M (1999). Estrogen activates telomerase. *Cancer Res*. **59**, 5917-5921.
- Lakatta EG (2003). Arterial and cardiac aging: major shareholders in cardiovascular disease enterprises: Part III: cellular and molecular clues to heart and arterial aging. *Circulation*. **107**, 490-497.
- Lansdorp PM, Verwoerd NP, van de Rijke FM, Dragowska V, Little MT, Dirks RW, Raap AK , Tanke HJ (1996). Heterogeneity in telomere length of human chromosomes. *Hum Mol Genet*. **5**, 685-691.
- Latron Y, Chautan M, Anfosso F, Alessi MC, Nalbone G, Lafont H , Juhan-Vague I (1991). Stimulating effect of oxidized low density lipoproteins on plasminogen activator inhibitor-1 synthesis by endothelial cells. *Arterioscler Thromb*. **11**, 1821-1829.
- Lee DC, Im JA, Kim JH, Lee HR , Shim JY (2005). Effect of long-term hormone therapy on telomere length in postmenopausal women. *Yonsei Med J*. **46**, 471-479.
- Lee HC, Yin PH, Lu CY, Chi CW , Wei YH (2000). Increase of mitochondria and mitochondrial DNA in response to oxidative stress in human cells. *Biochem J*. **348 Pt 2**, 425-432.
- Lee M, Martin H, Firpo MA , Demerath EW (2011). Inverse association between adiposity and telomere length: The Fels Longitudinal Study. *Am J Hum Biol*. **23**, 100-106.

- Leo R, Pratico D, Iuliano L, Pulcinelli FM, Ghiselli A, Pignatelli P, Colavita AR, FitzGerald GA, Violi F (1997). Platelet activation by superoxide anion and hydroxyl radicals intrinsically generated by platelets that had undergone anoxia and then reoxygenated. *Circulation*. **95**, 885-891.
- Li H, Forstermann U (2009). Resveratrol: a multifunctional compound improving endothelial function. Editorial to: "Resveratrol supplementation gender independently improves endothelial reactivity and suppresses superoxide production in healthy rats" by S. Soylemez et al. *Cardiovasc Drugs Ther*. **23**, 425-429.
- Libby P (2000). Changing concepts of atherogenesis. *J Intern Med*. **247**, 349-358.
- Libby P (2008). The molecular mechanisms of the thrombotic complications of atherosclerosis. *J Intern Med*. **263**, 517-527.
- Lin J, Epel E, Cheon J, Kroenke C, Sinclair E, Bigos M, Wolkowitz O, Mellon S, Blackburn E (2010). Analyses and comparisons of telomerase activity and telomere length in human T and B cells: insights for epidemiology of telomere maintenance. *J Immunol Methods*. **352**, 71-80.
- Lingner J, Hughes TR, Shevchenko A, Mann M, Lundblad V, Cech TR (1997). Reverse transcriptase motifs in the catalytic subunit of telomerase. *Science*. **276**, 561-567.
- Livak KJ, Schmittgen TD (2001). Analysis of relative gene expression data using real-time quantitative PCR and the 2(-Delta Delta C(T)) Method. *Methods*. **25**, 402-408.
- Luscher TF, Barton M (1997). Biology of the endothelium. *Clin Cardiol*. **20**, II-3-10.
- Lusis AJ, Mar R, Pajukanta P (2004). Genetics of atherosclerosis. *Annu Rev Genomics Hum Genet*. **5**, 189-218.
- M. C. Stuhlinger PST (2003). Etiology and pathogenesis of atherosclerosis. In *Peripheral Artery Disease*. (RTE J. D. Coffman, ed): Humana Press, pp. 1-19.
- Maechler P, Jornot L, Wollheim CB (1999). Hydrogen peroxide alters mitochondrial activation and insulin secretion in pancreatic beta cells. *J Biol Chem*. **274**, 27905-27913.
- Maedler K, Dharmadhikari G, Schumann DM, Storling J (2009). Interleukin-1 beta targeted therapy for type 2 diabetes. *Expert Opin Biol Ther*. **9**, 1177-1188.
- Mahmoudi M, Gorenne I, Mercer J, Figg N, Littlewood T, Bennett M (2008). Statins use a novel Nijmegen breakage syndrome-1-dependent pathway to accelerate DNA repair in vascular smooth muscle cells. *Circ Res*. **103**, 717-725.
- Maiti R, Agrawal NK (2007). Atherosclerosis in diabetes mellitus: role of inflammation. *Indian J Med Sci*. **61**, 292-306.
- Mangino M, Brouillette S, Braund P, Tirmizi N, Vasa-Nicotera M, Thompson JR, Samani NJ (2008). A regulatory SNP of the BICD1 gene contributes to telomere length variation in humans. *Hum Mol Genet*. **17**, 2518-2523.
- Mangino M, Richards JB, Soranzo N, Zhai G, Aviv A, Valdes AM, Samani NJ, Deloukas P, Spector TD (2009). A genome-wide association study identifies a novel locus on chromosome 18q12.2 influencing white cell telomere length. *J Med Genet*. **46**, 451-454.
- Maritim AC, Sanders RA, Watkins JB, 3rd (2003). Diabetes, oxidative stress, and antioxidants: a review. *J Biochem Mol Toxicol*. **17**, 24-38.
- Martens GA, Cai Y, Hinke S, Stange G, Van de Casteele M, Pipeleers D (2005). Glucose suppresses superoxide generation in metabolically responsive pancreatic beta cells. *J Biol Chem*. **280**, 20389-20396.

- Martens UM, Zijlmans JM, Poon SS, Dragowska W, Yui J, Chavez EA, Ward RK , Lansdorp PM (1998). Short telomeres on human chromosome 17p. *Nat Genet.* **18**, 76-80.
- Martin-Ruiz C, Saretzki G, Petrie J, Ladhoff J, Jeyapalan J, Wei W, Sedivy J , von Zglinicki T (2004). Stochastic variation in telomere shortening rate causes heterogeneity of human fibroblast replicative life span. *J Biol Chem.* **279**, 17826-17833.
- Matthews C, Gorenne I, Scott S, Figg N, Kirkpatrick P, Ritchie A, Goddard M , Bennett M (2006). Vascular smooth muscle cells undergo telomere-based senescence in human atherosclerosis: effects of telomerase and oxidative stress. *Circ Res.* **99**, 156-164.
- McCarthy MI , Zeggini E (2009). Genome-wide association studies in type 2 diabetes. *Curr Diab Rep.* **9**, 164-171.
- McCully KS , Wilson RB (1975). Homocysteine theory of arteriosclerosis. *Atherosclerosis.* **22**, 215-227.
- Melendez-Ramirez LY, Richards RJ , Cefalu WT (2010). Complications of type 1 diabetes. *Endocrinol Metab Clin North Am.* **39**, 625-640.
- Miller SA, Dykes DD , Polesky HF (1988). A simple salting out procedure for extracting DNA from human nucleated cells. *Nucleic Acids Res.* **16**, 1215.
- Minamino T, Miyauchi H, Yoshida T, Ishida Y, Yoshida H , Komuro I (2002). Endothelial cell senescence in human atherosclerosis: role of telomere in endothelial dysfunction. *Circulation.* **105**, 1541-1544.
- Molnar GA, Wagner Z, Wagner L, Melegh B, Koszegi T, Degrell P, Bene J, Tamasko M, Laczy B, Nagy J , Wittmann I (2004). [Effect of ACE gene polymorphism on carbohydrate metabolism, on oxidative stress and on end-organ damage in type-2 diabetes mellitus]. *Orv Hetil.* **145**, 855-859.
- Monteiro P, Duarte AI, Goncalves LM , Providencia LA (2005). Valsartan improves mitochondrial function in hearts submitted to acute ischemia. *Eur J Pharmacol.* **518**, 158-164.
- Morgan D, Oliveira-Emilio HR, Keane D, Hirata AE, Santos da Rocha M, Bordin S, Curi R, Newsholme P , Carpinelli AR (2007). Glucose, palmitate and pro-inflammatory cytokines modulate production and activity of a phagocyte-like NADPH oxidase in rat pancreatic islets and a clonal beta cell line. *Diabetologia.* **50**, 359-369.
- Morris RD, Rimm DL, Hartz AJ, Kalkhoff RK , Rimm AA (1989). Obesity and heredity in the etiology of non-insulin-dependent diabetes mellitus in 32,662 adult white women. *Am J Epidemiol.* **130**, 112-121.
- Mukherjee M, Brouillette S, Stevens S, Shetty KR , Samani NJ (2009). Association of shorter telomeres with coronary artery disease in Indian subjects. *Heart.* **95**, 669-673.
- Muller-Nordhorn J, Binting S, Roll S , Willich SN (2008). An update on regional variation in cardiovascular mortality within Europe. *Eur Heart J.* **29**, 1316-1326.
- Muoio DM , Newgard CB (2008). Mechanisms of disease: molecular and metabolic mechanisms of insulin resistance and beta-cell failure in type 2 diabetes. *Nat Rev Mol Cell Biol.* **9**, 193-205.
- Myers RH, Kiely DK, Cupples LA , Kannel WB (1990). Parental history is an independent risk factor for coronary artery disease: the Framingham Study. *Am Heart J.* **120**, 963-969.

- Nakamura H, Nakamura K , Yodoi J (1997). Redox regulation of cellular activation. *Annu Rev Immunol.* **15**, 351-369.
- Nakamura Y, Hirose M, Matsuo H, Tsuyama N, Kamisango K , Ide T (1999). Simple, rapid, quantitative, and sensitive detection of telomere repeats in cell lysate by a hybridization protection assay. *Clin Chem.* **45**, 1718-1724.
- Neil HA, Hammond T, Huxley R, Matthews DR , Humphries SE (2000). Extent of underdiagnosis of familial hypercholesterolaemia in routine practice: prospective registry study. *BMJ.* **321**, 148.
- Neil HA, Huxley RR, Hawkins MM, Durrington PN, Betteridge DJ , Humphries SE (2003). Comparison of the risk of fatal coronary heart disease in treated xanthomatous and non-xanthomatous heterozygous familial hypercholesterolaemia: a prospective registry study. *Atherosclerosis.* **170**, 73-78.
- Neil HA, Seagroatt V, Betteridge DJ, Cooper MP, Durrington PN, Miller JP, Seed M, Naoumova RP, Thompson GR, Huxley R , Humphries SE (2004). Established and emerging coronary risk factors in patients with heterozygous familial hypercholesterolaemia. *Heart.* **90**, 1431-1437.
- Newman B, Selby JV, King MC, Slemenda C, Fabsitz R , Friedman GD (1987). Concordance for type 2 (non-insulin-dependent) diabetes mellitus in male twins. *Diabetologia.* **30**, 763-768.
- Nishikawa T, Edelstein D, Du XL, Yamagishi S, Matsumura T, Kaneda Y, Yorek MA, Beebe D, Oates PJ, Hammes HP, Giardino I , Brownlee M (2000). Normalizing mitochondrial superoxide production blocks three pathways of hyperglycaemic damage. *Nature.* **404**, 787-790.
- Njajou OT, Cawthon RM, Damcott CM, Wu SH, Ott S, Garant MJ, Blackburn EH, Mitchell BD, Shuldiner AR , Hsueh WC (2007). Telomere length is paternally inherited and is associated with parental lifespan. *Proc Natl Acad Sci U S A.* **104**, 12135-12139.
- Nordestgaard BG (2009). Does elevated C-reactive protein cause human atherothrombosis? Novel insights from genetics, intervention trials, and elsewhere. *Curr Opin Lipidol.* **20**, 393-401.
- Nordfjall K, Svenson U, Norrback KF, Adolfsson R, Lenner P , Roos G (2009). The individual blood cell telomere attrition rate is telomere length dependent. *PLoS Genet.* **5**, e1000375.
- O'Callaghan N, Dhillon V, Thomas P , Fenech M (2008). A quantitative real-time PCR method for absolute telomere length. *Biotechniques.* **44**, 807-809.
- O'Rahilly S (2001). Uncoupling protein 2: Adiposity angel and diabetes devil? *Nat Med.* **7**, 770-772.
- Olivieri F, Lorenzi M, Antonicelli R, Testa R, Sirolla C, Cardelli M, Mariotti S, Marchegiani F, Marra M, Spazzafumo L, Bonfigli AR , Procopio A (2009). Leukocyte telomere shortening in elderly Type2DM patients with previous myocardial infarction. *Atherosclerosis.* **206**, 588-593.
- Olovnikov AM (1971). [Principle of marginotomy in template synthesis of polynucleotides]. *Dokl Akad Nauk SSSR.* **201**, 1496-1499.
- Orie NN, Zidek W , Tepel M (2000). Increased intracellular generation of reactive oxygen species in mononuclear leukocytes from patients with diabetes mellitus type 2. *Exp Clin Endocrinol Diabetes.* **108**, 175-180.

- Ornish D, Lin J, Daubenmier J, Weidner G, Epel E, Kemp C, Magbanua MJ, Marlin R, Yglecias L, Carroll PR, Blackburn EH (2008). Increased telomerase activity and comprehensive lifestyle changes: a pilot study. *Lancet Oncol.* **9**, 1048-1057.
- Oyama Y, Hayashi A, Ueha T, Maekawa K (1994). Characterization of 2',7'-dichlorofluorescein fluorescence in dissociated mammalian brain neurons: estimation on intracellular content of hydrogen peroxide. *Brain Res.* **635**, 113-117.
- Packer JE, Slater TF, Willson RL (1979). Direct observation of a free radical interaction between vitamin E and vitamin C. *Nature.* **278**, 737-738.
- Perneger TV (1999). Adjusting for multiple testing in studies is less important than other concerns. *Bmj.* **318**, 1288.
- Petersen KF, Shulman GI (2002). Pathogenesis of skeletal muscle insulin resistance in type 2 diabetes mellitus. *Am J Cardiol.* **90**, 11G-18G.
- Petersen S, Saretzki G, von Zglinicki T (1998). Preferential accumulation of single-stranded regions in telomeres of human fibroblasts. *Exp Cell Res.* **239**, 152-160.
- Pfaffl MW (2001). A new mathematical model for relative quantification in real-time RT-PCR. *Nucleic Acids Res.* **29**, e45.
- Pfaffl MW, Horgan GW, Dempfle L (2002). Relative expression software tool (REST) for group-wise comparison and statistical analysis of relative expression results in real-time PCR. *Nucleic Acids Res.* **30**, e36.
- Pfaffl MW, Tichopad A, Prgomet C, Neuvians TP (2004). Determination of stable housekeeping genes, differentially regulated target genes and sample integrity: BestKeeper--Excel-based tool using pair-wise correlations. *Biotechnol Lett.* **26**, 509-515.
- Piconi L, Quagliaro L, Assaloni R, Da Ros R, Maier A, Zuodar G, Ceriello A (2006). Constant and intermittent high glucose enhances endothelial cell apoptosis through mitochondrial superoxide overproduction. *Diabetes Metab Res Rev.* **22**, 198-203.
- Pillarsetti S, Saxena U (2004). Role of oxidative stress and inflammation in the origin of Type 2 diabetes--a paradigm shift. *Expert Opin Ther Targets.* **8**, 401-408.
- Poirier O, Nicaud V, Cambien F, Tiret L (2000). The Pro12Ala polymorphism in the peroxisome proliferator-activated receptor gamma2 gene is not associated with postprandial responses to glucose or fat tolerance tests in young healthy subjects: the European Atherosclerosis Research Study II. *J Mol Med.* **78**, 346-351.
- Poitout V, Amyot J, Semache M, Zarrouki B, Hagman D, Fontes G (2010). Glucolipotoxicity of the pancreatic beta cell. *Biochim Biophys Acta.* **1801**, 289-298.
- Quijada L, Moreira D, Soto M, Alonso C, Requena JM (1997). Efficient 5'-end labeling of oligonucleotides containing self-complementary sequences. *Biotechniques.* **23**, 658-660.
- Radak Z, Chung HY, Goto S (2008). Systemic adaptation to oxidative challenge induced by regular exercise. *Free Radic Biol Med.* **44**, 153-159.
- Raddatz E, Thomas AC, Sarre A, Benathan M (2011). Differential contribution of mitochondria, NADPH oxidases, and glycolysis to region-specific oxidant stress in the anoxic-reoxygenated embryonic heart. *Am J Physiol Heart Circ Physiol.* **300**, H820-835.
- Ravn-Haren G, Olsen A, Tjønneland A, Dragsted LO, Nexø BA, Wallin H, Overvad K, Raaschou-Nielsen O, Vogel U (2006). Associations between GPX1 Pro198Leu

- polymorphism, erythrocyte GPX activity, alcohol consumption and breast cancer risk in a prospective cohort study. *Carcinogenesis*. **27**, 820-825.
- Rehm J, Gmel G, Sempos CT , Trevisan M (2003). Alcohol-related morbidity and mortality. *Alcohol Res Health*. **27**, 39-51.
- Reich DE, Cargill M, Bolik S, Ireland J, Sabeti PC, Richter DJ, Lavery T, Kouyoumjian R, Farhadian SF, Ward R , Lander ES (2001). Linkage disequilibrium in the human genome. *Nature*. **411**, 199-204.
- Reusch JE , Draznin BB (2007). Atherosclerosis in diabetes and insulin resistance. *Diabetes Obes Metab*. **9**, 455-463.
- Reusens B, Ozanne SE , Remacle C (2007). Fetal determinants of type 2 diabetes. *Curr Drug Targets*. **8**, 935-941.
- Richter T , von Zglinicki T (2007). A continuous correlation between oxidative stress and telomere shortening in fibroblasts. *Exp Gerontol*. **42**, 1039-1042.
- Rimm EB, Stampfer MJ, Giovannucci E, Ascherio A, Spiegelman D, Colditz GA , Willett WC (1995). Body size and fat distribution as predictors of coronary heart disease among middle-aged and older US men. *Am J Epidemiol*. **141**, 1117-1127.
- Rimm EB, Williams P, Fosher K, Criqui M , Stampfer MJ (1999). Moderate alcohol intake and lower risk of coronary heart disease: meta-analysis of effects on lipids and haemostatic factors. *BMJ*. **319**, 1523-1528.
- Rivard A, Fabre JE, Silver M, Chen D, Murohara T, Kearney M, Magner M, Asahara T , Isner JM (1999). Age-dependent impairment of angiogenesis. *Circulation*. **99**, 111-120.
- Robert M. Berne MNL (1993a). The cardiovascular system. In *Physiology*. (MNL Robert M. Berne, ed): Mosby- Year Book, Inc., pp. 22-32.
- Robert M. Berne MNL (1993b). The endocrine system. In *Physiology*. (MNL Robert M. Berne, ed): Mosby- Year Book, Inc., pp. 851-875.
- Rocha VZ , Libby P (2009). Obesity, inflammation, and atherosclerosis. *Nat Rev Cardiol*. **6**, 399-409.
- Rogina B , Helfand SL (2004). Sir2 mediates longevity in the fly through a pathway related to calorie restriction. *Proc Natl Acad Sci U S A*. **101**, 15998-16003.
- Rosenblum JS, Gilula NB , Lerner RA (1996). On signal sequence polymorphisms and diseases of distribution. *Proc Natl Acad Sci U S A*. **93**, 4471-4473.
- Ross R (1993). The pathogenesis of atherosclerosis: a perspective for the 1990s. *Nature*. **362**, 801-809.
- Ross R (1999). Atherosclerosis--an inflammatory disease. *N Engl J Med*. **340**, 115-126.
- Rossi DJ, Bryder D, Seita J, Nussenzweig A, Hoeijmakers J , Weissman IL (2007). Deficiencies in DNA damage repair limit the function of haematopoietic stem cells with age. *Nature*. **447**, 725-729.
- Rothman KJ (1990). No adjustments are needed for multiple comparisons. *Epidemiology*. **1**, 43-46.
- Roy H, Bhardwaj S , Yla-Herttuala S (2009). Molecular genetics of atherosclerosis. *Hum Genet*. **125**, 467-491.
- Royle NJ, Mendez-Bermudez A, Gravani A, Novo C, Foxon J, Williams J, Cotton V , Hidalgo A (2009). The role of recombination in telomere length maintenance. *Biochem Soc Trans*. **37**, 589-595.

- Sahin E , Depinho RA (2010). Linking functional decline of telomeres, mitochondria and stem cells during ageing. *Nature*. **464**, 520-528.
- Sakuraba H, Mizukami H, Yagihashi N, Wada R, Hanyu C , Yagihashi S (2002). Reduced beta-cell mass and expression of oxidative stress-related DNA damage in the islet of Japanese Type II diabetic patients. *Diabetologia*. **45**, 85-96.
- Salpea KD , Humphries SE (2010). Telomere length in atherosclerosis and diabetes. *Atherosclerosis*. **209**, 35-38.
- Salpea KD, Nicaud V, Tiret L, Talmud PJ , Humphries SE (2008). The association of telomere length with paternal history of premature myocardial infarction in the European Atherosclerosis Research Study II. *J Mol Med*. **86**, 815-824.
- Salpea KD, Talmud PJ, Cooper JA, Maubaret CG, Stephens JW, Abelak K , Humphries SE (2009). Association of telomere length with type 2 diabetes, oxidative stress and UCP2 gene variation. *Atherosclerosis*. **209**, 42-50.
- Samani NJ, Boulby R, Butler R, Thompson JR , Goodall AH (2001). Telomere shortening in atherosclerosis. *Lancet*. **358**, 472-473.
- Sampson MJ, Gopaul N, Davies IR, Hughes DA , Carrier MJ (2002). Plasma F2 isoprostanes: direct evidence of increased free radical damage during acute hyperglycemia in type 2 diabetes. *Diabetes Care*. **25**, 537-541.
- Sampson MJ , Hughes DA (2006). Chromosomal telomere attrition as a mechanism for the increased risk of epithelial cancers and senescent phenotypes in type 2 diabetes. *Diabetologia*. **49**, 1726-1731.
- Sampson MJ, Winterbone MS, Hughes JC, Dozio N , Hughes DA (2006). Monocyte telomere shortening and oxidative DNA damage in type 2 diabetes. *Diabetes Care*. **29**, 283-289.
- Sanz J , Fayad ZA (2008). Imaging of atherosclerotic cardiovascular disease. *Nature*. **451**, 953-957.
- Satoh M, Ishikawa Y, Takahashi Y, Itoh T, Minami Y , Nakamura M (2008). Association between oxidative DNA damage and telomere shortening in circulating endothelial progenitor cells obtained from metabolic syndrome patients with coronary artery disease. *Atherosclerosis*. **198**, 347-353.
- Satoh M, Minami Y, Takahashi Y, Tabuchi T, Itoh T , Nakamura M (2009). Effect of intensive lipid-lowering therapy on telomere erosion in endothelial progenitor cells obtained from patients with coronary artery disease. *Clin Sci (Lond)*. **116**, 827-835.
- Savage DB, Petersen KF , Shulman GI (2007). Disordered lipid metabolism and the pathogenesis of insulin resistance. *Physiol Rev*. **87**, 507-520.
- Schonfeld P (1990). Does the function of adenine nucleotide translocase in fatty acid uncoupling depend on the type of mitochondria? *FEBS Lett*. **264**, 246-248.
- Scientific Steering Committee obotSBRG (1991). Risk of fatal coronary heart disease in familial hypercholesterolaemia. Scientific Steering Committee on behalf of the Simon Broome Register Group. *BMJ*. **303**, 893-896.
- Serra V, Grune T, Sitte N, Saretzki G , von Zglinicki T (2000). Telomere length as a marker of oxidative stress in primary human fibroblast cultures. *Ann N Y Acad Sci*. **908**, 327-330.
- Serrano AL , Andres V (2004). Telomeres and cardiovascular disease: does size matter? *Circ Res*. **94**, 575-584.

- Shah T, Casas JP, Cooper JA, Tzoulaki I, Sofat R, McCormack V, Smeeth L, Deanfield JE, Lowe GD, Rumley A, Fowkes FG, Humphries SE, Hingorani AD (2009). Critical appraisal of CRP measurement for the prediction of coronary heart disease events: new data and systematic review of 31 prospective cohorts. *Int J Epidemiol.* **38**, 217-231.
- Shay JW, Roninson IB (2004). Hallmarks of senescence in carcinogenesis and cancer therapy. *Oncogene.* **23**, 2919-2933.
- Shepherd PR, Withers DJ, Siddle K (1998). Phosphoinositide 3-kinase: the key switch mechanism in insulin signalling. *Biochem J.* **333 (Pt 3)**, 471-490.
- Slagboom PE, Droog S, Boomsma DI (1994). Genetic determination of telomere size in humans: a twin study of three age groups. *Am J Hum Genet.* **55**, 876-882.
- Slot JW, Geuze HJ, Freeman BA, Crapo JD (1986). Intracellular localization of the copper-zinc and manganese superoxide dismutases in rat liver parenchymal cells. *Lab Invest.* **55**, 363-371.
- Smith S, de Lange T (2000). Tankyrase promotes telomere elongation in human cells. *Curr Biol.* **10**, 1299-1302.
- Smogorzewska A, de Lange T (2002). Different telomere damage signaling pathways in human and mouse cells. *EMBO J.* **21**, 4338-4348.
- Smucker EJ, Turchi JJ (2001). TRF1 inhibits telomere C-strand DNA synthesis in vitro. *Biochemistry.* **40**, 2426-2432.
- Soerensen M, Christensen K, Stevnsner T, Christiansen L (2009). The Mn-superoxide dismutase single nucleotide polymorphism rs4880 and the glutathione peroxidase 1 single nucleotide polymorphism rs1050450 are associated with aging and longevity in the oldest old. *Mech Ageing Dev.* **130**, 308-314.
- Sozou PD, Kirkwood TB (2001). A stochastic model of cell replicative senescence based on telomere shortening, oxidative stress, and somatic mutations in nuclear and mitochondrial DNA. *J Theor Biol.* **213**, 573-586.
- Spyridopoulos I, Haendeler J, Urbich C, Brummendorf TH, Oh H, Schneider MD, Zeiher AM, Dimmeler S (2004). Statins enhance migratory capacity by upregulation of the telomere repeat-binding factor TRF2 in endothelial progenitor cells. *Circulation.* **110**, 3136-3142.
- St-Pierre J, Drori S, Uldry M, Silvaggi JM, Rhee J, Jager S, Handschin C, Zheng K, Lin J, Yang W, Simon DK, Bachoo R, Spiegelman BM (2006). Suppression of reactive oxygen species and neurodegeneration by the PGC-1 transcriptional coactivators. *Cell.* **127**, 397-408.
- Steer SE, Williams FM, Kato B, Gardner JP, Norman PJ, Hall MA, Kimura M, Vaughan R, Aviv A, Spector TD (2007). Reduced telomere length in rheumatoid arthritis is independent of disease activity and duration. *Ann Rheum Dis.* **66**, 476-480.
- Stephens JW, Dhamrait SS, Mani AR, Acharya J, Moore K, Hurel SJ, Humphries SE (2008). Interaction between the uncoupling protein 2 -866G>A gene variant and cigarette smoking to increase oxidative stress in subjects with diabetes. *Nutr Metab Cardiovasc Dis.* **18**, 7-14.
- Stephens JW, Gable DR, Hurel SJ, Miller GJ, Cooper JA, Humphries SE (2006). Increased plasma markers of oxidative stress are associated with coronary heart disease in males with diabetes mellitus and with 10-year risk in a prospective sample of males. *Clin Chem.* **52**, 446-452.

- Stephens JW , Humphries SE (2003). The molecular genetics of cardiovascular disease: clinical implications. *J Intern Med.* **253**, 120-127.
- Stephens JW, Hurel SJ, Cooper JA, Acharya J, Miller GJ , Humphries SE (2004). A common functional variant in the interleukin-6 gene is associated with increased body mass index in subjects with type 2 diabetes mellitus. *Mol Genet Metab.* **82**, 180-186.
- Stern MP (1995). Diabetes and cardiovascular disease. The "common soil" hypothesis. *Diabetes.* **44**, 369-374.
- Stocker R, Hunt NH, Weidemann MJ , Clark IA (1986). Protection of vitamin E from oxidation by increased ascorbic acid content within Plasmodium vinckei-infected erythrocytes. *Biochim Biophys Acta.* **876**, 294-299.
- Stolar M (2010). Glycemic control and complications in type 2 diabetes mellitus. *Am J Med.* **123**, S3-11.
- Su Y, Liu XM, Sun YM, Jin HB, Fu R, Wang YY, Wu Y , Luan Y (2008). The relationship between endothelial dysfunction and oxidative stress in diabetes and prediabetes. *Int J Clin Pract.* **62**, 877-882.
- Sun J, Folk D, Bradley TJ , Tower J (2002). Induced overexpression of mitochondrial Mn-superoxide dismutase extends the life span of adult Drosophila melanogaster. *Genetics.* **161**, 661-672.
- Suzuki YJ, Forman HJ , Sevanian A (1997). Oxidants as stimulators of signal transduction. *Free Radic Biol Med.* **22**, 269-285.
- Szostak JW , Blackburn EH (1982). Cloning yeast telomeres on linear plasmid vectors. *Cell.* **29**, 245-255.
- Tarry-Adkins JL, Chen JH, Smith NS, Jones RH, Cherif H , Ozanne SE (2009). Poor maternal nutrition followed by accelerated postnatal growth leads to telomere shortening and increased markers of cell senescence in rat islets. *FASEB J.* **23**, 1521-1528.
- Tentolouris N, Nzietchueng R, Cattan V, Poitevin G, Lacolley P, Papazafiropoulou A, Perrea D, Katsilambros N , Benetos A (2007). White blood cells telomere length is shorter in males with type 2 diabetes and microalbuminuria. *Diabetes Care.* **30**, 2909-2915.
- Terry DF, Nolan VG, Andersen SL, Perls TT , Cawthon R (2008). Association of longer telomeres with better health in centenarians. *J Gerontol A Biol Sci Med Sci.* **63**, 809-812.
- Tham WH , Zakian VA (2002). Transcriptional silencing at Saccharomyces telomeres: implications for other organisms. *Oncogene.* **21**, 512-521.
- Thong FS, Dugani CB , Klip A (2005). Turning signals on and off: GLUT4 traffic in the insulin-signaling highway. *Physiology (Bethesda).* **20**, 271-284.
- Thorogood M, Seed M , De Mott K (2009). Management of fertility in women with familial hypercholesterolaemia: summary of NICE guidance. *BJOG.* **116**, 478-479.
- Tiret L, Gerdes C, Murphy MJ, Dallongeville J, Nicaud V, O'Reilly DS, Beisiegel U , De Backer G (2000). Postprandial response to a fat tolerance test in young adults with a paternal history of premature coronary heart disease - the EARS II study (European Atherosclerosis Research Study). *Eur J Clin Invest.* **30**, 578-585.
- Trachootham D, Lu W, Ogasawara MA, Nilisa RD , Huang P (2008). Redox regulation of cell survival. *Antioxid Redox Signal.* **10**, 1343-1374.

- Tregouet DA, Escolano S, Tired L, Mallet A , Golmard JL (2004). A new algorithm for haplotype-based association analysis: the Stochastic-EM algorithm. *Ann Hum Genet.* **68**, 165-177.
- Tregouet DA , Tired L (2004). Cox proportional hazards survival regression in haplotype-based association analysis using the Stochastic-EM algorithm. *Eur J Hum Genet.* **12**, 971-974.
- Twigg SM, Kamp MC, Davis TM, Neylon EK , Flack JR (2007). Prediabetes: a position statement from the Australian Diabetes Society and Australian Diabetes Educators Association. *Med J Aust.* **186**, 461-465.
- Tyrberg B, Anachkov KA, Dib SA, Wang-Rodriguez J, Yoon KH , Levine F (2002). Islet expression of the DNA repair enzyme 8-oxoguanosine DNA glycosylase (Ogg1) in human type 2 diabetes. *BMC Endocr Disord.* **2**, 2.
- Ueland PM, Refsum H, Beresford SA , Vollset SE (2000). The controversy over homocysteine and cardiovascular risk. *Am J Clin Nutr.* **72**, 324-332.
- Ulaner GA , Giudice LC (1997). Developmental regulation of telomerase activity in human fetal tissues during gestation. *Mol Hum Reprod.* **3**, 769-773.
- Ushio-Fukai M, Zafari AM, Fukui T, Ishizaka N , Griendling KK (1996). p22phox is a critical component of the superoxide-generating NADH/NADPH oxidase system and regulates angiotensin II-induced hypertrophy in vascular smooth muscle cells. *J Biol Chem.* **271**, 23317-23321.
- Uziel O, Singer JA, Danicek V, Sahar G, Berkov E, Luchansky M, Fraser A, Ram R , Lahav M (2007). Telomere dynamics in arteries and mononuclear cells of diabetic patients: effect of diabetes and of glycemic control. *Exp Gerontol.* **42**, 971-978.
- Valdes AM, Andrew T, Gardner JP, Kimura M, Oelsner E, Cherkas LF, Aviv A , Spector TD (2005). Obesity, cigarette smoking, and telomere length in women. *Lancet.* **366**, 662-664.
- Vasa-Nicotera M, Brouillette S, Mangino M, Thompson JR, Braund P, Clemitson JR, Mason A, Bodycote CL, Raleigh SM, Louis E , Samani NJ (2005). Mapping of a major locus that determines telomere length in humans. *Am J Hum Genet.* **76**, 147-151.
- Vaziri H, Dragowska W, Allsopp RC, Thomas TE, Harley CB , Lansdorp PM (1994). Evidence for a mitotic clock in human hematopoietic stem cells: loss of telomeric DNA with age. *Proc Natl Acad Sci U S A.* **91**, 9857-9860.
- Vermes I, Haanen C, Steffens-Nakken H , Reutelingsperger C (1995). A novel assay for apoptosis. Flow cytometric detection of phosphatidylserine expression on early apoptotic cells using fluorescein labelled Annexin V. *J Immunol Methods.* **184**, 39-51.
- Verzola D, Gandolfo MT, Gaetani G, Ferraris A, Mangerini R, Ferrario F, Villaggio B, Gianiorio F, Tosetti F, Weiss U, Traverso P, Mji M, Deferrari G , Garibotto G (2008). Accelerated senescence in the kidneys of patients with type 2 diabetic nephropathy. *Am J Physiol Renal Physiol.* **295**, F1563-1573.
- von Zglinicki T (2000). Role of oxidative stress in telomere length regulation and replicative senescence. *Ann N Y Acad Sci.* **908**, 99-110.
- Wang H, Chu WS, Lu T, Hasstedt SJ, Kern PA , Elbein SC (2004). Uncoupling protein-2 polymorphisms in type 2 diabetes, obesity, and insulin secretion. *Am J Physiol Endocrinol Metab.* **286**, E1-7.

- Weinsaft JW , Edelberg JM (2001). Aging-associated changes in vascular activity: a potential link to geriatric cardiovascular disease. *Am J Geriatr Cardiol.* **10**, 348-354.
- Whitcombe D, Theaker J, Guy SP, Brown T , Little S (1999). Detection of PCR products using self-probing amplicons and fluorescence. *Nat Biotechnol.* **17**, 804-807.
- White H , Potts G (2006). Mutation scanning by high resolution melt analysis. Evaluation of Rotor-Gene 6000 (Corbett Life Science), HR-1 and 384 well LightScanner (Idaho Technology). *National Genetics Reference Laboratory (Wessex).*
- Whitehouse CJ, Taylor RM, Thistlethwaite A, Zhang H, Karimi-Busheri F, Lasko DD, Weinfeld M , Caldecott KW (2001). XRCC1 stimulates human polynucleotide kinase activity at damaged DNA termini and accelerates DNA single-strand break repair. *Cell.* **104**, 107-117.
- Williams GC (1957). PLEIOTROPY, NATURAL-SELECTION, AND THE EVOLUTION OF SENESCENCE. *Evolution.* **11**, 398-411.
- Wilson PW, D'Agostino RB, Parise H, Sullivan L , Meigs JB (2005). Metabolic syndrome as a precursor of cardiovascular disease and type 2 diabetes mellitus. *Circulation.* **112**, 3066-3072.
- Wilson WR, Herbert KE, Mistry Y, Stevens SE, Patel HR, Hastings RA, Thompson MM , Williams B (2008). Blood leucocyte telomere DNA content predicts vascular telomere DNA content in humans with and without vascular disease. *Eur Heart J.* **29**, 2689-2694.
- Wong KK, Maser RS, Bachoo RM, Menon J, Carrasco DR, Gu Y, Alt FW , DePinho RA (2003). Telomere dysfunction and Atm deficiency compromises organ homeostasis and accelerates ageing. *Nature.* **421**, 643-648.
- Wong LS, van der Harst P, de Boer RA, Codd V, Huzen J, Samani NJ, Hillege HL, Voors AA, van Gilst WH, Jaarsma T , van Veldhuisen DJ (2009). Renal dysfunction is associated with shorter telomere length in heart failure. *Clin Res Cardiol.* **98**, 629-634.
- Wright WE , Shay JW (1992). Telomere positional effects and the regulation of cellular senescence. *Trends Genet.* **8**, 193-197.
- Wu CH, Hsieh SC, Li KJ, Lu MC , Yu CL (2007). Premature telomere shortening in polymorphonuclear neutrophils from patients with systemic lupus erythematosus is related to the lupus disease activity. *Lupus.* **16**, 265-272.
- Wu KD, Orme LM, Shaughnessy J, Jr., Jacobson J, Barlogie B , Moore MA (2003). Telomerase and telomere length in multiple myeloma: correlations with disease heterogeneity, cytogenetic status, and overall survival. *Blood.* **101**, 4982-4989.
- Xing J, Chen M, Wood CG, Lin J, Spitz MR, Ma J, Amos CI, Shields PG, Benowitz NL, Gu J, de Andrade M, Swan GE , Wu X (2008). Mitochondrial DNA content: its genetic heritability and association with renal cell carcinoma. *J Natl Cancer Inst.* **100**, 1104-1112.
- Xu D, Neville R , Finkel T (2000). Homocysteine accelerates endothelial cell senescence. *FEBS Lett.* **470**, 20-24.
- Yudkin JS, Juhan-Vague I, Hawe E, Humphries SE, di Minno G, Margaglione M, Tremoli E, Kooistra T, Morange PE, Lundman P, Mohamed-Ali V , Hamsten A (2004). Low-grade inflammation may play a role in the etiology of the metabolic syndrome in patients with coronary heart disease: the HIFMECH study. *Metabolism.* **53**, 852-857.

- Yung LM, Laher I, Yao X, Chen ZY, Huang Y , Leung FP (2009). Exercise, vascular wall and cardiovascular diseases: an update (part 2). *Sports Med.* **39**, 45-63.
- Yusuf S, Gerstein H, Hoogwerf B, Pogue J, Bosch J, Wolffenbuttel BH , Zinman B (2001). Ramipril and the development of diabetes. *JAMA.* **286**, 1882-1885.
- Yusuf S, Hawken S, Ounpuu S, Dans T, Avezum A, Lanus F, McQueen M, Budaj A, Pais P, Varigos J , Lisheng L (2004). Effect of potentially modifiable risk factors associated with myocardial infarction in 52 countries (the INTERHEART study): case-control study. *Lancet.* **364**, 937-952.
- Zee RY, Michaud SE , Ridker PM (2009). Mean telomere length and risk of incident venous thromboembolism: a prospective, nested case-control approach. *Clin Chim Acta.* **406**, 148-150.
- Zeggini E, Weedon MN, Lindgren CM, Frayling TM, Elliott KS, Lango H, Timpson NJ, Perry JR, Rayner NW, Freathy RM, Barrett JC, Shields B, Morris AP, Ellard S, Groves CJ, Harries LW, Marchini JL, Owen KR, Knight B, Cardon LR, Walker M, Hitman GA, Morris AD, Doney AS, McCarthy MI , Hattersley AT (2007). Replication of genome-wide association signals in UK samples reveals risk loci for type 2 diabetes. *Science.* **316**, 1336-1341.
- Zhan H, Suzuki T, Aizawa K, Miyagawa K , Nagai R (2010). Ataxia telangiectasia mutated (ATM)-mediated DNA damage response in oxidative stress-induced vascular endothelial cell senescence. *J Biol Chem.* **285**, 29662-29670.